MYOFILAMENT AND MOLECULE:

A STUDY ON MYOSIN

by

CHARLES HAYWARD EMES, B.Sc.

A thesis submitted in partial fulfilment
of the regulations governing the Ph.D.
degree at the University of Leicester.

Department of Biochemistry,
School of Biological Sciences,
Adrian Building,
University of Leicester,
University Road,
Leicester, LE1 7RH.

May, 1977

ProQuest LLC
789 East Eisenhower Parkway
P.O. Box 1346
Ann Arbor, MI 48106-1346

To my family

Traveller, there is no path,

Paths are made by walking.

(Antonio Machado,

1875 - 1939)

Acknowledgements

I would like to express the deepest gratitude to my supervisor Dr A. J. Rowe for his help, encouragement and guidance during the course of this research.

My thanks also go to Professors H. L. Kornberg FRS and W. V. Shaw in whose department this work was carried out and to the Medical Research Council for the award of a Research Studentship.

I am indebted to Dr A. G. Weeds for instructing me in the SDS gel electrophoresis technique and for the gift of a sample of myosin light chains. I am particularly grateful to Messrs A. J. Gibbs and D. R. Boreham whose expertise and patience I relied heavily upon during the first few months of this study.

It is a pleasure to acknowledge the expert technical assistance of Mr J. R. Parkin with analytical ultracentrifugation and Ms J. Hunt with electron microscopy. My gratitude is also owed to the Computer Laboratory for the extensive use of facilities and to their Customer Services Section for pointing out the usefulness of the Econometric Software Package.

Finally I would like to thank my many friends and colleagues in the Department of Biochemistry whose enthusiasm and companionship have made my stay in Leicester such a pleasant one.

A portion of the results from the investigation into the alleged monomer-dimer equilibrium for myosin were presented at the British Biophysical Society meeting at Queen Elizabeth College London, 17th - 19th December, 1974.

Abstract

A procedure has recently been derived which makes it possible to determine the molecular weight of a particle from sedimentation velocity studies alone. Application of this new theory has enabled the molecular weight of both the myosin molecule and the myosin filament isolated from rabbit skeletal muscle to be determined. It has further been demonstrated by exhaustive curve-fitting that myosin A solutions contain no appreciable amounts of dimer at high ionic strength. This is in direct contradiction to the prediction by Godfrey and Harrington (1970a,b) and Harrington and Burke (1972) that a monomer-dimer equilibrium existed in myosin solutions. An analysis has been presented which shows that these latter results may be satisfactorily explained without recourse to a monomer-dimer hypothesis.

A detailed analysis of the hydrodynamic properties of synthetic A-filaments has shown that they display a feature not previously demonstrated heretofore; namely that they invariably possess a range of frictional ratios some 75% higher than can be accounted for in terms of the length-equivalent prolate ellipsoids of revolution. On the assumption that preparations of natural A-filaments exhibit similar frictional properties as those formed in vitro, it has been possible to determine the helical symmetry of purified natural A-filaments by measuring their sedimentation coefficient.

The sedimentation coefficient close to infinite dilution has been estimated for purified A-filaments by the technique of active enzyme centrifugation yielding a value of 132 ± 3S (in agreement with the earlier but less precise estimate of 136 ± 25S, Trinick, 1973). It was found that native A-filaments contain between 3.15 and 3.40 myosins/14.3nm axial repeat and this is regarded as good evidence in favour of a 3-stranded model for the A-filament.

CONTENTS

LIST OF FIGURES

LIST OF PLATES

LIST OF TABLES

CHAPTER I

The Problem and Method of Approach

I.1. Background Knowledge

Muscular contraction is brought about by the interaction of two proteins myosin and actin, and the energy required to produce tension is believed to be provided by the hydrolysis of ATP by myosin. The detailed arrangement of myosin and actin within muscle has been the subject of intensive research, not least in vertebrate skeletal (or striated) muscle, in which the contractile units, the 'sarcomeres', are all arranged in register. The vertebrate skeletal muscles most commonly used for both biochemical and physiological studies are the sartorius and gastrocnemius muscles of the frog and the psoas muscle of the rabbit for reasons which have been delightfully explained by Szent-Györgyi (1951). Information gained from vertebrate skeletal muscle from different species is usually considered to be interchangeable. With the development of the phase contrast microscope, vertebrate skeletal muscle was shown to have two bands alternating down the length of the fibre: the A- and I-bands (for anisotropic and isotropic, respectively). Selective removal of the proteins myosin and actin from muscle enabled myosin to be identified with the A-band structure and actin with the I-band (for a review see Huxley, 1972).

Electron microscope studies of longitudinal sections of skeletal muscle has shown that the I-band consists of I-filaments (or thin filaments) emanating from a centrally located Z-line. The A-band is formed from A-filaments (or thick filaments), which have a precisely defined length and are arranged in parallel with their ends in register. At normal rest-length the A- and I-filaments interdigitate such that there is total overlap. Cross-sections of muscle observed in the electron microscope and low angle X-ray diffraction of muscle have confirmed that the A- and I-filaments are arranged in a hexagonal lattice, thus each A-filament is surrounded by six I-filaments. Before considering the subunit structure of

the A- and I-filaments some of the properties of actin and myosin should be considered. Since the contractile proteins have been extensively reviewed (Gergely, 1966; Perry, 1967; Young, 1969; Oosawa and Kasai, 1971, Lowey, 1971, 1972; Pollard and Weihing, 1974) only a brief resumé of the pertinent features will be given here.

Actin is a globular protein of molecular weight 41700 (Elzinga et al., 1973) that can polymerize into a filamentous form, F-actin. Optical diffraction of electron micrographs of paracrystals of F-actin show that the actin monomers are arranged on a helix of pitch 2 x 35.5nm with a subunit repeat of 5.5nm (Ohtsuki and Wakabayashi, 1972). X-ray diffraction studies on live muscle shows a meridional reflection at a spacing of 38.5nm which is attributed to the periodicity in the I-filaments (Huxley and Brown, 1967). This spacing is slightly longer than the axial repeat of F-actin and is probably due to the presence of two additional protein components of the I-filament: troponin and tropomyosin. Troponin is a globular protein which binds to the I-filament with an approximate 40nm periodicity (Endo et al., 1966), whereas tropomyosin is a long fibrous protein which aggregates in an end-to-end fashion and lies in the grooves of the F-actin helix.

Myosin has the following properties: it is a highly asymmetric protein (axial ratio about 75); the molecular weight is about 470000; it has ATPase activity and actin-binding ability; it is soluble at ionic strengths greater than 0.3 but is insoluble below this ionic strength. Myosin can be split into two fragments by treatment with trypsin: light meromyosin (LMM) and heavy meromyosin (HMM). The LMM portion has a molecular weight of 140000, a length of 86.0nm and displays the solubility properties of myosin, being insoluble at physiological ionic strength. HMM on the other hand is soluble even at low ionic strength and has a molecular

weight of 340000. Digestion of HMM by papain forms two further fragments: HMM S-2 which is a short rod of length 40-50nm and HMM S-1 which is the globular head region of myosin (molecular weight, 115000) and contains the ATPase activity and actin-binding ability. Each myosin molecule therefore consists of two heads (HMM S-1) attached to a long tail of coiled-coil α-helix (LMM+HMM S-2). The trypsin-sensitive region between HMM S-2 and LMM is believed to have a more open and flexible structure than the rest of the myosin rod and may act as a 'hinge region' during cross-bridge formation in native muscle (see below).

Because of the solubility properties of the meromyosins previously mentioned, it is generally accepted that the LMM portions polymerize to form the backbone of the filament; the HMM portions, which are soluble at physiological ionic strength, lie close to the filament surface in resting muscle (Huxley and Brown, 1967). A detailed electron microscope study of synthetic myosin filaments and native A-filaments isolated from rabbit psoas muscle led Huxley (1963) to propose that the assembly of myosin filaments was initiated by antiparallel packing of myosin molecules, in a parallel manner, to the ends of the filament. X-ray diffraction of live frog sartorius muscle at rest gave layer lines indexing on a helical repeat of 43nm and it was suggested, but by no means proved, that this corresponded to a helical arrangement of myosin molecules in the A-filament (Huxley and Brown, 1967). As we shall see below, the number of strands in this helix is still in some doubt and it is the aim of this investigation to try to resolve this uncertainty. However, the proposed mechanism of muscular contraction is included at this point as a knowledge of the events that occur during the contraction cycle is essential in the discussion that follows on the symmetry of the A-filament. Once again the reader is referred to detailed reviews (Young, 1969; Huxley, 1972; Weber and Murray, 1973) and

the original papers (Huxley, 1957; Huxley and Brown, 1967; Huxley, 1968; Haselgrove, 1975).

From X-ray diffraction studies on muscle at rest, Huxley and Brown (1967) suggested that the first layer lines at a spacing of 43nm, and other orders of it, were produced from the helical arrangement of the myosin heads (HMM S-1 portions) on the A-filament. Upon contraction of the muscle the spacing of the reflections on the meridian remained unchanged although the intensity of the $14.3nm^{-1}$ reflection decreased slightly. Far greater changes were observed in the intensity of the reflections along the $43nm^{-1}$ layer lines which decreased to about one third of their resting value. Observations too, on the intensity of the 1,0 and 1,1 equatorial reflections (from the hexagonal lattice of the myosin and actin filaments), showed that the relative intensities of the two reflections were reversed when muscle changes from its resting state to rigor.

The interpretation of these X-ray diffraction results was that in resting muscle the S-1 subunits lie close to the myosin filament giving strong $43nm^{-1}$ layer lines and a prominent 1,0 equatorial reflection. During contraction or rigor, cross-bridges are formed between actin and myosin filaments (as evidenced by electron micrographs of muscle in rigor) as a result of the S-1 subunits attaching to the actin filament by bending at the LMM-HMM junction. The substantial mass transfer produces an increase in the intensity of the 1,1 reflection and a corresponding decrease in the 1,0 reflection. The $43nm^{-1}$ layer lines are diminished because the myosin heads are indexed on the actin filament helix and their original helical arrangement is reduced. Once attached to actin the myosin ATPase activity is greatly increased and it is presumed that during the release of the products of ATP hydrolysis (ADP and P_i) a conformational change in the myosin molecules occurs causing a movement of the actin filament relative

to the myosin filament. Shortening of muscle is permitted by the sliding of the actin filaments over the myosin filaments, the so-called 'sliding filament hypothesis' of Huxley. At the end of the cross-bridge cycle, ATP binds to S-1, actin and myosin dissociate, and the cross-bridges return to their starting position or proceed onto another cycle.

Let us now return to the structure of the A-filament and consider in more detail its helical symmetry. There are two reasons for studying the symmetry of the A-filament. Firstly it will help in a better understanding of how muscles work. For example there are many details that are still obscure: how are the cross-bridges distributed about the six surrounding I-filaments since the arrangement is different depending on the symmetry (see Squire, 1974 and section I.1.2); what percentage of the cross-bridges are attached at any one time; can the force generated per A-filament be reconciled with the total force generated by the whole muscle? The second reason is that the structure of the A-filament is an interesting one from an intellectual point of view in determining how A-filament assembly is accomplished in vivo. Indeed, the mechanism by which the length of the A-filament is determined so precisely (1.57μm in rabbit skeletal muscle, Craig and Offer, 1976a) is unknown. Other details that remain to be elucidated are the way in which radial growth of the A-filament is prevented in vivo, particularly since synthetic myosin filaments formed in vitro show a variation in diameter (10-40nm); also there is a high turnover of structural proteins in living muscle (Koizumi, 1974) but how this replacement is achieved remains undisclosed.

I.1.1. The Symmetry of the A-filament

From X-ray diffraction studies on resting muscle, Huxley and Brown (1967) suggested that the A-filament exhibited 2-fold helical symmetry,

a proposal which was consistent with the variation in intensity along the first layer lines, provided that the centre of mass of the S-1 subunits was at a radius of 10.0 to 11.0nm. However, Squire (1971) proposed that a 4-stranded helix could also comply with the X-ray diffraction pattern if the centre of mass of the myosin heads was at a radius of about 16.0 to 17.0nm, thus, even in relaxed muscle, the myosin heads are in a position quite close to actin filaments. But Huxley (1968) has interpreted the large mass transference from myosin filaments to actin filaments, when a muscle passes from the relaxed state into the rigor state, as a movement of the myosin heads from positions close to the myosin filament to positions where they attach to actin (see above). Squire (1972) was able to reconcile his 4-stranded model with the mass transfer observations by considering the effective mass radius of the myosin filament. The mass ratio of myosin filament to actin filament for muscle at rest (5:1) and in rigor (1.7:1 or less) has been calculated from X-ray diffraction patterns (Huxley, 1968). This mass ratio for myofilaments in resting muscle is slightly higher than that found from interference microscopy (4:1, Huxley and Hanson, 1957). The predicted mass ratios for myofilaments of muscle at rest and in rigor (using the effective mass radius) are equally as good, or as poor, for a 4-stranded model as for a 2-stranded model with 2 myosins/cross-bridge. Thus, on this basis, 4-stranded and 2-stranded symmetry are equally as likely to represent the true symmetry of the A-filament.

However, another possible type of symmetry was considered by Squire (1972), namely 3-stranded. Three-stranded symmetry can also comply with the intensity distribution along the first, second and third layer lines and gives a total myosin filament to total actin filament mass ratio of 3.9:1, which is in excellent agreement with the 4:1 ratio estimated from interference microscopy (Huxley and Hanson, 1957). The effective mass

ratios of thick to thin filament in relaxed and rigor muscles are 2.9:1 and 0.9:1, respectively, for a 3-stranded model (Squire, 1972). Once again these values are not sufficiently different from the observed mass ratios (Huxley, 1968) to rule out the 3-stranded model. Thus the X-ray diffraction results from relaxed and rigor muscles may be interpreted by three possible types of symmetry: 2-, 3- or 4-stranded. Furthermore, the number of myosins per cross-bridge (or lattice point) cannot be determined from X-ray diffraction. But biochemical evidence of the total myosin content of muscle (Hanson and Huxley, 1957; Huxley and Hanson, 1957) provides an upper limit to the number of myosins per A-filament (384, Huxley, 1972). On the basis that there are 98 'crowns' per A-filament (i.e. 98 transverse planes at which cross-bridges project, Craig and Offer, 1976a) this means that 3- or 4-stranded models can have only one myosin per cross-bridge but a 2-stranded model may have one or two myosins/cross-bridge (Huxley and Brown, 1967).

If a more accurate estimate of the myosin content of muscle can be obtained some of these possible types of symmetry could be ruled out. One such approach has been to use quantitative SDS gel electrophoresis. By solubilising whole myofibrils in the detergent SDS and separating the myosin and actin by polyacrylamide gel electrophoresis, in the presence of SDS, then the mass ratio of myosin to actin can be measured. This ratio, together with the relative lengths of thick and thin filaments, suffices to calculate N, the number of myosins/14.3nm repeat or crown. From the argument above it will be appreciated that if N is 2 or 3 the A-filament is 2- or 3-stranded, respectively, with 1 myosin/cross-bridge. If N is 4, there are two possibilities: either 4-stranded with 1 myosin/cross-bridge or 2-stranded with 2 myosins/cross-bridge.

Three groups of researchers have independently determined the symmetry of the A-filament from quantitative SDS gels of solubilised,

glycerinated myofibrils. Morimoto and Harrington (1974a) found N was 3.9 ± 0.3 favouring either 4-stranded symmetry or 2-stranded with 2-myosins per cross-bridge. Tregear and Squire (1973), on the other hand, suggested that the symmetry was 3-fold or possibly four. The third study, by Potter (1974) gave an estimate of 254 myosins/A-filament, a finding consistent with either a 3-stranded or a 2-stranded helix with 1 myosin/cross-bridge. There are inherent difficulties in this procedure:

(i) myosin dissociates in the presence of SDS into its component polypeptide chains and the myosin : actin ratio is estimated from the area under one of the myosin polypeptide peaks and correcting for the weight fraction of this polypeptide present in myosin

(ii) the staining intensity of actin and myosin polypeptide chains is different and must be measured

(iii) one must be certain that all the protein of the myofibril has entered the gel

(iv) there must be no proteolysis occurring.

On this last point it is disconcerting to note that SDS has been reported to promote proteolysis (Fairbanks et al., 1971; Trinick, 1973). Quantitative SDS gels have therefore been unable to unambiguously determine the symmetry of the A-filament, although the evidence probably favours 3-stranded symmetry to some limited extent.

I.1.2. Experimental Evidence Concerning Symmetry

Huxley and Brown (1967) have shown myosin filaments in frog sartorius muscle are arranged in a hexagonal superlattice in which adjacent filaments are rotated by $^2/_3$ of a turn relative to each other (i.e. by 360x2/3n degrees, where n is the number of strands). An argument presented by Squire (1974) was that this myosin filament superlattice is not a chance

arrangement but one designed to produce an even spacing of cross-bridges directed towards actin filaments. By this reasoning, a 2- or 4-stranded model integrated into the superlattice would create a non-equivalent actin filament environment in which short regions of an actin filament are approached by 6 or 12 HMM S-1 subunits (depending on the number of myosins per cross-bridge). Only with a 3-stranded model for the myosin filament can a quasi-equivalence of actin filaments be achieved (Squire, 1974); the superlattice arrangement of myosin filaments is essential to ensure that an actin filament is approached by single cross-bridges, evenly spaced at 14.3nm intervals. Thus only a 3-stranded model provides an adequate explanation for the existence of the superlattice.

The second piece of evidence has come from computer-simulation of the intensity distribution along the layer lines of the X-ray diffraction pattern for the three alternative types of symmetry (Squire, 1975). Comparison of the predicted distribution with that observed in the layer lines of the X-ray diffraction pattern (Huxley and Brown, 1967) should, in principle, distinguish between the three types of symmetry. But, for a realistic model, the assumptions that have to be made are numerous and consequently the results predicted from it are more open to criticism. The main parameters included for each symmetry model were the relative positions of the two S-1 subunits in the cross-bridge, the radial distance of the cross-bridge from the filament axis and the orientation of the cross-bridge in space (defined by the angles ϕ and θ). Only poor agreement could be obtained between the 4-stranded model and the observed intensity distribution. Good agreement was obtained with a 2- or 3-stranded model although the angle of tilt, ϕ, of the cross-bridge in the 2-stranded model (between 0 and 45°) makes this possibility unlikely (Squire, 1975).

Further evidence for a 3-stranded model has come from this laboratory

(Trinick, 1973). Purified A-filaments were prepared for electron microscopy by shadowing with platinum after critical-point drying. Negatively contrasted A-segments were also studied. Optical diffraction of electron micrographs of shadowed filaments showed a strong off-meridional reflection at 21.5nm spacing which dominated the pattern. A recent development in image analysis (Gibbs and Rowe, 1974) has enabled this reflection to be identified in micrographs of negatively contrasted filaments, also. The $21.5nm^{-1}$ reflection was believed to be generated from the spacing between one myosin molecule and its nearest neighbour (along the surface of the filament) and its intensity was suggested to be due to the myosin heads being 'slewed' along the 21.5nm helix, in the relaxed state (Figure 1.).

The angle between the equator and the line through the $21.5nm^{-1}$ reflection (θ) was measured from the optical diffraction pattern and was $50 \pm 2^{\circ}$. Values of θ may also be computed for a range of filament diameters for a 2-, 3- or 4-stranded model and it is therefore possible to determine which model provides the best fit to the experimental data. Figure 2 shows the computer-simulated curves (Rowe, unpublished, after Trinick, 1973) for the three types of symmetry showing that θ decreases both as the number of strands increases and as the diameter of the filament decreases. From the measured θ and the estimated diameter of the metal-shadowed filament (after correcting for the metal-cap thickness) it can be seen that the best fit is obtained for a 3-stranded model. The 4-stranded model is incompatible with the data, although a 2-stranded model could be included if a substantial over-estimation of the diameter of the filament is assumed.

I.1.3. Models for the Myosin Packing Arrangement

The weight of evidence therefore favours a 3-stranded model, but it

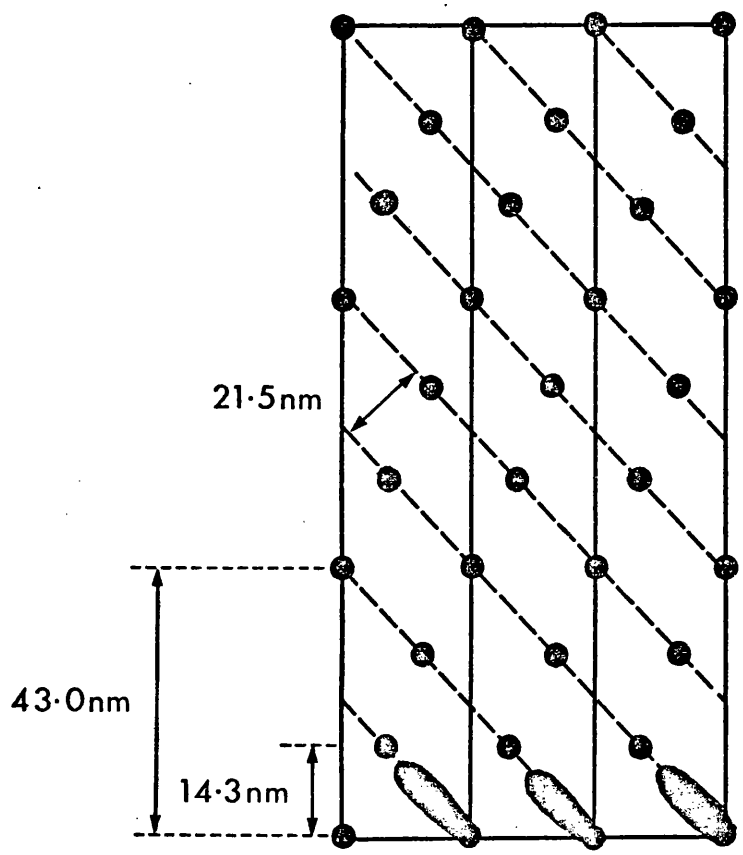

Figure 1 Surface lattice of myosin heads on a shadowed A-filament with a postulated 3-stranded helix

It is supposed that the intensity of the 21.5nm^{-1} reflection seen in optical diffraction patterns of electron micrographs of shadowed A-filaments is due to the myosin heads being slewed along the 21.5nm helix, Trinick (1973).

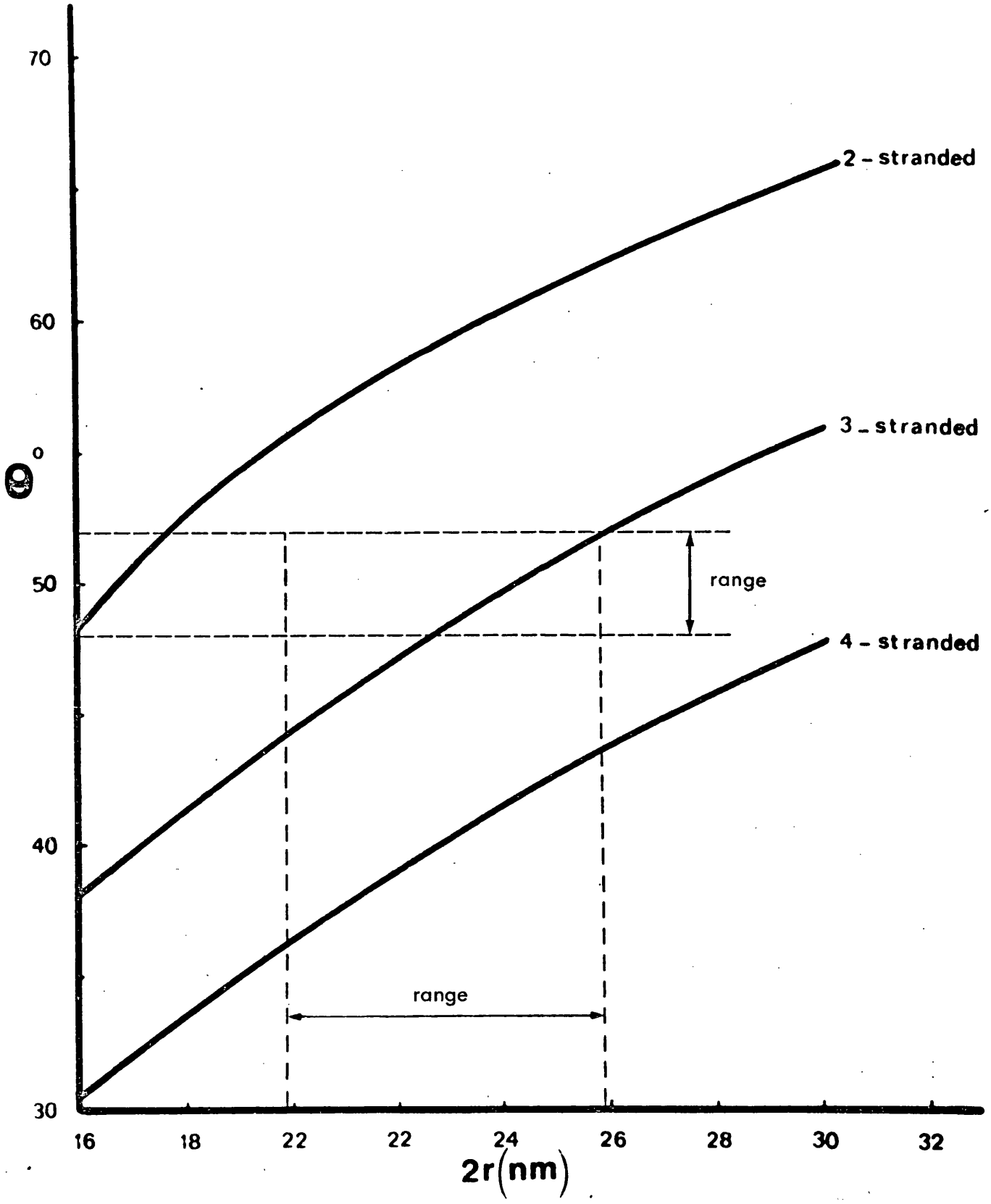

Figure 2 The angle between the equator and the 21.5nm^{-1} reflection (θ) computed for three types of symmetry as a function of diameter

The observed θ and diameter lie within the ranges indicated.

is not possible to discount entirely the other types of symmetry. In spite of this uncertainty, four detailed models for the packing arrangement of myosin molecules into the A-filament have been proposed: two on the basis of 3-fold helical symmetry (Squire, 1973; Rowe, unpublished) and two assuming 2-fold symmetry exists (Pepe, 1967, 1971; Young et al., 1972). Any model describing the packing arrangement of myosin molecules must be consistent with the following points: (i) it must of course obey one of the three types of symmetry, (ii) the polarity of the myosin molecules must be reversed on either side of the M-line (Huxley, 1963), (iii) it must take into account the known dimensions and solubility properties of the LMM and HMM fragments of myosin, (iv) the packing arrangement must be consistent with the electron microscope observations that the A-filament has a triangular cross-sectional profile on either side of the M-line (Pepe, 1967, 1971) and that in the M-line region the cross-section appears circular with a hollow centre (Pepe, 1971), (v) the packing in the M-line region must explain the appearance of the five transverse lines seen in longitudinal sections of muscle of which the three middle lines are often more prominent than the outer two (Pepe, 1967, 1971), (vi) the diameter of the filament must be compatible with electron microscope observations (12 to 14nm, Huxley, 1963; Trinick, 1973) and X-ray diffraction results (a predicted maximum diameter of 13.0 and 15.0nm, for a 2- and 3-stranded model, respectively, Squire, 1973).

(a) Young et al. model

The model by Young et al.(1972) is based upon the assumption that the LMM subunit is flexible and can twist into a helix of pitch about 43nm. This supposition is founded upon the observation of a single type of LMM aggregate obtained by gradual dialysis to 0.2M-NH_4Cl, pH 8.1, over a period of six months (King and Young, 1972). In the author's opinion there are

other interpretations for the appearance of these LMM aggregates without the need to assume a helical twist. There is no other evidence to suggest that LMM is flexible and a helical twist is incompatible with the X-ray diffraction results on live muscle (Huxley and Brown, 1967) and optical diffraction of electron micrographs of purified A-filaments (Trinick, Gibbs and Rowe, unpublished). In view of this discrepancy the Young et al. model will not be considered in detail here.

(b) Pepe model

The Pepe model is based upon the following observations and assumptions. (i) Labelling of glycerinated chicken breast muscle with 'antibody to myosin' results in a periodicity of 43.0nm, consisting of seven equally spaced stripes in the middle of each half of the A-band (Pepe, 1967, 1971). It was assumed that this periodicity reflects the arrangement of myosin molecules along the entire length of the A-filament and that the periodicity was only observed in a limited region of the A-filament because of slight disorders in the packing arrangement in the M-line region (where tail-to-tail abutment of myosin molecules occurs) and in the taper at the ends.

(ii) Two stranded helical symmetry was assumed, such that there are six cross-bridges per 43.0nm repeat. The model could accommodate one or two myosins/cross-bridge. (iii) In the electron microscope, cross-sections of muscle taken in the pseudo-H-zone (a region defined by the edge of the bare-zones of the A-filaments) show a triangular profile, the orientation of which is reversed on either side of the M-line (Pepe, 1967, 1971). Pepe proposed that the myosin molecules are all aggregated parallel to the filament axis and that there are twelve rows in all: three centrally located and nine peripherally located, an arrangement consistent with this triangular cross-sectional profile. This arrangement of LMMs in the

backbone of the filament was later supported by the image enhancement of the subunits seen in cross-sections of A-filaments using the Markham rotation technique (Pepe and Drucker, 1972). The reversal of the orientation of the triangular profiles was accounted for by assuming that a helical twist through 180° occurred between M-bridges (a distance of about 22nm). The helical twist would also lead to a circular profile for the A-filament in the M-line region in agreement with electron microscope observations (Pepe, 1967, 1971).

(iv) The five transverse lines seen in the M-line in longitudinal sections of muscle were attributed to M-bridges formed between neighbouring A-filaments. Pepe suggested that an M-bridge forms between two A-filaments at the point where tail-to-tail abutment of oppositely orientated myosin molecules on one filament is exactly opposite a similar point on a neighbouring filament. This model predicts that neighbouring filaments show exactly the same orientation, which contradicts the X-ray diffraction results on frog sartorius muscle from which it was concluded that neighbouring filaments were rotated by 120° relative to each other (for a 2-stranded model, Huxley and Brown, 1967). The Pepe model was later modified (Pepe, 1972) to conform with this observation by introducing a gap of 2/3 of a period (28.6nm) between the tails of oppositely orientated myosin molecules. The M-bridge was then suggested to connect between tails of antiparallel myosin molecules on neighbouring filaments.

(v) The length of the bare-zone predicted from the Pepe model was about 172nm, which is greater than the best estimate for this length (154nm, Craig and Offer, 1976a) although Pepe claims that the helical twist in the M-line region could reduce the length by 2/3 of a repeat (giving a bare-zone length of 144nm).

Several criticisms can be made of the Pepe model. (i) The model is

based upon the observation of seven stripes seen in each half of the A-band when labelled with 'anti-myosin', but the original antibody was contaminated by other antibodies to impurities present in myosin (including C-protein). It was later shown that these stripes are due entirely to antibody to C-protein, both in chicken muscle (Pepe, 1972) and rabbit muscle (Craig and Offer, 1976b). But since C-protein binds to myosin it was suggested that it reflects the underlying periodicity of the myosin molecules. (ii) A 'close-packed' arrangement of myosin molecules was initially proposed in which the diameter of the filament (including HMM S-2 portions) was 9 - 12nm (Pepe, 1967). Results from image enhancement of electron micrographs of cross-sections of A-filaments (Pepe and Drucker, 1972) and from optical diffraction of ultra-thick sections of the same (Pepe, 1975) required that the close packing arrangement be 'expanded' to agree with the measured centre-to-centre distance between subunits of 3.7 to 4.0nm. From this measurement I have calculated the diameter of the A-filament (including HMM S-2 portions) as 15 to 16nm, assuming Pepe's model for the arrangement of myosin tails to be correct. This diameter is consistent with that of a filament showing 3-fold symmetry rather than 2-fold symmetry (Squire, 1973). It is unlikely however that a stable filament structure could be formed in which the subunits are separated by a distance of about 4nm and an alternative explanation is presented below (see Rowe model).

(iii) The myosin molecules are not all in equivalent positions and it was necessary to propose a mechanism by which the heads of the centrally located myosin molecules reached the surface of the filament so that they could interact with actin. Pepe (1967) postulated that there was a kink in the myosin molecules in the trypsin-sensitive region which provided enough flexibility for the HMM portions to reach the surface of the filament. This is one of the most important features of the Pepe model and one that

is essential to the proposed packing arrangement, yet there is no evidence to suggest that such a kink exists in myosin molecules.

(iv) Pepe (1967) predicted that there were 192 cross-bridges per A-filament and that they extended in an unbroken array from the edge of the bare-zone to the end of the filament, but Craig and Offer (1976a) by labelling glycerinated rabbit psoas muscle with antibody to S-1 found a single gap near the end of the filament. (v) The modification of the original model which created gaps between antiparallel myosin molecules has two consequences. Firstly, to maintain the original bare-zone length of 172nm (ignoring the 'helical twist' for a moment), additional myosin molecules were included in the bare-zone region (Pepe,1972). The additional myosin tails created antiparallel overlaps within the bare-zone region of 4 x 14.3nm (57.2nm) but no such overlap has been detected in LMM paracrystals or myosin aggregates. Cross-sections of A-filaments in the M-line region would show 14 subunits as opposed to the 12 subunits seen in cross-sections in the pseudo-H-zone. The mechanism by which these extra subunits pack into the backbone of the filament remains to be explained. Secondly, the condition for the formation of M-bridges between A-filaments (namely that M-bridges can only form between oppositely orientated myosin molecules on the surface of the filament) requires, from the author's interpretation, an axial translation of one A-filament relative to its neighbour of 2/3 of a repeat (which is equivalent to a 120° shift in rotation for a 2-stranded model). Although this arrangement would then satisfy the requirements of the A-filament superlattice, it would be inconsistent with the antibody labelling studies of muscle (Craig and Offer, 1976a,b), which suggest that there is no axial shift between A-filaments.

(vi) The Pepe model is based upon 2-fold helical symmetry but present information suggests that this type of symmetry is unlikely.

(c) Squire model

Squire (1971, 1972) proposed that the structure of different myosin filaments were related and followed this with a general myosin filament model (Squire, 1973). The model is founded upon the proposed structure of myosin ribbons found in vertebrate smooth muscle (Small and Squire, 1972): two 4nm thick layers of myosin molecules separated by a flat core of protein about 7.5nm thick. The axial repeat of the myosin projections of smooth muscle was the same as that seen in other filaments (that is about 14.3nm). It was suggested that a myosin filament could be formed by bending this flat myosin layer into a cylinder; by including different numbers of projections in the lateral direction in the myosin ribbon, myosin filaments showing 3, 4 or 6-fold symmetry could be formed.

Thus, in the general model for the myosin filament the assumptions made in the model for the myosin ribbon also apply to the structures of the myosin filament of vertebrate skeletal muscle and insect flight muscle. The following points therefore apply to myosin ribbons and to myosin filaments alike. (i) All of the rod portion of myosin (i.e. LMM + HMM S-2, 145nm long) is involved in packing. In point of fact, the HMM S-2 portions are insoluble at physiological ionic strength and when relaxed muscle is activated they are able to move away from the ribbon or filament surface, but this movement of HMM S-2 (Pepe, 1966, 1967) was assumed not to affect the packing arrangement of the LMM portions. (ii) Close-packing of the myosin molecules is assumed in myosin ribbons but formation of a cylindrical filament from a close-packed layer will inevitably result in less dense packing at the periphery of the filament.

(iii) There is one myosin molecule per lattice point in ribbons of vertebrate smooth muscle (Small and Squire, 1972), a conclusion that was confirmed by the estimation of the weight ratio of actin to myosin in

vertebrate smooth muscle from SDS gel electrophoresis (Tregear and Squire, 1973). (iv) All myosin molecules are in equivalent positions in myosin ribbons and filaments. (v) The packing arrangement of myosin is related to the lateral repeat of the core protein. In vertebrate skeletal muscle and insect flight muscle, the core protein, if it exists, was suggested to pack hexagonally in contrast to the tetragonal arrangement proposed for myosin ribbons.

(vi) To allow for overlapping of myosin molecules, the rod portion was assumed to be tilted slightly away from the filament axis, about 1.5°. In this way, the tail end of the myosin molecule is on the inner surface of the myosin layer, whereas the head end is on the outer surface where it is free to move out from the myosin layer (for example during cross-bridge formation). The myosin filament shows a similar tilt of myosin molecules both towards and around the filament axis. To avoid confusion, I will henceforth refer to 'tilt' as the angle between the myosin rod and the filament axis in a radial direction, and 'slew' as the angle between these two axes but in a circumferential direction. The angle of 'slew' in the Squire model is about 3° and the angle of tilt is about 1.5°. Squire (1973) reported that a 0.51nm^{-1} reflection seen in wide-angle X-ray diffraction patterns of muscle was consistent with a maximum angle of tilt + slew of 5° (tilt and slew are indistinguishable in diffraction patterns).

A detailed model of the packing arrangement of myosin molecules in the bare-zone region of the A-filament of vertebrate skeletal muscle was also presented (Squire, 1973) and was consistent with the following observations. Firstly, in the bare-zone region where there is antiparallel overlap of myosin rods, overlaps of 43.0 and 130nm are formed in agreement with the major overlaps seen in LMM paracrystals (mainly 43.0nm, Huxley, 1963; Lowey et al., 1967; Katsura and Noda, 1973b) and in myosin aggregates

(90 and 130nm overlaps, Harrison et al., 1971). A 90nm overlap seen in bipolar aggregates of myosin and myosin rod (Harrison et al., 1971) was not produced in this packing arrangement. Secondly, the bare-zone region was 160nm long which is in good agreement with the estimate of 154nm (Craig and Offer, 1976a).

Thirdly, both the triangular cross-sectional profile in the pseudo-H-zone and the circular profile in the M-line region (Pepe, 1967, 1971) can be generated by the Squire model. The orientation of the triangular profiles on either side of the M-line could be accounted for without the need to assume a sudden 180° helical twist in the A-filament as proposed by Pepe (1967, 1971). The model also predicts that the filament has a hollow centre about 5nm in diameter and this is compatible with the less densely stained region seen in the electron micrographs of transverse sections of A-filaments. Fourthly, the model satisfies the observed diameter of the A-filament of 12.0 to 14.0nm: the outer diameter of the model of the filament is about 15.5nm, although the discrepancy can be accounted for by the less dense packing arrangement on the outside of the filament. A slightly narrower diameter in the M-line region is also predicted.

There are three major points in which the Squire model for the structure of the A-filament of vertebrate skeletal muscle is inadequate. Firstly, there is no evidence of a core protein in vertebrate skeletal muscle. The maximum amount of core protein in the myosin filament predicted by the Squire model is 4% by weight, assuming that the core protein has the same density as that of myosin rod. It is possible that the core protein may be F-protein (an impurity in myosin A preparations present in about 2-3% by weight, Starr and Offer, 1971) but evidence will be presented in this thesis that the A-filament core contains substantial amounts of solvent. But the existence of core protein, while providing a

close link between different myosin filaments, is not essential to the packing arrangement proposed by Squire (1973).

The second point is that Squire did not attempt to present a full explanation of the appearance of transverse stripes in electron micrographs of the M-line region. However, Squire (1973) did suggest that three out of the five stripes might be formed by attachment of M-bridges to the centre of 43.0nm overlaps of antiparallel myosins, but there is no evidence to support this assumption. The remaining two stripes were reported to occur where M-bridges attach to the point of tail-to-tail abutment of oppositely orientated myosin molecules (following the original proposal by Pepe, 1967). What Squire does not point out is that under this proviso, two additional stripes should appear close to the edge of the bare-zone. If M-bridges are attached solely at points of tail-to-tail abutment, Squire's model predicts that four stripes will be observed at 43.0nm intervals. This clearly is inconsistent with the five stripes at 22.0nm intervals seen in electron micrographs (Pepe, 1967).

The third and most important point is that a complete array of myosin heads is not developed until 4 x 43.0nm or 5 x 43.0nm from the M-line. This follows as a natural consequence of the proposed packing arrangement in the bare-zone and a similar restriction at the tapered ends predicts that the myosin heads array is incomplete at 3 x 43.0nm from the ends until the filament terminates. But evidence collected by Craig and Offer (1976b) from antisubfragment-1 labelling of glycerinated rabbit psoas muscle showed that the packing is complete from the edge of the bare-zone to the end of the filament except for a single gap near the ends. Furthermore, the length of the constant packing region in the Squire model is about 375nm out of a filament half-length of about 785nm, which is inconsistent with the known physiological behaviour of muscle: that is, the tension generated

is proportional to the A-I-filament overlap (Gordon et al., 1966). The Squire model therefore has serious flaws.

(d) Rowe model

Another model for A-filament structure has been proposed by Rowe from evidence gained from optical diffraction of electron micrographs of purified A-filaments and A-segments (Trinick, Gibbs and Rowe, unpublished observations). Since the details of this model have not been published as yet, a brief account of it is included here. The Rowe model assumes that the myosin molecules are tilted to the filament axis in a radial direction, as does the Squire model, but the difference is that the Rowe model considers an all tilt arrangement as opposed to the model of Squire which has both tilt and slew. That a small amount of tilt in the myosin molecules may be allowed is supported from wide-angle X-ray diffraction of whole muscle (the maximum amount of tilt or tilt + slew is now thought to be only 3°, K. C. Holmes, personal communication) and optical diffraction of negatively contrasted purified A-filaments from this laboratory. The latter observation is a pair of off-meridional spots produced by a periodicity of 6.6nm; these reflections are believed to arise from the 2-fold coiled-coil α-helix of the myosin rod. The angle of these reflections to the meridian is also consistent with a maximum angle of tilt of 3°. It should be noted that optical diffraction patterns from electron micrographs of A-filaments do not usually show 'order' because of the unfavourable signal to noise ratio, but the transforms obtained by Gibbs and Rowe were produced by using a new technique of linear integration (Gibbs and Rowe, 1974).

The Rowe model is also based on the 'tile-roof' packing arrangement of LMMs deduced by Katsura and Noda (1973b) from studies on negatively stained paracrystals of LMM. The filament in the Rowe model consists of

nine doublet strands in each of which the myosin molecules are arranged in a tile-roof array with a 43nm overlap. Each doublet is staggered by 14.3nm relative to its neighbour, so that there are three myosin S-1 subunits projecting at 14.3nm intervals. The myosin tails are not slewed but are tilted in a radial direction by 3° with respect to the filament axis. There are 18 LMM portions in any infinitely thin cross-section of the filament but a section of conventional EM thickness would show 27 subunits because of overlap (see Figure 3). The model predicts that the profile of the filament seen in cross-sections taken through the cross-bridge-bearing region and the pseudo-H-zone will be triangular and is therefore compatible with the electron microscope observations (Pepe and Drucker, 1972; Pepe, 1975). In addition, the fine detail seen in the cross-sections revealed by the Markham rotation technique (Pepe and Drucker, 1972) can also be interpreted by the Rowe model. In a section of finite thickness, the Rowe model predicts that 27 subunits will be observed and of all these, twelve may be exactly superimposed upon the Markham rotated electron micrographs. Rowe has suggested that the 'missing subunits' lie between the three centrally located and the nine peripherally located LMMs and that the subunit spacing is 2.0nm rather than 4.0nm measured from electron micrographs. There are two explanations as to why these subunits are not observed. (i) They are stained in cross-sections but are less well ordered than the other subunits and the Markham rotation technique tends to suppress rather than enhance their appearance. However, this explanation is inconsistent with the optical diffraction results from electron micrographs of 250nm thick sections of myosin filaments which show a spacing of 4nm (Pepe, 1975). (ii) The alternative explanation is that in spite of the precautions taken to ensure that the stain penetrated the entire thickness of the section, the 'middle ring' of subunits is less densely stained than

Figure 3 The Rowe model for the structure of the thick filament of vertebrate skeletal muscle.

(a) Appearance of the A-filament in a cross-section of infinite thinness as predicted by the Rowe model.* The open circles represent the LMM portions, the filled circles the HMM S-2 portions; the HMM S-1 fragments are also shown.

(b) The dimensions of the myosin molecule upon which the Rowe model is based.

(c) The arrangement predicted for the M-line region. Only three strands are shown, each staggered by 14.3nm with respect to its neighbour. The polarity of the myosin molecules is indicated by the arrows; the helical twist that occurs in the bare-zone region is not shown. It is postulated that the M-line protein attaches to the points of tail-to-tail abutment.

*the section is through a plane where new LMMs are incorporated, i.e. there are 18 + 3 subunits.

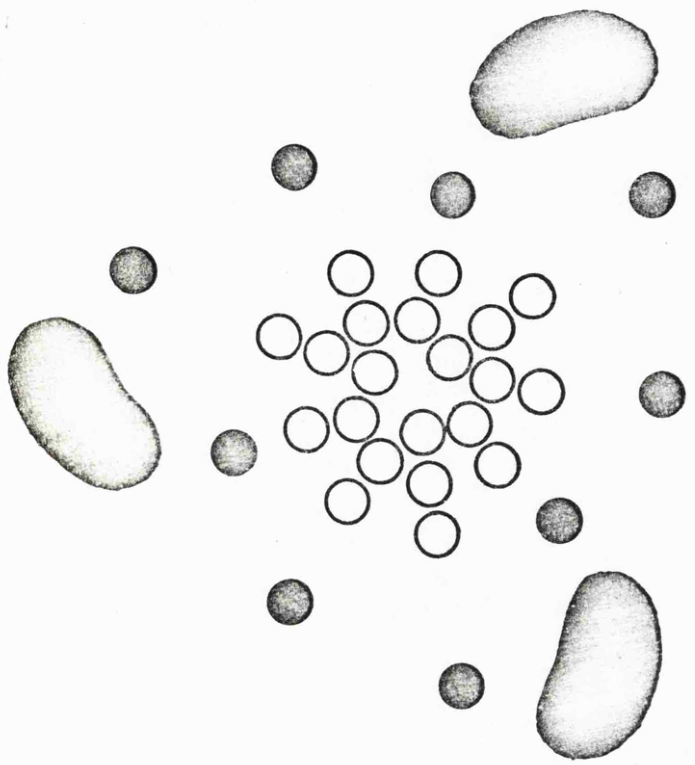

(a)

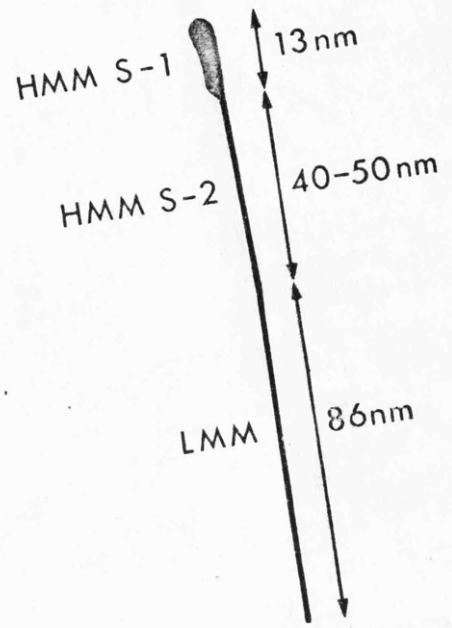

(b)

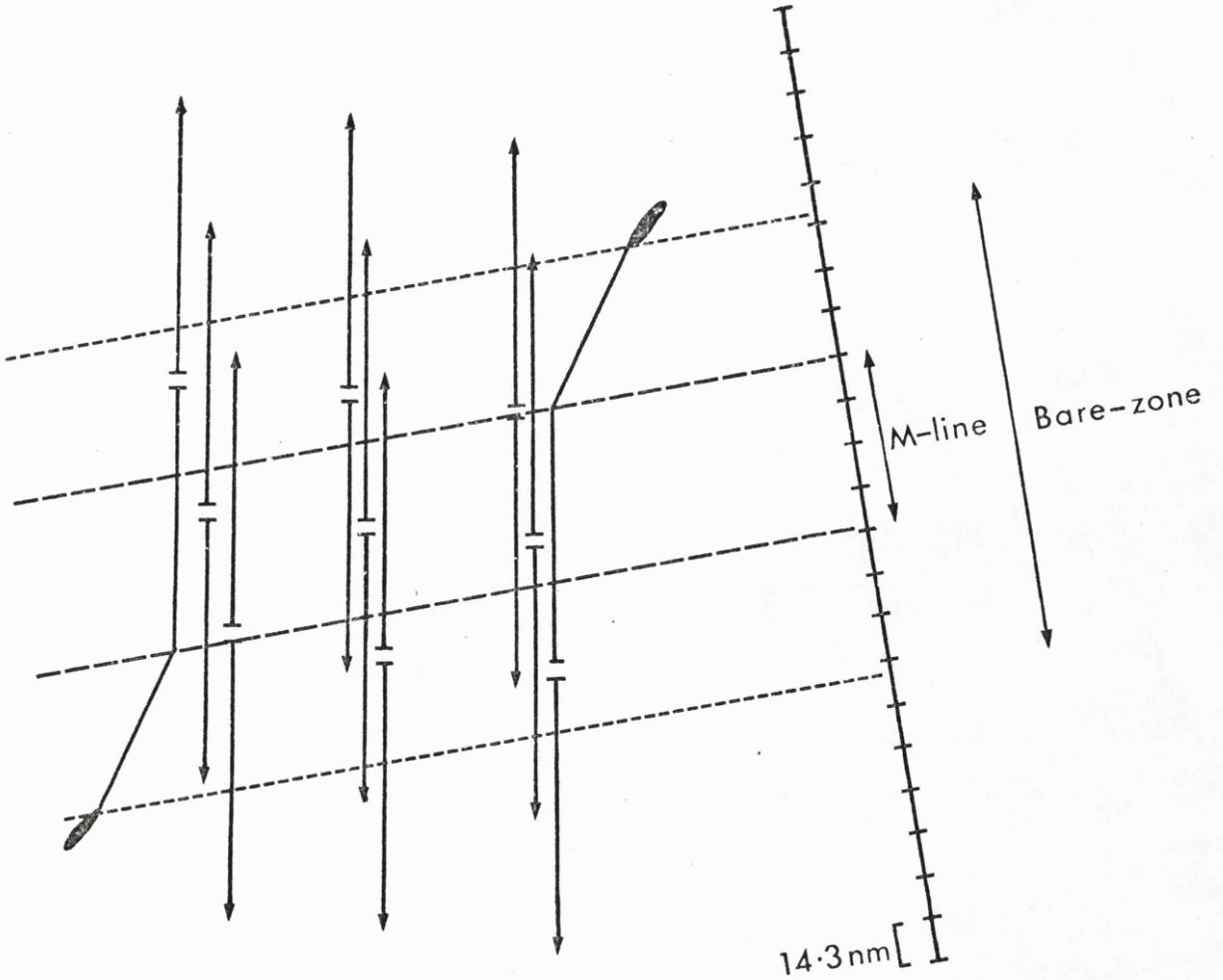

(c)

the other subunits. This non-uniform staining could account for the 4nm spacing measured by both types of image analysis. Clearly, the assumption that additional subunits are present but merely not observed in electron micrographs provides an adequate explanation for the otherwise large centre-to-centre distance between subunits.

Turning now to the packing arrangement in the bare-zone region, the Rowe model predicts that the length of the bare-zone is in the range 137 to 157nm. The exact length cannot be deduced from the model because of the uncertainty in the length of the HMM S-2 portion (40 - 50nm). However, the measured length of the bare-zone (154nm, Craig and Offer, 1976a) lies within the predicted range of lengths for the bare-zone. Three points arise from the packing arrangement in the bare-zone. Firstly, there are two possible types of antiparallel overlaps seen in the bare-zone: 43.0 and 86.0nm, which are consistent with the 43.0nm overlaps (Katsura and Noda, 1973b) and 86.0nm overlaps (Chowrashi and Pepe, 1971) seen in LMM paracrystals. A 130nm overlap is not postulated, in contrast to the Squire model which predicts 43 and 130nm overlaps but no 86 or 90nm overlap.

Secondly, if one considers that M-line protein attaches only to the point where there is tail-to-tail abutment of antiparallel molecules, then there is a total of nine possible sites for M-line stripes. The three middle stripes are observed because M-bridge formation is not hindered by overlying HMM S-2 portions. Moving away from the M-line, the next stripe on either side will be less readily observed because at this point HMM S-2 portions begin to project from the filament surface and may hinder M-bridge formation, but the remaining sites will not form M-bridges because they will be totally obscured by the overlying HMM S-2 portions. Thus of a total of five M-line stripes, the three centrally located ones will appear more prominent than the outer two, in agreement with electron micrographs

(Pepe, 1967, 1971). Admittedly, if there is precise tail-to-tail abutment, the Rowe model would predict five stripes with an axial separation of 14.3nm as opposed to the 22.0nm actually observed (Pepe, 1967). The explanation may lie in a small gap between the ends of antiparallel molecules (about 7 - 10nm wide), possibly filled with M-line protein itself. With this slight modification, the M-line stripes would be separated by approximately 22nm.

Another feature of the packing scheme is that since a tile-roof arrangement is proposed, a helical twist in the A-filament must be introduced into the bare-zone region. This helical twist through 180° inevitably results in a less well ordered packing arrangement and the whole filament structure will tend to 'loosen up'. In this way, not only can a circular cross-sectional profile with a hollow centre be accounted for, but also the extra tails caused by the overlap in the pseudo-H-zone can fit into the 'wells' between the doublet strands. The helical twist mentioned here differs from that in the Pepe model as it does not need to be completed within the distance between M-bridges but can occur over the entire length of the bare-zone. The reversal of the orientation of the triangular cross-sectional profiles on either side of the M-line can also be accounted for by the model.

It has already been noted that antisubfragment-1 labelling of glycerinated psoas muscle has shown that a single gap exists near the end of the A-band (Craig and Offer, 1976a). This missing crown is succeeded by two more crowns, the last marking the end of the filament. The Rowe model can be shown to be consistent with this observation by the following argument. It is postulated that radial bonding between members of a doublet strand is more important in maintaining the subunit structure than the circumferential bonding between neighbouring strands. If one further

postulates that a myosin molecule is 'omitted' from the filament structure, then the subsequent members of the doublet strand will also be absent since there are insufficient sites to form a stable structure. But, on the other hand, the neighbouring doublet strands will not be affected. Assuming three myosin molecules are omitted (remembering that the Rowe model is based upon 3-fold helical symmetry) then inspection of the model reveals that the sequence of crowns at the end of the filament will be: 'empty, full, full', which is exactly the prediction made by Craig and Offer (1976a). As to why myosin molecules may be omitted, remains obscure, although perhaps the tapering at the ends of the filament (which in no way alters the above argument) may be relevant here. Further suppositions must await more detailed knowledge on the structure of the A-filament.

The Rowe model has the following features:

(i) it obeys 3-fold helical symmetry

(ii) all myosin molecules are equivalent for most of the length of the filament (except in the bare-zone and at the ends of the filament)

(iii) the myosin heads project in an array that is complete from the edge of the bare-zone to the end of the filament (a gap near the end of the filament is also predicted if certain assumptions are made)

(iv) the model predicts cross-sectional profiles that are compatible with electron microscope observations

(v) the diameter of the filament, including HMM S-2 portions, is 15 to 16nm in excellent agreement with predictions for a 3-stranded model from X-ray diffraction results and with electron microscope observations (Huxley, 1963; Trinick, 1973)

(vi) no 'kink' in the myosin molecule need be assumed

(vii) no core protein is necessary

(viii) the bare-zone shows overlaps of 43 and 86nm as do myosin aggregates

and LMM paracrystals

(ix) M-bridges connect between regions of tail-to-tail abutment of antiparallel myosin molecules and five stripes are predicted, the outer two being less prominent

(x) the stripes in the M-line region are unaffected by the helical twist in this region as all the A-filaments are precisely aligned (i.e. there is no longitudinal stagger)

(xi) in a superlattice arrangement of A-filaments showing 3-fold symmetry, each A-filament is rotated by 80° with respect to its neighbour. At each level where a stripe is seen in the M-line region, three M-bridges project from each A-filament and connect with neighbouring filaments in a similar way to cross-bridge formation between A- and I-filaments.

The observation of seven stripes in each half of the A-band when muscle is labelled with antibody to C-protein, may be explained by the Rowe model in the same way as the Pepe model. If, as is generally supposed (Pepe, 1972; Pepe and Drucker, 1975) the C-protein periodicity reflects the underlying repeat of the myosin molecules, the location of C-protein in the A-filament infers that constant packing is confined to a limited region. Although the Rowe model predicts that there is constant packing from the edge of the bare-zone to the end of the filament, it could be argued that distortions caused by the packing in the bare-zone region and in the tapered ends could extend into the constant packing region. Thus it is conceivable that the location of C-protein along the A-filament does reflect a constant packing arrangement in this region only.

The disadvantage of the Rowe model is that it is unable to explain why C-protein binds at 43nm intervals and not at every 14.3nm, since the myosin molecules are all equivalent. There are four possible reasons for the observed periodicity of C-protein. (i) The C-protein extends along the

surface of the filament for a distance of 30nm or thereabouts and thus effectively blocks the next two potential sites. But evidence from labelling of glycerinated rabbit psoas muscle with antibody to C-protein, suggests that the C-protein molecule extends over an axial distance of less than 10nm (Craig and Offer, 1976b). (ii) The other two binding sites per 43nm may be blocked by other proteins as yet unidentified. This seems unlikely on the basis of the amount of other protein components present in the thick filament and in any case one is left to speculate as to why these proteins do not bind at every 14.3nm interval. (iii) The binding of C-protein to the first site may perturb the next two sites so that C-protein is permitted to bind to the third site and so on down the filament. However, negatively stained A-segments show a 43nm periodicity beyond the region where C-protein stripes appear (Trinick, 1973; Craig, 1977). (iv) The fourth possibility is that C-protein binding reflects a true 43nm periodicity in the myosin filament and that all the myosin molecules are not in equivalent positions (Craig and Offer, 1976b). There is as yet insufficient detail on the structure of the A-filament to design meaningful models which show myosin molecules in non-equivalent positions. Thus at present, the Rowe model for the packing arrangement of myosin molecules into the A-filament provides the best scheme to satisfy the experimental observations, with the notable exception of the periodicity of C-protein.

It is therefore apparent that the weight of experimental evidence presently available suggests that the symmetry of the A-filament is 3-fold and that, on this basis, a suitable model for the packing arrangement of myosin molecules can be postulated. However, 2- or 4-stranded symmetry cannot be categorically ruled out. This investigation provides additional support for a 3-stranded helix by an entirely different approach than that used previously. The aim is to determine the molecular weight of purified

A-filaments isolated from rabbit psoas muscle, from whence the number of myosins/14.3nm (N) can be estimated. [There has been one other approach to determine the molecular weight of the A-filament by the particle counting method (Morimoto and Harrington, 1974a). However, this technique may introduce errors, leading to a substantial over-estimate of molecular weight and it will be considered more fully later (IV.1).].

I.1.4. Molecular Weight of the A-filament

To estimate the molecular weight of the A-filament there are three essential requirements: (i) a method to obtain purified A-filaments, (ii) a means of measuring molecular weight and (iii) the molecular weight of myosin must be known. The molecular weight of myosin has been an elusive quantity to estimate and values quoted in the literature have been varied.

In 1970, a monomer-dimer equilibrium was reported for myosin solutions at high ionic strength (Godfrey and Harrington, 1970a,b) and this was offered as an explanation as to why values of the molecular weight of myosin measured by different researchers have been inconsistent. This investigation was begun with a study of the alleged monomer-dimer equilibrium by sedimentation velocity experiments. In the course of this research, a method was devised by Rowe (1977) by which the molecular weight of a particle could be calculated from its s^o (the sedimentation coefficient at infinite dilution) and k_s (the concentration dependence of the sedimentation coefficient). The procedure is based on a theoretically-derived equation that relates k_s to the frictional ratio (f/f_o) of the sedimenting particle. The determination of molecular weight from s^o and k_s is particularly useful for purified A-filaments which, because of their fragility and cohesive properties, preclude the use of more conventional techniques for molecular weight determination. However, the s^o and k_s

method requires a concentrated solution of purified A-filaments (in excess of 1mg/ml) and it is this criterion that has been difficult to satisfy. Attempts described herein to obtain concentrated purified A-filaments failed, but a technique using H_2O-D_2O gradients, developed in this laboratory (Trinick, 1973), has been used to acquire purified A-filaments in dilute form (0.1mg/ml). An alternative approach to determine the molecular weight of the A-filament was pursued to see if f/f_o of the A-filament could be predicted from that of an equivalent prolate ellipsoid of revolution of the same length and mass. But first it was necessary to establish if an equivalent prolate ellipsoid of revolution was a good hydrodynamic model for the myosin filament by using synthetic myosin filaments as a model system. A relationship was found between f/f_o of the 'length-equivalent' prolate ellipsoid and f/f_o of the myosin filament and therefore the molecular weight of the A-filament was estimated by measuring s^o and predicting f/f_o. The sedimentation coefficient at infinite dilution, s^o, was obtained by active enzyme centrifugation, a useful technique by which the catalytically active form of the enzyme is followed by a reaction-induced change in absorbance.

The advantages of calculating N, the number of myosins/14.3nm, from the molecular weight estimated from s^o and f/f_o are: (i) the native form of the A-filament is studied in its catalytically active state, thus the effect of any proteolysis is immediately apparent, (ii) since the sedimentation coefficient is measured close to infinite dilution, the absolute concentration of the A-filaments is not critical, (iii) s^o is independent of length, i.e. a partially degraded A-filament preparation has about the same s^o as that of a non-degraded preparation, (iv) the problems mentioned for quantitative SDS gels do not arise, (v) the symmetry of the A-filament can be established unequivocally (except where $N = 4$).

On this last point, there are two possible models for the structure of the A-filament: 2-stranded with 2 myosins/cross-bridge or 4-stranded with 1 myosin/cross-bridge. The former possibility is much more favoured by any of the myosin packing arrangements mentioned if a myosin dimer exists at high ionic strength, since as the ionic strength is lowered and filament formation proceeds, the myosin dimer will predominate in solution (Godfrey and Harrington, 1970a). Thus an investigation into the alleged association of the myosin molecule is important for two reasons: not only to establish the molecular weight of myosin but also to determine if a myosin dimer does exist in substantial amounts at high ionic strength. This thesis therefore describes hydrodynamic studies performed on solutions of myosin both as individual molecules and in the aggregated form of the myosin filament. Additional information on the amount of water associated with the myosin filament and molecule has also been obtained and the usefulness of some new hydrodynamic techniques is also high-lighted. The conclusion drawn from the results described herein is that the A-filament shows 3-stranded helical symmetry.

C H A P T E R - II

Materials and Methods

II.1. Materials

All chemicals used were of analytical grade or the finest grade commercially available. Deuterium oxide (99.79% deuterated) was from the United Kingdom Atomic Energy Research Establishment, Winfrith, Dorset; New Zealand White rabbits were from Hop Rabbits, Canterbury; ADP, ATP, phosphoenolpyruvate (PEP), ethyleneglycol-bis-(β-aminoethyl ether) NN'-tetraacetic acid (EGTA), NADH from yeast, and firefly lantern extract in $MgSO_4$ - arsenate buffer were all from Sigma (London) Chemical Co. Ltd., Kingston-upon-Thames, Surrey; pyruvate kinase and lactate dehydrogenase, both from rabbit muscle, were from Boehringer Corporation (London) Ltd., Colnbrook, England; NN-bis(2-hydroxyethyl)-glycine (Bicine), dithiothreitol (DTT) and NNN'N'-tetramethylethylene-diamine (Temed) were from BDH Chemicals Ltd., Poole, England; bovine serum albumin was from Calbiochem, Los Angeles; 2-(3-acetamido-5-N-methylacetamido-2,4,6-triiodobenzamido)-2-deoxy-D-glucose (metrizamide) was from Nyegaard and Co., Oslo; polystyrene latex spheres were from Serva, Heidelberg; DEAE-Sephadex A-50 was obtained from Pharmacia (Great Britain) Ltd., London, and EDTA was from Fisons Scientific Apparatus, Loughborough, England.

II.2. Methods

II.2.1. Preparation of Samples for SDS gel Electrophoresis

(a) Myosin and synthetic myosin filaments used in ultracentrifugation studies were dialysed against 0.5M-NaCl, 0.05M-sodium phosphate buffer, pH 6.7, with two changes of the solution.

(b) Myofibril and crude A-filament samples were dialysed for 16h in 1% (v/v) β-mercaptoethanol and 1% (w/v) SDS which was found to solubilise both samples (Potter, 1974). Duplicate samples, dialysed against 1% SDS, were

used to determine protein concentration.

(c) Purified A-filaments were prepared for electrophoresis as described in V.2.6.

(d) C-protein was prepared by the method of Offer et al.(1973). The C-protein precipitate, formed at very low ionic strength and collected by centrifugation (3000g for 15min), was redissolved in 0.5M-NaCl, 0.05M-sodium phosphate buffer, pH 7.0. A mixture of C- and F-proteins was obtained in the same way but without ammonium sulphate fractionation of myosin prior to DEAE-Sephadex chromatography.

(e) The sample of light chains from skeletal muscle myosin in 1% SDS was a gift from Dr A. Weeds.

The samples for SDS polyacrylamide gel electrophoresis were either used at once or stored at -15°C. Protein concentration was estimated by the method of Lowry et al.(1951). Samples to be electrophoresed were diluted to not less than 50% (v/v) of sample buffer: 0.01M-Tris-Bicine, 1% (w/v) SDS, 10% (v/v) β-mercaptoethanol, 40% (v/v) glycerol, 0.015% (w/v) bromophenolblue. SDS was added where necessary to give five times excess by weight of SDS per mg protein. Samples were boiled for 2 - 3min and then cooled. The following amounts were applied to 10% gels: 100µg solubilised myofibrils, 20µg light chains or 80µg myosin.

II.2.2. SDS Polyacrylamide gel Electrophoresis

Gel tubes 15cm long were soaked in 'Decon 90', rinsed in distilled water and then in 1% SDS. Polymerization of the 10% gel solution containing 10% (w/v) acrylamide, 0.3% (w/v) bis-acrylamide, 1% (w/v) SDS, 0.2% (v/v) Temed, was accomplished by adding 15mg ammonium persulphate to 25ml of the solution. On to the top of the gels was layered a small amount of water and the gels left to stand overnight. The following day, the

gel tubes were assembled into the electrophoresis apparatus, the samples were applied, and electrophoresis was performed at 1mA/tube, until the tracking dye had entered the gel, then continued at 4mA/tube. The running buffer used was 0.1M-Tris-Bicine, 0.1% (v/v) SDS. The current was switched off when the tracking dye was about 1cm from the end of the tube. Gels were removed by forcing water from a syringe between the gel and the wall of the glass tube. Staining was carried out at 45°C for 1h with 0.5% (w/v) coomassie brilliant blue (Sigma) in a methanol, acetic acid, water solvent (5:1:4 by volume). The gels were destained electrophoretically in methanol, acetic acid, water (2:1:7 by volume) at 1A (or 100V) for 3/4h and then left in methanol, acetic acid, water (0.5:1:8.5 by volume) until fully destained and finally stored in 7% (v/v) acetic acid.

A Joyce-Loebl microdensitometer was used to scan the gels at a wavelength of 500nm. Care was taken to ensure that the long axis of the gels was exactly parallel to the scanning direction.

II.2.3. Ultracentrifugation

Two analytical ultracentrifuges have been used throughout this study: an MSE Centriscan 75 equipped with two optical filters for work at a wavelength of 500 or 280nm, and an MSE Mk. 1 Analytical Ultracentrifuge, fitted with a u-v scanner. Several modifications to this latter instrument have enabled us to carry out routine work more efficiently and also supplied us with several new techniques (e.g. 'bright-field' and 'dark-field' scanning Toepler optics).

(a) Logic pulse

A 0.5mW Helium/Neon laser as the light source for the 'logic pulse' (the pulse which switches on the sample and hold circuits of the u-v scanner) has replaced the original infra-red source. The laser is located

above the monochromator and this arrangement allows for easier adjustment of the 'logic pulse' without affecting the optical system.

(b) Analogue multiplexer

An analogue multiplexer was designed and constructed by J. R. Parkin and used when multiple schlieren patterns were photographed. Movement of protein boundaries in three centrifuge cells with different loading concentrations can be followed simultaneously when 2° wedge windows are used in two of the centrifuge cells. The wedge windows displace the analogue beam so that three schlieren peaks, separated in the x-direction, can be observed in the final image plane. However, each schlieren pattern is partially obscured by the light from the other two cells, resulting in poor definition. The analogue multiplexer eradicates this problem. It is essentially an adjustable mask placed in the back focal plane of the condensing lens (i.e. just behind the phase plate) which separates the information from each of the three cells (Trautman, 1956). The definition is greatly enhanced, Plate 1, and permits easier measurement of schlieren patterns from photographs.

(c) Dark-field schlieren optics

Detection of protein boundaries by conventional schlieren optics (using a phase plate and cylindrical lens) is limited to protein concentrations above 0.1mg/ml. Another problem is that schlieren peaks may only be recorded photographically, as the information (dc/dr and r) is provided in two dimensions (in the x- and z-directions, respectively). Dark-field schlieren optics not only permit the detection of very small protein boundaries (down to 0.5μg/ml for bovine serum albumin, A. J. Rowe, unpublished observations) but the resulting image may be scanned by the photomultiplier of the u-v scanner. The dark-field optical system is a modification of the original Toepler arrangement in which a horizontal

Plate 1. Multiple schlieren patterns obtained (a) without and (b) with the analogue multiplexer.

10mm double sector centre-pieces were used together with 2 wedge windows. The samples contain synthetic myosin filaments at different concentrations. Speed: about 12000rev./min; temperature: 5°C. The direction of sedimentation is from right to left.

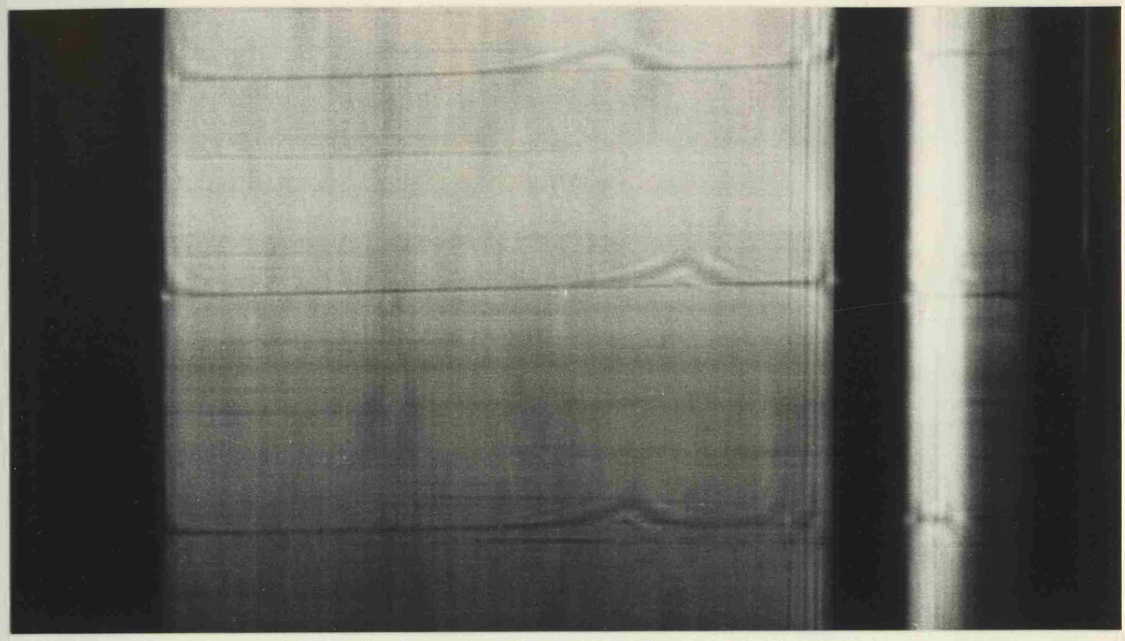

(a)

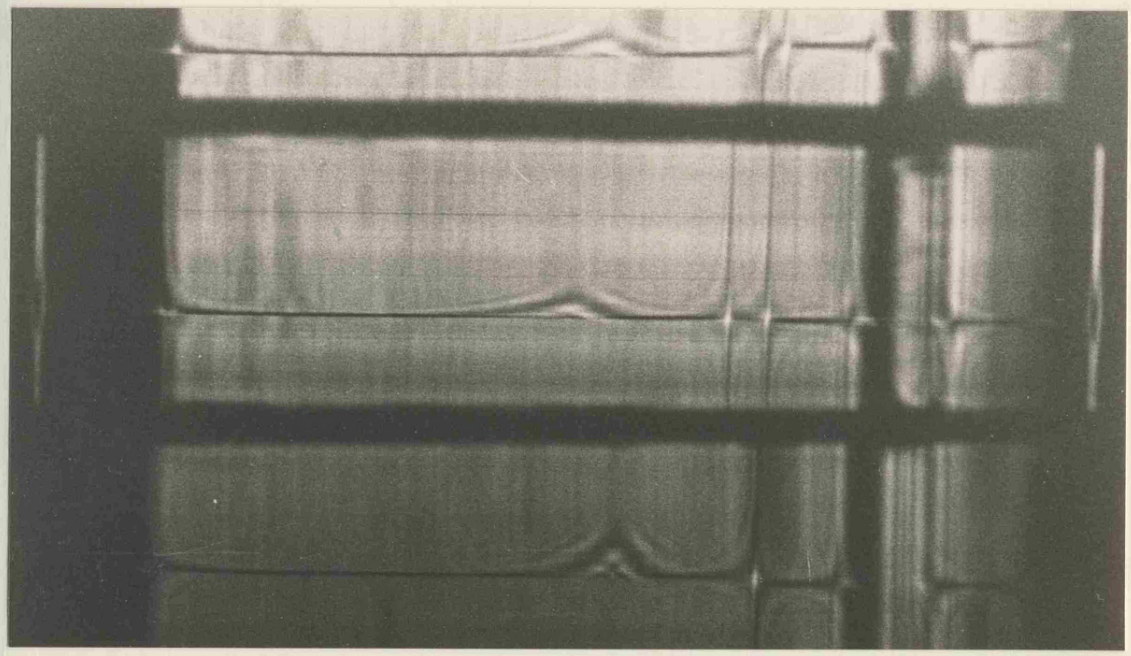

(b)

knife edge is situated in the back focal plane of the condensing lens; both the phase plate and the condensing lens are removed (Reisner and Rowe, 1971). The knife edge intercepts the analogue beam, leaving the beam refracted away from the optical axis to be detected by the photomultiplier. In the final image plane a bright line, representing the position of the maximum concentration gradient, is seen against a dark background (hence the name dark-field). There are two great advantages in the dark-field scanning system: (i) there is much increased sensitivity in the detection of protein boundaries, (ii) upto nine samples can be multiplexed by the u-v scanner using dark-field optics.

The MSE Centriscan 75 is equipped with a bright-field scanning optical system, which is simply the converse of the dark-field system in which the diffracted beam is intercepted. Any wavelength of light may be chosen for dark-field or bright-field optics, provided of course that the macromolecule under study does not absorb at the chosen wavelength, but in practice 500nm was routinely used.

II.2.4. Choice of Optical System

Four optical systems have been used in this research: absorption, schlieren, dark-field and bright-field.

(a) Myosin solutions

The absorption optical system (wavelength, 280nm) was used to follow moving myosin boundaries at concentrations above 0.5mg/ml. At protein concentrations below this, the dark-field scanning system was used with the MSE Analytical Ultracentrifuge. Scans were recorded automatically by the u-v scanner and measurements of the position of the protein boundary, r, were usually taken from the differential trace. Where the MSE Centriscan 75 was used, the protein boundary was followed by the bright-field optical

system; scans were recorded on a flat-bed recorder and superimposed upon each other.

(b) Synthetic myosin filament solutions

Because of the presence of ATP in synthetic filament solutions, absorption optics (at wavelength 280nm) could not be used to follow the protein boundary. Instead, the schlieren optical system, in conjunction with the 'analogue multiplexer', was used to detect the position of the concentration gradient. The schlieren patterns were recorded photographically on Ilford HP4 film. No other optical system was used.

(c) Purified A-filament solutions

In active enzyme centrifugation (Cohen, 1963) of purified A-filaments and synthetic myosin filaments, absorption optics (wavelength, 340nm) were used to follow the movement of the enzyme layer by linking the enzyme reaction to the oxidation of NADH to NAD^+.

II.2.5. Calculation of Sedimentation Coefficients

Where photographs were taken, enlargements were made on Ilford 'Ilfoprint' photographic paper; the prints were not permanently fixed or washed, but were placed on a flat surface and left to dry at room temperature. Under these conditions there was negligible shrinkage or distortion of the paper. The measurement of the distance from the second reference line to the position of the maximum concentration gradient, made from chart paper or photographic print, was aided by a specially constructed linear comparator. The results were analysed either by a linear least squares regression of ln r versus time using a program written for a Hewlett-Packard 9100B Calculator or, for accurate work, by an ALGOL program written by the author and used on the CDC Cyber 72 of the Leicester University Computer Laboratory. This latter program not only corrects for

minor changes in temperature during a run, but also corrects for the progressive discrepancy between the set interval-time of scanning and the actual interval-time at which the moving boundary is scanned as it progresses down the cell.

Standard errors on the s values were always less than 1% for myosin solutions analysed by sedimentation velocity, but were sometimes worse than this for active enzyme centrifugation of myosin filaments (over 4%). All s values were corrected to 20°C and water ($s_{20,w}$) from measured density and viscosity values for the buffer and from tabulated values of the same for water from 'The Handbook of Chemistry and Physics', 43rd edition, published by the Chemical Rubber Publishing Co. USA. In sedimentation velocity experiments, cell loading protein concentrations were always corrected for radial dilution using the equation:

$$\frac{c_t}{c_o} = \frac{r_m^2}{r_t^2} \qquad (1)$$

where r_t is the radial position of the boundary halfway through the run, r_m is the meniscus position and c_o is the initial concentration. The concentration so corrected, c_t, is referred to as the 'true sedimenting concentration'.

II.2.6. Electron Microscopy

A Siemens Elmiskop 1A was used for electron microscopy at an accelerating voltage of 80kV, with a 50μm objective aperture. The magnification was calibrated for each session from measurements of the diameter of polystyrene latex spheres (0.481μm diameter) taken directly from the EM plates using a Projectina Microscope (magnification x10), fitted with a two dimensional micrometer stage. Grids used were 200 mesh

copper grids, 3.05mm diameter, coated with a celloidin-carbon support film. A drop of synthetic myosin filaments or native A-filaments (at about 40μg/ml) was placed on the grid, left for a few seconds, then washed with 0.1M-KCl, stained with 2% uranyl acetate and dried in air. The grids obtained showed mainly positively stained filaments, but with some areas of true negative staining. For true negative staining, the grids were first 'glow-discharged' in an NGN Coating Unit and then used immediately. The filament lengths were measured directly from the EM plates using the Projectina Microscope; 100 to 150 filaments were measured for each filament preparation.

II.2.7. Estimation of Protein Concentration

Myosin concentration was determined by a modified Biuret method which was calibrated against the nitrogen content of myosin by the micro-Kjeldahl method (Rowe, 1960). The procedure was as follows: to 1ml protein solution was added 1ml 10M-NaOH and 1ml H_2O; after mixing, 0.2ml of 1% (w/v) $CuSO_4$ was added, mixed again and left for 10min. The absorbance was read at 552nm in an SP 500 spectrophotometer; the absorbance at 700nm was always close to zero. The concentration of myosin was also checked by measuring the absorbance at 280 and 320nm and using a fourth power term to correct for scattering. The extinction coefficient used was $E^{1\%}_{1cm} = 5.52$, at 280nm (Godfrey and Harrington, 1970a).

For estimation of protein concentration prior to SDS gel electrophoresis, the Lowry et al.(1951) procedure was used with bovine serum albumin as standard.

II.2.8. pH Measurement

A Pye-Unicam pH meter was used with a glass-calomel electrode. The

pH electrode was calibrated using a standard buffer, pH 7.0 at 25°C. If cold solutions were used, the temperature compensator was turned to the temperature of the solution and the pH adjusted; solutions so treated will be referred to throughout as having 'pH ... at 4°C'. For D_2O solutions, the same apparatus and standard were used, but the pD was adjusted to 0.4 units higher than that for the equivalent H_2O solution (Glascoe and Long, 1960).

II.2.9. Estimation of Errors

The error on the mean of a number of measurements was estimated by using library routines for the Hewlett-Packard 9100B Calculator. Where graphs have been plotted, lines or curves through experimental points have been computed by 'least squares' statistical procedures and then drawn with the aid of a 9125A Graph Plotter attached to the 9100B Calculator, using a program written by the author. The error limits quoted represent the standard error of the mean, unless expressly stated otherwise.

C H A P T E R III

Investigation of the Alleged Monomer-Dimer Equilibrium for Myosin

III.1. Introduction

Myosin is the major contractile protein of muscle and it may be extracted from a skeletal muscle mince by using a 0.68 ionic strength phosphate buffer (Guba and Straub, 1943). The myosin obtained after short extraction periods (about 10min) contains small amounts of actin and is called 'myosin A' so as to distinguish it from the actin-rich myosin obtained after longer extraction periods (myosin B or actomyosin), Szent-Györgyi (1945). When analysed by SDS polyacrylamide gel electrophoresis, myosin A dissociates into a heavy chain component (molecular weight, 200000) and several light chain species. The number of classes of light chains and their molecular weight depends on the muscle from which the myosin was extracted (Lowey and Risby, 1971; Sarkar et al., 1971). In skeletal fast muscle from the rabbit, there are three light chain species which are labelled in order of decreasing molecular weight: LC1 (21000), LC2 (19000) and LC3 (17000), Weeds and Lowey (1971). LC1 and LC3 have been identified as the alkali light chains (alkali-1 and alkali-2, respectively) which can be removed from myosin at alkali pH and result in the loss of ATPase activity (Stracher, 1969; Dreizen and Gershman, 1970). The LC2 species corresponds to the DTNB-light chains, so called because they dissociate from myosin in the presence of DTNB (5,5'-dithiobis-(2-nitro-benzoic acid)) without loss of ATPase activity. For each mole of myosin there are two moles of heavy chains, two moles of DTNB-chains and a variable amount of alkali-1 and alkali-2 (Starr and Offer, 1973). It has been proposed that myosin exists in two isoenzymic forms, one containing two moles of alkali-1 and the other containing two moles of alkali-2. The different amounts of alkali-1 and alkali-2 can therefore be explained by the proportion of these isoenzymic forms within a muscle (Starr and Offer, 1973).

In addition to the heavy chains and light chains seen on SDS gels of

myosin A there are several other components: B-, C- and F-proteins are the major impurities, together with a small amount of actin (Starr and Offer, 1971). The most significant impurity is C-protein which has been extensively characterised by Offer et al.(1973) and confirmed as a distinct and separate protein of the A-filament. Actin and C- and F-proteins may be removed from myosin A by ammonium sulphate fractionation followed by ion-exchange chromotagraphy (Starr and Offer, 1971), the myosin so obtained is called 'column-purified myosin'. From SDS gels, the weight fraction of the component polypeptide chains present in myosin gives a minimum molecular weight of about 467000, assuming that they all show the same staining intensity. However, determinations of the molecular weight of intact myosin by a variety of means have been unreliable with most estimates being greater than 500000.

In 1970, Godfrey and Harrington (1970a,b) reported that a rapidly reversible monomer-dimer equilibrium existed in myosin solutions at high ionic strength. The conclusion was substantiated by evidence from three sources, namely sedimentation equilibrium (Godfrey and Harrington, 1970b), viscosity studies at low concentration (Harrington and Burke, 1972) and laser light scattering (Herbert and Carlson, 1971). It should be pointed out that a distinction between myosin A and column-purified myosin was not always made in these studies, yet results from the work described here indicate that there is indeed a difference between the two preparations. However, the original deduction was made from sedimentation equilibrium experiments performed on column-purified myosin. It was suggested (Godfrey and Harrington, 1970b) that the molecular weight determined at a finite myosin concentration and extrapolated to zero concentration, did not represent the ideal molecular weight of the monomer, but was a weight-average of a mixture of monomer and dimer. Thus, the existence of a

monomer-dimer equilibrium for myosin provided an explanation for the variation of s^{o} and molecular weight reported in the literature, see Table 2 in section III.4. In view of this hypothesis and the importance of knowing the precise molecular weight of myosin to determine the symmetry of the A-filament, it would be worthwhile to confirm or refute the alleged equilibrium for myosin. But a further implication arises for a monomer-dimer equilibrium for myosin: since the dimer was apparently favoured upon decreasing the ionic strength (Godfrey and Harrington, 1970a), it may be that the basic building block in filament formation is the dimer. In section I.1.1 it was explained that there are four possibilities for the structure of the A-filament of vertebrate skeletal muscle: 2, 3 or 4-stranded models with 1 myosin/cross-bridge, or a 2-stranded model with 2 myosins/cross-bridge. If myosin dimers are involved in filament formation, are any of these four possible structures particularly favoured?

III.1.1. The Myosin Dimer and the Symmetry of the A-filament

There are two classes of myosin dimer that may be formed: the antiparallel dimer (tail-to-tail) or the parallel dimer (head-to-tail). The antiparallel dimer may be dismissed from this discussion, for although it is easy to imagine how the central bare-zone may be formed by side-to-side aggregation of these dimers, it is impossible to imagine how the bipolar structure of the A-filament may be created by further polymerization of antiparallel dimers. Parallel dimers, on the other hand, may form the bare-zone by tail-to-tail abutment (possibly mediated by M-line protein) and further filament growth accomplished by head-to-tail addition of more parallel dimers.

Parallel dimers can be divided into two subclasses: those with total overlap and those with partial overlap. Polymerization of total-overlap

dimers can give rise to only one of the four possible A-filament structures, that is 2-stranded with 2 myosins acting as a single functional cross-bridge. The partial-overlap dimers would presumably show an overlap in multiples of 14.3nm to concur with the X-ray diffraction data of relaxed muscle which indicate that the myosin molecules are arranged on a helix with a periodicity of 43.0nm. These parallel dimers may polymerize to produce any of the four possible A-filament structures, although the 2-stranded helical symmetry with 2 myosins per lattice point is the most highly favoured.* To produce a structure with 1 myosin/lattice point by partial-overlap dimers would require a complex polymerization system and the arrangement of myosin molecules in the final structure would not be equivalent or quasi-equivalent. In summary, therefore, if a parallel dimer does exist and is intimately involved in filament formation, the 2-stranded model with 2 myosins/cross-bridge becomes an extremely likely possibility for the structure of the A-filament.

III.1.2. Reinvestigation of the Myosin Monomer-Dimer Equilibrium

Because the existence of a monomer-dimer equilibrium for myosin not only affects the estimated molecular weight of the monomer but also favours the 2-stranded model with 2 myosins/cross-bridge for the A-filament structure, it was decided to reinvestigate the reported equilibrium by sedimentation velocity experiments performed on myosin solutions at high ionic strength. The Gilbert-Jenkins theory for a rapidly reversible monomer-dimer equilibrium predicts that during sedimentation velocity the protein boundary exhibits a single asymmetrical schlieren peak and, as the concentration decreases, the weight-average s value, $\bar{s}$, approaches that of the monomer (Gilbert, 1959). It was suggested that as a result of the magnitude of the equilibrium constant reported ($K = 10^3$ml/g, Godfrey and

*but only where the overlap is not a multiple of 43.0nm.

Harrington, 1970b), the decrease in $\bar{s}$ value towards that of the monomer occurred at a concentration lower than can be detected by conventional optical techniques used with the analytical ultracentrifuge.

Since dark-field optics are now available and can detect very low protein concentrations (about 0.5μg/ml for bovine serum albumin, A. J. Rowe, unpublished observations), it was decided to test this prediction by obtaining an s *versus* concentration plot down to low protein concentrations. A decrease in $\bar{s}$ value at low concentrations would be indicative of a monomer-dimer equilibrium. During this study, the relationship between k_s (the concentration dependence of the sedimentation coefficient) and f/f_o, the frictional ratio, was elucidated by Rowe (1977). The importance of this relationship is that it enables the calculation of the ideal molecular weight (M^o) from a knowledge of s^o, k_s and $\bar{v}$ (provided that the usual conditions for 2-component sedimentation are attained, i.e. absence of charge effects and no self-interaction, see Appendix I). There is a further advantage in being able to relate k_s and f/f_o: where molecular weight, $\bar{v}$ and s^o of the monomer are known, k_s for the monomer is automatically fixed. Thus divergence of the experimentally determined $\bar{s}$ values from the theoretical dependence of s with concentration is indicative of self-association. It is also possible to compute the s *versus* concentration curves, for the simple case of a monomer-dimer equilibrium, for a range of equilibrium constants and, by comparing these with the experimental s values, obtain an estimate of the equilibrium constant.

Thus sedimentation velocity studies on myosin solutions at high ionic strength can confirm or refute the hypothesis of a monomer-dimer equilibrium. Initial sedimentation velocity runs were performed on column-purified myosin solutions so as to directly compare these results with those from sedimentation equilibrium experiments (Godfrey and Harrington, 1970b).

But because of the presence of irreversible aggregates, column-purified myosin was later abandoned in favour of myosin A. However, a variation in f/f_o was found in myosin A solutions which had been stored for long periods in 50% glycerol ('glycerolated myosin A') and thus most of the experiments described here have been performed on fresh myosin A solutions. It might be argued that small amounts of actin present in myosin A solutions could affect the s value or concentration dependence of myosin, so attempts were made to obtain actin-free myosin by extracting whole muscle with 0.266M-K_2HPO_4 (Mihalyi and Rowe, 1966).

Additional information on the hydrodynamic properties of myosin has been gained by combining sedimentation velocity and viscosity studies. This Chapter describes these investigations and the following conclusions have been drawn:-

(i) sedimentation velocity runs on myosin A solutions show a linear concentration dependence of the sedimentation coefficient over the entire concentration range studied, suggesting that no appreciable monomer-dimer equilibrium exists.

(ii) the molecular weight of myosin has been successfully obtained from s^o and k_s alone (i.e. without independent measurement of the diffusion coefficient) and is 470000.

(iii) a variation in f/f_o for myosin was found and it is proposed that this variation in frictional ratio can be explained in terms of a variable separation of the myosin heads. This hypothesis will be discussed with reference to the predicted f/f_o of myosin computed from the Kirkwood-Bloomfield theory (Bloomfield et al., 1967).

(iv) combination of sedimentation and viscosity experiments has provided an estimate of $V_s/\bar{v}$ (the swelling) of the myosin molecule in aqueous solution. This value of $V_s/\bar{v}$ will be used in a new procedure which is able

to quantitatively test the 'goodness of fit' of hydrodynamic models.

III.2. Methods

III.2.1. Extraction and Purification of Myosin A

New Zealand White rabbits were killed by severing the jugular vein and the back muscles were removed immediately. Myosin A was extracted from the muscle by the procedure of Szent-Györgyi (1945) as modified by Johnson and Rowe (1960); the scheme is summarised in Figure 4. All manipulations were carried out in a cold room (4°C) and centrifugations were performed in pre-cooled rotors. Twice glass-distilled water was used during the extraction and to make up the solutions. The solutions used were: 'Guba-Straub' (0.3M-KCl, 0.15M-potassium phosphate buffer, pH 6.5 at 4°C) and 'stock buffer' (0.55M-KCl, 0.02M-KH_2PO_4, 0.01M-$Na_2HPO_4.12H_2O$, the pH was adjusted to 6.7 at 4°C with 10M-NaOH). After one or two reprecipitations at ionic strength 0.28, the myosin A was dialysed against stock buffer overnight. No lipid material was present in any of these preparations and they were clear of any 'threads' of denatured protein. Myosin A to be used for ultracentrifugation studies was centrifuged at 50000rev./min (157000g) for 2h at 5°C in an MSE 65 Centrifuge.

III.2.2. Glycerolated Myosin A

Solutions of myosin A were stored for long periods in 50%(v/v) glycerol at -15°C; glycerolated myosin A was prepared from these solutions by dilution to I 0.05 followed by centrifugation at 2500rev./min (1470g) for 40min. The supernatant was discarded and the precipitate was redissolved in stock buffer, precipitated once more and finally dialysed against stock buffer overnight.

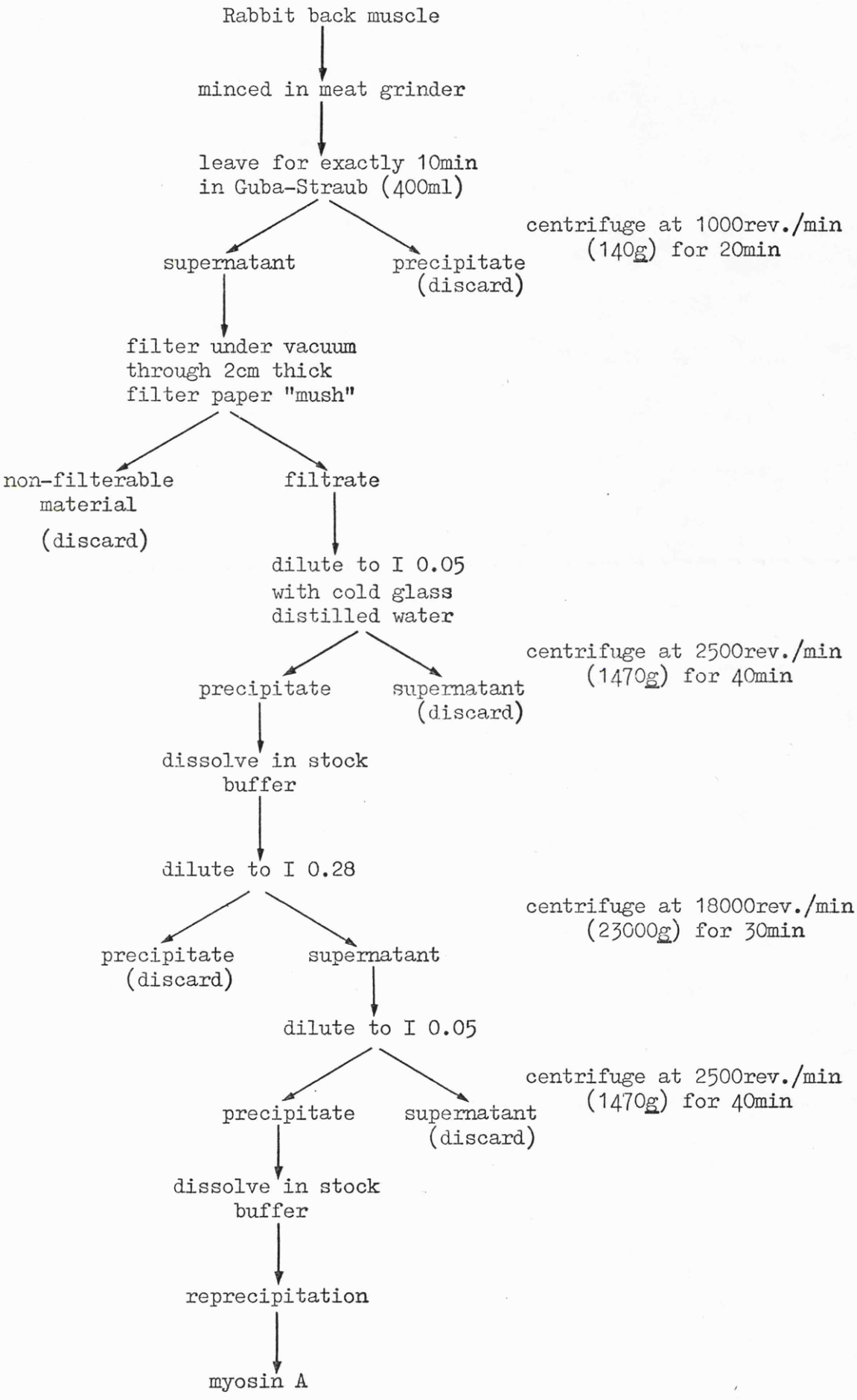

Figure 4 Extraction of myosin A from rabbit muscle

III.2.3. Preparation of Column-Purified Myosin

The procedure of column purification of myosin A using DEAE-Sephadex A-50 was that used by Godfrey and Harrington (1970b).

(a) Ammonium Sulphate Precipitation

To a sample of myosin A solution, stirred slowly on ice, was added solid ground ammonium sulphate. The first fraction, 0 - 35%(w/v) saturation, was removed by centrifugation at 8000rev./min (10000g) for 15min. The second fraction, 35 - 40%(w/v)saturation, contains myosin; the supernatant, containing F-protein, was discarded. The myosin fraction, dissolved in stock buffer, was dialysed against 0.15M-potassium phosphate, 10mM-EDTA, pH 7.5 at 4°C and then chromatographed as described below.

(b) DEAE-Sephadex A-50 Chromatography

A column of DEAE-Sephadex A-50, 25 - 35cm long and 6.6cm^2 in cross-section, was equilibrated with 0.15M-potassium phosphate, 10mM-EDTA, pH 7.5. Myosin A, prepared as above and at a concentration of less than 14mg/ml, was applied to the top of the column. After the C-protein was eluted in the void volume, a linear KCl gradient was applied using 0.15M-potassium phosphate, 10mM-EDTA and 0.5M-KCl, 0.15M-potassium phosphate, 10mM-EDTA, both at pH 7.5. Absorbance at 280nm was measured for each 10ml fraction collected. Myosin appeared in fractions corresponding to a volume of 450 - 600ml of eluent. Pooled myosin fractions were dialysed against 0.04M-KCl (in the absence of phosphate as this tends to inhibit precipitation at low ionic strength) with several changes. The column-purified myosin precipitate was collected by centrifugation at 4000rev./min (1600g) for 20min in the cold, and the sediment redissolved in the minimum volume of stock buffer.

III.2.4. Secondary Phosphate Extracted Myosin

Since 0.266M-K_2HPO_4 solution specifically solubilises myosin and stabilises the Z-disk and I-filament structure (Mihalyi and Rowe, 1966) it can be used as the basis of a simple method to obtain actin-free myosin from muscle. In order to minimise breakage and solubilisation of I-filaments, myosin was extracted by soaking the whole muscle in 0.266M-K_2HPO_4. Psoas muscle from the rabbit was dissected out, teased into strips and the ends tied with cotton. The muscle strips were immersed in about 75ml of 0.266M-K_2HPO_4 so that the ends of the muscle remained above the solution. After 2h the muscle was removed; the solution was stirred and adjusted to pH 6.7 and then dialysed against 6mM-potassium phosphate buffer, pH 6.7, with several changes. The myosin was collected by centrifugation on a bench centrifuge at 4000rev./min (1600g) for 20min at 4°C. The supernatant was discarded and the precipitate dissolved in stock buffer.

III.2.5. SDS gel electrophoresis

Samples of all four types of myosin used (fresh myosin A, glycerolated myosin A, column-purified myosin and K_2HPO_4-extracted myosin) were analysed by SDS gel electrophoresis as described in II.2.1 and II.2.2.

III.2.6. Ultracentrifugation of Myosin

Runs were carried out in the MSE Analytical Ultracentrifuge within the temperature range 5 - 7°C (with an average fluctuation of $\pm$0.05°C) and at a speed between 50000 - 60000rev./min. Absorption optics (wavelength, 280nm) and 10mm double sector cells were used for concentrations of myosin down to 0.5mg/ml. Below this concentration, 20mm double sector cells or synthetic boundary cells were used in conjunction with dark-field optics (wavelength, 500nm) to increase sensitivity. Both temperature and speed

were monitored frequently throughout the run and scans were taken every 5min. For reasons of accuracy and expediency, 3 - 5 samples were 'multiplexed' in a single run. From measurements of the radial position of the myosin boundary, r, accurate sedimentation coefficients were calculated using an ALGOL program written by the author, see II.2.5.

III.2.7. Computer-Simulated Graphs

The computer-simulated graphs for the s versus concentration dependence of a monomer-dimer equilibrium were drawn with the aid of a 9125A Graph Plotter attached to a Hewlett-Packard Calculator, There are two problems involved in computing a theoretical s against concentration profile for a monomer-dimer equilibrium for myosin:

(i) the precise value of s^o_m and s^o_d (the s^o values of monomer and dimer, respectively) are unknown

(ii) the concentration dependence of monomer and dimer ($k_{s,m}$ and $k_{s,d}$) are not known.

The first problem was overcome by using a range of s^o_m and s^o_d in which the true values are likely to lie (s^o_m = 5.0 - 6.0S; s^o_d = 7.0 - 9.0S). On the second point, the published curves for a monomer-dimer equilibrium are based upon the assumption that $k_{s,m} = k_{s,d}$ = 7.1ml/g (Gilbert and Gilbert, 1973). The value 7.1ml/g is an estimate of k_s for spherical globular proteins (a poor assumption for myosin which is far from spherical and has a k_s of about 94ml/g). However, there is now a procedure available to calculate k_s of a particle from its molecular weight, s^o and $\bar{v}$ (see Appendix I). The k_s of monomer and dimer for myosin have been calculated over a range of the feasible values of s^o_m and s^o_d by the following method. For a given s^o_m, the frictional ratio may be calculated from the relationship $f/f_o = s^o_{sp}/s^o_m$, where s^o_{sp} is the extrapolated s value of an equivalent

sphere of the same mass. The value of s^o_{sp} is obtained via equation 16 in Appendix I, with $f/f_o = 1$ and assuming a molecular weight of 460000. As f/f_o is related to k_s by $k_s = 2\bar{v}(V_s/\bar{v} + (f/f_o)^3)$, the k_s of the monomer can be found using only s^o_m, molecular weight of the monomer and $\bar{v}$; $V_s/\bar{v}$ was assumed to be 1.0. The k_s of dimer is calculated in the same way but using twice the molecular weight.

The weight-average sedimentation coefficient, $\bar{s}$, for a monomer-dimer mixture was calculated by substituting $k_{s,m}$ and $k_{s,d}$ into the Gilbert equations (Gilbert and Gilbert, 1973):

$$\bar{s} = \left(\frac{1 - k_{s,m}\, c}{c}\right) c_m s^o_m + \left(\frac{1 - k_{s,d}\, c}{c}\right) c_d s^o_d \qquad (2)$$

$$c_m = \frac{-1+\sqrt{1 + 4Kc}}{2K} \qquad (3)$$

$$c_d = K c_m^2 \qquad (4)$$

K is the equilibrium constant, c is the total protein concentration, c_m and c_d are the equilibrium concentrations of monomer and dimer, respectively. The $\bar{s}$ values are calculated over a total protein concentration of 0 - 4mg/ml. The plotter program automatically increments K from 10 to 10^4ml/g in logarithmic steps (by a factor of $10^{0.2}$ so that K = 1.000, 1.5849, 2.519, 3.9811, 6.3096, 10.000, 15.849ml/g etc.).

III.2.8. Predicted Frictional Ratio of Myosin

The Kirkwood-Bloomfield theory predicts that the frictional coefficient of a particle can be estimated by assuming that the hydrodynamic properties of a particle can be represented by a surface shell

consisting of a large number of small spheres (Bloomfield et al., 1967). A somewhat simpler version of the Kirkwood-Bloomfield theory has been used to calculate the frictional coefficient of myosin by assuming that the myosin rod and each head (HMM S-1) may be represented by a string of spheres of diameter 2.0nm (Bloomfield et al., 1967). The frictional coefficient is then calculated by summing the hydrodynamic interaction of each sphere with every other one and a FORTRAN program, written by the author, was used for this purpose. The equation used was

$$f = \frac{n\, 6\pi\eta\, r}{1 + \frac{r}{n}\sum_{i=1}^{n}\sum_{j=1}^{n}\left(R_{i,j}^{-1}\right)} \qquad (5)$$

η is the viscosity (taken as the viscosity of water at 20°C, η = 1.005cp); r is the radius of the spherical subunits (1.0nm) ; n is the number of subunits and $\Sigma\Sigma(R_{ij}^{-1})$ is the double sum of the inverse of the distance between the i^{th} and j^{th} subunits, assuming that the structure is rigid. The dimensions of the myosin molecule were taken as 148nm for the total length (Slayter and Lowey, 1967; Lowey et al.,1969) with the two heads dividing at a point 24nm distant from the head end. A diameter of 2.0nm was used for the tail (Huxley, 1963; Slayter and Lowey, 1967) but no account was taken for the larger diameter of the S-1 portions. Two conformational states of myosin were assumed: one with the heads together and the other with the heads apart and at an angle of 45° to the longitudinal axis of the rod, Figure 13. The frictional coefficient so obtained was substituted into the Svedberg equation: $fs^{o} = M(1 - \bar{v}\rho)/N_A$, to calculate s^{o} assuming M = 460000. The frictional ratio was computed from $f/f_o = s^{o}_{sp}/s^{o}$, where s^{o}_{sp} was determined from M and $\bar{v}$ assuming $f/f_o = 1$ (see III.2.7 and Appendix I).

III.2.9. Viscosity Determinations

Myosin A, prepared as in III.2.1, was diluted with stock buffer and centrifuged at 25000rev./min (39000g) for 1h to remove any surface-denatured protein formed in the diluting and mixing. A Cannon-Fenske viscometer (BS. IP. CF. 71/62) was used and after each viscosity measurement was washed with concentrated nitric acid, millipore-filtered water and acetone and then dried in air. A Townsen and Mercer bridge-controlled water bath set at 5°C maintained the temperature to within ±0.05°C. Into the viscometer was carefully pipetted 6ml of solution and flow times measured with a National Physical Laboratory stop watch with 0.05s divisions until consecutive readings agreed to within 0.1s. Flow-times were adjusted for the kinetic energy correction, then Tanfords correction was used to convert solvent density to solution density (Yang, 1961), using $\bar{v}$ = 0.720ml/g at 5°C (Kay, 1960). Concentration was estimated after the viscosity measurement on duplicate samples using a modified Biuret method (II.2.7). This precaution was included to prevent over-estimation of the protein concentration involved in the viscosity measurement due to adsorption of protein to the glass walls of the viscometer (III.4).

III.3. Results

III.3.1. Purification of Myosin A

SDS gel electrophoresis of myosin A samples used in ultracentrifugation studies showed no anomalous features, Plate 2. The C- and F-protein bands and the myosin light chains were identified by coelectrophoresis with the purified proteins. The remaining bands were identified by their molecular weight and by comparison with published gel patterns (Starr and Offer, 1971). All the myosin A samples showed only small amounts of actin

Plate 2. SDS gels of myosin A and column-purified myosin

The electrophoresis procedure is given in section II.2.2. The major bands were identified as (from the top): heavy chain (HC), C-protein (C), F-protein (F) and light chains (LC1, LC2, LC3).

(a) 100μg myosin A applied

(b) 60μg myosin A + 20μg light chain marker

(c) 75μg column-purified myosin (LC3 can be seen in the original gel).

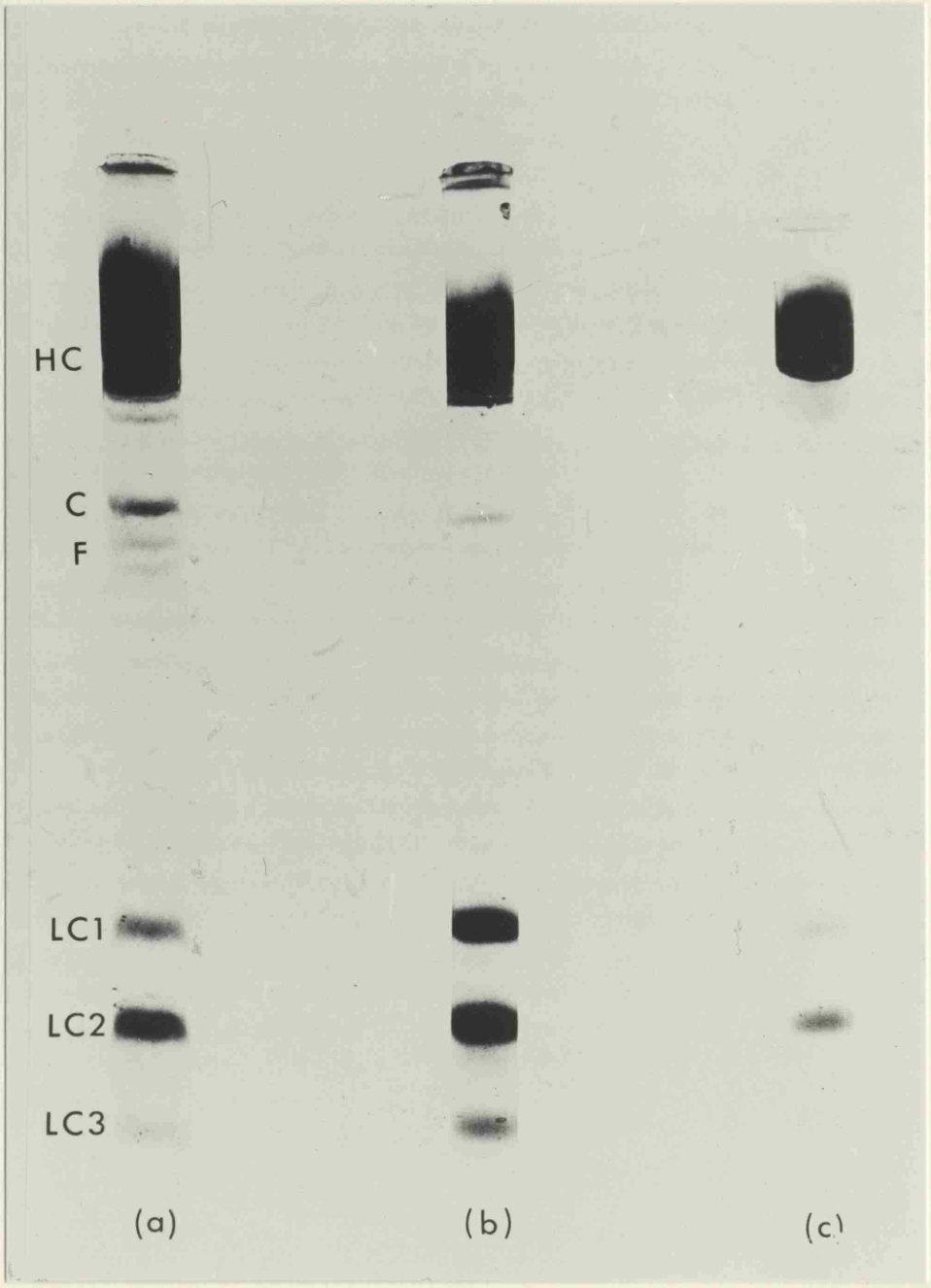
HC
C
F
LC1
LC2
LC3
(a)
(b)
(c)

(less than 0.5% by weight); most of the actin was removed after just one reprecipitation of myosin A at ionic strength 0.28.

III.3.2. Column-Purified Myosin

A typical elution profile from a DEAE-Sephadex A-50 column is shown in Figure 5. The SDS gel pattern of column-purified myosin is shown in Plate 2. Note that C- and F-proteins have been removed and that there is no actin band.

Sedimentation velocity of column-purified myosin revealed the presence of irreversible aggregates sedimenting ahead of the main myosin boundary. Several approaches were tried in an attempt to remove these aggregates. (i) Column-purified myosin was centrifuged at 50000rev./min (157000g) for 2h at 5°C in an effort to selectively precipitate these aggregates, but the supernatant, when analysed in the ultracentrifuge, still showed the presence of n-mers. (ii) Dreizen et al. (1967) reported that ammonium sulphate precipitation caused aggregation of myosin. However, omission of the ammonium sulphate fractionation stage failed to prevent formation of aggregates. (iii) The concentration of column-purified myosin involves dialysis at low ionic strength and it is well known that myosin tends to aggregate under these conditions, so this stage of the purification was excluded. In spite of this precaution, column-purified myosin collected from the DEAE-Sephadex column and centrifuged immediately in the analytical ultracentrifuge showed an aggregate peak, whereas the untreated myosin A showed none. It was decided therefore, in the absence of any suitable procedure to remove these aggregates, that further attempts to determine s values on column-purified myosin would be abandoned.

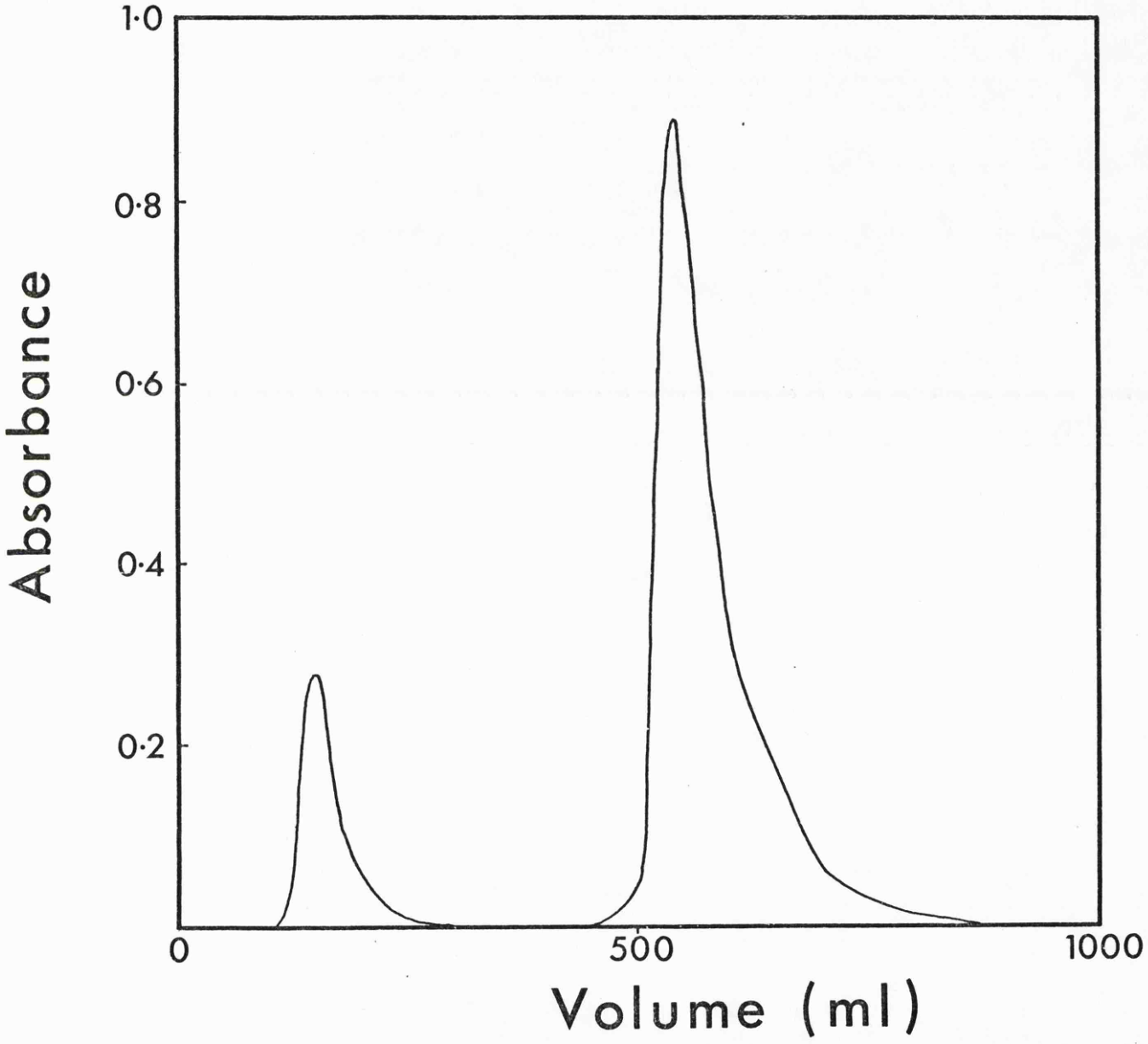

Figure 5 Elution profile of DEAE-Sephadex A-50 column loaded with myosin A

C-protein is eluted in the void volume. Myosin is eluted when a linear KCl gradient is applied. Sample: 2.52g of myosin A; buffer: 0.15M-potassium phosphate, 10mM-EDTA, pH7.5.

III.3.3. Secondary Phosphate Extracted Myosin

The SDS gels of myosin extracted with 0.266M-K_2HPO_4 are shown in Plate 3. A faint band, identified from its molecular weight as actin, can be seen and is about 0.2% by weight of the total protein. In spite of the precautions taken, this contaminant may be due to the breakage of myofibrils and the subsequent release of F-actin. But whatever the cause may be, it is clear that myosin cannot be extracted from muscle without some trace of actin accompanying it.

Sedimentation of K_2HPO_4-extracted myosin in the ultracentrifuge gave single schlieren peaks. The $s_{20,w}$ values determined at several different concentrations showed exactly the same concentration dependence as that for fresh myosin A solutions. A full s *versus* concentration plot was not obtained because of the low yield of myosin from this extraction procedure, but it is apparent that the trace of actin in these myosin solutions does not affect the sedimentation of the myosin.

III.3.4. Ultracentrifugation Studies on Myosin

Sedimentation coefficients for myosin A solutions at very low protein concentration (below 50μg/ml) could not be obtained because the protein boundaries formed during centrifugation were unstable. This instability of the protein boundary was not due to convective disturbances within the ultracentrifuge cell as identical experiments with bovine serum albumin have been consistently successful. Rather, this phenomenon may be due to adsorption of myosin to the windows of the ultracentrifuge cell: prior treatment of the windows with a mixture of nitric acid and ethanol or with a hydrophobic coating (fluorocarbon spray) failed to reduce this instability. Alternatively, the unstable boundary may be caused by dissociation of myosin, below 50μg/ml, into its component polypeptide

Plate 3. SDS gels of secondary phosphate extracted myosin

120μg of K_2HPO_4-extracted myosin were applied. The actin band is signified by A, the other bands are labelled as in Plate 2.

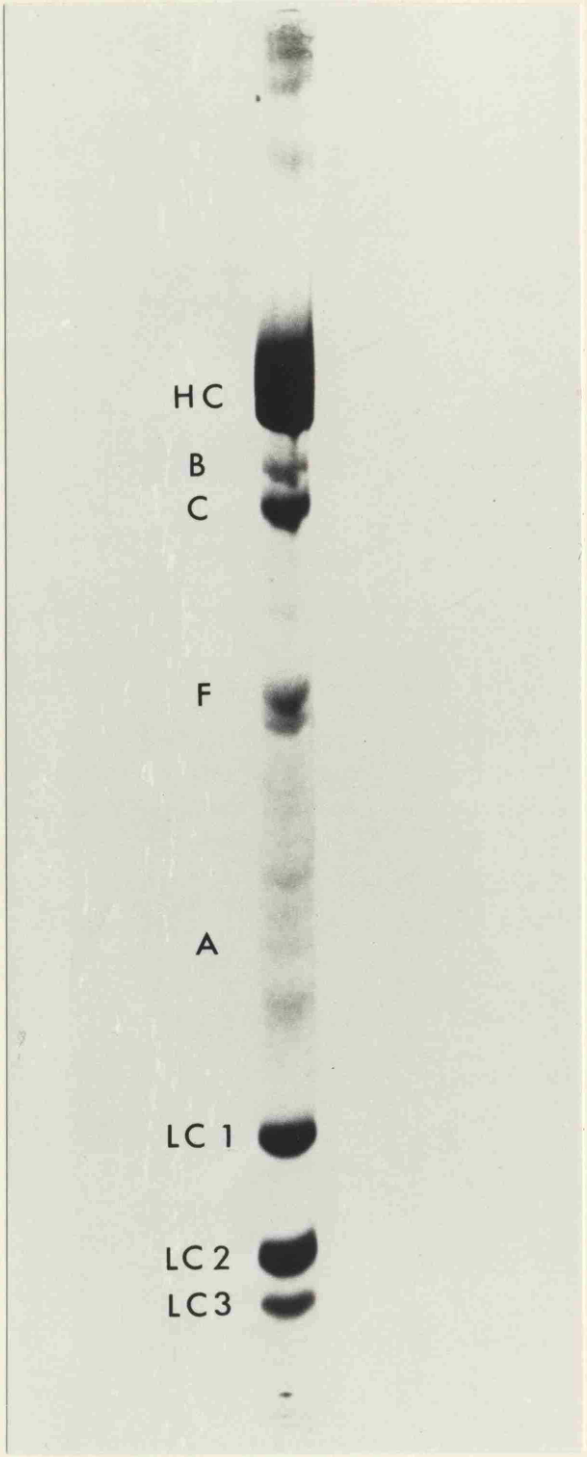
HC
B
C
F
A
LC 1
LC 2
LC 3

chains, as reported by Siemankowski and Dreizen (1975).

However, s values for protein concentrations down to 100μg/ml have been determined for myosin A solutions by using dark-field optics (at a wavelength of 500nm). The protein boundary appears as a bright band against a dark background and may be recorded photographically, Plate 4, or, more usually, by scanning with a photomultiplier. A typical scan together with its differential trace is illustrated in Plate 5. The MSE Centriscan 75 has also been used to measure s values of myosin solutions. With this instrument the protein boundary may be detected by bright-field scanning optics and the scans can be superimposed to provide an easily measurable trace, Plate 6. Results from sedimentation velocity experiments on three myosin A preparations are shown in the graph of $s_{20,w}$ *versus* concentration, Figure 6. The correlation coefficient for all the points is 0.95. The equation $1/s = (1 + k_s c)/s^o$ was used to determine the best straight line through all the points shown, as it describes a better linear relationship upto higher concentrations than the equation $s = s^o(1 - k_s c)$. The solution is $s^o_{20,w} = 5.52 \pm 0.05S$ and $k_s = 94.1 \pm 8.2ml/g$.

III.3.5. *Myosin Dimer – Fact or Fiction?*

Although the s *versus* concentration profile for fresh myosin A solutions appears linear, is it possible that the predicted s *versus* concentration dependence for a monomer-dimer equilibrium could still fit the experimental results? In other words, since s^o_m and s^o_d are not precisely known for myosin, is there any combination of these parameters that can be chosen such that the s against concentration profile for a monomer-dimer equilibrium is indistinguishable from a straight line, within experimental error? To answer this question, exhaustive curve fitting has been applied over a wide range of s^o_m and s^o_d and equilibium constants (K).

Plate 4. The appearance of a protein boundary as seen through the eyepiece of the ultracentrifuge.

The protein boundary appears as a bright line against a dark background. The sample was myosin A at 1.34mg/ml. Speed: 60000rev./min; temperature: 5°C. Direction of sedimentation is from bottom to top.

Plate 5. A trace recorded by the u-v scanner of a protein boundary detected by dark-field optics.

The lower trace records dc/dr (vertical direction) as a function of r (horizontal direction). The direction of sedimentation is from right to left. The upper trace is the differential of the lower one. The sample was myosin A at 0.5mg/ml. Speed: 59700rev./min; temperature: 6.0°C.

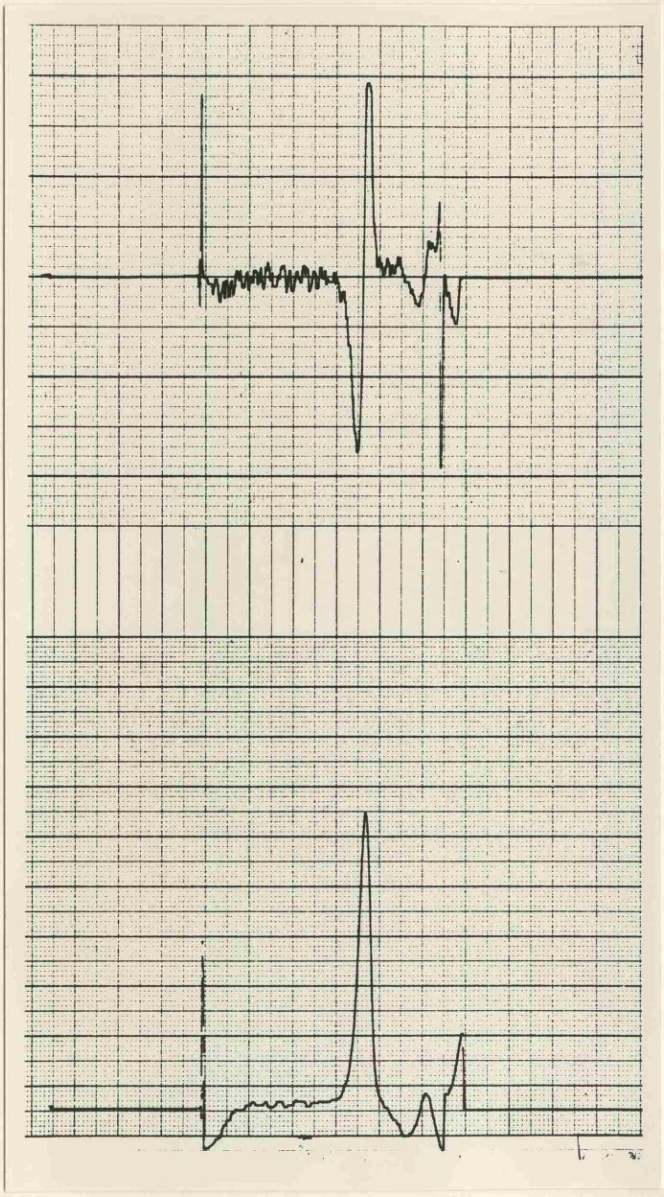

Plate 6. Movement of a protein boundary as recorded by the Centriscan 75 using bright-field scanning optics.

The trace records the concentration gradient, dc/dr, (vertical direction) as a function of radial position, r, (horizontal direction). The sample was myosin A at 1.34mg/ml. Speed: 59000rev./min; temperature: 6.0°C. The direction of sedimentation is from left to right.

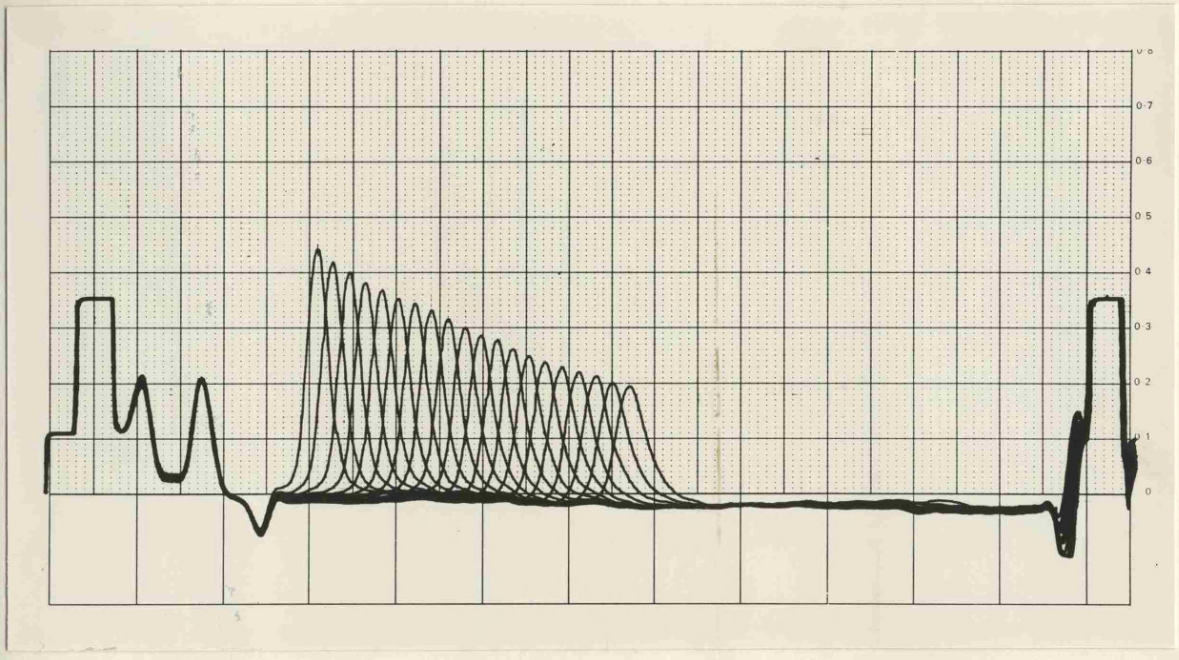
0·7
0·6
0·5
0·4
0·3
0·2
0·1
0

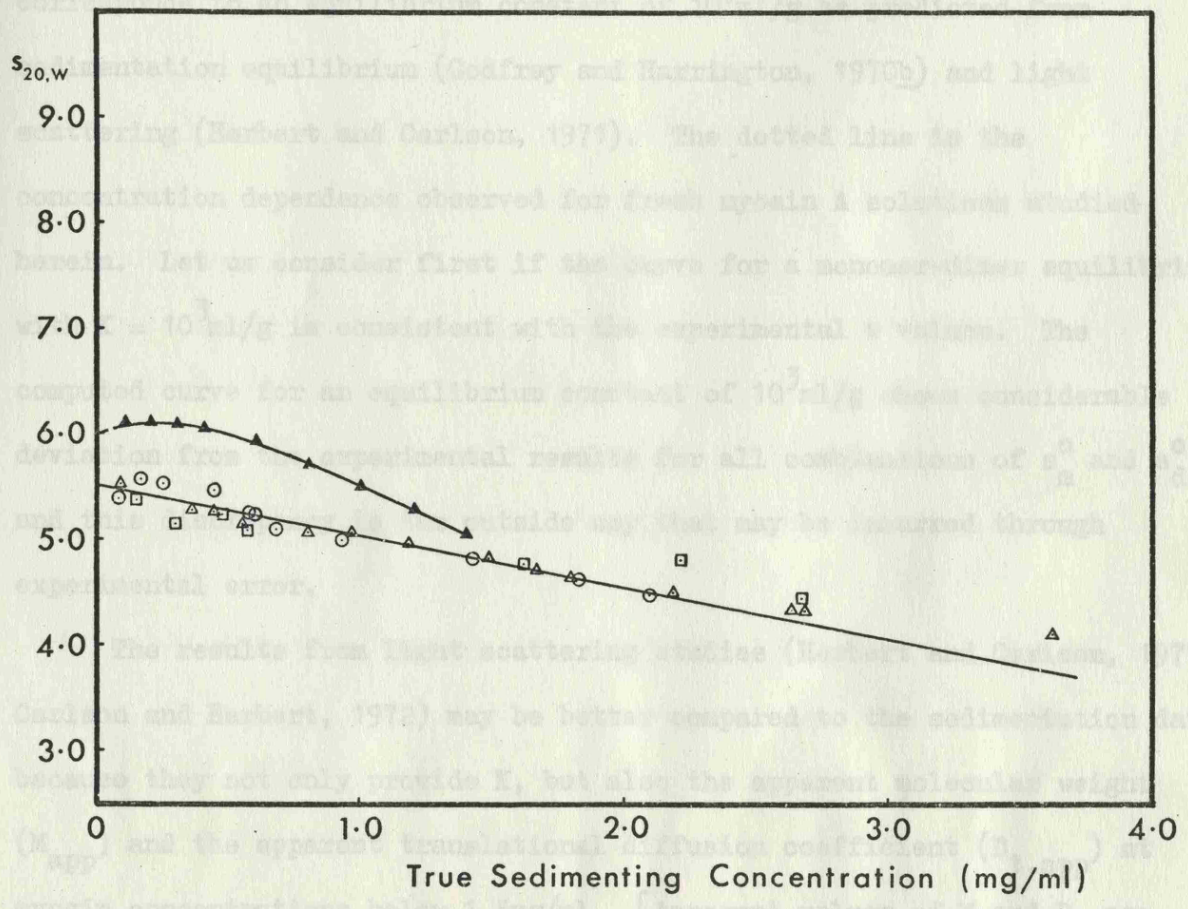

Figure 6 s versus concentration plot for myosin A

The line shown was computed form the 1/s versus concentration dependence. The open symbols represent different myosin A preparations; the dependence predicted for the alleged monomer-dimer equilibrium from Herbert and Carlson's (1971) light scattering data is also shown, (▲).

The s versus concentration curves were computed over the concentration range 0 to 4mg/ml as described in section III.2.7. Figures 7 to 11 show the curves so obtained for five values of s^o_m. A list of the parameters used to construct the curves is given in Table 1. The equilibrium constant, K, was, in most cases, incremented from 10 to 10^4ml/g in logarithmic steps; the limiting lines are for pure monomer and pure dimer. The dashed line corresponds to an equilibrium constant of 10^3ml/g as predicted from sedimentation equilibrium (Godfrey and Harrington, 1970b) and light scattering (Herbert and Carlson, 1971). The dotted line is the concentration dependence observed for fresh myosin A solutions studied herein. Let us consider first if the curve for a monomer-dimer equilibrium with K = 10^3ml/g is consistent with the experimental s values. The computed curve for an equilibrium constant of 10^3ml/g shows considerable deviation from the experimental results for all combinations of s^o_m and s^o_d and this discrepancy is far outside any that may be incurred through experimental error.

The results from light scattering studies (Herbert and Carlson, 1971; Carlson and Herbert, 1972) may be better compared to the sedimentation data because they not only provide K, but also the apparent molecular weight (M_{app}) and the apparent translational diffusion coefficient ($D_{t,app}$) at myosin concentrations below 1.5mg/ml. [Apparent values of M and D_t are obtained because they are measured at a finite myosin concentration.]. By substituting M_{app} and $D_{t,app}$ into the equation: $M_{app} = RT\bar{s}/(1 - \bar{v}\rho)D_{t,app}$, where $\bar{v}$ is the partial specific volume and ρ is the solvent density, then $\bar{s}$, the weight-average sedimentation coefficient, can be estimated. The $\bar{s}$ versus concentration dependence predicted from Herbert and Carlson's (1971) results bear no resemblance to the experimental dependence determined herein (Figure 6) and, paradoxically, to none of the theoretical curves for

Figure 7. Computer-simulated s versus concentration plot for a myosin monomer-dimer equilibrium with $s^{o}_{m} = 5.0S$.

The dotted line is the concentration dependence observed in this study. The limiting lines are the dependence for pure monomer and pure dimer; the dashed line represents the equilibrium constant predicted by Godfrey and Harrington (1970b), 10^{3}ml/g. Equilibrium constants are (from monomer to dimer): (a) 10, 10^{2}, then incremented by $10^{0.2}$ to 10^{4}, 10^{5}ml/g; (b), (c), (d) and (e) 10, then incremented by $10^{0.2}$ to 10^{4}, 10^{5}ml/g.

Graphs (a) to (e) represent different values of s^{o}_{d} as assigned in Table 1 (b).

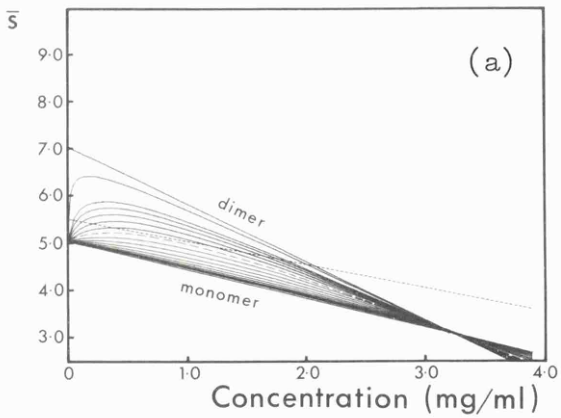
$\bar{s}$
9·0
8·0
7·0
6·0
5·0
4·0
3·0
(a)
dimer
monomer
0
1·0
2·0
3·0
4·0
Concentration (mg/ml)

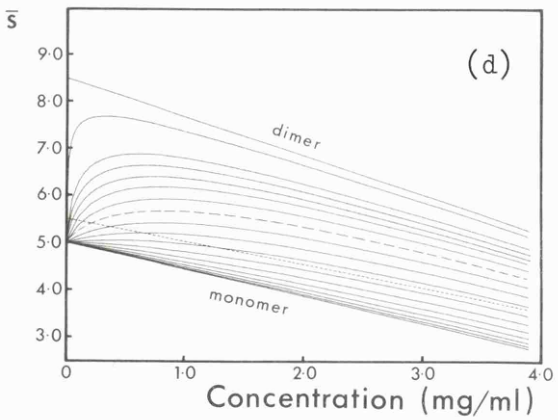
$\bar{s}$
9·0
8·0
7·0
6·0
5·0
4·0
3·0
(d)
dimer
monomer
0
1·0
2·0
3·0
4·0
Concentration (mg/ml)

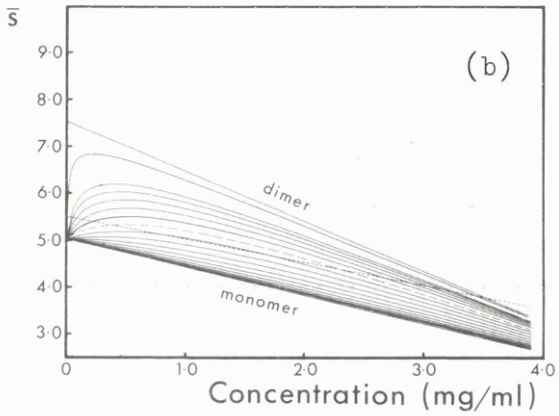
$\bar{s}$
9·0
8·0
7·0
6·0
5·0
4·0
3·0
(b)
dimer
monomer
0
1·0
2·0
3·0
4·0
Concentration (mg/ml)

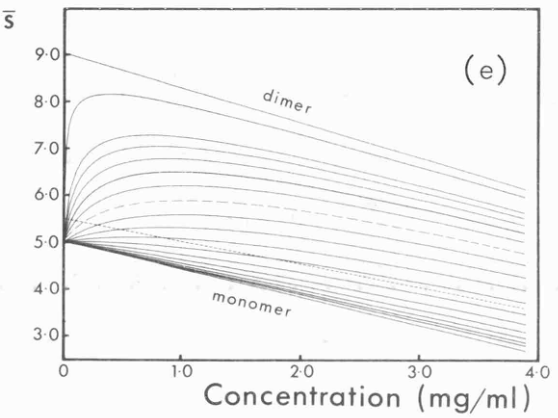
$\bar{s}$
9·0
8·0
7·0
6·0
5·0
4·0
3·0
(e)
dimer
monomer
0
1·0
2·0
3·0
4·0
Concentration (mg/ml)

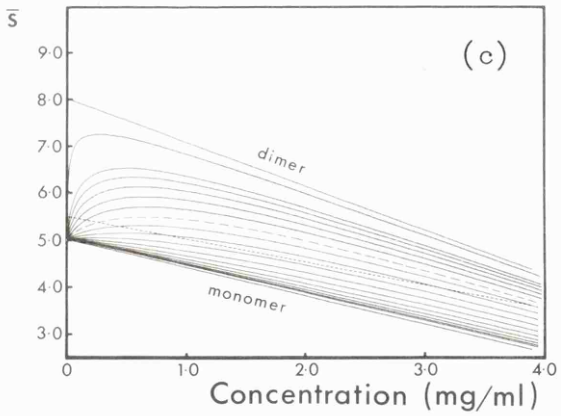
$\bar{s}$
9·0
8·0
7·0
6·0
5·0
4·0
3·0
(c)
dimer
monomer
0
1·0
2·0
3·0
4·0
Concentration (mg/ml)

Figure 8. Computer-simulated s versus concentration plot for a myosin monomer-dimer equilibrium with $s^{o}_{m} = 5.25S$

The dotted line is the concentration dependence observed in this study. The limiting lines are the dependence for pure monomer and pure dimer; the dashed line represents the equilibrium constant predicted by Godfrey and Harrington (1970b), 10^{3}ml/g. Equilibrium constants are (from monomer to dimer): (a) 10, 10^{2}, then incremented by $10^{0.2}$ to 10^{4}, 10^{5}ml/g; (b), (c), (d), and (e) 10, then incremented by $10^{0.2}$ to 10^{4}, 10^{5}ml/g.

Graphs (a) to (e) represent different values of s^{o}_{d} as assigned in Table 1 (b).

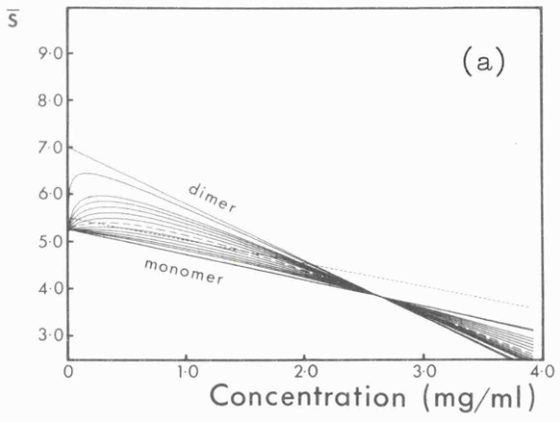
$\bar{s}$
9·0
8·0
7·0
6·0
5·0
4·0
3·0
(a)
dimer
monomer
0
1·0
2·0
3·0
4·0
Concentration (mg/ml)

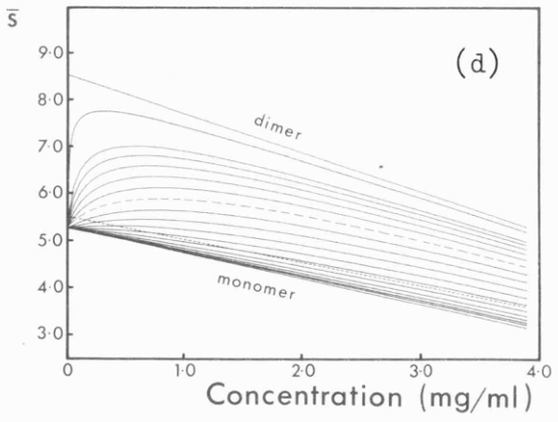
$\bar{s}$
9·0
8·0
7·0
6·0
5·0
4·0
3·0
(d)
dimer
monomer
0
1·0
2·0
3·0
4·0
Concentration (mg/ml)

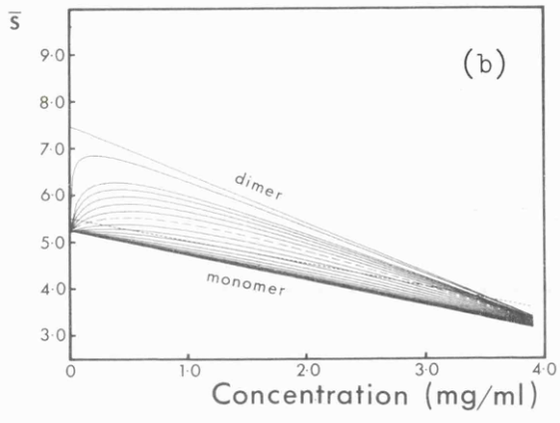
$\bar{s}$
9·0
8·0
7·0
6·0
5·0
4·0
3·0
(b)
dimer
monomer
0
1·0
2·0
3·0
4·0
Concentration (mg/ml)

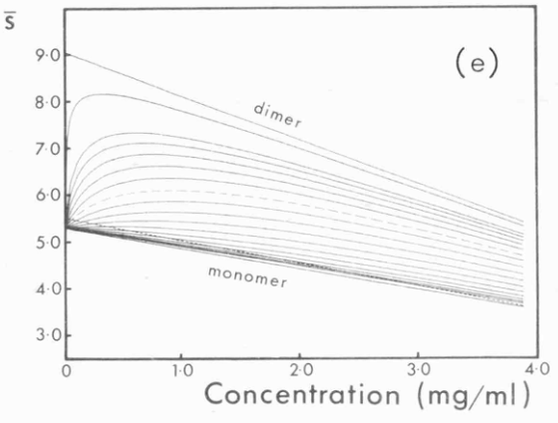
$\bar{s}$
9·0
8·0
7·0
6·0
5·0
4·0
3·0
(e)
dimer
monomer
0
1·0
2·0
3·0
4·0
Concentration (mg/ml)

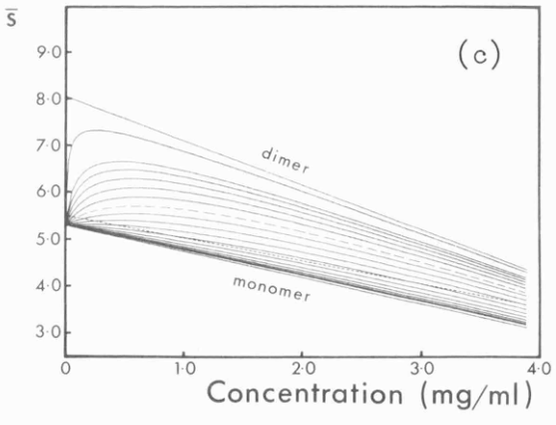
$\bar{s}$
9·0
8·0
7·0
6·0
5·0
4·0
3·0
(c)
dimer
monomer
0
1·0
2·0
3·0
4·0
Concentration (mg/ml)

Figure 9. Computer-simulated s versus concentration plot for a myosin monomer-dimer equilibrium with $s^{o}_{m} = 5.5S$

The dotted line is the concentration dependence observed in this study. The limiting lines are the dependence for pure monomer and pure dimer; the dashed line represents the equilibrium constant predicted by Godfrey and Harrington (1970b), 10^{3}ml/g. Equilibrium constants are (from monomer to dimer): (a) 10, 10^{2}, then incremented by $10^{0.2}$ to 10^{4}, 10^{5}ml/g; (b), (c), (d) and (e) 10, then incremented by $10^{0.2}$ to 10^{4}, 10^{5}ml/g.

Graphs (a) to (e) represent different values of s^{o}_{d} as assigned in Table 1 (b).

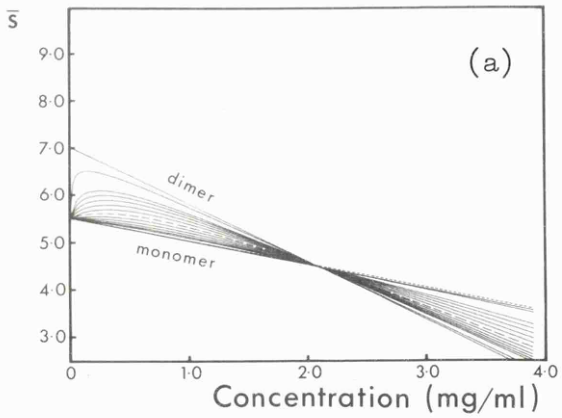
$\bar{s}$
9·0
8·0
7·0
6·0
5·0
4·0
3·0
(a)
dimer
monomer
0
1·0
2·0
3·0
4·0
Concentration (mg/ml)

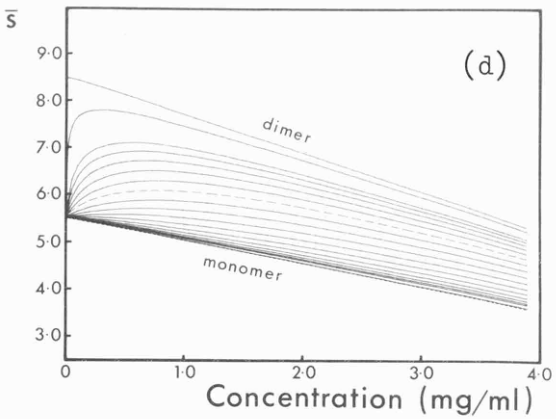
$\bar{s}$
9·0
8·0
7·0
6·0
5·0
4·0
3·0
(d)
dimer
monomer
0
1·0
2·0
3·0
4·0
Concentration (mg/ml)

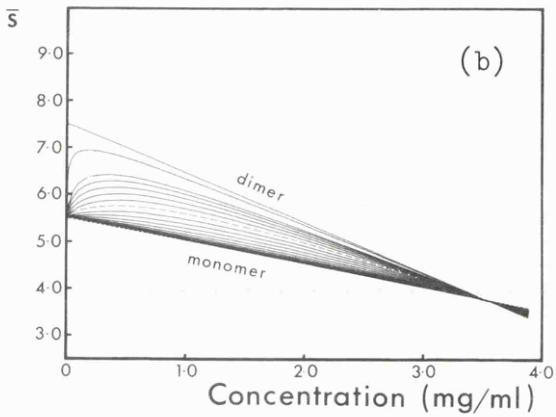
$\bar{s}$
9·0
8·0
7·0
6·0
5·0
4·0
3·0
(b)
dimer
monomer
0
1·0
2·0
3·0
4·0
Concentration (mg/ml)

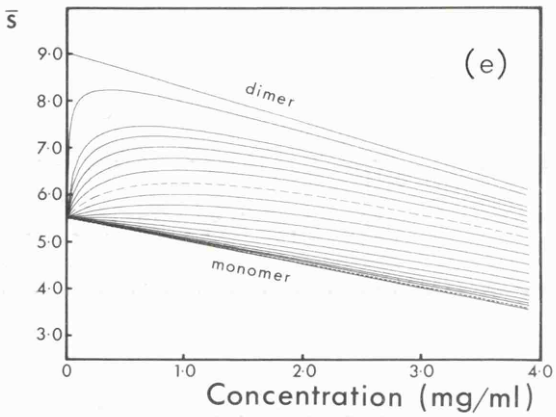
$\bar{s}$
9·0
8·0
7·0
6·0
5·0
4·0
3·0
(e)
dimer
monomer
0
1·0
2·0
3·0
4·0
Concentration (mg/ml)

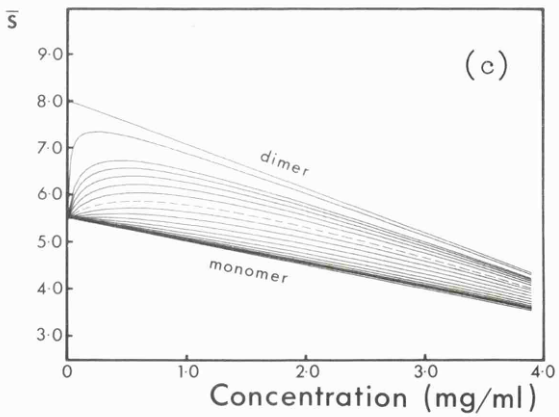
$\bar{s}$
9·0
8·0
7·0
6·0
5·0
4·0
3·0
(c)
dimer
monomer
0
1·0
2·0
3·0
4·0
Concentration (mg/ml)

Figure 10. Computer-simulated s versus concentration plot for a myosin monomer-dimer equilibrium with $s^o_m = 5.75S$

The dotted line is the concentration dependence observed in this study. The limiting lines are the dependence for pure monomer and pure dimer; the dashed line represents the equilibrium constant predicted by Godfrey and Harrington (1970b), 10^3ml/g. Equilibrium constants are (from monomer to dimer): (a) and (b) 10, 10^2, then incremented by $10^{0.2}$ to 10^4, 10^5ml/g; (c), (d) and (e) 10, then incremented by $10^{0.2}$ to 10^4, 10^5ml/g.

Graphs (a) to (e) represent different values of s^o_d as assigned in Table 1 (b).

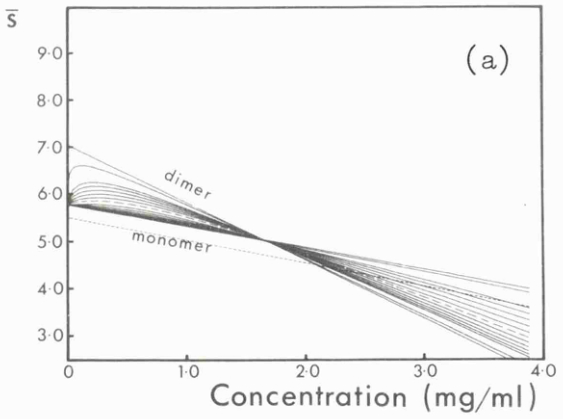
$\bar{s}$
9·0
8·0
7·0
6·0
5·0
4·0
3·0
(a)
dimer
monomer
0
1·0
2·0
3·0
4·0
Concentration (mg/ml)

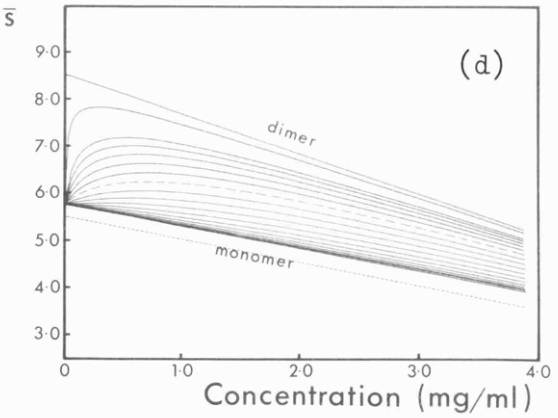
$\bar{s}$
9·0
8·0
7·0
6·0
5·0
4·0
3·0
(d)
dimer
monomer
0
1·0
2·0
3·0
4·0
Concentration (mg/ml)

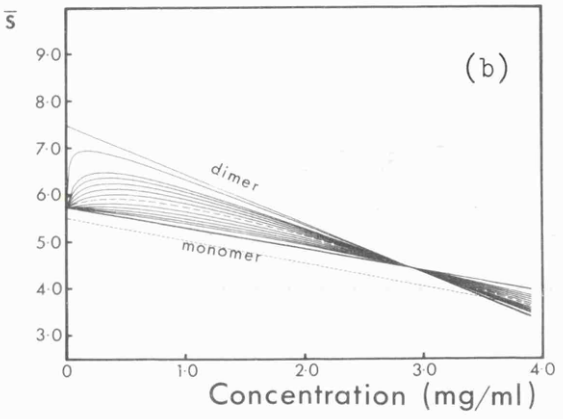
$\bar{s}$
9·0
8·0
7·0
6·0
5·0
4·0
3·0
(b)
dimer
monomer
0
1·0
2·0
3·0
4·0
Concentration (mg/ml)

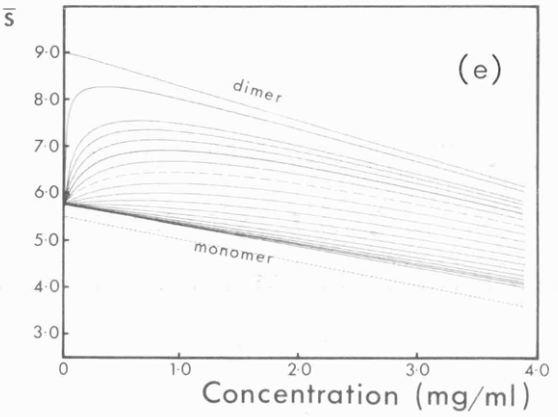
$\bar{s}$
9·0
8·0
7·0
6·0
5·0
4·0
3·0
(e)
dimer
monomer
0
1·0
2·0
3·0
4·0
Concentration (mg/ml)

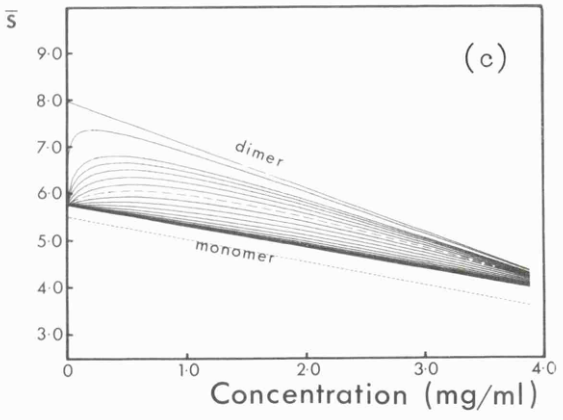
$\bar{s}$
9·0
8·0
7·0
6·0
5·0
4·0
3·0
(c)
dimer
monomer
0
1·0
2·0
3·0
4·0
Concentration (mg/ml)

Figure 11. Computer-simulated s versus concentration plot for a myosin monomer-dimer equilibrium with $s^{o}_{m} = 6.0S$

The dotted line is the concentration dependence observed in this study. The limiting lines are the dependence for pure monomer and pure dimer; the dashed line represents the equilibrium constant predicted by Godfrey and Harrington (1970b), 10^{3}ml/g. Equilibrium constants are (from monomer to dimer): (a), (b) and (c) 10, 10^{2}, then incremented by $10^{0.2}$ to 10^{4}, 10^{5}ml/g; (d) and (e) 10, then incremented by $10^{0.2}$ to 10^{4}, 10^{5}ml/g.

Graphs (a) to (e) represent different values of s^{o}_{d} as assigned in Table 1 (b).

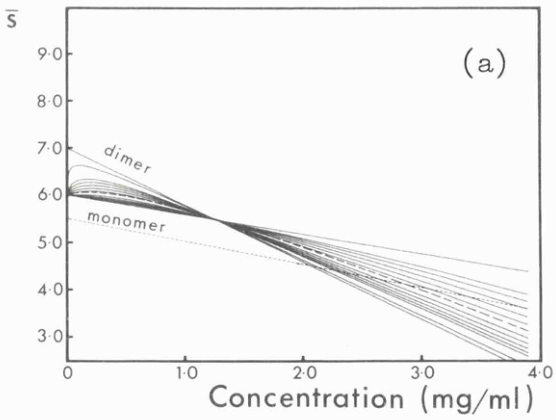
$\bar{s}$
9·0
8·0
7·0
6·0
5·0
4·0
3·0
(a)
dimer
monomer
0
1·0
2·0
3·0
4·0
Concentration (mg/ml)

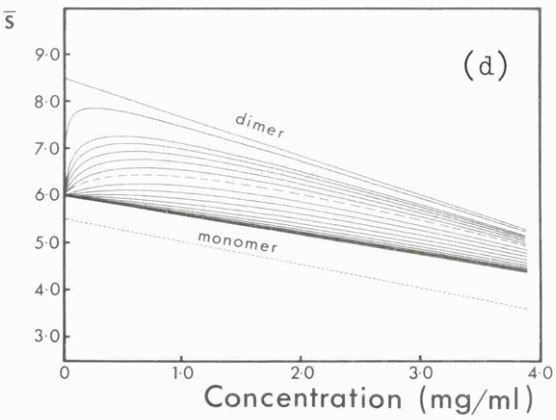
$\bar{s}$
9·0
8·0
7·0
6·0
5·0
4·0
3·0
(d)
dimer
monomer
0
1·0
2·0
3·0
4·0
Concentration (mg/ml)

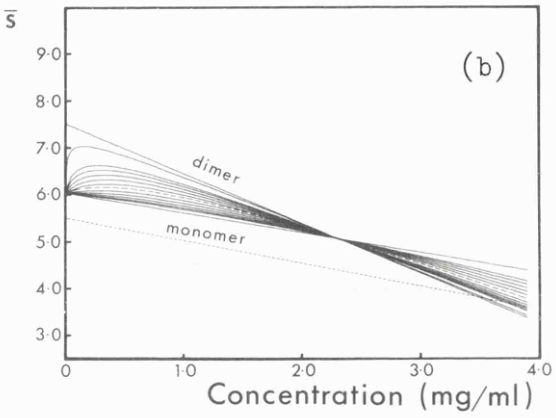
$\bar{s}$
9·0
8·0
7·0
6·0
5·0
4·0
3·0
(b)
dimer
monomer
0
1·0
2·0
3·0
4·0
Concentration (mg/ml)

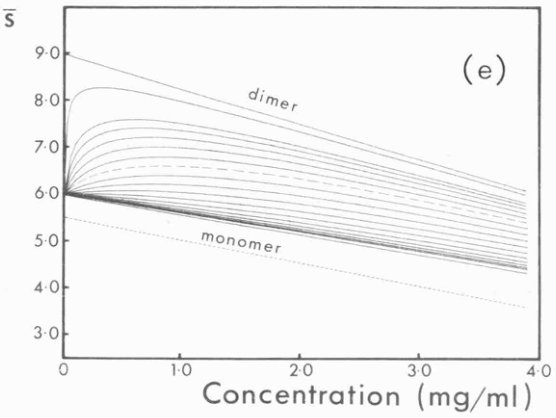
$\bar{s}$
9·0
8·0
7·0
6·0
5·0
4·0
3·0
(e)
dimer
monomer
0
1·0
2·0
3·0
4·0
Concentration (mg/ml)

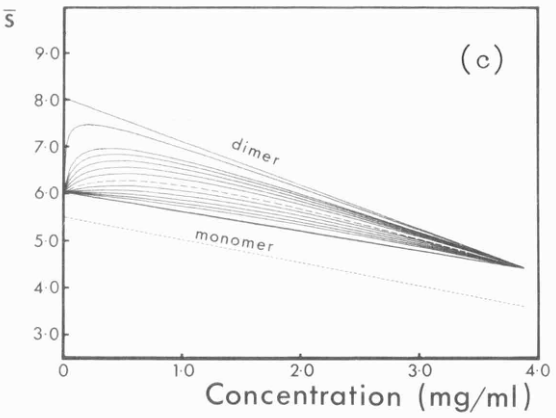
$\bar{s}$
9·0
8·0
7·0
6·0
5·0
4·0
3·0
(c)
dimer
monomer
0
1·0
2·0
3·0
4·0
Concentration (mg/ml)

Table 1. List of the parameters used to compute the concentration dependence of s for a monomer-dimer equilibrium for myosin.

(a) Range of parameters for the monomer

s^o_m (S)	f/f_o	$k_{s,m}$ (ml/g)
5.0	4.32	119.0
5.25	4.17	103.0
5.5	3.93	89.8
5.75	3.76	78.8
6.0	3.60	69.5

(b) Range of parameters for the dimer

	s^o_d (S)	f/f_o	$k_{s,d}$ (ml/g)
a	7.0	4.90	172.9
b	7.5	4.57	140.8
c	8.0	4.29	116.3
d	8.5	4.04	97.2
e	9.0	3.81	82.1

a monomer-dimer equilibrium, although Herbert and Carlson (1971) point out that their data cannot distinguish between a monomer-dimer, monomer-trimer, or monomer-dimer-trimer equilibrium.

It can be concluded that the published equilibrium constants for the monomer-dimer equilibrium of myosin cannot be applied to the myosin solutions analysed here. This being so, what is the largest equilibrium constant that can be assumed and still satisfy the results? There is a difficulty in answering this question owing to the uncertainty in s^o_m and s^o_d. However, it will be shown that the predicted s value for the myosin monomer is between 5.5 and 6.0S, from the Kirkwood-Bloomfield theory (Bloomfield et al., 1967), see section III.3.7. Assuming s^o_d lies in the range 8.0 to 9.0S, only an equilibrium constant of less than 10ml/g at most could comply with the experimental data. A higher equilibrium constant, upto 100ml/g, could fit the data only if s^o_m is less than 5.5S and s^o_d is less than 8.0S, but under these conditions the frictional ratio of the monomer (e.g. for s^o_m = 5.0S, f/f_o = 4.32) would be much higher than that predicted from the Kirkwood-Bloomfield theory (the predicted f/f_o for a heads apart molecule is 3.97). Therefore we may conclude that there is little or no reversible dimerization of myosin at high ionic strength. On the basis of this finding, the molecular weight of myosin 'monomer' can be confidently determined by a new procedure from s^o and k_s (Rowe, 1977), since the conditions for its application are now fulfilled (i.e. no charge effects and no significant self-interaction).

III.3.6. Estimation of the Molecular Weight of Myosin from s^o and k_s

From the relationship between k_s and f/f_o (see Appendix I) and by use of the Svedberg equation, the ideal molecular weight (M^o) of myosin may be determined from $s^o_{20,w}$, k_s, $V_s/\bar{v}$ and $\bar{v}$. The molecular weight of myosin A

samples analysed here has been calculated using a value for $V_s/\bar{v}$ of 1.1 (see III.3.8). By substituting $\bar{v}$ = 0.728ml/g, $s^o_{20,w}$ = 5.52S and k_s = 94ml/g, the molecular weight of myosin is 470000 ± 27000. This molecular weight of myosin agrees well with the range estimated from the molecular weights of the meromyosins: 450000 - 500000 (Lowey et al., 1969) and is further evidence that there can be little or no dimer present in these myosin solutions.

III.3.7. Variation of f/f_o

It was inferred above that a monomer-dimer equilibrium with an equilibrium constant of greater than 10ml/g did not exist in myosin solutions at high ionic strength. But the monomer-dimer equilibrium theory provided an explanation for the variation of published values of s^o for myosin: the $s^o_{20,w}$ values, obtained by extrapolation to infinite dilution from regions of 'high' concentration, were suggested to be weight-averages of a mixture of monomer and dimer (Godfrey and Harrington, 1970a). It is certainly surprising that careful ultracentrifugation studies on myosin A solutions have yielded a range of $s^o_{20,w}$ values from 5.5 to 6.5S (see Table 2). Since it now seems likely that a monomer-dimer equilibrium could not be responsible for this inconsistency, can an alternative explanation be offered?

A possible explanation for this variation of $s^o_{20,w}$ values was indicated during initial experiments with glycerolated myosin. The dependence of the sedimentation coefficient upon concentration was linear for glycerolated myosin A solutions, Figure 12, although s^o and k_s varied depending upon the length of the storage period. The variation in s^o and k_s appeared only between different preparations and never within the same preparation at a given time of storage. The effect of a monomer-dimer

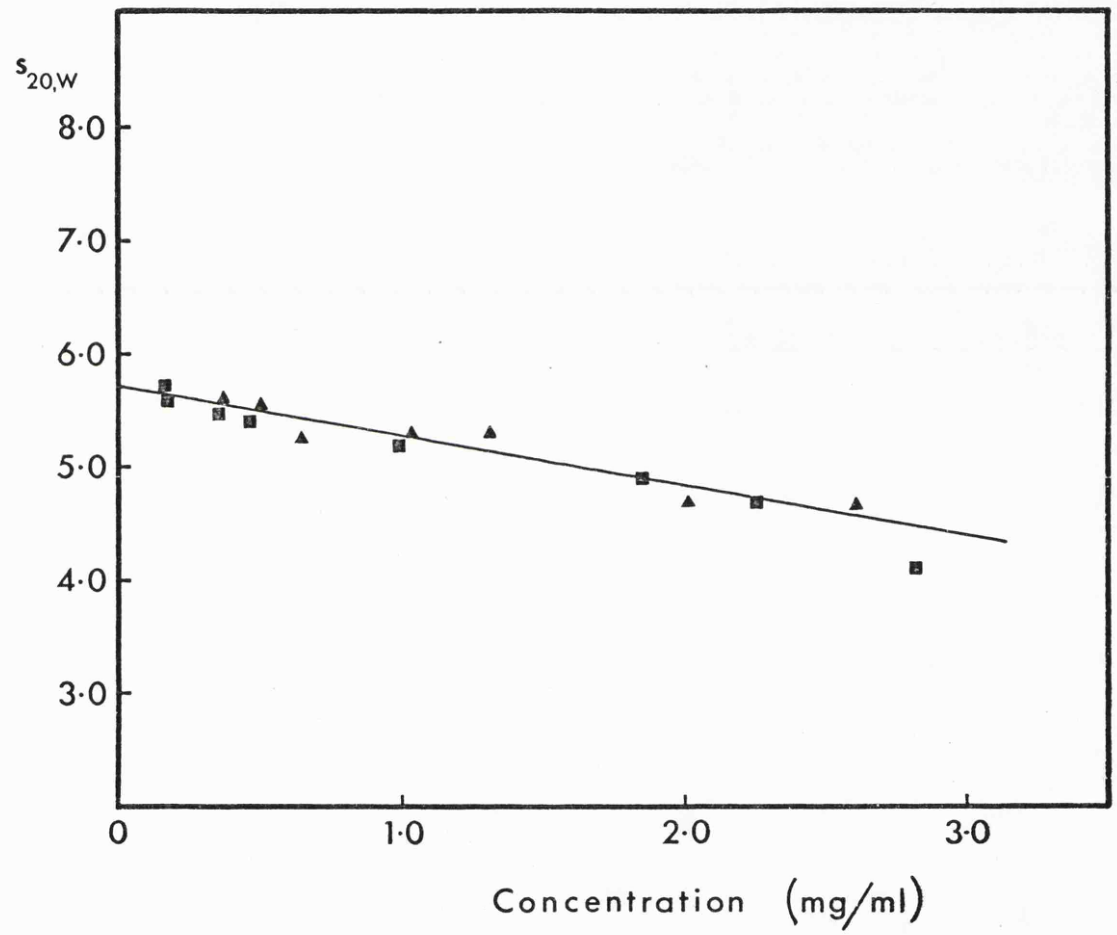

Figure 12 s versus concentration plot for glycerolated myosin A solutions

The symbols signify two different preparations of myosin A, both stored in 50% glycerol at -18°C for 1 month.

Concentration has been corrected for radial dilution.

equilibrium in glycerolated myosin solutions can be discounted because not only was the s against concentration dependence linear, but the molecular weight, estimated from k_s and s^o, was the same as that for fresh myosin solutions. The different s^o and k_s can only be interpreted as a change in f/f_o occurring during storage in glycerol, possibly caused by the separation of the two myosin heads. Two attempts were made to test this hypothesis, the first to measure the frictional ratio of two myosin models, one with 'heads apart', the other with 'heads together' and the second to predict the frictional ratio from the Kirkwood-Bloomfield theory.

For the first approach, two points were considered; firstly, as the myosin molecules move through solution during sedimentation they undergo random Brownian motion, thus the frictional ratio must be averaged over all the possible orientations of the model. Secondly, the velocity of the myosin molecule in the ultracentrifuge is slow so that the condition of 'laminar flow' prevails; hydrodynamic experiments must be carried out under the same condition so that the effect of turbulence is negligible. To measure the difference in frictional ratios, scale models of the two myosin conformations were built and the drag on each model measured in a water flow channel. By constructing a suitable harness, the drag (which is proportional to the frictional coefficient) can be measured for different orientations of the model, so fulfilling the first condition. The second criterion of laminar flow was more difficult to attain. Laminar flow is achieved at a Reynold's Number (R_e) of less than 10, for a sphere or rod, where the Reynold's Number is a dimensionless constant given by $R_e = \rho.u.d/\eta$, where d is the diameter of the model and u is the velocity. For a R_e of less than ten, the velocity of the water over the model would have to be less than 1mm/s and, with the apparatus available, this flow rate could not be reliably obtained nor the drag on the model accurately

measured. It may yet be possible to measure the drag on models of myosin at low R_e by using a fluid of high kinematic viscosity (η/ρ); for example air (η/ρ = 15.2cSt) or sucrose solution (a 74% sucrose solution (w/w) has a kinematic viscosity of 1188cSt).

The second approach, to predict the frictional ratio of myosin via the Kirkwood-Bloomfield theory, proved more successful. The 'shell model' for estimating frictional coefficients was not applied to myosin as it would require complex calculations and, to be meaningful, detailed knowledge of the structure of the myosin molecule. Instead, an approximate frictional coefficient was estimated (Bloomfield et al., 1967) by assuming the myosin molecule was made up of spheres 2.0nm in diameter (see section III.2.8). The two conformations of myosin are shown in Figure 13 and they do indeed have different frictional coefficients. Substituting the frictional coefficients so obtained, together with M^o, into the Svedberg equation gave s^o as 5.98S for a 'heads together' model and 5.45S for the 'heads apart' model. The predicted s^o values are, of course, only as accurate as the assumptions on which they are based (i.e. the size and shape of the myosin molecule); by choosing slightly different dimensions and a greater angle between the myosin heads, it would be possible to predict an s^o range of 5.5 to 6.5S. Thus from these calculations, it is shown that a change in the conformation of the myosin molecule can account, at least in part, for the observed range of s^o (5.5 - 6.5S). In passing, it is interesting to note that the predicted value of 5.45S agrees well with the experimentally determined s^o found in this study, suggesting that these myosin solutions consist mostly of 'heads apart' molecules.

III.3.8. Determination of $V_s/\bar{v}$

A combination of results from both sedimentation velocity and

(a)

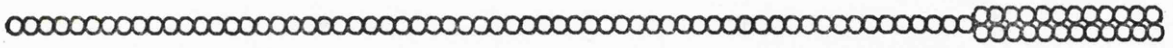

Predicted $s^0_{20,w} = 5{\cdot}98S$

(b)

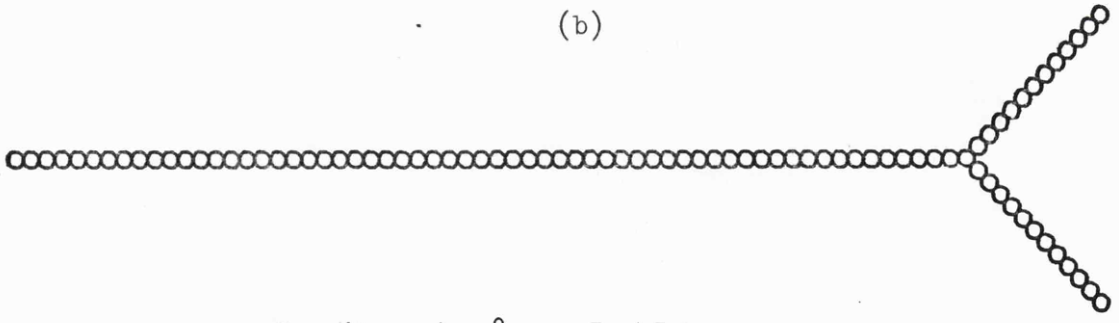

Predicted $s^0_{20,w} = 5{\cdot}45S$

Figure 13 The two models used to calculate the frictional coefficient of myosin from the Kirkwood-Bloomfield theory

The diameter of each sphere is 2.0nm; no account has been taken of the larger diameter of the myosin heads.

(a) 'heads together', (b) 'heads apart'.

viscosity studies has been much used in the past to elucidate the hydrodynamic behaviour of macromolecules. Although by these procedures it is usually possible to choose between a prolate or oblate ellipsoid of revolution as the more suitable hydrodynamic model, up until now there has been no method to test the 'goodness of fit' of these models. A new approach by Rowe (1977, and in Appendix II) has provided a means of testing quantitatively the plausibility of an assumed model. The procedure involves estimating $V_s/\bar{v}$ (the swelling of a macromolecule) from the ratio k_η/k_s (the derivation of this relationship is given in Appendix II), where k_η is the concentration dependence of reduced viscosity (η_{sp}/c) given by the equation: $\eta_{sp}/c = [\eta](1 + k_\eta c)$; $[\eta]$ is the intrinsic viscosity. The $V_s/\bar{v}$ so determined is independent of any assumed model and its value can be compared to that obtained by an alternative procedure in which a hydrodynamic model is assumed; if the two values are the same then the model is valid under the experimental conditions used, if they are different then the model is unsuitable.

(a) <u>The Model-Independent $V_s/\bar{v}$</u>

In Appendix II the derivation of the equation $V_s/\bar{v} = k_\eta/k_s$ is given. The usual conditions for the application of sedimentation theory must be met (i.e. no charge effects and no self-interaction) and k_η and k_s should be determined on the same sample. Figure 14 shows the reduced viscosity (η_{sp}/c) <u>versus</u> concentration profile for myosin A solutions in stock buffer, pH 6.7. A least squares regression procedure was used to estimate the line through the experimental points, which is given by the equation $\eta_{sp}/c = [\eta](1 + k_\eta c)$. From the slope and the intercept, the intrinsic viscosity, $[\eta]$, is 234 $\pm$ 1ml/g, k_η = 92 $\pm$ 4ml/g and the Huggins constant ($k_\eta/[\eta]$) is 0.39 $\pm$ 0.02. The intrinsic viscosity agrees well with other published values for myosin (see III.4). The $s_{20,w}$ <u>versus</u> concentration

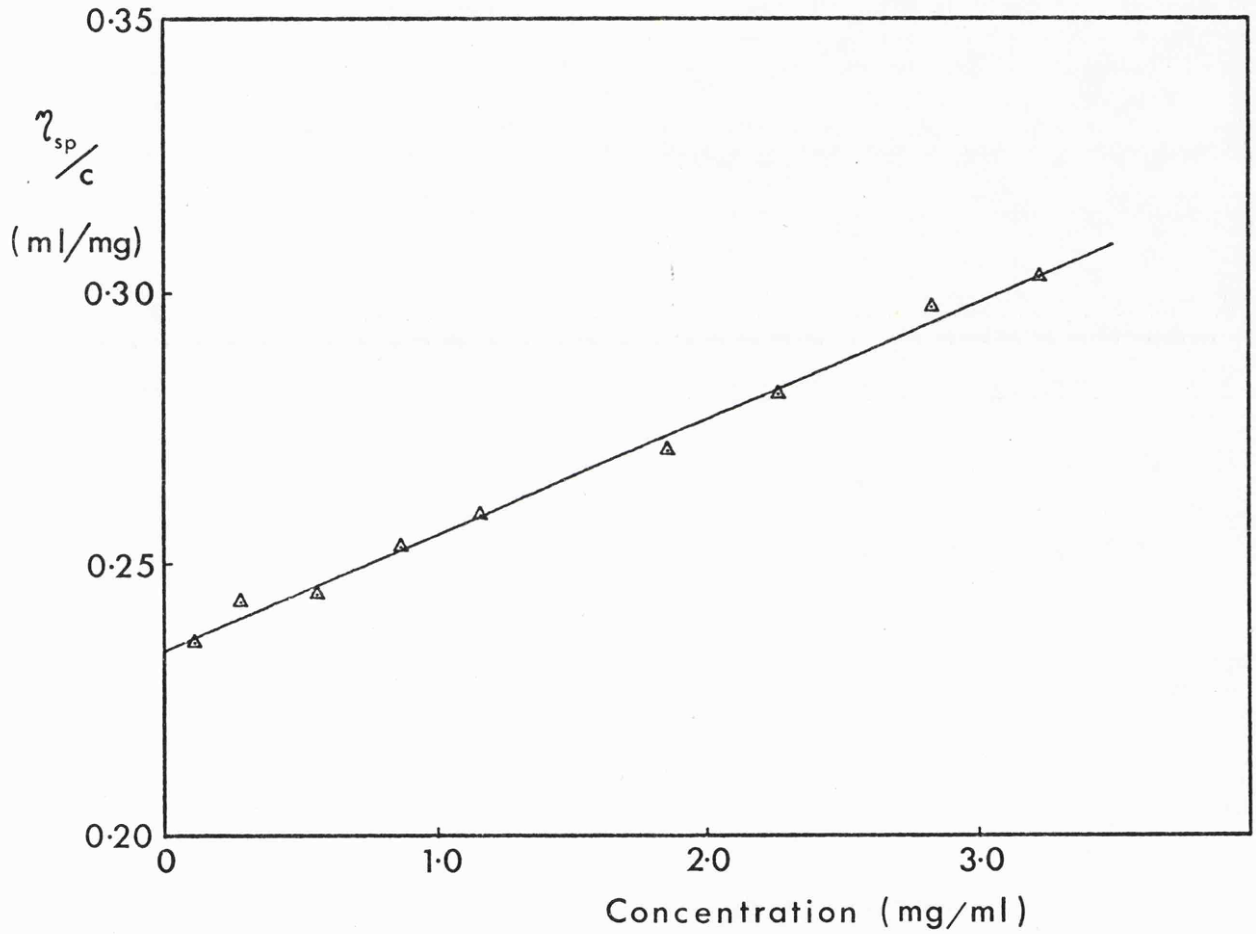

Figure 14 Reduced viscosity versus concentration profile of myosin A in stock buffer

Before viscosity measurements the diluted myosin A samples were centrifuged at 25000 rev./min to remove any denatured protein. Viscosity was measured at 5 °C and concentration was determined afterwards.

plot for the same myosin A sample is shown in Figure 15, where $s^{o}_{20,w}$ is 5.95 ± 0.06S and k_s (corrected to solution density) is 88.4 ± 8.0ml/g. The molecular weight, estimated from s^{o} and k_s (and using $V_s/\bar{v} = 1.1$), is 513000 ± 28000 for this myosin A preparation, although this is not significantly greater than the previous value of 470000 ± 27000.

The $V_s/\bar{v}$ value estimated from k_η/k_s, without any assumptions as to the shape of the particle, is 1.1 ± 0.1. The validity of any assumed model can be tested by comparing the model-dependent $V_s/\bar{v}$ value with the model-free estimate quoted above. In practice only two hydrodynamic models are applied to proteins: the prolate and oblate ellipsoids of revolution. The axial ratio must be determined first and there are two methods for doing so, both of which use information from sedimentation and viscosity studies.

(b) The Model-Dependent $V_s/\bar{v}$

The first approach has been outlined by Scheraga and Mandelkern (1953) who defined the β-function:

$$\beta = \frac{N_A\, s^{o}\, [\eta]\, \eta_o}{M^{2/3}(1-\bar{v}\rho)} \qquad (6)$$

where N_A is Avogadro's Number; $[\eta]$ is the intrinsic viscosity in dl/g; η_o is the viscosity of the solvent. The following conditions apply to this equation: $[\eta]$ and s^{o} must be measured in the same solvent (in order that the axial ratio and hydrodynamic volume do not vary) and both refer to the extrapolated values at infinite dilution. The β-function has been computed over a range of axial ratios for prolate and oblate ellipsoids of revolution (see Figure 3 in Appendix II). The β-function calculated for myosin ($2.95 \pm 0.15 \times 10^{6}$) corresponds to a prolate ellipsoid of axial ratio 48 ± 16; an oblate ellipsoid can be ruled out, as at large axial ratios, the β-function is constant at 2.15×10^{6}. The viscosity increment,

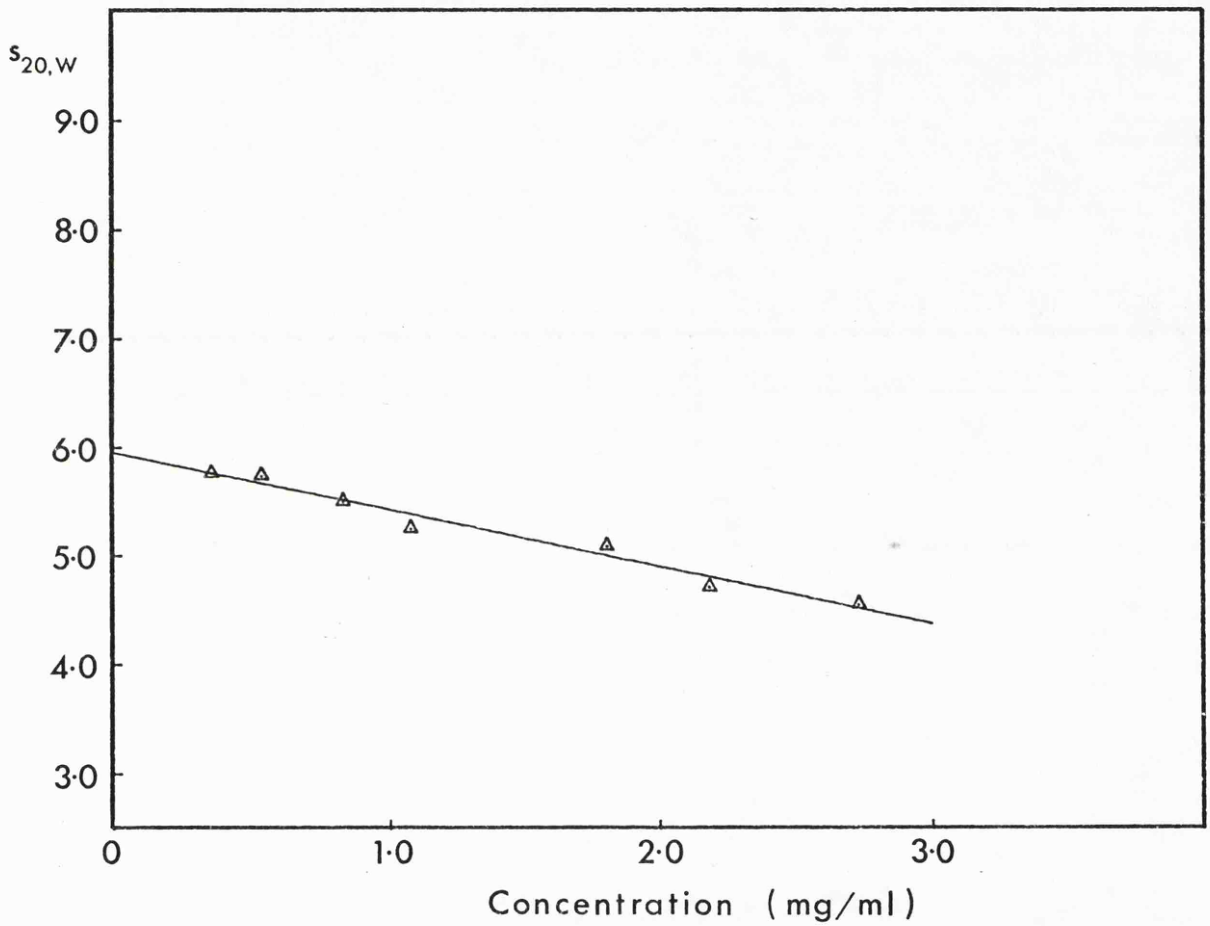

Figure 15 s versus concentration plot for the myosin A sample used in viscosity measurements

Sedimentation coefficients were measured at 5 - 7 °C within the rotor speed range 55000 - 60000rev./min.

ν, was found by interpolation from a graph of ν *versus* axial ratio, where ν was calculated using the Simha (1940) equation (see Table VII in Yang, 1961). Estimation of $V_s/\bar{v}$, using $V_s/\bar{v} = [\eta]/\bar{v}\nu$, gave 2.0 ± 1.0 for a prolate ellipsoid of revolution.

The second method of estimating $V_s/\bar{v}$ from axial ratio involves the R-function, which is numerically equal to $k_s/[\eta]$ (the derivation is given in Appendix II). The R-function has several advantages over the β-function in that it is more precise and more sensitive (once again Appendix II should be consulted for more details). The following conditions must be fulfilled: there must be an absence of charge effects and self-interaction and the treatment only applies to dilute solutions where specific solute-solute interactions can be neglected. The value of the R-function for this myosin preparation is 0.38 ± 0.04, corresponding to an axial ratio of 30 ± 6 for a prolate ellipsoid and, once again, an oblate ellipsoid may be discounted as the R-function is too low. The value of $V_s/\bar{v}$ calculated from the axial ratio, by the same method as above, is 4.3 ± 1.3 for a prolate ellipsoid.

III.4. Discussion

The sedimentation velocity studies described here on myosin A solutions have demonstrated that if a monomer-dimer equilibrium does exist, its equilibrium constant is less than 10ml/g (i.e. at least 100 times less than that described by Harrington and his coworkers). The evidence for this conclusion is drawn from the linearity of the $s_{20,w}$ *versus* concentration plot and by comparison with computer-simulated curves for a monomer-dimer equilibrium. Although the myosin A solutions studied contained small amounts of actin, the presence of this contaminant in no way affected the linear concentration dependence of the sedimentation coefficient. On the contrary, column-purification of myosin to remove actin and other

contaminants resulted in the formation of irreversible myosin aggregates (upto 20% of the total protein concentration) and prohibited meaningful interpretation of the sedimentation velocity data. Since the evidence presented here contradicts the monomer-dimer equilibrium theory for myosin, can alternative explanations be offered for the supporting evidence from sedimentation equilibrium, light scattering and viscosity studies?

The high-speed sedimentation equilibrium results obtained by Godfrey and Harrington (1970b) from column-purified myosin at high ionic strength (0.5M-KCl, 0.1M-EDTA, 0.2M-phosphate buffer, pH 7.3) was analysed with the aid of a Roark-Yphantis computer program. This program fits the best curve to the experimental data by using a sliding least squares curve-fitting program and by varying the parameters M^o, K and B (the second virial coefficient). The second virial coefficient postulated for the myosin monomer was very much higher than those values previously reported. For example, B obtained by Godfrey and Harrington (1970b) was 6.6×10^{-4} mol.ml/g^2, whereas earlier estimates are: $B = 0.98 \pm 0.16 \times 10^{-4}$ mol.ml/g^2 from light scattering (Gellert and Englander, 1963, as corrected by Tomimatsu, 1964); $B = 1.12 \times 10^{-4}$ mol.ml/g^2 (Woods et al., 1963) and $B = 1.10 \times 10^{-4}$ mol.ml/g^2 (Mueller, 1964), both by the Archibald sedimentation equilibrium technique. We may estimate the most plausible value of B for myosin by using the equation:

$$B = \frac{N_A \pi d l^2}{4 M^2} \qquad (7)$$

The assumptions involved in the derivation of this equation are: (i) the protein can be represented by a rigid rod of uniform diameter, d, (ii) the length, l, is at least ten fold greater than the diameter and (iii) there are no charge effects in the macromolecular solution (Zimm,

1946). Now conditions (ii) and (iii) can be applied to myosin, but the assumption that myosin can be represented by a long cylinder is a poor one. However, in the absence of any more suitable relationships between B and other hydrodynamic models, I have estimated B from the dimensions of the myosin molecule *via* eqn. 7. With a molecular weight of 470000, length equal to 150nm and diameter equal to 2.5nm, B is 1.2×10^{-4}mol.ml/g^2. Even if a somewhat higher estimate for the length of the myosin molecule is used, length = 175nm (taking the length of the tail as 150nm, Elliott *et al.*, 1976 and the heads as 25nm long), B is only 1.64×10^{-4}mol.ml/g^2. Thus, even considering the assumption of a cylindrical model for myosin and the uncertainty in the size of the myosin molecule, it seems highly unlikely that a second virial coefficient as high as 6.60×10^{-4}mol.ml/g^2 can be correct.

The second point to be considered is that the solution for the equilibrium constant, K, may not be a unique one. Indeed, Pitt and Rowe (unpublished observations) have demonstrated by computer-simulation that analysis of sedimentation equilibrium data can provide more than one pair of values (K, B) as a solution and that *exhaustive* curve fitting is required to confirm that only one equilibrium constant prevails. So, on the basis that the solution for K may not be unique and that the predicted value of B is incompatible with previous estimates of B and with the known dimensions of the myosin molecule, I suggest that the equilibrium constant reported by Godfrey and Harrington (1970*b*) may be incorrect. Rather, the curvature in $1/M_{w,app}$ *versus* concentration plots may not be the result of a monomer-dimer equilibrium but the expression of one or more of the following phenomena: (i) dissociation of myosin at low concentration into low molecular weight components (as postulated by Siemankowski and Dreizen, 1974, 1975), (ii) adsorption of myosin to the windows of the ultracentrifuge

cell (as supposed herein to account for the instability of the protein boundary in sedimentation velocity experiments) and (iii) the high molecular weight aggregate found in sedimentation equilibrium experiments (Godfrey and Harrington, 1970b) may effect the distribution of the lower molecular weight species throughout the rest of the cell. Concerning this last point, irreversible aggregates may be particularly prevalent in column-purified myosin solutions, as has been demonstrated by my own initial sedimentation velocity experiments and also in sedimentation equilibrium runs (Siemankowski and Dreizen, 1975). In support of this finding is the report by Pinset-Härström and Morel (1975) that myosin solutions left for long periods in 0.45M-KCl contain large amounts of oligomers; since column purification of myosin is performed in a phosphate buffer at I 0.38, this may be the explanation for the appearance of aggregates in these myosin solutions.

As for the light scattering results of Herbert and Carlson (1971), one may note that they have used a new, and as yet untested, technique for laser light scattering and that their results are neither consistent with those obtained in this work, nor with the theoretical $s_{20,w}$ *versus* concentration dependence curves predicted for a monomer-dimer equilibrium, nor indeed with the $1/s_{20,w}$ *versus* concentration data of Godfrey and Harrington (1970a) for that matter. The third source of support for the monomer-dimer equilibrium came from the viscosity experiments of Harrington and Burke (1972). The evidence for a monomer-dimer equilibrium relies heavily upon the observation of a downward curvature in reduced viscosity (η_{sp}/c) *versus* concentration plots at low concentrations (below 0.2mg/ml). There are two effects that may alter the concentration dependence of η_{sp}/c, namely adsorption of protein onto the capillary walls, causing a decrease in its diameter and producing anomalously high values of η_{sp}/c and secondly, decrease in the

bulk concentration of protein as a result of adsorption of protein to all the glass surfaces to which the solution is exposed.

In a careful study of the intrinsic viscosity of myosin by Johnson and Rowe (1961), the effect of a decrease in the diameter of the capillary due to protein adsorption was shown to have a negligible effect upon η_{sp}/c. In the later study by Harrington and Burke (1972) a similar conclusion was reached, however, these investigators failed to consider the effect of decrease in the bulk protein concentration which has a significant effect at low myosin concentrations. As a result of this phenomenon, η_{sp}/c is under-estimated, thus the downward curvature in the η_{sp}/c <u>versus</u> concentration plot at low concentrations can equally well be explained by protein adsorption. Johnson and Rowe (1961) have emphasised the importance of measuring protein concentration <u>after</u> viscosity determination in order to obtain an accurate estimate of the actual concentration used. By observing this precaution, linear η_{sp}/c against concentration dependence has been observed for myosin at concentrations from 2mg/ml down to 0.1mg/ml.

The intrinsic viscosity reported by Harrington and Burke (1972) was higher than any other previously reported for skeletal muscle myosin: they found $[\eta]$ = 245ml/g compared to 235ml/g (Johnson and Rowe, 1961) and 217ml/g (Holtzer and Lowey, 1959). If one assumes that the η_{sp}/c against concentration plot should be linear, the intrinsic viscosity predicted from Harrington and Burke's (1972) data is even higher (258ml/g), yet no explanation was offered for this discrepancy.

In summary, therefore, it is possible to offer perfectly viable alternative interpretations for the sedimentation equilibrium and viscosity experiments from which a monomer-dimer equilibrium for myosin was deduced. But the monomer-dimer equilibrium theory did provide an explanation for the variation of the published values of s^o and M^o for myosin. Since s^o and M^o

are obtained by measuring s and M_{app} at finite concentrations and extrapolating to infinite dilution, both s^o and M^o would be weight-averages of a mixture of monomer and dimer and their values would be dependent upon the ratio of the two species in the concentration range used. However, it has been shown that a variation of s^o for myosin may originate from a change in f/f_o caused by the opening of the myosin heads. The Kirkwood-Bloomfield theory (Bloomfield et al., 1967) applied to two myosin conformations has shown that a difference in s^o values of about 0.5S can occur and even greater differences can be predicted by increasing the angle between the myosin heads. The different s^o values published for myosin, Table 2, may therefore be explained by a conformational change occurring in the myosin molecule, either during preparation or during storage in glycerol, such that the angle between the heads is altered. One must assume that this conformational change is not rapidly reversible and that myosin populations are fairly homogeneous for a given preparation so as to account for the linear dependence of s upon concentration and the appearance of single, hypersharp schlieren peaks in the ultracentrifuge.

The similarity between the predicted s^o value for myosin (with heads apart) and the experimental value determined here is better than the information on the size and shape of the myosin molecule warrants. In recent measurements from electron micrographs of shadowed myosin molecules, Elliott et al.(1976) have estimated that the length of the rod portion of myosin is 150 $\pm$ 20nm and that the heads are pear-shaped and 20nm long. It is possible that by using this latest model for myosin and the full shell model theory of Kirkwood and Bloomfield (Bloomfield et al., 1967) a different s^o may be predicted than that determined for the rather crude model used here. Notwithstanding these criticisms, the approximate form of the Kirkwood-Bloomfield theory has been useful in predicting an alteration

in f/f_o for myosin.

One is left to speculate on how a change in the angle between the myosin heads is accomplished at the molecular level. The SDS gels of different myosin samples and the molecular weights calculated from s^o and k_s are not significantly different and so one may rule out proteolysis as the cause of the change in f/f_o. Since the conformational change occurs during myosin preparation and/or during storage in glycerol, it is possible that denaturation of some of the polypeptide chains of myosin may be responsible. One suggestion is that the DTNB-light chains, whose function in the myosin molecule remains obscure, may be responsible for maintaining the angle between the heads and that their denaturation causes a change in the angle. Finally, it is of interest to note that in muscle the myosin heads (HMM S-1) are assumed to act individually on actin sites, so a 'heads apart' configuration may be a distinct advantage.

Sedimentation velocity experiments have demonstrated that the existence of a myosin monomer-dimer equilibrium is unlikely and alternative explanations have been presented both for the evidence on which a monomer-dimer equilibrium is based (Godfrey and Harrington, 1970b; Harrington and Burke, 1972) and for the predictions made from it (i.e. to account for the variation of s^o). Let us now recount the properties of the myosin molecule deduced from this study:

(i) there is no significant monomer-dimer equilibrium at high ionic strength

(ii) a variation in f/f_o has been demonstrated between different myosin preparations

(iii) the molecular weight estimated from s^o and k_s is 470000.

The s^o and k_s procedure for molecular weight determination has been particularly useful in this study in which a change in f/f_o has altered both s^o and k_s. The molecular weight obtained agrees well with the range

450000 - 500000 predicted from a knowledge of the molecular weights of the purified meromyosin fragments (Lowey et al., 1969). A list of published s^o and k_s values is given in Table 2 together with the molecular weight as estimated by conventional methods, e.g. light scattering (L.S.), sedimentation equilibrium (EQUIL.), the Archibald procedure or osmometry (OSM.). The mean of the molecular weights quoted is 506000 ± 40000 (S.D.), excluding the very eccentric values for dog cardiac myosin. For comparison, the molecular weights estimated from s^o and k_s have been included. Only reliable sedimentation velocity data have been selected (i.e. no actomyosin solutions have been considered and only myosin samples that give single schlieren peaks when centrifuged at 5°C). In all cases, k_s was corrected for an assumed radial dilution of 5% so as to correct it to true sedimenting concentration.

The mean molecular weight from s^o and k_s was 505000 with a standard deviation of 62000; this standard deviation is remarkably good when one considers that previous researchers were not overly concerned in obtaining extraordinarily accurate k_s values. It is also pleasing to note that for dog cardiac myosin, the molecular weight from s^o and k_s was calculated to be 430000, whereas the molecular weight from the Archibald method gave, for two different authors, the patently incorrect values of 758000 and 222000. Thus the technique for determining molecular weight from s^o and k_s gives a mean molecular weight in excellent agreement with that obtained by procedures specifically designed to measure molecular weight.

Two other pieces of information can be added to the list of the hydrodynamic properties of myosin:

(iv) the swelling, $V_s/\bar{v}$, is 1.1 ± 0.1

(v) it has been confirmed that a prolate ellipsoid is not a good hydrodynamic model for myosin.

Table 2. Published values of s°, k_s and M° for myosin

The molecular weight calculated from s° and k_s by the method of Rowe (1977) is given in column 4.

ANIMAL Type of myosin	$s^{\circ}_{20,w}$ (S)	k_s ml/g	M° from s° & k_s	M° from other methods		References
RABBIT myosin A	6.50	56.9	498000	493000 ± 50000	(L.S.)	Holtzer and Lowey (1959)
RABBIT myosin A	6.43	66.9	489000	540000	(s° & D)	Johnson and Rowe (1960)
RABBIT myosin A	6.15	-	-	500000	(s° & D)	Laki and Carroll (1955)
RABBIT myosin A	6.13	89.7	576000	468000	(EQUIL.)	Gershman et al. (1969)
RABBIT myosin A	6.10	50.8	431000	550000	(L.S.)	Ellenbogen et al. (1960)
RABBIT myosin A	-	-	-	470000 ± 25000	(ARCH.)	Lowey and Cohen (1962)
RABBIT myosin A	-	-	-	470000 (M_n) 490000 (M_w)	(OSM.) (EQUIL.)	Tonomura et al. (1966)
RABBIT myosin A	-	-	-	520000	(L.S.)	Gellert and Englander (1960) as corrected by Tomimatsu (1964)
RABBIT myosin A	-	-	-	524000	(ARCH.)	Mueller (1964)
RABBIT myosin A	-	-	-	525000 ± 12000	(L.S.)	Holtzer et al. (1961)
RABBIT CP-myosin [a] (DEAE-Sephadex)	6.15	84.6	562000	510000	(EQUIL.)	Chung et al. (1967)
RABBIT CP-myosin (DEAE-Sephadex)	6.06	97.7	553000	458000	(EQUIL.)	Godfrey and Harrington (1970a,b)
RABBIT CP-myosin (DEAE-cellulose)	5.88	68.7	471000	504000	(s° & D)	Trayer and Perry (1966)
CHICKEN CP-myosin (DEAE-Sephadex)	5.96	88.9	550000	500000	(EQUIL.)	Richards et al. (1967)
DOG cardiac myosin	6.00	98.3	584000	500000	(ARCH.)	Luchi et al. (1965)
DOG cardiac myosin	6.16	50.3	431000	222000	(EQUIL. & ARCH.)	Ellenbogen et al. (1960)
DOG cardiac myosin	5.80	58.6	426000	758000	(ARCH.)	Brahms and Kay (1962)
LOBSTER myosin A	5.82	38.7	345000	595000	(EQUIL.)	Woods et al. (1963)
COD myosin	6.50	48.9	460000	480000 ± 20000	(EQUIL.)	Connell (1958)
COD myosin	-	-	-	530000 590000	(s° & D) (ARCH.)	Connell and Mackie (1964)
MULLET myosin	6.05	49.6	416000	-		Hamoir et al. (1960)

[a] CP-myosin is the abbreviation for column-purified myosin. The type of ion-exchange resin used for the purification is shown in brackets.

Abbreviations: L.S., light scattering; EQUIL., sedimentation equilibrium; ARCH., Archibald; OSM., osmometry.

The model-independent $V_s/\bar{v}$ determined for myosin as 1.1 ± 0.1 is lower than that usually estimated for globular proteins (1.3 - 1.4). This model-independent value contrasts strongly with the large value earlier suggested for myosin (Rowe, 1964) on the basis of an assumed ellipsoidal model. Comparison of the $V_s/\bar{v}$ of myosin with that of other asymmetric particles is hampered by the lack of reliable published data. The reason lies in the fact that some fibrous protein solutions (i) exhibit self-interaction or (ii) sedimentation and viscosity experiments were not performed in the same buffer and on the same sample or (iii) sedimentation data were simply not fully corrected to infinite dilution. One may, however, speculate that proteins which have an extended coiled-coil α-helical structure, but are soluble by virtue of numerous charge groups, may contain less water of hydration (by volume) because of the effect of electrostriction (Edsall, 1953; Waugh, 1954). Measurement of the amount of electrostriction in myosin and tropomyosin (Kay, 1960) has shown that these muscle proteins do indeed show pronounced electrostriction, although estimation of $\bar{v}$ of these proteins from the specific volumes of the constituent amino acids suggest that the electrostriction effect is compensated for by the presence of 'excluded volume' (in the Linderstrøm-Lang, 1949, sense) within the molecule. Further discussion on whether this low $V_s/\bar{v}$ for myosin is unique or one which is displayed by other highly elongated particles will have to wait for reliable measurements of $V_s/\bar{v}$ on other proteins.

I shall digress for a moment to consider the effect of the hydration of the myosin molecule upon the amount of 'bound water' in muscle. This latter quantity is of interest in the study of muscular contraction because it affects the charge distribution on the myofilaments, the viscosity of the myoplasm and the frictional resistance created during shortening.

Since a substantial amount of the protein in muscle is myosin (about 38% of all protein, Huxley and Hanson, 1957; Hanson and Huxley, 1957), one might expect at first sight that the amount of water in muscle associated with the myosin filaments is small. As we shall see in the next Chapter this is not so, because myosin filaments contain large amounts of 'entrained solvent'.

Let us now return to the consideration of the swelling of the myosin molecule and its use in testing the validity of a prolate ellipsoid model. In the present study, estimates of $V_s/\bar{v}$ for a rigid prolate ellipsoid of revolution have given values of 2.0 ± 1.0 from the β-function and 4.3 ± 1.3 from the R-function. Of the two, the latter provides the more precise and accurate value of $V_s/\bar{v}$, but even so, this is inconsistent with the model-independent value. Thus the $V_s/\bar{v}$ method clearly demonstrates quantitatively that the supposition that the hydrodynamic properties of the myosin molecule can be adequately represented by a smooth, rigid prolate ellipsoid of revolution is invalid. Consequently, one must treat with scepticism any predictions of the molecular properties of myosin from hydrodynamic studies where this premise has been made (Lowey and Cohen, 1962; Herbert and Carlson, 1971).

It will be remembered from section III.1 that the presence of a monomer-dimer equilibrium has two important consequences: (a) it made one possibility for the structure of the A-filament extremely likely (namely a 2-stranded model with 2 myosins per cross-bridge), (b) it cast doubt onto the molecular weight of myosin. From the experiments described in this Chapter, the following conclusions may be made:

(i) There can be no significant monomer-dimer equilibrium in myosin solutions at high ionic strength, thus, the 2-stranded model with 2 myosins per cross-bridge is no more likely than any other possibility.

(ii) The molecular weight of myosin has been confirmed by a new method involving s^o and k_s and this clearly illustrates the usefulness of this procedure. It will be shown in the next Chapter that the s^o and k_s method for molecular weight determination may be used to calculate the molecular weight of the A-filament.

(iii) Estimation of $V_s/\bar{v}$ from k_η and k_s provides a means of quantitatively testing the validity of hydrodynamic models for macromolecules. Once again, this combined viscosity and sedimentation analysis will be used in the following Chapter to investigate the hydrodynamic behaviour of synthetic myosin filaments.

Having established these facts for myosin, we may now move on to consider the problems involved in determining the molecular weight of the A-filament.

CHAPTER IV

Hydrodynamic Studies on Synthetic Myosin Filaments

IV.1. Introduction

In section I.1.4 it was explained that the symmetry of the A-filament may be determined by measuring the molecular weight of a purified A-filament preparation provided that the molecular weight of myosin is precisely known. The previous Chapter presented evidence arguing against a monomer-dimer equilibrium and has removed the doubt on the molecular weight of the myosin monomer, so that, in principle, the determination of M^o of the A-filament can provide the symmetry. But the very nature of the A-filament makes measurement of molecular weight extremely difficult by conventional techniques; the problems are mainly caused by the high asymmetry of the A-filament: it has a diameter of 12 - 14nm (Huxley, 1963) and a length of 1.57μm (Craig and Offer, 1976a).

Let us consider the commonly used procedures for determining molecular weight and how suitable each may be for the particular problem of the A-filament molecular weight. (i) Light scattering requires dust-free solutions for analysis and the difficulty with purified A-filament solutions is to remove dust particles that are of the same size as the A-filament. However, Jolly and Josephs (1975) have announced that they have successfully measured the M^o of A-filaments by light scattering, although how they managed to overcome the aforementioned difficulty has not been published as yet. (ii) Sedimentation equilibrium is inapplicable as the A-filaments have a very small diffusion coefficient and would therefore take a very long time to reach equilibrium, if indeed equilibrium could be attained. (iii) The molecular weight of the A-filament (of the order of 10^8) precludes the use of calibrated gel columns for the determination of molecular weight. The filaments would appear in the void volume and therefore M^o would be indeterminable. (iv) Osmometry procedures cannot be used to estimate the molecular weight of A-filaments as the osmotic

pressure would be too low to be measured by conventional means. (v) The particle counting method has been used to determine the molecular weight of purified A-filaments (Morimoto and Harrington, 1974a). The principle of the procedure is to count the number of particles (n) in a known volume (V) of suspension at a known concentration (c); the molecular weight is then given by $M = N_A cV/n$. The method used by Morimoto and Harrington (1974a) was modified from the original procedure (Williams and Backus, 1949; Williams et al., 1951) since in the latter, the volume V was estimated by mixing the suspension with a sample of Dow Latex polystyrene particles at known number concentration and this created an uncertainty in V of about 5%. Instead, Morimoto and Harrington estimated the volume of the suspension when transferred to an analytical ultracentrifuge cell (c.f. IV.2.4); the filaments were then sedimented onto three electron microscope grids fixed to the bottom of the cell. These researchers claim that this technique produces an uncertainty in V of only 0.5% and they calculate M^o to be $204 \pm 11 \times 10^6$, giving the number of myosins/A-filament as 445 ± 24 and $N = 4.3 \pm 0.2$. But the M^o obtained by this method is critically dependent upon n (as estimated from electron microscopy) and c (Lauffer, 1951), and the following points should be considered.

(a) The distribution of A-filaments must be uniform so that the area sampled for counting is representative.

(b) All the filaments in the sampling area must be counted.

(c) The purified A-filaments were first fixed with formaldehyde and this may create aggregates by cross-linking. If these aggregates, or A-segments, go undetected in electron micrographs (because of their low concentration) this could lead to a serious under-estimation of n.

(d) The concentration was estimated by the Lowry et al. (1951) procedure, but these A-filament solutions were contaminated with about 4% by weight

of thin filaments and also other protein components of the myofilaments. (e) The presence of small fragments of A-filaments that are undetected by electron microscopy but do contribute towards the weight concentration was not considered. This is particularly important since it is later suggested (V.4) that these A-filaments are highly degraded.

Thus it seems that the particle counting method used by Morimoto and Harrington (1974a) may yield a large M^o due to under-estimation of n and/or over-estimation of c.

However, there is a new procedure which can be applied to give a more reliable estimate of the molecular weight of the A-filament. The technique is that of calculating M^o from s^o, k_s and $\bar{v}$ (Rowe, 1977) which has been successfully applied to myosin solutions (see previous Chapter). The concentration dependence of the sedimentation coefficient (k_s) is related to the frictional ratio of any sedimenting particle by the equation: $k_s = 2\bar{v}(V_s/\bar{v} + (f/f_o)^3)$ where $V_s/\bar{v}$ is the 'swelling' of the particle. Thus the frictional ratio of the particle estimated from k_s can be substituted into the Svedberg equation: $s^o = M^o(1 - \bar{v}\rho)/N_A f$, where $f = f/f_o \times f_o$, to obtain the molecular weight (see Appendix I).

There is, however, one draw-back. A concentrated sample of purified A-filaments (at least 1mg/ml) is required in order to determine k_s and the only two successful reports of purification of A-filaments (Morimoto and Harrington, 1973; Trinick, 1973) have produced solutions containing, at most, 0.1mg/ml of A-filaments. The problem arises from the difficulty in separating A- and I-filaments from homogenised myofibrils: as the A-filaments are sensitive to small changes in ionic strength and pH and tend to aggregate easily (and once aggregated are difficult to dissociate again), the procedures available to separate A- and I-filaments are limited. The two reports of purified A-filaments have both used the zone velocity

technique to separate A- and I-filaments by virtue of their different s values and it is the strong concentration dependence of the A-filament that is responsible for dilution. For the same reasons mentioned above, concentration of A-filaments by the usual methods (e.g. pervaporation, pelleting, ammonium sulphate precipitation) is unsuitable. The next Chapter describes attempts to obtain concentrated, purified A-filaments by an alternative procedure of isopycnic banding which, unfortunately, failed.

So, as only a dilute solution of purified A-filaments is available to us, k_s cannot be measured although, as will be shown in Chapter V, s^o can be directly obtained by active enzyme centrifugation (Cohen, 1963). If M^o for A-filaments is to be determined from s^o and k_s we therefore require a means of predicting k_s or f/f_o. It is possible to predict f/f_o for a prolate ellipsoid of revolution from its axial ratio (Perrin, 1936), so in theory, the molecular weight of the A-filament can be computed from s^o and f/f_o provided that an equivalent prolate ellipsoid can be applied as a hydrodynamic model. But it has been suggested elsewhere (Trinick, 1973) that A-filaments may exhibit an anomalous f/f_o compared with that of the equivalent prolate ellipsoid. For the first time, the suitability of ellipsoids of revolution as hydrodynamic models for biological macromolecules can be tested quantitatively by the $V_s/\bar{v}$ ($= k_\eta/k_s$) method (see III.4 and Appendix I). Since both k_η and k_s are unobtainable for purified A-filaments because of their low concentration in solution, it was decided to revert to synthetic myosin filaments as a model system for native A-filaments.

Synthetic myosin filaments can be obtained at high concentrations by diluting myosin solution to an ionic strength between 0.1 and 0.3 (Jakus and Hall, 1947; Noda and Ebashi, 1960; Zobel and Carlson, 1963) and they show several features similar to those of native A-filaments (Huxley, 1963). The similarities are: a bare central zone (0.15 - 0.2μm in length);

irregular surface projections down the rest of the filament length; tapered ends. These observations led Huxley (1963) to propose a model for the assembly of myosin molecules into bipolar filaments. However, subsequent studies (Kaminer and Bell, 1966; Moos et al., 1975) have uncovered discrepancies within this general model and, if synthetic filaments are to be used as a model system for A-filaments, the following points need to be explained:

(i) the absence of a bare-zone in some synthetic filaments

(ii) most synthetic filaments show no $43nm^{-1}$ reflection in optical transforms of electron micrographs, although there is good evidence to suggest that the $43nm^{-1}$ layer lines seen in X-ray diffraction patterns of resting muscle are due to native A-filaments.

(iii) most filaments formed in vitro show a range of lengths (0.2 - 12μm) whereas A-filaments of vertebrate skeletal muscle have a precisely defined length of 1.57μm.

If points (i) and (ii) reflect a difference in the packing arrangement of myosin molecules in A-filaments and synthetic filaments (for example a disruption of the helical symmetry in the latter) this may lead to a considerable difference in frictional ratio and hence invalidate the usefulness of synthetic filaments as a model system. There are several reasons that make this possibility of a different packing arrangement unlikely. Kaminer and Bell (1966), in observations made on synthetic filaments lacking a bare-zone, report the reappearance of the bare-zone when myosin molecules are dissociated from the filament by raising the pH from 6.5 to 8.0. There have been three reports of a 43nm or 14nm longitudinal repeat in synthetic myosin filaments: in the first report Eaton and Pepe (1974) observed myosin aggregates at I 0.3 and pH 7.0 that had no bare central zone but possessed a clear 43nm repeat down their

entire length. In the other two reports, Moos et al. (1975) observed a 14nm longitudinal repeat in filaments formed from column-purified myosin and Pinset-Härström and Morel (1975) detected a 43nm repeat by optical diffraction of electron micrographs of similar filaments.

That a 43.0nm repeat is not always observed in synthetic filaments may reflect the different specimen preparation procedures used for synthetic filaments and native thick filaments. Because of the random orientation of synthetic filaments in solution, X-ray diffraction cannot be used to detect axial repeats; instead, the filaments must be dried down onto grids after negative staining and electron micrographs of the filaments analysed by optical diffraction (a similar procedure may be used for samples of isolated A-filaments). It may be that the strong surface tension forces exerted on synthetic filaments (or purified A-filaments) during drying perturbs the regular arrangement of myosin heads. In support of this hypothesis, reflections analogous to those from X-ray diffraction of resting muscle have been obtained by optical diffraction of electron micrographs of purified A-filaments by (a) ensuring that surface tension effects are avoided or (b) by using sophisticated image analysis procedures. Trinick (1973) avoided surface tension forces by critical-point drying purified A-filaments from rabbit psoas muscle; optical diffraction of electron micrographs of these specimens showed reflections at 14.3, 43.0 and 21.5nm^{-1} (the last being the strongest reflection seen). The 21.5nm repeat was suggested to arise from the circumferential distance between one myosin head and its nearest neighbour and its intensity was considered to be caused by the myosin heads being 'slewed' at an angle to the longitudinal axis along the 21.5nm helix (Trinick, 1973), Figure 2.

Gibbs and Rowe (1974) have used a 'linear integration' procedure for image analysis to show that similar transforms can be obtained from

electron micrographs of conventionally prepared negatively contrasted specimens, though with a very large background 'noise'. Considering these points, the lack of a 43.0nm repeat in synthetic filaments may be caused by disruption of the regular arrangement of myosin heads during specimen preparation for the electron microscope rather than as a consequence of a different packing scheme for the myosin tails. It should be remembered that the myosin heads only act as a 'pointer' to the underlying repeat of the myosin tails (Huxley, 1963): simply because the myosin heads are disordered in synthetic filaments does not immediately infer a disorder in the packing of the LMM portions.

Thus, observations of the absence of a bare-zone or a 43nm repeat in synthetic filaments can be accounted for without assuming a difference in the packing arrangement between synthetic filaments and native A-filaments. The synthetic filaments are, by this argument, likely to show the same hydrodynamic properties as purified A-filaments. But there is a third consideration: that of the length of synthetic filaments. There has been no report to date of a homogeneous population of synthetic filaments made from vertebrate skeletal muscle myosin that has an average length of 1.57μm (i.e. that of native A-filaments). Indeed, synthetic filaments formed by myosin from various sources (smooth muscle myosin: Kaminer, 1969; Sobieszek, 1972; Pollard, 1974; cardiac muscle myosin: Carney and Brown, 1966; non-muscle myosin: Pollard and Weihing, 1974) show a range of lengths. For skeletal muscle myosin, the average length has been shown to be a function of ionic strength and pH (Josephs and Harrington, 1966; Kaminer and Bell, 1966; Sunouchi et al., 1966; Sanger, 1971). The method of lowering the ionic strength, by dilution or dialysis, has also been recognised to influence filament length (Huxley, 1963; Katsura and Noda, 1971; Sanger, 1971) and Pinset-Härström and Morel (1975) have interpreted

this as due to the length of time spent at a critical ionic strength. Therefore, by controlling I, pH and speed of dilution it is possible to alter the length distribution of synthetic filaments.

For this study, the most suitable preparation would be one containing a homogeneous population of synthetic filaments of length 1.57μm but, as already mentioned, this has not been achieved to date. Longer filament preparations show extensive heterogeneity and tend to produce more than one schlieren peak in the ultracentrifuge (the reason for this is considered in IV.4.9), but short filaments (0.5 - 0.7μm) produced by rapid dilution to I 0.13, pH 7.0, show a unimodal length distribution and single schlieren peaks (Katsura and Noda, 1971). It is these shorter filaments that have been used as a model system for A-filaments since the advantage of their monodispersity more than compensates for their short length. Now the procedure mentioned earlier for determining $V_s/\bar{v}$ (from k_η and k_s) requires that there is no self-interaction and that k_η and k_s are determined upon the same sample. With these criteria satisfied, the goodness of fit of an equivalent prolate ellipsoid of revolution may be tested by determining the model-dependent value of $V_s/\bar{v}$ from the R-function.

This Chapter describes sedimentation and viscosity experiments performed on synthetic myosin filament preparations. Although this investigation was prompted by the need to determine $V_s/\bar{v}$ and test the suitability of an equivalent prolate ellipsoid as a hydrodynamic model, further useful information can be obtained. For the first time it is possible to estimate the ideal molecular weight of synthetic myosin filaments (from s^o and k_s) without any assumptions as to their shape. From the molecular weight and length-average length of the filament preparation (estimated from electron microscopy), the number of myosin molecules/14.3nm repeat, and hence the symmetry, may be found.

It will be shown that:

(i) there is a variation of s^o and k_s for different synthetic filament preparations and this is reflected in a variation in N (the number of myosins/14.3nm interval). This is interpreted not as a change in symmetry but as radial growth of a basic filament structure.

(ii) the model-independent $V_s/\bar{v}$, from k_η and k_s, shows that an equivalent prolate ellipsoid cannot account for the hydrodynamic behaviour of synthetic filaments

(iii) the f/f_o of a 'length-equivalent' prolate ellipsoid of revolution can be related to the true f/f_o of synthetic filaments.

IV.2. Methods

IV.2.1. Preparation of Synthetic Filaments

Myosin A, prepared as described in section III.2.1 and at a concentration of 25mg/ml, was dialysed against stock buffer, the pH of which was adjusted to 7.0 with potassium hydroxide. The myosin solution was then diluted to I 0.13 by rapidly adding, from a pipette, 6mM-potassium phosphate buffer, pH 7.0 at 4°C. The solution became very turbid as is usual for preparations of synthetic filaments. A buffer of I 0.13, pH 7.0, was made up in exactly the same way except for using stock buffer in place of myosin A solution. To the buffer was added solid EGTA to a final concentration of 1mM, the pH readjusted to 7.0 and the synthetic filaments dialysed against this buffer: the diffusate was used in dilutions of synthetic filaments and as a reference solution in ultracentrifugation. Addition of EGTA to the myosin A solution prior to synthetic filament formation resulted in the formation of a precipitate, but synthetic filaments made as described above, showed no such precipitate and were

stored at 4°C for a maximum of seven days when unused material was discarded. The presence of myosin monomer in synthetic filament solutions was investigated by centrifuging three 6ml samples, with starting concentrations of 1, 2 and 5mg/ml, at 60000rev./min (295000g) for 2h. The concentration of protein in the supernatant was estimated from the absorbance at 280nm, corrected for the turbidity measured at 320nm, using a fourth power wavelength exponent, see II.2.7.

IV.2.2. SDS gel Electrophoresis

SDS gel electrophoresis of myosin A samples used for synthetic filament formation was carried out as described in II.2.1 and II.2.2.

IV.2.3 Electron Microscopy

Synthetic myosin filaments were prepared for electron microscopy and the lengths measured from electron micrographs as described in II.2.6. The 'length-average length' was calculated from the equation:

$$l_{ave} = \frac{\sum l_i^2 N_i}{\sum l_i N_i} \qquad (8)$$

where N_i is the number of filaments in the length range $l_i \pm 0.05\mu m$ and l_i has the values 0.05, 0.15, 0.25μm etc.

IV.2.4. Ultracentrifugation Studies

All sedimentation velocity experiments were performed at 5 - 7°C and 15000 - 18000rev./min. Double sector cells of 10mm pathlength fitted with wedge windows were used to analyse three different synthetic filament samples simultaneously (over a concentration range of 3 to 0.5mg/ml). Conventional schlieren optics were used, together with the 'analogue

multiplexer', taking photographs every 2min. For concentrations below 0.5mg/ml single runs were carried out using 20mm double sector cells, again with schlieren optics.

Immediately prior to cell loading, 10µl of a solution containing 1.0M-$MgCl_2$ and 0.5M-ATP, adjusted to pH 7.0 with potassium hydroxide, was added to a 1ml sample of synthetic filaments to give a final concentration of 10mM-$MgCl_2$ and 5mM-ATP. The buffer used in the reference cell was made up to contain the same concentrations of $MgCl_2$ and ATP. The concentration of synthetic filaments was measured in each sample by the modified Biuret method, see II.2.7. Mg-ATP was added in order to prevent myosin - actin interaction and to reduce possible interaction between myosin filaments during centrifugation (see IV.4.10). The presence of 1mM-EGTA in the synthetic filament preparation chelated any free Ca^{2+} which normally causes superprecipitation of myosin A samples upon addition of ATP. No superprecipitation was observed in synthetic filament preparations over the time span of the centrifugation.

A control run was carried out on identical synthetic filament samples in the presence and absence of Mg-ATP to test: (a) if the presence of ATP affected the sedimentation coefficient and (b) if the plateau concentration was altered during the course of the experiment after correcting for radial dilution. The concentration in the 'plateau region' during sedimentation is defined by the radial dilution law for sector-shaped cells:

$$c_t = c_o \times \frac{r_m^2}{r_t^2} \qquad (9)$$

where c_o is the initial concentration, r_m is the radial position of the meniscus and r_t is the position of the boundary after a time t. The plateau concentration, c_t, might decrease in the presence of ATP due to

superprecipitation occurring during centrifugation: the large myosin filament - actin complexes sedimenting rapidly to the bottom of the cell. If the plateau concentration decreases, the sedimentation coefficient in the presence of ATP will be higher than that in its absence (because of the dependence of s upon concentration).

The change in the plateau concentration was investigated in the following manner. The initial concentration was measured by the modified Biuret method (II.2.7) and the volume of sample in the centrifuge cell calculated from r_m and the dimensions of the cell. After centrifugation for a time t (taking photographs every 2min in order to determine s), the centrifuge was slowed taking photographs at 20 second intervals to check that no mixing occurred and to determine the final boundary position. When the centrifuge was stopped, the total supernatant was removed very carefully without disturbance of the pellet and the concentration of myosin in the supernatant measured. Now the concentration of myosin in the protein-containing phase between the final boundary position, r_t, and the cell bottom, has been diluted by the protein-free phase between r_m and r_t. So correction of the concentration of myosin in the supernatant for this dilution yields the actual concentration in the plateau region. This may then be compared with the predicted plateau concentration, c_t, assuming that the radial dilution law is obeyed (i.e. $c_t = c_o \times r_m^2 / r_t^2$). The results have been summarised below:

	Initial concn. (mg/ml)	Predicted plateau concn. (mg/ml)	Actual concn. in plateau region (mg/ml)	$s_{20,w}$ (S)
+ATP	1.44	1.33	1.32 ± 0.02	107.0 ± 2.0
-ATP	1.44	1.34	1.35 ± 0.02	104.7 ± 1.9

One may conclude that there is no significant depletion of the plateau concentration by superprecipitation (or self-interaction) of myosin filaments during centrifugation in the presence of ATP. This finding is confirmed by the fact that the synthetic filaments did not sediment appreciably faster in the presence of ATP than in its absence.

IV.2.5. Viscosity Measurements

Since the viscosity of synthetic myosin filaments is dependent upon shear rate (Josephs and Harrington, 1966), the viscosity was measured at various shear rates and extrapolated to zero rate of shear. Different flow rates and hence different shear rates, G (since G is inversely proportional to flow rate), were produced by a constant pressure apparatus, Figure 16, which was connected to the viscometer and a manometer by a three-way tap. Pressures, which were all less than atmospheric, were measured by the difference in the liquid levels in the arms of the manometer both before (Δh_1) and after (Δh_2) viscosity measurements. The pressure decreased slightly during a viscosity measurement and an average (Δh) was taken (the difference between Δh_1 and Δh_2 was about 0.1 - 0.3cm). The same viscometer, water bath and cleaning procedure was used as described previously (see III.2.9). All flow times were measured at a temperature of 5.0°C.

The stock synthetic filament solution was diluted with buffer, and 1M-$MgCl_2$ 0.5M-ATP, pH 7.0, was added to each dilution just before viscosity measurement to give a final concentration of 10mM-$MgCl_2$, 5mM-ATP. Once again the reason for this addition of Mg-ATP was to try to eliminate myosin filament interaction during viscosity determinations (IV.2.4). The buffer was similarly made up to 10mM-$MgCl_2$ and 5mM-ATP and flow times (t_o) were measured over a wide range of Δh. A least squares quadratic fit was used to compute the best curve through the experimental points. Since Δh was

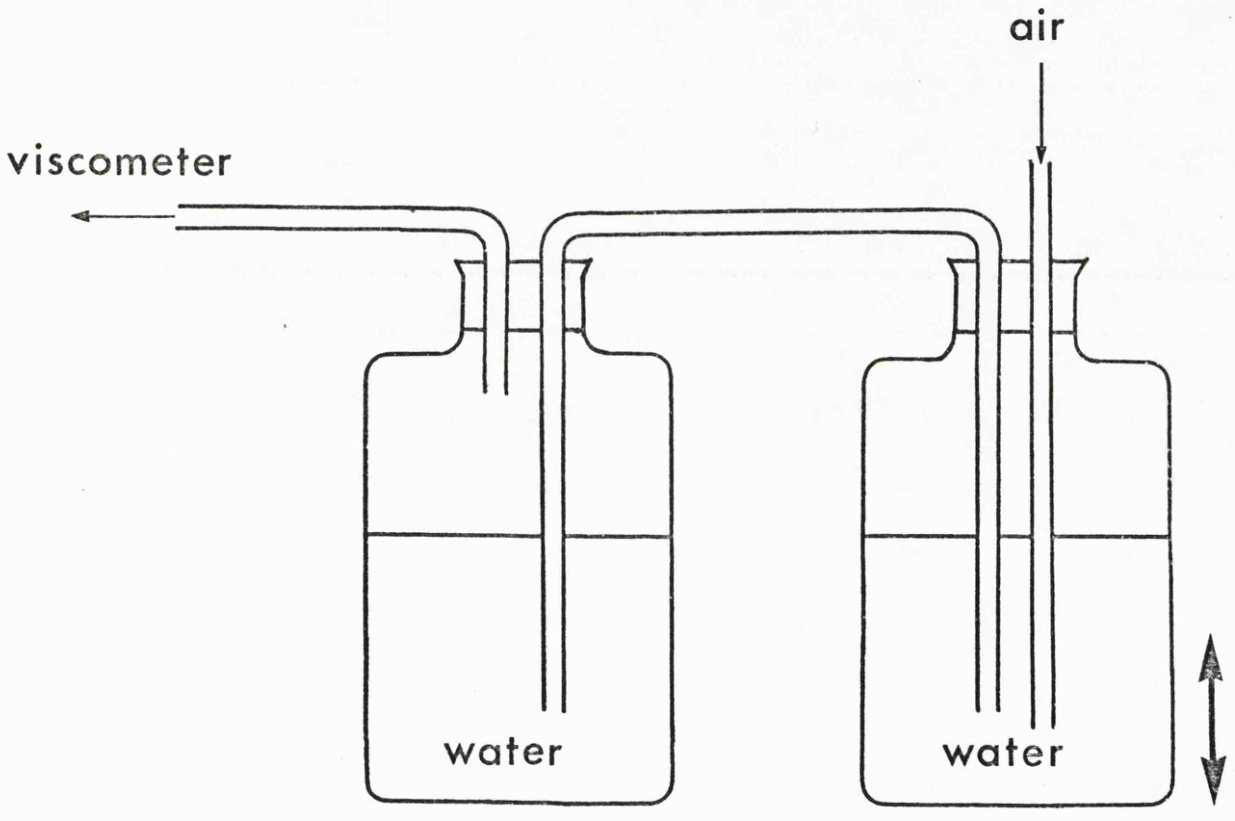

Figure 16 Constant pressure apparatus used to generate different shear rates.

not exactly reproducible, the flow time of buffer at the actual Δh used in viscosity determinations of synthetic filament solutions was found by interpolation. The kinetic energy correction was negligible (less than 1%) and was ignored; Tanford's correction to solution density (Yang, 1961) was applied using $\bar{v}$ = 0.720ml/g, Kay (1960). The reduced viscosity at concentration, c, and shear rate, G, is given by

$$\left(\frac{\eta_{sp}}{c}\right)_{G,c} = \left(\frac{\eta}{\eta_o} - 1\right)/c \qquad (10)$$

where

$$\frac{\eta}{\eta_o} = \frac{\rho t}{\rho_o t_o} \qquad (11)$$

ρ is the solution density; ρ_o is the solvent density; t is the flow time and t_o is the solvent flow time. The shear rate, G, is given by $G = 4V/\pi R^3 t$, where V is the volume of the viscometer bulb, R is the radius of the capillary. The reduced viscosity, $(\eta_{sp}/c)_{G,c}$, was extrapolated to zero rate of shear and zero concentration to yield $[\eta]$, the intrinsic viscosity, in the usual manner. The data were also treated using an Econometric Software Package (provided by the Leicester University Computer Laboratory) run on the CDC Cyber 72. The program was a multiple least squares regression to solve a set of over-determined simultaneous linear equations for more than one variable. The equations used are:

$$\left(\frac{\eta_{sp}}{c}\right)_{G,c} = \left(\frac{\eta_{sp}}{c}\right)_{G=0,c} + \alpha\left(\frac{\eta_{sp}}{c}\right)_{G=0,c} . G \qquad (12)$$

where $\alpha(\eta_{sp}/c)_{G=0,c}$ is the slope of the line obtained from a plot of $(\eta_{sp}/c)_{G,c}$ <u>versus</u> G.

$$\left(\frac{\eta_{sp}}{c}\right)_{G=0,c} = [\eta] + k_\eta[\eta]c \qquad (13)$$

where

$$[\eta] = \left(\frac{\eta_{sp}}{c}\right)_{G=0,\,c=0} \qquad (14)$$

Substituting eqn. 13 into eqn. 12 we have:

$$\left(\frac{\eta_{sp}}{c}\right)_{G,c} = [\eta] + k_\eta[\eta]c + \alpha[\eta]G + \alpha k_\eta[\eta]Gc \qquad (15)$$

The variables are c, G and Gc. Concentration, c, was measured after viscosity determinations on duplicate samples by the modified Biuret method (II.2.7). The presence of ATP prevents the use of absorbance at 280nm to determine concentration and the Lowry et al. (1951) procedure is affected by K^+ (Vallejo and Lagunas, 1970) and Mg^{2+} (Kuno and Kihara, 1967). The modified Biuret method, on the other hand, was not affected by either ion and gave reproducible results if the filaments were first solubilised by allowing the solution to stand for 10min after the addition of 10M-NaOH.

IV.3. Results

IV.3.1. SDS gel Electrophoresis

The SDS gels of myosin A samples used to prepare synthetic filaments are identical to those in the previous Chapter, see Plate 2 (III.3.1). A small amount of actin is always present in these myosin A samples.

IV.3.2. Electron Microscopy

A general view of 'positively stained' filaments at low magnification is shown in Plate 7. At higher magnification, Plate 8, the filaments can be seen to have tapered ends; surface projections may also be observed. A clear bare-zone is only rarely discernible in these synthetic filament preparations.

The length distributions of filament preparations are featured as histograms in Figure 17. The length-average length is also given (see section IV.2.3 for the method of calculation). Note that in all synthetic filament preparations a narrow length distribution was obtained with 90 - 95% of the filaments falling in the range 0.2 to 1.0μm. The distribution was always unimodal.

IV.3.3. Ultracentrifugation Studies

Total precipitation of synthetic filaments in the absence of Mg-ATP was accomplished by centrifugation at 60000rev./min for 2h, see section IV.2.1. Less than 0.05mg/ml of protein remained in the supernatant, indicating that most of the myosin was polymerized into filaments under these conditions. In ultracentrifugation experiments no peak corresponding to myosin monomer was ever detected, indicating that there is no monomer-polymer equilibrium, Plate 9. All synthetic filament preparations sedimented as a single hypersharp peak as seen by schlieren optics; the hypersharp boundary is created because of the strong s upon concentration dependence of these synthetic filaments (see below).

Sedimentation coefficients were calculated as described previously (II.2.5). Standard errors on individual $s_{20,w}$ values were between 1 and 2%, the errors arising largely from the difficulty in estimating the centre of a schlieren peak that becomes broader as centrifugation proceeds because of

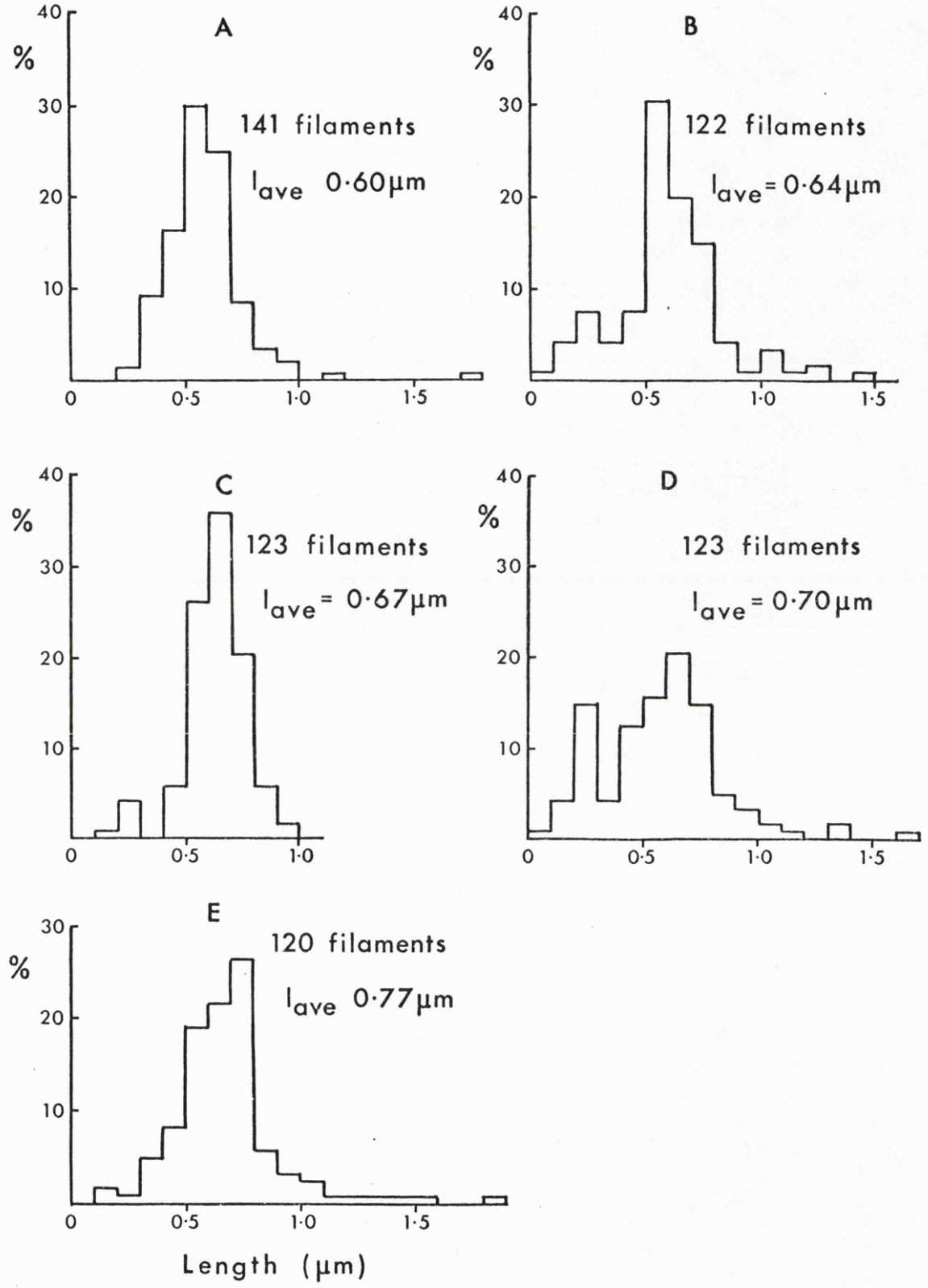

Figure 17 Length distributions for five synthetic filament preparations

The number of filaments counted and the length-average length (l_{ave}) are indicated.

Plate 7. Electron micrograph of positively stained synthetic myosin filaments.

Magnification: x64000.

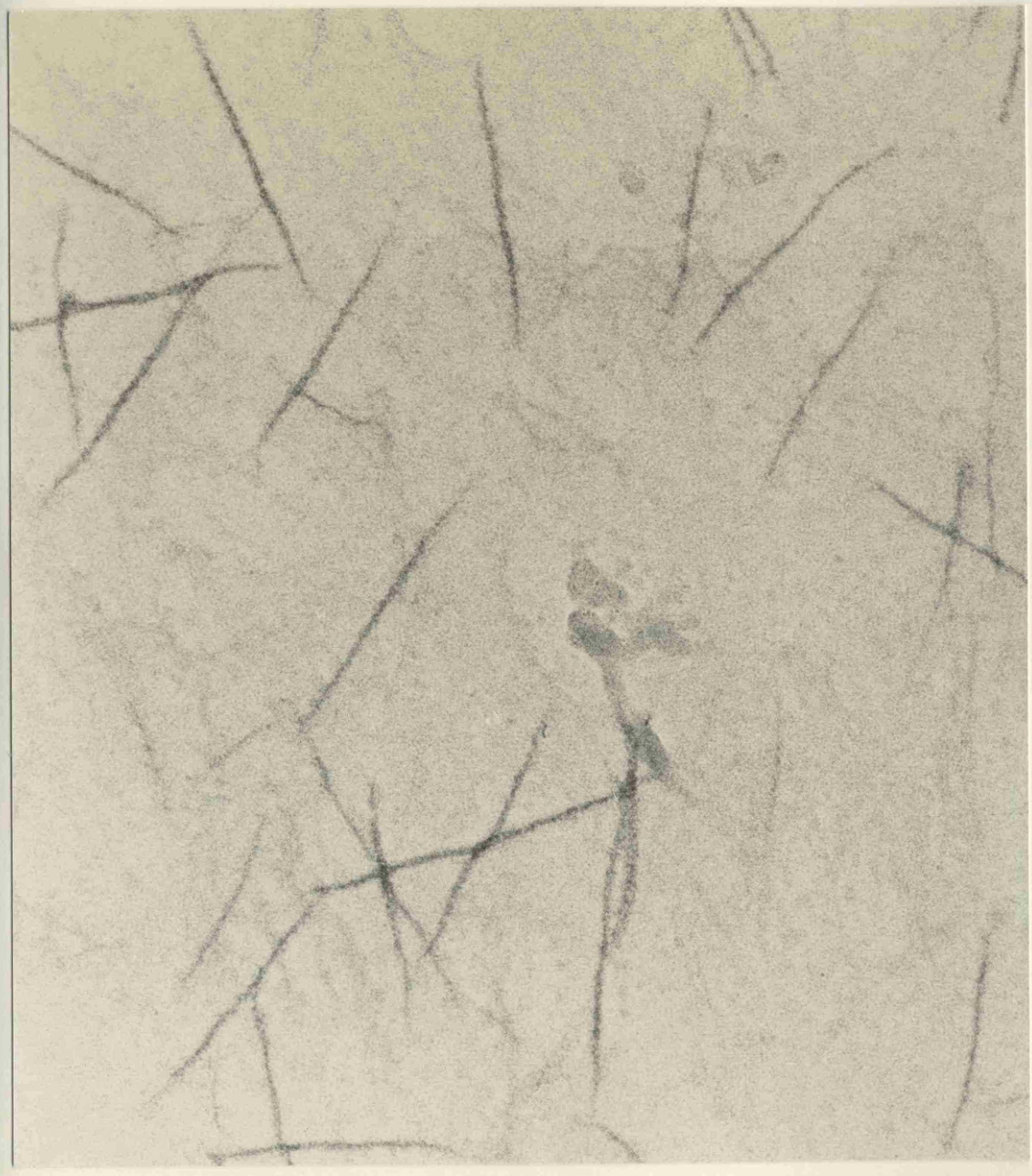

Plate 8. Electron micrograph of synthetic myosin filaments at high magnification.

The synthetic filaments have tapered ends and surface projections. A bare-zone is only occasionally observed. Magnification: x160000.

Plate 9. Schlieren pattern of synthetic filaments.

The concentration of synthetic filaments was 0.95mg/ml. Speed: 15760rev./min; temperature: 6.3°C. The direction of sedimentation is from right to left.

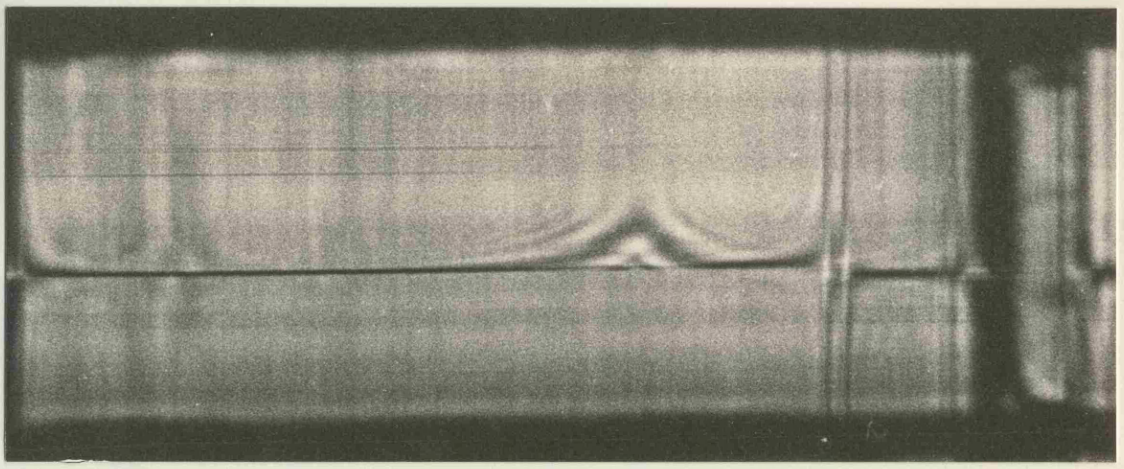

polydispersity. The $s_{20,w}$ *versus* concentration plot for five synthetic filament preparations are shown in Figure 18. All preparations show linear concentration dependence over the concentration range studied (0.3 to 3.0mg/ml). It can be seen that there is a wide range of $s^o_{20,w}$ and k_s for these synthetic filament preparations, although the length-average length varies from 0.60 to 0.77μm, Table 3, only.

IV.3.4. Molecular Weight and Symmetry of Synthetic Filaments

The molecular weight of each filament preparation was calculated from k_s and s^o via equation 15 in Appendix I. The value of $V_s/\bar{v}$ used in the equation: $k_s = 2\bar{v}(V_s/\bar{v} + (f/f_o)^3)$ was 2.3, as determined from the ratio of k_η and k_s (see section IV.3.5). The number of myosin molecules/14.3nm, N, was calculated after first correcting the molecular weight of the filament for the weight fraction due to C-protein (3.5%, see Morimoto and Harrington, 1974a).

$$N = \frac{\text{mol. wt. of filament} \times 0{\cdot}965}{\text{mol. wt. of myosin}} \times \frac{14{\cdot}3}{l_{ave}}$$

where the molecular weight of myosin used was 470000 and l_{ave} refers to the weight-average length in nm. The results are presented in Table 3. Column six of the table shows that N obtained in this manner varies with the synthetic filament preparation, as would be expected, in qualitative terms. from the variability of s^o and k_s. The diameter of a prolate ellipsoid of revolution with the same length and M^o as the synthetic filaments (shown in Table 3, column 7) was calculated from

$$b = \left(\frac{3M\bar{v}}{4\pi N_A a}\right)^{1/2} \qquad (16)$$

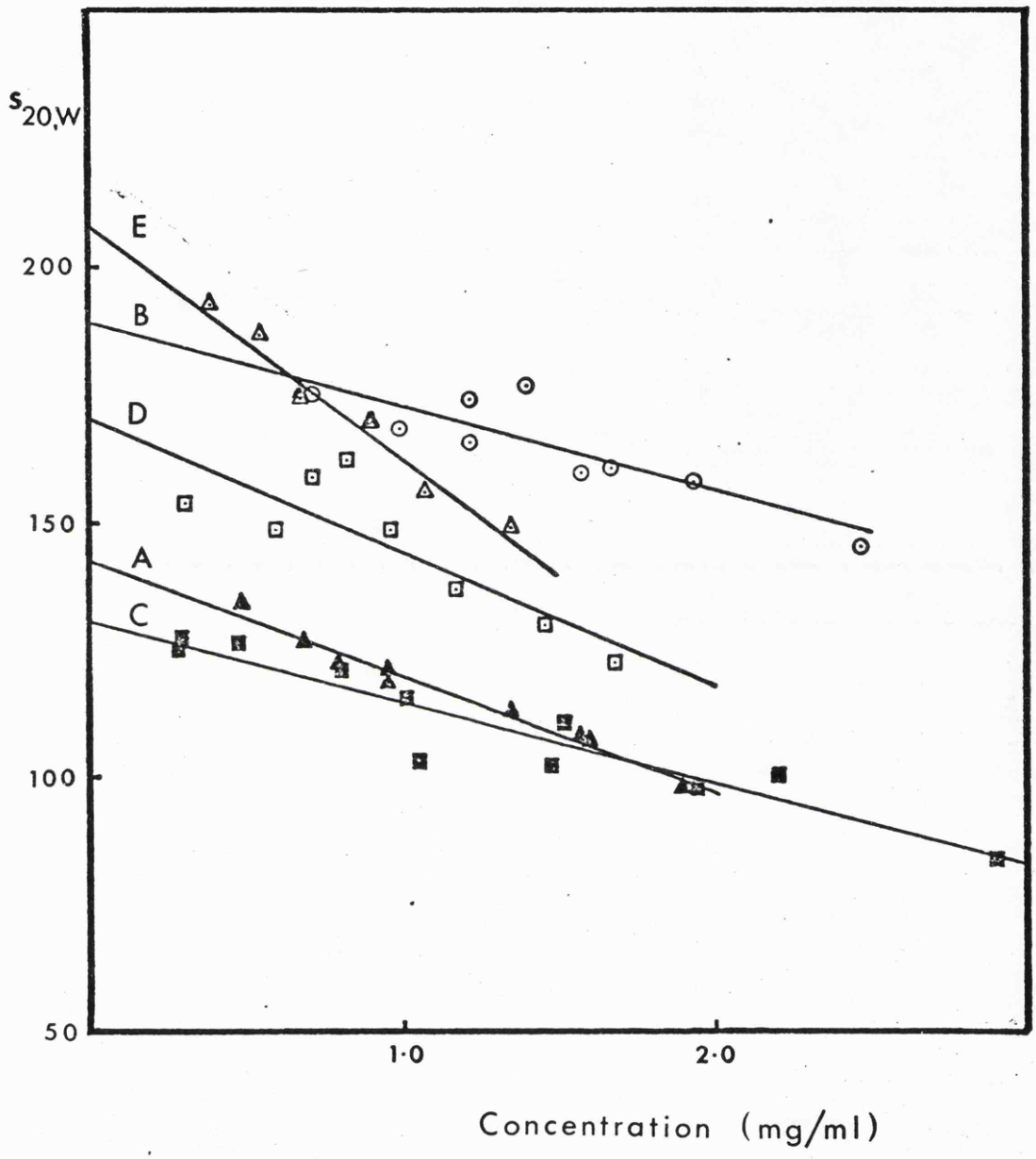

Figure 18 The concentration dependence of s for five synthetic filament preparations

The length histogram for each preparation, identified by A,B,C,D or E, is shown in Figure 17.

Table 3. The molecular weight and number of myosins/14.3nm for synthetic myosin filaments.

Prep.	Length average length (μm)	k_s (ml/g)	$s^o_{20,w}$ (S)	M.W.[a] via s^o and k_s $x10^{-7}$	N ± S.E.	Radius of [b] prolate ellipsoid (nm)
A	0.60	161	143	8.15	3.7 ± 0.2	8.4
B	0.64	86	189	8.97	4.2 ± 1.6	9.0
C	0.67	121	132	6.20	2.8 ± 0.3	7.3
D	0.70	154	170	10.3	4.4 ± 0.9	9.2
E	0.77	218	208	16.7	6.5 ± 0.6	11.2

[a] $V_s/\bar{v}$ used was 2.3

[b] Radius of the length-equivalent prolate ellipsoid from the equation: $b = (3M\bar{v}/4\pi N_A a)^{\frac{1}{2}}$ where M is the molecular weight (column 5) and 'a' is half of the length average length (column 2).

a is half the length-average length, N_A is Avogadro's Number and $\bar{v}$ is 0.728ml/g at 20°C (Kay, 1960).

IV.3.5. Determination of $V_s/\bar{v}$ ('swelling')

(a) Estimation of k_η

The dependence of η_{sp}/c with shear rate (G) is shown in Figure 19. The extrapolated values of η_{sp}/c at zero rate of shear were replotted against concentration, Figure 20. From the slope and the intercept, the following values were obtained: intrinsic viscosity, $[\eta]$, was 176ml/g; k_η = 366ml/g; Huggins constant ($k_\eta/[\eta]$) was 2.08 (estimation of errors on these values is difficult because of the double plot used). An alternative way of representing the results is by a Zimm-type plot. A Zimm plot (Zimm, 1948) is used in the presentation of light scattering data and includes extrapolations to both zero scattering angle and zero concentration. The same procedure was used here to extrapolate to zero concentration and zero rate of shear. Experimental points were smoothed by the application of a linear least squares statistical procedure and the η_{sp}/c values at constant shear rate interpolated. The smoothed points were plotted against G + kc where k is a scaling constant (chosen as 100). The lines in Figure 21 are the extrapolations to zero concentration at constant shear rate, and to zero shear rate at constant concentration. The symbol (▲) represents η_{sp}/c at zero concentration and (●) represents η_{sp}/c values at zero shear rate.

The results give two estimates of $[\eta]$: one from the extrapolation at zero shear rate, $[\eta]$ = 176.1ml/g and the other from extrapolation at zero concentration, $[\eta]$ = 174.5ml/g. The difference between the two values is not significant. The experimental data were also treated using the simultaneous least squares regression for more than one variable (the Econometric Software Package, ESP, provided by the Leicester University

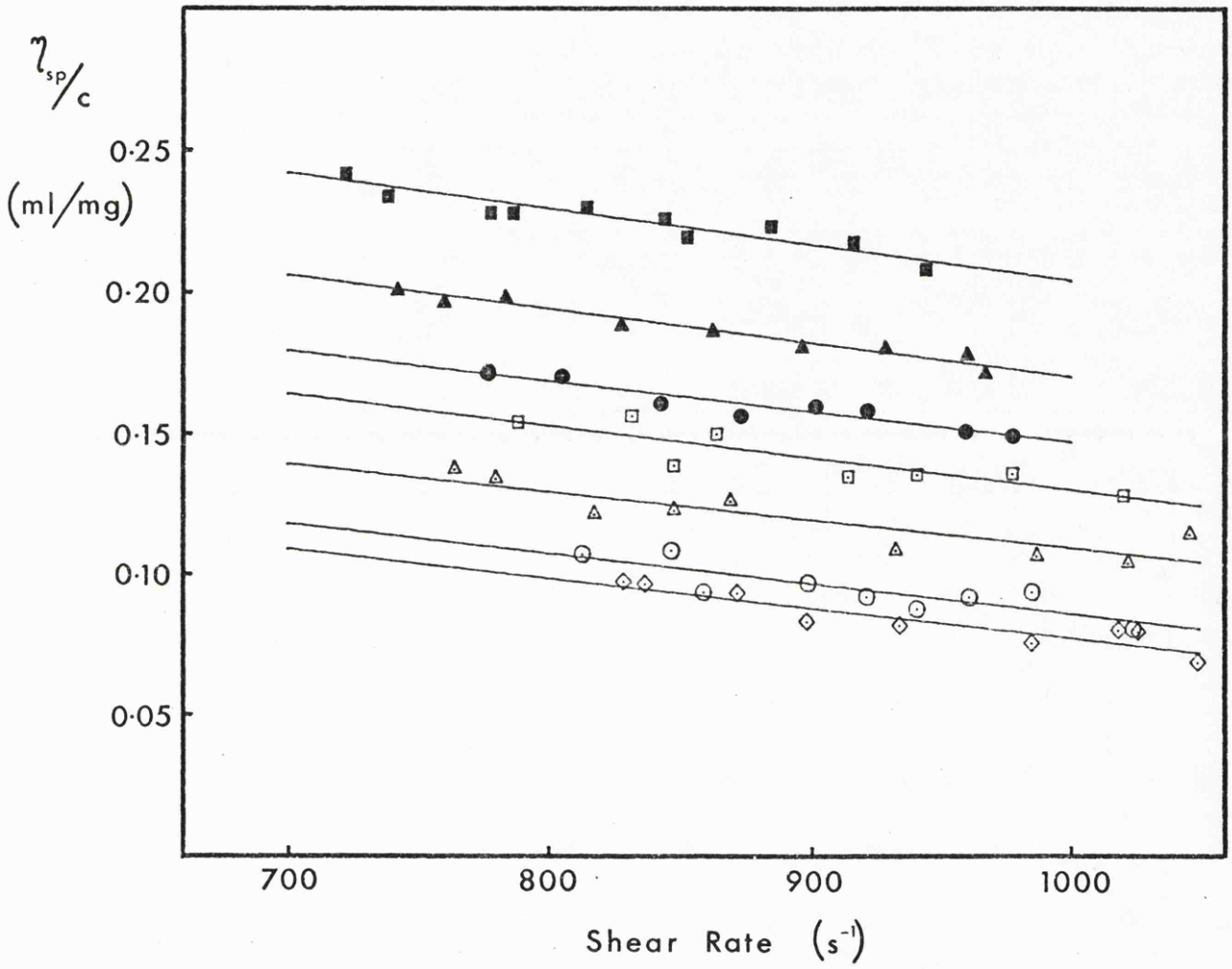

Figure 19 Reduced viscosity versus shear rate for synthetic myosin filaments in 0.13M-KCl, pH 7.0, at 5°C

The concentrations (mg/ml) are: 0.13 (◇), 0.26 (⊙), 0.53 (△), 1.05 (⊡), 1.31 (●), 1.67 (▲) and 2.25 (■).

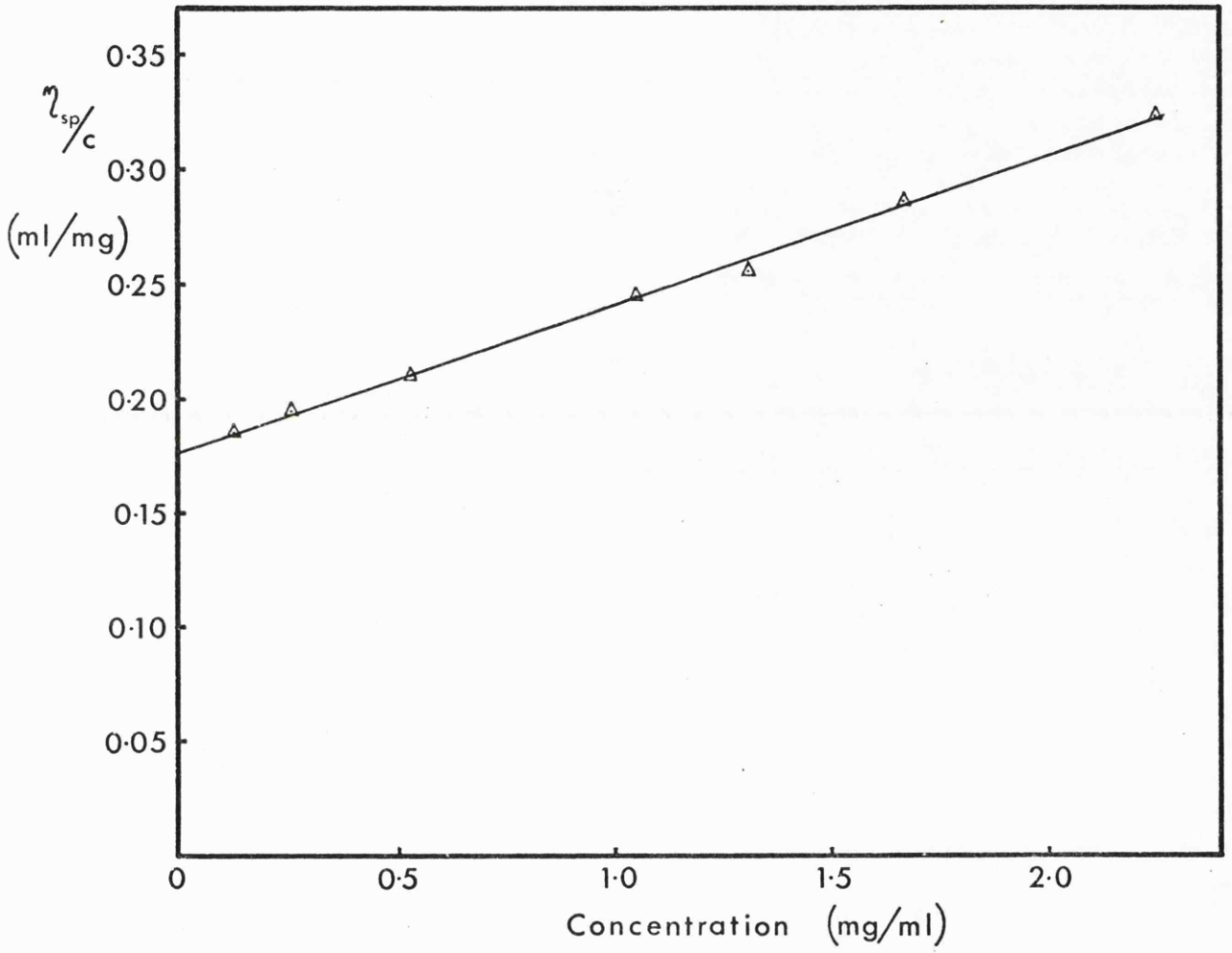

Figure 20 Reduced viscosity at zero shear rate against concentration of synthetic myosin filaments

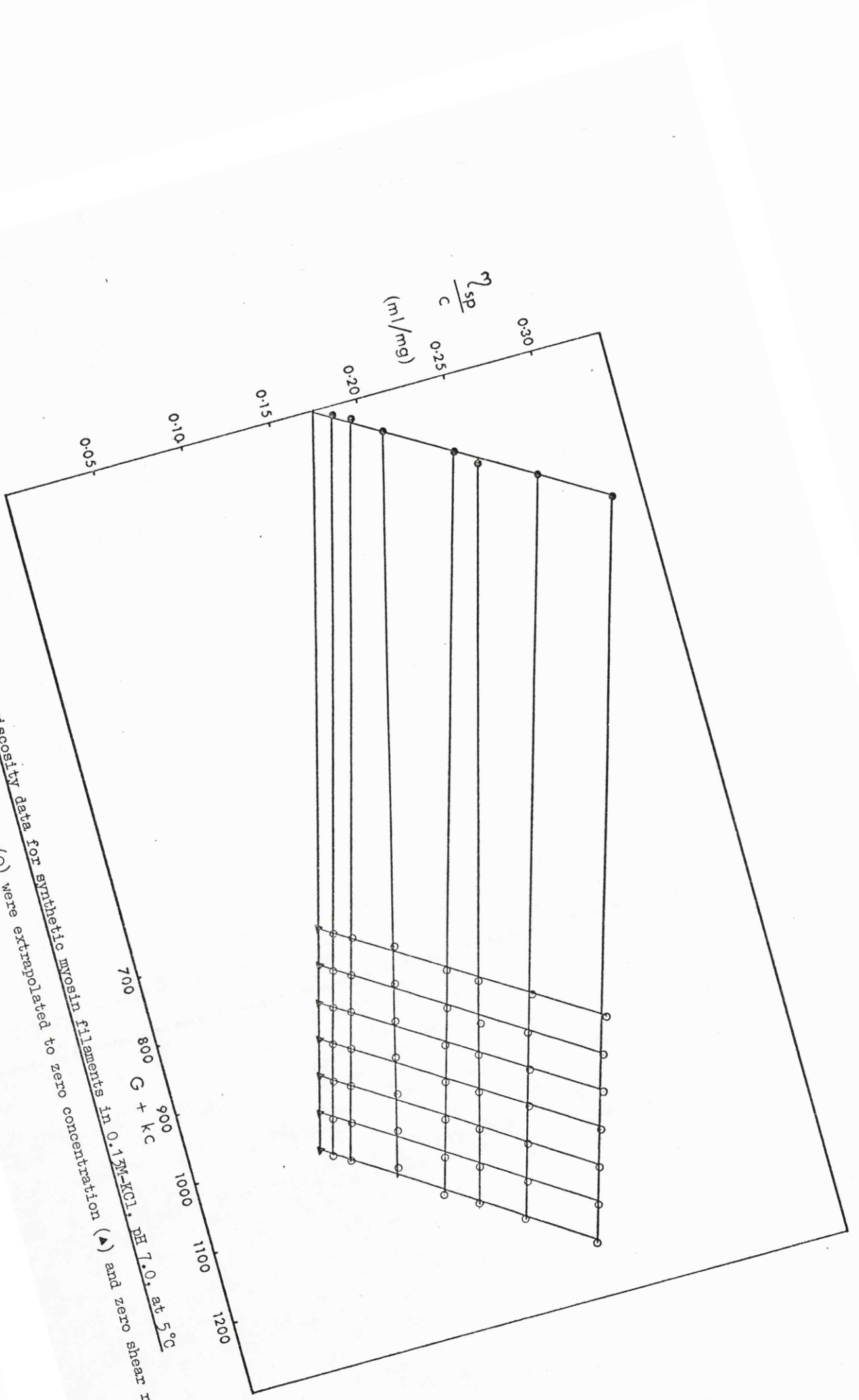

Figure 21 Ziimm-type plot of viscosity data for synthetic myosin filaments in 0.13M-KCl, pH 7.0, at 5°C. The smoothed experimental points (○) were extrapolated to zero concentration (▲) and zero shear rate (●).

Computer Laboratory). The print-out is shown in Figure 22 and gives the actual (*) and fitted points (+) together with an estimate of the residual of each point from the line. On the right-hand side of the Figure, the residuals are plotted to show how each point lies in relation to the standard error limits (dotted lines) on the 'best straight line' through all the points. The following values were obtained: $[\eta]$ = 176.8 ± 11.7ml/g; k_η = 375 ± 75ml/g and Huggins constant = 2.1 ± 0.6. Use of the ESP computer program is more convenient than the conventional method of obtaining $[\eta]$ and k_η and more importantly provides an estimate of the errors involved.

(b) Estimation of k_s

The $s_{20,w}$ against concentration plot obtained for the same synthetic filament preparation used in the viscosity measurements is shown in Figure 23. A least squares regression of the points gave $s^o_{20,w}$ = 143.0 ± 2.0S and k_s = 160.7 ± 10.0ml/g. Now k_η/k_s is numerically equal to $V_s/\bar{v}$ (Appendix II) but the viscosity results have been corrected to solution density (using Tanford's correction): the value of k_s when corrected likewise to solution density is 160.8 ± 10.0ml/g. The ratio $V_s/\bar{v}$ was calculated to be 2.3 ± 0.2, and this value has been used to calculate the molecular weight of synthetic filaments from $s^o_{20,w}$ and k_s (IV.3.4).

(c) Estimation of $V_s/\bar{v}$

The $V_s/\bar{v}$ determined from k_η/k_s is independent of any assumed model (and of the absolute concentration of synthetic filaments). The validity of an equivalent prolate ellipsoid or oblate ellipsoid of revolution as a model for synthetic filaments can be tested by using the R-function ($R = k_s/[\eta]$, see Appendix II) to determine axial ratio (a/b) and from thence, using the viscosity increment, to find the model-dependent $V_s/\bar{v}$. The viscosity increment, ν, was found from the axial ratio via Table VII of Yang (1961) in which ν is computed for a range of a/b's using the Simha

PLOT OF ACTUAL(*) AND FITTED(+) VALUES

PLOT OF RESIDUALS(*)

ID	ACTUAL	FITTED	RESIDUAL
1	.2421	.2379	.425E-02
2	.2341	.2358	-.175E-02
3	.2283	.2310	-.275E-02
4	.2282	.2300	-.179E-02
5	.2303	.2266	.370E-02
6	.2262	.2230	.319E-02
7	.2198	.2220	-.217E-02
8	.2236	.2181	.552E-02
9	.2180	.2142	.381E-02
10	.2085	.2108	-.227E-02
11	.2008	.2002	.585E-03
12	.1965	.1981	-.159E-02
13	.1961	.1953	.276E-02
14	.1884	.1902	-.176E-02
15	.1863	.1891	-.198E-03
16	.1808	.1821	-.130E-02
17	.1803	.1783	.202E-02
18	.1780	.1746	.342E-02
19	.1716	.1738	-.216E-02
20	.1722	.1744	-.217E-02
21	.1707	.1711	-.647E-03
22	.1610	.1668	-.585E-02
23	.1567	.1633	-.655E-02
24	.1602	.1601	.126E-03
25	.1584	.1578	.630E-03
26	.1512	.1534	-.219E-02
27	.1495	.1513	-.184E-02
28	.1545	.1573	-.285E-02
29	.1567	.1525	.421E-02
30	.1391	.1507	-.116E-01
31	.1503	.1489	.145E-02
32	.1352	.1432	-.796E-02
33	.1359	.1401	-.424E-02
34	.1363	.1360	.276E-03
35	.1285	.1312	-.266E-02
36	.1378	.1286	.917E-02
37	.1344	.1269	.751E-02
38	.1215	.1228	-.102E-02
39	.1232	.1196	.364E-02
40	.1265	.1172	.930E-02
41	.1089	.1103	-.137E-02
42	.1069	.1044	.253E-02
43	.1045	.1005	.401E-02
44	.1147	.9789E-01	.168E-01
45	.1077	.1071	.625E-03
46	.1083	.1035	.541E-02
47	.9410E-01	.1022	-.808E-02
48	.9740E-01	.9791E-01	-.505E-03
49	.9250E-01	.9546E-01	-.296E-02
50	.8610E-01	.9138E-01	-.528E-02
51	.9230E-01	.9124E-01	.106E-02
52	.9420E-01	.8807E-01	.613E-02
53	.8100E-01	.8447E-01	-.347E-02
54	.9780E-01	.9756E-01	.204E-03
55	.9700E-01	.9675E-01	.248E-03
56	.9380E-01	.9302E-01	.782E-03
57	.8370E-01	.9023E-01	-.653E-02

Figure 22. A sample of output from the Econometric Software Package

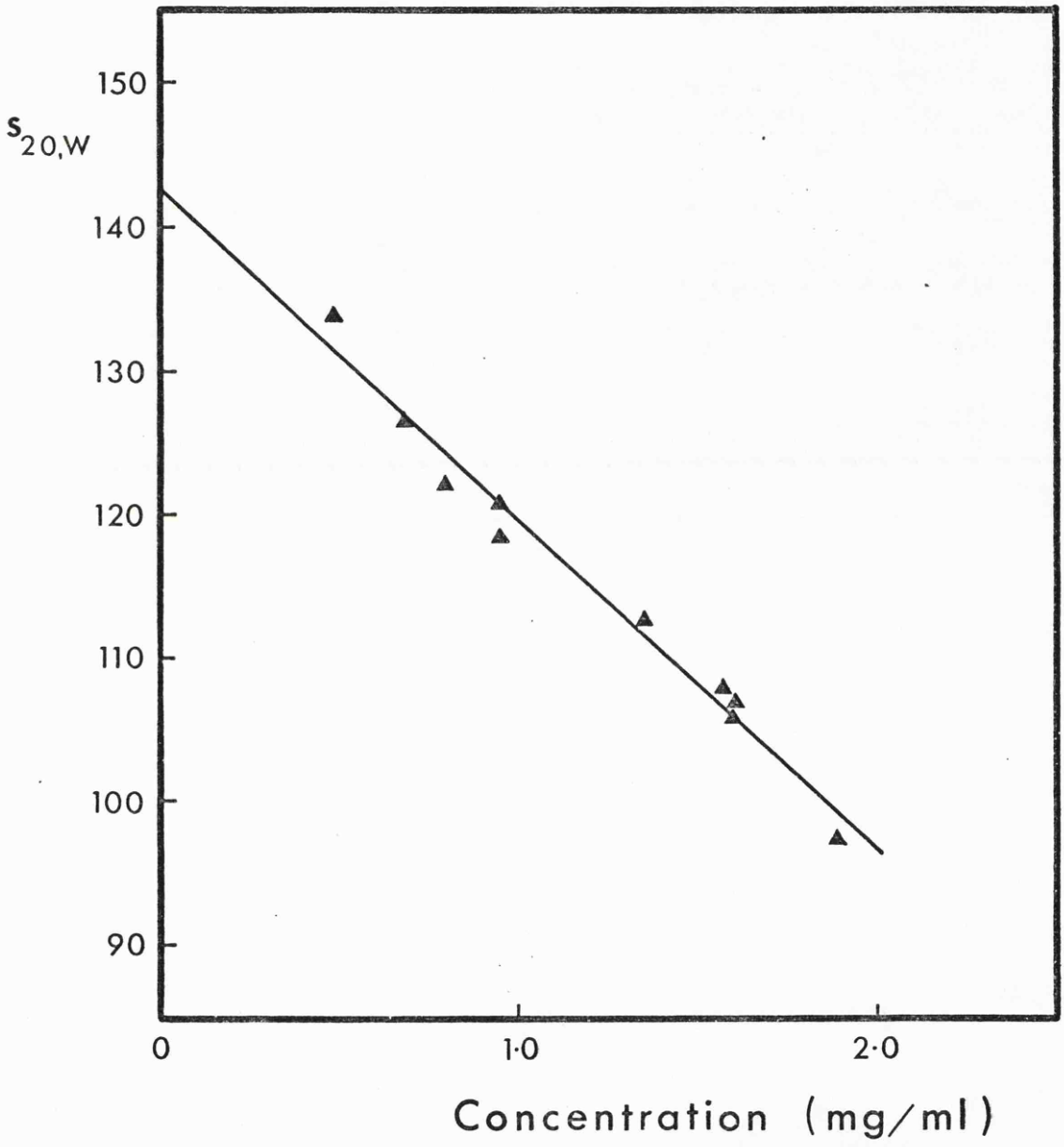

Figure 23 s versus concentration plot of the synthetic filament preparation used in viscosity measurements

(1940) equations for prolate and oblate ellipsoids of revolution. The model-dependent $V_s/\bar{v}$ was calculated from the equation: $V_s/\bar{v} = [\eta]/\bar{v}\nu$. The value of R was 0.9 ± 0.1, giving for a prolate ellipsoid: a/b = 19.5 ± 1.5; ν = 14.8 ± 5.0; $V_s/\bar{v}$ = 16 ± 5.

IV.4. Discussion

IV.4.1. Comparison of these Viscosity Results with those of a Previous Study

Intrinsic viscosity, $[\eta]$, and k_η, calculated using the Econometric Software Package computer program, have the values: $[\eta]$ = 176.8 ± 11.7ml/g, k_η = 375 ± 75ml/g and agree well with those obtained by the conventional method of extrapolation to zero rate of shear and zero concentration ($[\eta]$ = 176ml/g; k_η = 366ml/g). The advantage of the computer program is that it provides a realistic estimate of the errors involved and is far less tedious to perform.

The $[\eta]$ determined here, together with the Huggins constant (2.1 ± 0.6) are both very much lower than those reported by Josephs and Harrington (1966). The viscosity experiments performed by Josephs and Harrington were upon solutions in which polymer was in equilibrium with monomer at pH 8.3, 0.137M-KCl. Usually the interpretation of viscosity results obtained from solutions in which a reversible equilibrium exists, is hampered by (a) the uncertainty in the individual concentration of the two species and (b) the effect the presence of one component has on the intrinsic viscosity of the other. Josephs and Harrington (1966) claim to have corrected their results for both these effects. In contrast, the solutions used here showed no such equilibrium, a conclusion deduced from the schlieren pattern in the ultracentrifuge and the very low protein concentration in the supernatant

of polymer-depleted solution (IV.3.3). Additional support may be derived from the report by Morimoto and Harrington (1974a) that there is no significant amount of monomer in purified A-filament preparations in 0.1M-KCl, 10mM-$MgCl_2$, 5mM-ATP, 1mM-EGTA, 7mM-potassium phosphate, pH 7.0.

Furthermore, the reduced viscosity measurements made by Josephs and Harrington (1966) showed strong dependence upon shearing stress and extrapolated to give exceptionally high values at zero shearing stress, as a result the $[\eta]$ obtained is some 17% higher than that found here. An unusually high value of the Huggins constant (5.2) was also reported and attributed to a large solvent-solute interaction. Some of these differences may be accounted for by the different ionic conditions used (in this study a buffer of I 0.13, pH 7.0 was used throughout).

IV.4.2. Swelling ($V_s/\bar{v}$)

The model-independent $V_s/\bar{v}$ found from the ratio of k_η and k_s is 2.3 ± 0.2. This large value for the swelling of synthetic myosin filaments cannot be accounted for simply on the basis of hydration, especially when one remembers that $V_s/\bar{v}$ of the myosin molecule was fairly low (1.1 ± 0.1). The explanation probably lies in the packing arrangement of the myosin molecules into the myosin filament. During polymerization of myosin molecules there would be a tendency for $V_s/\bar{v}$ to decrease because of the expulsion of water of hydration during hydrophobic bond formation. But the imperfect packing of LMM portions into the filament backbone inevitably results in solvent being trapped within the core of the filament. This 'entrained solvent' as it is known is unable to diffuse freely with the surrounding solvent and contributes towards $V_s/\bar{v}$. Entrained solvent is by no means unique to myosin filaments and is presumed to be present in many protein aggregates (including multisubunit enzymes): although reliable

hydrodynamic data from which $V_s/\bar{v}$ may be estimated is scanty, the data of Nishihara and Doty (1958) for a range of collagen sonicates — like A-filaments in general conformation — can be interpreted to show a $V_s/\bar{v}$ similar to that measured here (Rowe, personal communication).

Can this entrained solvent account for the large $V_s/\bar{v}$ found here? There is evidence from electron micrographs of cross-sections of vertebrate skeletal muscle that indicates that the A-filament has a 'less densely stained' centre, about 5nm in diameter (Pepe, 1971; Squire, 1973). Squire (1973) has suggested that the centre of the filament contains core protein, although examination of SDS gels of solubilised myofibrils and purified A-filaments from rabbit psoas muscle (Morimoto and Harrington, 1973, 1974a; Trinick, 1973) argues against this supposition. A solvent-filled core within the myosin filament is one interpretation of these observations and hydrodynamic measurements, like those described here, will include this entrained solvent in the $V_s/\bar{v}$ ratio.

IV.4.3. Comparison of $V_s/\bar{v}$ with the Total Bound Water in Muscle

The $V_s/\bar{v}$ value found here for myosin filaments formed *in vitro* may be compared to the total bound water in muscle (i.e. water of hydration) estimated by using pulsed nuclear magnetic resonance techniques. The amount of hydration in whole vertebrate skeletal muscle is still in some doubt, although some discrepancies may be accounted for by species differences. In general, the % of hydration falls in the range 7 - 20% (Belton *et al.* 1972; Belton and Packer, 1974; Caillé and Hinke, 1974; Fung and McGaughy, 1974; Fung *et al.*, 1975; Hazlewood *et al.*, 1974). Now since there is agreement that the total amount of water in muscle is 80% by mass, one may calculate that the % of bound water *by volume* is 5.6 - 16%. Assuming an average $\bar{v}$ of 0.75, the % of protein by volume in muscle is

15% which gives a $V_s/\bar{v}$ ratio of between 1.4 and 2.1. There are several comments that should be made about this $V_s/\bar{v}$ ratio: (a) it is an integrated value for all the proteins in muscle and only about 38% of this protein is myosin (Hanson and Huxley, 1957; Huxley and Hanson, 1957), (b) the extent of hydration varies with ionic strength, temperature and possibly species, (c) the $V_s/\bar{v}$ from hydrodynamic studies may be different from that calculated from n.m.r. studies. With reference to this last point, it should be remembered that only 'bound water' has been used in the calculation. One would expect that entrained solvent would show different properties not only from the bound water but also from the free water in the intracellular volume. In support of this hypothesis is the finding by Hazlewood et al. (1974) that there is a third fraction of water accounting for some 8% of the total tissue water which does display the features mentioned above. It is not known whether the other estimates mentioned for the amount of bound water in muscle have included this additional 'ordered water' or not, but in any event one may conclude that the $V_s/\bar{v}$ for myosin filaments measured here is not inconsistent with the n.m.r. studies on the total water associated with proteins in vertebrate skeletal muscle.

IV.4.4. Suitability of Ellipsoids of Revolution as Hydrodynamic Models for Synthetic Filaments

A $V_s/\bar{v}$ value of 2.3 is, by the above argument, perfectly plausible if one considers the effect of entrained solvent and this model-independent $V_s/\bar{v}$ has been used to test the validity of ellipsoids of revolution in representing the hydrodynamic behaviour of synthetic filaments. The model-dependent $V_s/\bar{v}$ values for an equivalent prolate ellipsoid and oblate ellipsoid of revolution are 34 ± 13 and 16 ± 5, respectively, so it is clear that neither ellipsoid of revolution is a suitable hydrodynamic

model. This conclusion, then, confirms the suggestion made by Trinick (1973) that there is a difference in the frictional ratio of purified A-filaments and of the equivalent prolate ellipsoid. The assumption that the hydrodynamic properties of synthetic filaments can be represented by the equivalent prolate ellipsoid has been made previously (Noda and Ebashi, 1960; Josephs and Harrington, 1966) primarily because of the lack of any more suitable model. But it is, after all, hardly surprising that a structure covered with many large surface projections cannot be represented by a smooth, rigid prolate ellipsoid.

IV.4.5. The Origin of the Variation in f/f_o

The frictional ratio of synthetic filaments may be estimated from k_s provided that the usual conditions for the application of sedimentation theory are obeyed: (a) no interaction and (b) no charge effects, the latter may be achieved by ensuring that the pH is near the isoelectric point of the protein and that there is a swamping excess of neutral electrolyte. The frictional ratios so obtained are listed in column 3 of Table 4 and show a range of values from 3.9 to 5.3 for five synthetic filament preparations analysed here. Let us consider first to what factor this variation in f/f_o may be attributed.

The argument that follows applies to a prolate ellipsoid of revolution but it will be shown, IV.4.7, that the frictional properties of synthetic filaments can be related to those of an equivalent prolate ellipsoid via a 'frictional increment'. The length-average length for each synthetic filament preparation is different but this cannot be the sole factor affecting f/f_o. The reason is that although an increase in length would increase the axial ratio, a/b, (and through it, the frictional ratio and k_s), the extrapolated sedimentation coefficient, s^o, would remain

Table 4. The frictional ratio of synthetic filaments compared to that of the length-equivalent prolate ellipsoid of revolution.

Prep.	Axial Ratio	$(f/f_o)_{fil}$ via k_s (x)	$(f/f_o)_{prol}$ via Perrin eqn. (y)	frictional increment $f_i = x/y$	Number of myosins /14.3nm
A	39	4.78	2.64	1.81	3.7
B	36	3.87	2.55	1.52	4.2
C	46	4.36	2.84	1.54	2.8
D	38	4.71	2.61	1.80	4.4
E	34	5.30	2.50	2.12	6.5

MEAN = 1.76 $\pm$ 0.11

largely constant since it is relatively insensitive to changes in length at constant mass/unit length and high axial ratio (Peacocke and Schachman, 1954). However, the experimentally determined s^{o} values (Table 3) show a wide distibution and this may be interpreted as a variation in diameter, since s^{o} shows a much greater dependence upon diameter than length. An increase in diameter with length has been reported for synthetic filaments: Kaminer and Bell (1966) in a detailed electron microscope study showed that in general as the length of synthetic filaments increased from 0.2 to 1.7μm, the diameter increased from 5.0 to 30.0nm. In contrast, Katsura and Noda (1971) proposed a width-limiting mechanism for synthetic filaments and a maximum diameter of 12.5nm. Two criticisms of this proposal may be made: firstly it does not account for the several reports of synthetic filaments with diameters very much greater than 12.5nm (Kaminer and Bell, 1966; Moos et al., 1975; Pinset-Härström and Morel, 1975) and secondly, width was estimated by assuming a cylindrical model for myosin and this may involve substantial errors.

The cause of this change in diameter (see Table 3, column 7) cannot be due to swelling by the following reasoning. Diameter is related to s^{o} and s^{o} is proportional to mass/unit length and is therefore approximately independent of swelling (Peacocke and Schachman, 1954). On the other hand, an alteration in diameter and hence s^{o}, can be attributed to radial growth of the filament brought about by further aggregation of myosin molecules. Thus an increase in s^{o} may be accomplished by an increase in mass/unit length, a conclusion that is supported by the concomitant increase in N, the number of myosins/14.3nm interval (Table 3). The significance of this alteration in N is considered below (section IV.4.11).

IV.4.6. The Concept of the 'Length-Equivalent' Prolate Ellipsoid of Revolution

It was shown above that the variation of f/f_o (and hence s^o and k_s) can be accounted for by a change in diameter of synthetic filaments. But the original aim of this investigation was to examine ways in which f/f_o of synthetic filaments may be predicted. What is required is a means of comparing the frictional ratio of synthetic filaments as a function of length. To make this comparison it is essential to choose a frame of reference to which f/f_o of the filament may be related. The frame of reference chosen was a smooth, rigid prolate ellipsoid of the same length and mass as the 'average synthetic filament' and one that is also close-packed and unhydrated (the inclusion of hydration merely introduces a constant and its effect upon f/f_o will be discussed later).

The use of a 'length-equivalent' prolate ellipsoid is unusual and deserves some comment. An equivalent ellipsoid of revolution has been much used in the past to represent the hydrodynamic behaviour of macromolecules: it is, by definition, the ellipsoid of revolution that has the same f/f_o as the particle. Because both solvation and asymmetry contribute towards the frictional ratio, a minimum f/f_o is usually taken, assuming that solvation is zero (Tanford, 1963). It has been emphasised that this is an equivalent ellipsoid and that its axial ratio and over-all shape do not necessarily bear any relationship to those of the particle. Indeed, the $V_s/\sqrt{v}$ method used in this thesis to examine the validity of equivalent ellipsoids of revolution as hydrodynamic models for myosin (III.3.8) and synthetic myosin filaments (IV.4.4) is a means of quantitatively testing this last point. Under different ionic conditions it is possible that an equivalent prolate ellipsoid would be valid for, say, myosin and could predict the axial ratio.

In this discussion I have considered a prolate ellipsoid of

revolution whose length is the same as the length-average length of a synthetic filament preparation. Unlike the equivalent prolate ellipsoid, which has two variables: length and diameter, this 'length-equivalent' prolate ellipsoid has but one variable: diameter. The length-equivalent prolate ellipsoid therefore has two features: (a) its f/f_o can be computed from mass and length and (b) its mass is extremely sensitive to diameter. The first feature has been used here to compare the frictional ratios of synthetic filament samples of different length-average length; the second feature has been used in the following Chapter to calculate the molecular weight of the A-filament from s^o and length-average length (V.3.9). Again it should be emphasised that the diameter of the length-equivalent prolate ellipsoid is not necessarily the same as that of the myosin filament. Let us now return to consider how f/f_o of the length-equivalent prolate ellipsoid for synthetic filaments is estimated.

IV.4.7. Comparison of f/f_o of Synthetic Filaments with that of the Length-Equivalent Prolate Ellipsoid

The radius of a prolate ellipsoid (b) having the same molecular weight and length (2a) as that of the 'length-average synthetic filament' was calculated from the equation: $b = (3M\bar{v}/4\pi N_A a)^{\frac{1}{2}}$ and the axial ratio (a/b) then determined. Perrin's (1936) equation has been used to calculate the frictional ratio of the length-equivalent prolate ellipsoid from its axial ratio and is shown for each filament preparation in Table 4, column 4. Comparing the frictional ratios of synthetic filaments and the length-equivalent prolate ellipsoid, it is clear that for each filament preparation the frictional ratio of the filament, estimated from k_s, is always greater. As mentioned previously, the frictional ratio of a particle may be considered to be the result of two effects: solvation and asymmetry.

Since an unhydrated model was chosen, the influence of hydration (or swelling) upon frictional ratio may be estimated. The extent of swelling in synthetic filaments was calculated from k_η and k_s as 2.3. For a prolate ellipsoid of revolution, volume is proportional to b^2a (where b is the short semi-axis and a is the long semi-axis) and, if swelling is considered, the volume of the hydrated prolate ellipsoid will be greater by a factor of 2.3. Provided that the increase in length during swelling is negligibly small, the radius, b, increases by a factor of $\sqrt{2.3}$, causing the axial ratio to decrease by a similar amount. Swelling then, produces a decrease in axial ratio so f/f_o for a hydrated prolate ellipsoid is smaller than that of the unhydrated ellipsoid. Clearly the difference between f/f_o for synthetic filament and unhydrated prolate ellipsoid cannot be accounted for on the basis of swelling. It may be inferred that the difference in f/f_o's is due to a difference in shape. For the ratio of the two frictional ratios, an average value has been estimated as 1.76 ± 0.11. I shall henceforth refer to this ratio as the 'anomalous frictional increment' or f_i.

IV.4.8. The Anomalous Frictional Increment

The most obvious feature of f_i is its magnitude: it indicates that frictional ratios 76% higher than those of the length-equivalent prolate ellipsoids are found for synthetic filaments. The presence of surface projections (i.e. the myosin heads) along the synthetic filament may account for this large increase in frictional ratio. The frictional ratio for the asymmetric synthetic filament is a summation over all the possible orientations of the filament (since during hydrodynamic measurements they are undergoing random Brownian motion), but a large change in the frictional coefficient at one particular orientation will, none-the-less, be reflected in the over-all f/f_o. Such a change could be induced by the helical

arrangement of the cross-bridges which, when the filament axis is parallel to the 'flow', could create a torque upon the filament causing it to revolve about its own axis. [An analogous turning motion is observed in the propellor of a motorized-yacht: when the yacht is under sail and the motor disengaged, the propellor turns as a result of the movement of the yacht.].

There are two ways of testing this hypothesis: (a) by measuring the frictional ratio of a model, or (b) by predicting the frictional ratio from the Kirkwood-Bloomfield theory. The problems involved in measuring the frictional ratios of models under the condition of laminar flow have been outlined in the previous Chapter (III.3.7). The same limitations apply here, although the achievement of a low Reynold's Number would be even more difficult as the model of a synthetic filament, because of its complexity, will inevitably be large. The complexity of the synthetic filament structure would also make calculation of the frictional coefficient from the Kirkwood-Bloomfield theory (Bloomfield et al., 1967) much more complex (although by no means impossible). In view of these difficulties, no attempts have been made, as yet, to test this hypothesis.

IV.4.9. Independence of Frictional Increment and Axial Ratio

The second feature of the f_i is that the standard error of the mean estimated for five filament preparations, is low ($f_i = 1.76 \pm 0.11$) yet there is considerable variation in axial ratio (from 34 to 46 for the length-equivalent prolate ellipsoid). No obvious increase in f_i was observed over this range of axial ratios. To check that f_i is independent of axial ratio upto higher axial ratios (100 - 120) is difficult for two reasons: (a) the polydispersity of the filament preparation must be kept to a minimum because the hydrodynamic equations are restricted to solutions which are reasonably monodisperse and (b) diameter tends to increase and s^o

is highly dependent upon diameter. Concerning the first point, the polydispersity must be kept fairly low if anomalies are to be avoided. There is, however, evidence from several authors that indicates that under the conditions where long synthetic filaments form, the length distribution becomes extremely broad (Josephs and Harrington, 1966; Sanger, 1971; Katsura and Noda, 1971, 1973a).

As for the second point, it has been inferred that s^o is sensitive to changes in diameter, a deduction supported by the observation that with long filament preparations (in which there is a variation in width, Kaminer and Bell, 1966), two or more schlieren peaks are detected in the ultracentrifuge (Kaminer and Bell, 1966; Josephs and Harrington, 1966; Sanger, 1971). For these reasons, further sedimentation velocity experiments were not performed on synthetic filaments with high axial ratio (from 50 to 100), but the independence of f_i with axial ratio was assumed to hold up to these high axial ratios. If the cross-bridges do have the effect on f/f_o as proposed, then it would follow that f_i is independent of axial ratio. The f_i can therefore be used to predict the frictional ratio of purified A-filaments from that of the length-equivalent prolate ellipsoid of revolution, thus fulfilling the main objective of this investigation into synthetic filaments.

IV.4.10. Is the Variation of N Artefactual?

This study on the hydrodynamic properties of synthetic filaments has provided the first estimate of the number of myosins/14.3nm repeat (N). This has been achieved by using a new hydrodynamic treatment (Rowe, 1977, and Appendix I) which enables molecular weight to be determined from s^o and k_s. Table 3 shows that N varies over the range 2.8 to 6.5 and this may be attributed either to a genuine change in N or to one of the following

effects.

(a) Polydispersity

Each synthetic filament preparation exhibits polydispersity in length so that s values are weight-averages. But it has already been shown that s^o is insensitive to small changes in length so it is unlikely that length distribution has any significant effect upon s^o (and hence N).

(b) Estimation of Length

Errors in N could arise from miscalculation of the length-average length from electron microscopy measurements. However, substantial changes in length (upto two-fold) would be required to produce the observed changes in N and there is no evidence to suggest that synthetic filaments are particularly susceptible to mechanical damage during preparation for electron microscopy. Depolymerization, caused by an increase in ionic strength upon addition of uranyl acetate, was discounted as similar length distributions were obtained for concentrations of uranyl acetate from 0.2 to 4.0% (w/v).

(c) Myosin Filament Interaction During Centrifugation

Mg-ATP was added to synthetic filament solutions immediately prior to ultracentrifugation or viscosity measurements in order to minimise filament interaction. The logic behind this is that since myosin binds Mg-ATP the net charge on the myosin filaments will be increased slightly and this may help to keep the filaments separated in solution. (This slight increase in net charge does not enhance the 'primary charge effect' since the latter is greatly reduced by operating near the isoelectric point of myosin.). But since myosin hydrolyses ATP (admittedly at a slow rate in the presence of Mg^{2+}), if all the ATP were used up during the course of an ultracentrifuge experiment, myosin filament interaction would be permitted and could yield an erroneously high s value. However control experiments in the presence

and absence of Mg-ATP have indicated that substantial filament interaction does not occur.

(d) Effect of Ca^{2+} on s

The possible influence of Ca^{2+} on the sedimentation coefficient of synthetic filaments, as reported by Morimoto and Harrington (1974b), was avoided by performing all sedimentation velocity experiments in the presence of the calcium chelator, EGTA.

(e) Other Protein Components of the Thick Filament

The molecular weight of synthetic filaments estimated from s^o and k_s was corrected for the weight fraction of C-protein (3.5%) as calculated by Morimoto and Harrington (1974a) from SDS gel electrophoresis of solubilised glycerinated myofibrils of rabbit psoas muscle. This correction makes the assumption that the C-protein removed from muscle during myosin A extraction binds to synthetic myosin filaments in the same weight ratio as in the native thick filament. In this regard, it should be noted that there is no evidence as yet to indicate that C-protein binds to synthetic filaments with a 43nm periodicity seen in vertebrate skeletal muscle. No correction was made for the other minor protein components present in myosin A extracts (B- and F-proteins and actin), but this has negligible effect upon N.

IV.4.11. Is the Variation in N due to a Change in Symmetry or to a Change in Mass/Unit Length?

It is safe to assume therefore that the variation of N shown by synthetic filaments is real and not artefactual. Two possibilities must be considered to account for this variation in N: (a) it reflects a genuine change in symmetry, or (b) the symmetry is constant but further aggregation of myosin molecules occurs in a radial direction.

(a) Change in Symmetry

A change in symmetry to account for the variation of N is supported by Squire's (1973) hypothesis that there is a general packing scheme determining the structure of different myosin filaments. One may envisage myosin filament formation to occur by head-to-tail and side-to-side aggregation of myosin molecules into a flat sheet which is then 'rolled-up' into the filament. Several criticisms can be made against this scheme. Firstly, the Squire (1973) model has been discussed in detail in section I.1.3(c) and is inconsistent with a number of experimental observations. Secondly, whereas the highest value of N found here (6.5 ± 0.6) is consistent with a six-fold helical symmetry for the myosin filament (as found in insect flight muscle, Squire, 1972), by this argument N values greater than six may occur, particularly since synthetic filaments with very large diameters have been reported (for example upto 30.0nm, Kaminer and Bell, 1966; upto 40.0nm, Pinset-Härström and Morel, 1975). Thirdly, synthetic filaments are dynamic structures whose length and diameter can be reversibly altered by changing the ionic strength or pH (Kaminer and Bell, 1966; Sanger, 1971). The rolled-up sheet model would, in the author's opinion, place severe restrictions on the reversible nature of synthetic filaments because of the large entropy changes that would be required.

(b) Change in Mass/Unit Length but with Constant Symmetry

The second suggestion was that the symmetry of the filament was constant and that the changes in N were brought about by addition of myosin molecules to the outside, causing an increase in diameter. This theory can immediately explain several observations. The absence of a bare-zone in some synthetic filaments (Kaminer and Bell, 1966) can be interpreted by the aggregation of myosin molecules to the outside of a 'basic filament

structure', in a random fashion, such that the bare-zone is obliterated by myosin heads. The reappearance of the bare-zone upon raising the ionic strength or pH can be interpreted as the removal of these peripheral molecules to reveal the 'basic filament' once more. By a similar argument, the reversibility of synthetic filaments can be explained. Here, as the ionic strength is lowered, longitudinal growth proceeds by addition of myosin molecules to the ends of the filament and radial growth proceeds by side-to-side aggregation of myosin molecules to the filament. In this way, longitudinal and radial growth are apparently limitless, a prediction consistent with the electron microscope measurements of Kaminer and Bell (1966). Increasing the ionic strength would reverse this process.

It is further tentatively suggested that the 'basic filament' structure referred to corresponds to the smallest N found here (2.8 ± 0.3), which is consistent with 3-fold helical symmetry. However, the existence of a 2-stranded filament that has escaped detection in these experiments cannot be ruled out. As a final point it should be noted that this model for aggregation of myosin molecules into synthetic filaments is by no means inconsistent with that of Huxley (1963). Rather it should be considered an extension of it to account for the radial growth displayed by synthetic filaments. Both the 'basic filament' described here and the A-filament formed *in vivo* may still be formed by the method of Huxley (1963). The difference between synthetic filament and native A-filament assembly is that, *in vivo*, further radial growth is somehow prevented. The mechanism for controlling radial growth *in vivo* and its absence or failure to work *in vitro* remains to be elucidated.

IV.5. Summary

The conclusions drawn from this investigation into the hydrodynamic

properties of synthetic myosin filaments may be summarised by the following points.

(i) Synthetic filaments show a variation in s^o and k_s and this can be accounted for by a difference in axial ratio between filament preparations.

(ii) For the first time, the molecular weight and the number of myosins per 14.3nm has been calculated for synthetic filaments without any assumptions as to their shape. A range of N values has been detected, consistent with the hypothesis that radial growth, beyond the diameter of the native A-filament, is unrestricted in myosin filaments formed in vitro.

(iii) $V_s/\bar{v}$ has been determined and its magnitude has been interpreted as due to the presence of a volume of 'entrained solvent' within the filament core.

(iv) By using new hydrodynamic techniques the validity of an equivalent prolate ellipsoid as a model for synthetic filaments has been tested.

(v) A method has been outlined by which it is possible to predict the f/f_o of the length-equivalent prolate ellipsoid from length-average length and mass of synthetic filaments. The frictional ratio of the synthetic filament is some 76% higher than that of the length-equivalent prolate ellipsoid of revolution and it has been proposed that this 'frictional increment' is due to the helical arrangement of myosin heads on the filament backbone.

At the beginning of this Chapter it was explained that the determination of M^o from s^o and k_s was hampered by the inability to determine k_s. These investigations into synthetic filaments were instigated to see if either k_s or f/f_o (since the two are related) may be predicted for A-filaments as s^o can be measured. By establishing a length-equivalent prolate ellipsoid of revolution as a system of reference, it has been possible to show that its f/f_o (determined from length and mass) is related

to f/f_o of synthetic filaments. Exactly the same procedure cannot be used for purified A-filaments as 'mass' is of course unknown. But since M^o is related to the axial ratio of the length-equivalent prolate ellipsoid by $M = 4N_A\pi b^2 a/3\bar{v}$ and to s^o of purified A-filaments by the Svedberg equation, there is a unique solution for M^o. In this way, the measurement of s^o and the length-average length is sufficient to determine the molecular weight of the A-filament and, from thence, its symmetry.

CHAPTER V

The Molecular Weight and Helical Symmetry of the A-filament

V.1. Introduction

In section I.1.4 it was stated that to determine the helical symmetry of the A-filament from its molecular weight, three criteria had to be met: (i) purified A-filaments must be obtained and (ii) a method to determine the molecular weight, (iii) the molecular weight of myosin must be precisely known. The sedimentation velocity studies reported in Chapter III confirmed that the molecular weight of myosin is 470000 and also high-lighted the usefulness of M^o determination from s^o and k_s. It has also been explained (see IV.1) that the procedure used to purify A-filaments yields a solution containing only 0.1mg/ml of A-filaments and that this concentration is insufficient to measure k_s. But hydrodynamic studies on synthetic myosin filaments have shown that f/f_o of the filament can be related to that of the length-equivalent prolate ellipsoid of revolution and thus provides a means of predicting f/f_o of purified A-filaments. This Chapter describes (a) attempts to obtain a concentrated sample of purified A-filaments, (b) estimation of f/f_o of A-filaments from f/f_o of the length-equivalent prolate ellipsoid, correcting for the 'anomalous frictional increment' and (c) measurement of s^o for purified A-filaments at low concentration by active enzyme centrifugation.

The purification of A-filaments from vertebrate skeletal muscle is hampered by the fact that A-filaments are sensitive to slight changes in ionic strength and pH and tend to either aggregate or depolymerize easily. Furthermore, they are fragile and are damaged by 'sticking' to surfaces (e.g. dialysis tubing or filter paper) or by pelleting in a centrifuge. It is therefore not surprising that successful reports of purification of A-filaments from rabbit skeletal muscle have been few (Morimoto and Harrington, 1973; Trinick, 1973). Purified A-filaments have been obtained by using the 'zone velocity' technique to separate A- and I-filaments by

virtue of their different s values. However, the large concentration dependence of the sedimentation coefficient of A-filaments is the cause of the spreading of the leading edge of the sedimenting band and the result is dilution of the A-filaments.

A second approach is described here: that of separating A- and I-filaments by differences in density. It is well known that proteins have a narrow density range ($\bar{v}$, which is inversely proportional to density, has a range from about 0.72 to 0.74ml/g) but there is no simple way of predicting the density of proteins in solution (their 'buoyant density') from their 'unhydrated' density ($1/\bar{v}$). The difficulty is that the extent of hydration of the protein affects the observed density in solution. One cannot therefore predict if a difference between the buoyant densities of A- and I-filaments exists and one must turn to experimentation to provide the answer. Separation of macromolecules according to density can be achieved on a density gradient by creating the 'isopycnic condition' during centrifugation. At the isopycnic condition the forces acting on the macromolecule (centrifugal force, diffusion and buoyancy) are at equilibrium so there is no net movement of the macromolecules and a band is formed. The resolution can be increased by using high centrifugal forces and a shallow density gradient (Hüttermann and Wendlberger, 1975).

There are two ways of carrying out isopycnic centrifugation, both of which have been used here: either on a stable preformed gradient or on an equilibrium density gradient formed during centrifugation starting from a homogeneous mixture of both the macromolecule and the small molecules that form the gradient. The advantage of the equilibrium density gradient is that a large increase in concentration of the macromolecule can be achieved: by adding solute directly to the macromolecular solution to reach the desired starting density, a many fold increase in concentration within the

protein band may be obtained. The disadvantages are that resolution is poor because the steepness of the gradient is a function of angular velocity and secondly, the time necessary to form the equilibrium density gradient is inversely proportional to the square of the length of the solvent column (Hüttermann and Wendlberger, 1975). Both these disadvantages may be reduced by using a fixed angle rotor. During centrifugation the density gradient is formed along the horizontal axis and the length of the solvent column is therefore shortened. The steepness of the density gradient is still a function of the rotor speed but when the centrifuge tube is reoriented to the vertical, the gradient becomes shallower and the resolution is increased.

Preformed density gradients offer two advantages over equilibrium gradients. Firstly, the steepness of the gradient is independent of angular velocity, provided the preformed gradient remains stable. There will be a tendency for the gradient-forming molecules to redistribute, under centrifugal force, to their equilibrium distribution but the effect can be greatly reduced by increasing the length of the solvent column. The steepness of the density gradient can thus be chosen independently of the centrifugal speed. Secondly, the sample is usually loaded on top of the preformed gradient and the time for the macromolecule to reach its isodensity position is dependent only upon its s value. In contrast with equilibrium density gradients, the time for the macromolecule to reach its isodensity position is dependent upon the speed at which the density gradient is formed, which in its turn is a function of the length of the solvent column. The use of preformed density gradients then, enables the resolution to be increased and the time to reach the isopycnic condition to be decreased. The disadvantage is that large volumes of the macromolecular solution cannot be applied to the top of the preformed

gradient because of the problem of density inversion.

For both types of density gradient it is an essential requirement that the viscosity of the density gradient medium should be low so that the time for the protein to reach its isodensity position is short. Sucrose is unsuitable as a solute since the concentration required to deliver a density range of 1.2 to 1.4g/ml (the range of buoyant densities of proteins, Hu et al., 1962) also has a very high viscosity. By using D_2O in place of H_2O, the density can be increased by a factor of 1.11 so that less solute is required to reach the same density (hence the viscosity is lower). The medium chosen for the equilibrium density gradients was a mixture of D_2O and fructose. Fructose was chosen in preference to sucrose as the former has a significantly lower viscosity at the same density (25% lower at $\rho = 1.28$). To increase resolution and decrease the time to reach equilibrium, a fixed angle rotor was used.

During this investigation the author's attention was drawn to the advantages of D_2O-metrizamide as a density gradient medium (A. Hüttermann, personal communication). Metrizamide is a derivative of glucose (see II.1 for the full systematic name) and its most important feature is that in a solution of density 1.33, the viscosity is low (24.7cp at 5°C). Equilibrium density gradients are slow to form in metrizamide solutions but this fact ensures long term stability of preformed gradients. One disadvantage of metrizamide is that at high concentrations it interacts reversibly with proteins and heavy sattelite bands are formed during isopycnic banding of proteins (Rickwood et al., 1974). Replacing H_2O with D_2O reduces the reversible interaction between metrizamide and protein (as well as decreasing the time to reach the isopycnic condition). A further disadvantage of metrizamide is that it shows a strong absorbance at 280nm. Never the less, attempts were made to purify A-filaments from a crude preparation

contaminated by I-filaments (and A- and I-segments) using isopycnic banding on (a) equilibrium density gradients of D_2O-fructose and (b) preformed density gradients of D_2O-metrizamide.

These isopycnic banding experiments unfortunately failed to yield purified A-filaments, for reasons given in V.4. However, the investigation into the symmetry of the A-filament need not be abandoned because of the failure to obtain concentrated purified A-filaments. In the previous Chapter it was shown that the frictional ratio of synthetic filaments having a range of s^o values was higher than the calculated frictional ratio of equivalent prolate ellipsoids of the same length and mass, although the two could be related by the 'anomalous frictional increment'. If therefore it is possible to measure s^o for a dilute sample of purified A-filaments, it will be possible to determine the molecular weight (M^o) and hence the symmetry of the A-filament, provided that an algorithm can be devised to determine the value of M^o which simultaneously satisfies the equations involving M^o and a/b of the equivalent prolate ellipsoid, and M^o, s^o and f/f_o (the last parameter is calculated for a length-equivalent prolate ellipsoid and corrected for the anomalous frictional increment).

There are two ways in which the s value of a dilute A-filament solution (about 0.1mg/ml) can be measured: either by using sedimentation velocity in conjunction with dark-field optics or by active enzyme centrifugation. But since the A-filaments described here are still contaminated with small amounts of actin filaments after purification, there is a danger that the s value may be under-estimated by sedimentation velocity runs due to the presence of slower moving I-filaments. Active enzyme centrifugation, as its name implies, detects only the active form of the enzyme and the presence of 'non-active' contaminants has no effect. Cohen (1963) first showed the feasibility of determining sedimentation

coefficients of enzymes in their catalytically active forms. The technique involves layering a small amount of enzyme onto a 'reaction mixture' by means of which the sedimenting enzyme layer can be followed by its enzyme-catalysed reaction. The method has several advantages:

(i) only the active form of the enzyme is monitored

(ii) extensive purification of the enzyme is unnecessary (crude extracts from sonicated cells have been successfully used; see Kemper and Everse, 1973)

(iii) the normal spectrophotometric assay may be suitable, with minor modifications, for use in active enzyme centrifugation.

It might be thought that the sedimentation coefficient of a 'crude' A-filament preparation could be measured by active enzyme centrifugation without the need for purification. But this is not so. A crude A-filament preparation contains other 'active' forms of the enzyme, the A-segments, which have a very much higher s value than the A-filament, and it would be the movement of A-segments that would be monitored. Purification of A-filaments on H_2O-D_2O gradients separates A-segments from A-filaments (Trinick, 1973) and therefore solves this problem.

The movement of the enzyme layer is followed by monitoring optical changes in the reaction mixture either caused directly by accumulation of product or decrease in substrate concentration, or by linking to a secondary reaction (the latter may be a chemical or enzymic reaction). There have been several reports of sedimentation coefficients of enzymes estimated by using a linked enzyme system in active enzyme centrifugation (Mire, 1967; Kolb, 1974; Schmitt, 1975) but I shall describe here the first successful report of a linked enzyme system involving <u>two</u> enzyme-catalysed reactions used to detect the 'primary enzyme'. In the discussion that follows, the following points are considered: (a) a linked enzyme system

used to detect A-filaments, (b) the conditions necessary for active enzyme centrifugation, (c) fulfilling these conditions and (d) problems specific to active enzyme centrifugation of A-filaments.

(a) Linked Enzyme System

A-filaments, for the most part, consist of myosin, an enzyme catalysing the hydrolysis of ATP to ADP and inorganic phosphate. The hydrolysis of ATP by myosin can be followed by an absorbance change by the use of a dual linked enzyme system:

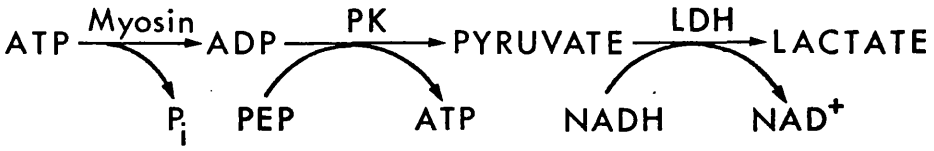

The two enzymes involved are pyruvate kinase (PK) and lactate dehydrogenase (LDH), the latter oxidising NADH to NAD^+ resulting in a loss in absorbance at 340nm. The concentrations of reactants and enzymes were established by performing trial experiments on synthetic myosin filaments (prepared as described in IV.2.1) in an SP 1800 spectrophotometer. The following general points need to be considered.

(i) The initial NADH concentration must be high enough to be detected by the photomultiplier of the ultracentrifuge.

(ii) The hydrolysis of ATP by myosin is activated by Ca^{2+} and inhibited by Mg^{2+} (Szent-Györgyi, 1951).

(iii) K^+ (Boyer et al., 1942) and Mg^{2+} (Boyer et al., 1943; Lardy and Zeigler, 1945) are essential for pyruvate kinase activity. Pyruvate kinase is inhibited by Ca^{2+}, the inhibition being partially overcome by K^+ (Kachmar and Boyer, 1956; Boyer et al., 1942). ATP shows competitive inhibition with PEP and ADP for active sites on pyruvate kinase (K_I is 0.12mM-ATP, Reynard et al., 1961).

(iv) Lactate dehydrogenase undergoes substrate inhibition by pyruvate at

concentrations above 0.2 to 1.0mM-pyruvate (Stambaugh and Post, 1966; Busch and Nair, 1957) and product inhibition by lactate (K_I = 130mM, Stambaugh and Post, 1966). LDH is also inhibited by NAD^+ (K_I = 0.2mM, Zewe and Fromm, 1962).

The concentration of constituents in the reaction mixture was adjusted to give the optimum rate of hydrolysis of ATP by synthetic myosin filaments (followed by the loss of absorbance at 340nm). Before this linked enzyme system can be used in active enzyme centrifugation, the following four conditions must be fulfilled.

(b) Conditions for Active Enzyme Centrifugation

Condition 1. 'Positive density gradient throughout the cell'

As the enzyme band sediments it creates a negative density gradient at its leading edge and a positive gradient at its trailing edge, If convection-free sedimentation is to be maintained, this negative gradient must be everywhere compensated by a stabilising density gradient, such that the total density gradient is always positive (Cohen and Mire, 1971a).

Condition 2. 'Constant enzymic rate throughout the run'

The validity of active enzyme centrifugation in determining s^o is based upon the assumption that the enzyme rate is constant throughout the run. In practice, this is achieved in one of two ways: (a) by using an initial substrate concentration that is saturating for the enzyme (e.g. 20 times K_m, where K_m is the Michaelis constant), or (b) by using lower substrate concentrations but ensuring that the concentration of substrate is not reduced by the enzyme by more than a few percent. If this condition is not fulfilled, an erroneously high sedimentation coefficient is obtained (Cohen and Mire, 1971a).

Condition 3. 'Sedimentation of the secondary enzyme must be slower than the primary enzyme'

For a coupled enzyme system the sedimentation of the secondary enzyme must be slower than the primary enzyme (Mire, 1967).

Condition 4. 'The secondary enzyme must be in excess'

The secondary enzyme must be in excess of the primary enzyme so that the product of the primary reaction is immediately used up. If this condition is not fulfilled then what is monitored is not the movement of the enzyme band, but the speed at which the product of its reaction is utilised. The result is that an anomalously low sedimentation coefficient is obtained (Cohen and Mire, 1971b).

(c) Fulfilling the Conditions

To obtain accurate sedimentation coefficients for myosin filaments (either synthetic myosin filaments or purified A-filaments) each of these conditions must be fulfilled.

Condition 1.

Condition 1 is fulfilled by increasing the concentration of neutral electrolyte in the reaction mixture. Under centrifugation, the small molecules set up a concentration gradient resulting in a positive density gradient throughout the cell. For dilute enzyme concentrations, 0.1M-KCl is sufficient to maintain a positive gradient (Cohen and Mire, 1971a). However, since synthetic myosin filaments are prepared at 0.13M-KCl, no additional KCl need be added. Purified A-filaments too, are prepared at physiological ionic strength (I 0.13) but the density of a sample of A-filaments purified on an H_2O-D_2O density gradient, is high (ρ = 1.07 to 1.08). To prevent density inversion when the A-filaments are layered on top of the reaction mixture, the latter was made up in 100% D_2O (the pD was adjusted to 7.4, Glascoe and Long, 1960).

Condition 2.

Condition 2 requires that the substrate concentration is saturating. As far as the author is aware there have been no measurements of the Michaelis constant for myosin in a solution of I 0.13 at 25°C, but trial experiments have shown that an ATP concentration of 10mM is more than sufficient to ensure saturation. It is essential that the ATP concentration is also saturating after the enzyme band has passed or, if not, that the concentration is decreased by only a few percent (Cohen and Mire, 1971a). The maximum rates of ATP hydrolysis measured in the spectrophotometer for both synthetic myosin filaments and purified A-filaments (150 and 920nmol ATP/min/mg of protein, respectively) means that in active enzyme centrifugation only 0.3% and 1.6%, respectively, of the original ATP is hydrolysed after the enzyme band has passed.

Condition 3.

The sedimentation coefficients of myosin filaments (about 136S, Trinick, 1973) pyruvate kinase ($s^{o}_{20,w}$ = 9.8S, Mire, 1967) and lactate dehydrogenase ($s^{o}_{20,w}$ = 7.0S, Cohen and Mire, 1971b) comply with condition 3. That pyruvate kinase has a greater $s^{o}_{20,w}$ than lactate dehydrogenase will not affect the enzyme reaction because of the very much larger $s^{o}_{20,w}$ of myosin filaments.

Condition 4.

Condition 4 requires that the linked enzyme system be in excess so that the enzyme reaction rate is faster than the velocity of the enzyme band. To determine the concentration of PK and LDH required, active enzyme centrifugation was performed on synthetic myosin filaments as described in V.2.9(c). It will be shown for purified A-filaments that this condition only holds below a certain critical rotor speed.

(d) Specific Problems with A-filaments

There are several problems which relate specifically to the problem of determining $s^{o}_{20,w}$ for purified A-filaments by active enzyme centrifugation. Firstly, the sensitivity of A-filaments to changes in ionic strength and pH have already been mentioned, thus the optimum rate of ATP hydrolysis by A-filaments must be chosen without significant alteration of these two parameters. Secondly, the A-filament has an $s^{o}_{20,w}$ value twice as large as that of any enzyme previously measured by active enzyme centrifugation. The problem of ensuring that the linked enzyme rate is fast enough to follow the sedimenting enzyme band becomes a very real one. Thirdly, since A-filaments are purified in an ATP medium and are continuously hydrolysing it to ADP, there is bound to be some ADP present in the enzyme layer. It was found that diffusion of this ADP into the reaction mixture can seriously affect the estimated s value, particularly at high concentrations and low rotor speeds. As the concentration of ADP is critical, the amount of ATP hydrolysed to ADP has been estimated in some purified A-filament fractions, using the firefly lantern assay procedure for ATP.

In spite of these difficulties, the sedimentation coefficient of purified A-filaments has been measured as a function of rotor speed. By combining s^{o} with the predicted value of f/f_{o}, it has been possible to estimate the molecular weight of the A-filament. The molecular weight is consistent with 3-fold helical symmetry for the A-filament.

V.2. Methods

V.2.1. Synthetic Filament Preparation

Synthetic myosin filaments were prepared by diluting myosin A

solutions to an ionic strength of 0.13 as described previously (see IV.2.1.).

V.2.2. Myofibril Preparation

The procedure used was that of Huxley (1963) as modified by Trinick (1973). A modified sodium-Ringer was used by Trinick (1973), in which the psoas muscle was soaked at least 24h. The solution depletes the level of calcium in the muscle, thus preventing the onslaught of potassium contracture when the muscle is transferred to physiological ionic strength potassium chloride. This 'calcium-depleting medium' has the following constituents: 0.1M-NaCl, 2mM-$MgCl_2$, 2mM-KCl, 1mM-EGTA, 0.1% (w/v) glucose in 6mM-potassium phosphate buffer, pH 7.0 at 4°C. The solution used by Huxley (1963) in which the muscle was homogenised ('homogenising buffer') contains 0.1M-KCl, 10mM-$MgCl_2$, and 1mM-EGTA in 6mM-potassium phosphate buffer, pH 7.0 at 4°C.

Freshly excised rabbit psoas muscle was teased into strips 4 - 5mm in diameter, fastened with cotton to perspex strips at approximately rest length and soaked in calcium depleting medium for 24h with several changes. After this time, the muscle was removed and teased into fibre bundles of about 1mm in diameter, washed in homogenising buffer and then cut into lengths of about 3mm. The fibril preparation, cooled on ice, was blended in an MSE homogeniser that was run at top speed for three 30 second periods, interspersed with 15s periods at low speed to allow cooling to occur. The homogenate was spun in a bench centrifuge at 3000rev./min (900g) for 2min and the supernatant discarded. The precipitate was resuspended in 45ml of homogenising buffer and the centrifugation step repeated: this procedure was repeated twice more to remove soluble proteins. The final myofibril suspension was examined in a Watson Microsystem 70 phase contrast microscope, and a sample taken for SDS gel electrophoresis (II.2.1 and

II.2.2). Removal of M-line protein from A-filaments was carried out overnight by soaking the myofibrils in a freshly made up solution of 5mM-Tris-HCl, 1mM-dithiothreitol, pH 7.8 at 4°C.

V.2.3. 'Crude A-filament' Preparation

Myofibrils, prepared as above, were centrifuged at 3000rev./min (900g) for 4min and the pellet was resuspended in 'relaxing medium' (0.1M-KCl, 10mM-$MgCl_2$, 5mM-ATP, 1mM-EGTA in 6mM-potassium phosphate buffer, pH 7.0 at 4°C). The centrifugation was repeated and 4 - 5ml of relaxing medium added to the pellet. A Potter-Elvehjm blender (5ml capacity) was used to disrupt the myofibrils into myofilaments (also A- and I-segments). Only gentle blending (4 'strokes') was necessary for optimum yield of A-filaments. Intact fibrils were removed by centrifugation in a Unipan (Poland) bench centrifuge at 14000rev./min (9400g) for 1 minute. The supernatant contained dissociated myofilaments, a sample of which was taken for examination in the electron microscope and for SDS gel electrophoresis.

V.2.4. Purification of A-filaments

(a) Isopycnic Banding

(i) Equilibrium density gradients of D_2O-fructose

Relaxing medium was made up in 100% D_2O and the pD adjusted to 7.4 (Glascoe and Long, 1960). Fructose was added to the 100% D_2O-relaxing medium to make a concentrated solution containing 74% (w/w) fructose. To this fructose solution was added a suspension of crude A-filaments to make the final concentration of fructose 46% (w/w), ρ = 1.28 at 5°C. Centrifugation was performed at 5°C and 65000rev./min (265000g) in an 8 x 14ml fixed-angle rotor for 30h. In V.1 it was explained that a fixed-angle rotor ensures a short solvent column, hence decreasing the time to

reach equilibrium. Furthermore, after the run when the tube is reoriented to the vertical, a flattening of the gradient takes place resulting in higher resolution. Fractions (1ml in volume) were collected and samples taken for electron microscopy (see II.2.6).

(ii) Preformed gradients of D_2O-metrizamide

A preformed gradient of four 0.95ml steps of 20, 25, 30 and 35% (w/w) of metrizamide in 100% D_2O-relaxing medium, pD 7.4 at 4°C, (ρ = 1.224 to 1.323) was made up and left overnight in the dark (metrizamide is light-sensitive). To the top of the gradient was layered 1.5ml of crude A-filament suspension and centrifugation performed at 60000rev./min (295000g) at 6°C for 16h in a 3 x 6.5ml swing-out rotor. In this case, the longer solvent column slows down the redistribution of molecules in the preformed gradient into an equilibrium gradient. A shallower D_2O-metrizamide gradient (ρ = 1.224 - 1.293) was also used with three 1.3ml steps containing 20, 25 and 30% (w/w) metrizamide. Centrifugation was carried out as before but for 2 or 4h. About 0.5ml fractions were collected and analysed by electron microscopy and SDS gel electrophoresis.

(b) Zone Velocity on H_2O-D_2O Gradients

The second approach to purification of A-filaments was taken from Trinick (1973). His method separates A- and I-filaments and also A- and I-segments from a crude preparation of A-filaments using the 'zone velocity' technique. The principle is to layer the crude A-filament suspension onto a stabilising gradient and separate the components by virtue of their different s values. The stabilising gradient used by Trinick (1973) was an H_2O-D_2O density gradient and has several advantages over the more conventional gradients (e.g. sucrose, glycerol etc.):

(i) for most purposes D_2O is chemically identical to water

(ii) it is readily available in highly purified form

(iii) its viscosity is relatively low (2.0cp at 5°C).

Trinick (1973) used both swing-out and zonal rotors but, of the two, I have found that the swing-out rotor is preferable: it requires less material – both A-filament suspension and supporting gradient; it is quicker, not only to set up the gradient and collect the fractions, but also in 'run-time'; it is more reliable (Trinick, 1973, reported a 16% success rate with zonal rotors, although I have found an 86% success rate with swing-out rotors). The only other modification of the Trinick (1973) procedure was to increase the concentration of ATP in the relaxing medium to 10mM in order to ensure that dissociation of A- and I-filaments persisted during centrifugation.

A 6ml linear gradient was made using a gradient-former (Buchler Instruments, New Jersey) from 3.1ml of 20% D_2O-relaxing medium (light end) and 2.9ml of 100% D_2O-relaxing medium (heavy end). About 250µl of the myofilament suspension was immediately applied to the top of the H_2O-D_2O gradient. Centrifugation was carried out at 5°C using a 3 x 6.5ml swing-out rotor in an MSE 65 centrifuge at either 20000rev./min (30000g) for 1h or 28000rev./min (60000g) for 1/2h. The gradients were displaced upwards by relaxing medium made up in 60% (v/v) glycerol; 15 drop fractions were collected and stored on ice. The fractions were analysed by SDS gel electrophoresis (see II.2.1 and II.2.2) and electron microscopy (II.2.6). The fractions least contaminated by I-filaments were used for active enzyme centrifugation.

V.2.5. Electron Microscopy

The procedures used in electron microscopy (specimen preparation, determination of magnification, measurement of length) have all been described earlier (II.2.6). The length-average length of the A-filament

preparations was calculated as before (IV.2.3).

V.2.6. SDS gel Electrophoresis

Purified A-filament fractions were prepared for SDS gel electrophoresis in the following manner. Cold trichloroacetic acid was added to 0.5ml of the purified A-filament fraction to give a final concentration of 50mM-trichloroacetic acid, and then left in the cold for 20min. The precipitate, collected by centrifugation at 14000rev./min (9400g) for 1min, was made neutral by adding 20mM-Tris base and then solubilised by adding SDS to a final concentration of 2% (v/v) and macerating with a glass rod. Samples were either used at once or stored for upto a week at -18°C. The concentration of protein in the samples was estimated by the Lowry procedure (II.2.7), and electrophoresis was carried out as described previously (II.2.1 and II.2.2). Gels were scanned when fully destained with the aid of a Joyce Loebl microdensitometer, wavelength 500nm.

V.2.7. Estimation of Concentration of A-filaments

Estimation of the concentration of A-filaments is difficult because of their low concentration in solution and the effect of K^+ and Mg^{2+} on the Lowry procedure (IV.2.5). The concentration of A-filaments in the original fractions was calculated during preparation for SDS gel electrophoresis (V.2.6). This is not an accurate method of protein determination (within $\pm$ 15%) but concentration is not critically important in active enzyme centrifugation.

V.2.8. Linked Enzyme Assay for Myosin Filaments

The concentrations of the constituents of the reaction mixture for the linked enzyme assay of myosin filaments were established by experiments

performed in an SP 1800 spectrophotometer. All enzyme rates were recorded at a wavelength of 340nm in a 1cm pathlength cuvette; the temperature of the cuvette holder was maintained at 25°C by a thermostatted water bath. In these trial experiments, synthetic myosin filaments were used at a final concentration of 100μg/ml.

K^+ Potassium ions are essential for pyruvate kinase activity but must be present in any case to maintain the ionic strength close to physiological. The final concentration of KCl used was 0.1M.

Ca^{2+} and Mg^{2+} Magnesium ions are also essential for pyruvate kinase activity but inhibit the activity of myosin (Szent-Györgyi, 1951). Ca^{2+} activates myosin but inhibits PK activity (the latter effect being partially overcome by K^+). The optimum rate of oxidation of NADH was obtained at 10mM-$MgCl_2$ and 5mM-$CaCl_2$ (the final concentration of Ca^{2+} will be lower than this because it is chelated by EGTA).

PEP and ATP For active enzyme centrifugation, ATP must be at a saturating concentration for myosin. A concentration of 10mM-ATP fulfills this condition, but ATP inhibits PK (K_I = 0.12mM-ATP, Reynard et al., 1961). The inhibition is competitive with PEP and ADP and is negligibly small at a concentration of 8mM-PEP, which is two orders of magnitude higher than the K_m (K_m = 0.07mM-PEP, McQuate and Utter, 1959).

NADH A concentration of 100μM-NADH was used which has an absorbance of 0.62 units.

PK and LDH In order that there should be no accumulation of pyruvate it is necessary to ensure that LDH is in excess of PK. Fast, linear enzyme rates were obtained with 20μg/ml PK and 50μg/ml LDH.

Inhibition of LDH Substrate-inhibition by pyruvate and product-inhibition by lactate on LDH is dependent upon the isozyme used. Since the LDH from rabbit muscle (Boehringer Corporation (London) Ltd.) is predominantly M_4,

this discussion will be confined to this isozyme only. Pyruvate inhibits the activity of LDH-M_4 above a concentration of 1mM (Stambaugh and Post, 1966; Busch and Nair, 1957), but provided LDH is in excess of PK, pyruvate will not accumulate. Product inhibition of LDH by lactate has a K_I of 130mM (Stambaugh and Post, 1966) but this concentration of lactate would never be reached because the amount of NADH present (100μM) becomes limiting. Inhibition by NAD^+ has been suggested to be caused by the formation of an abortive ternary complex: LDH-NAD^+, the K_I being 0.2mM-NADH (Zewe and Fromm, 1962). Whereas NAD^+ might have an inhibitory action in the late stages of a spectrophotometric assay, in active enzyme centrifugation the local concentration of NAD^+ in the enzyme band would be much lower so inhibition would only be slight.

pH To maintain the conditions as close to physiological as possible, the pH must be adjusted to 7.0. Fortunately pH 7.0 is near the optimum pH for all three enzymes (PK, LDH and myosin). Where purified A-filaments have been used the reaction mixture was made up in 100% D_2O and the pD adjusted to 7.4 (Glascoe and Long, 1960).

To summarise, the optimum rate of oxidation of NADH to NAD^+ was obtained under the following conditions: synthetic myosin filaments, 100μg/ml at I 0.13, pH 7.0; reaction mixture, 0.1M-KCl, 10mM-$MgCl_2$, 10mM-ATP, 8mM-PEP, 5mM-$CaCl_2$, 1mM-EGTA, 100μM-NADH, 50μg/ml LDH, 20μg/ml PK in 6mM-potassium phosphate buffer, pH 7.0.

V.2.9. Active Enzyme Centrifugation

(a) Control Runs

(i) NADH

The concentration of NADH remained constant in the reaction mixture in the absence of myosin (as shown by the absorbance at 340nm monitored

in the SP 1800 spectrophotometer). The reaction mixture was also tested in the analytical ultracentrifuge to check (a) the absorbance remained stable and (b) that the NADH did not sediment appreciably. The reaction mixture was made up as described above and transferred to one sector of a double-sector cell with 10mm pathlength. Into the other sector was placed a reference solution (relaxing medium made up to 10mM-ATP, pH 7.0) and the cell was spun in the MSE Analytical Ultracentrifuge at 20000rev./min and 22°C; scans were taken every 5min at a wavelength of 340nm.

(ii) ADP

In V.1.(d) it was explained that purified A-filament samples contained ADP (the amount can be estimated by measuring the amount of ATP hydrolysed using the luciferin-luciferase assay procedure, V.2.11). During active enzyme centrifugation the purified A-filaments are layered onto the top of the reaction mixture and ADP diffuses into it; ADP acts as a substrate for PK and ultimately causes the oxidation of NADH to NAD^+. It will be shown that the diffusion of ADP only becomes a problem at (a) high ADP concentrations and (b) low rotor speeds. Under either of these conditions the diffusion of ADP occurs at a faster rate than the movement of the A-filament layer and it is the former that is followed by the loss of absorbance at 340nm. Because of this problem, control runs were carried out at different speeds and by layering different concentrations of ADP onto the reaction mixture. Diffusion of ADP can be followed by the movement of the 'boundary' produced by the oxidation of NADH to NAD^+, and in this way an apparent s value may be calculated. This boundary caused by the diffusion of ADP shows several features that distinguish it from the boundary produced by the movement of A-filaments (see V.4). It should be emphasised that diffusion is of course <u>independent</u> of rotor speed and that apparent s values have been calculated merely to compare them with the

s value of A-filaments.

The reaction mixture was made up as before and 0.4ml introduced into one sector of a synthetic boundary cell (the over-filling type with 20mm pathlength). Into the other sector was carefully placed 0.45ml of a solution containing ADP and 0.1M-KCl, 10mM-$MgCl_2$, 1mM-EGTA in 6mM-potassium phosphate buffer, pH 7.0. The concentrations of ADP used were 1 or 10mM, and centrifugation was carried out at various speeds and at temperatures in the range 22 - 25°C. Scans were taken every 2min at a wavelength of 340nm.

(b) Synthetic Myosin Filaments

To test the feasibility of determining the $s^{o}_{20,w}$ of myosin filaments by active enzyme centrifugation, initial experiments were attempted with synthetic myosin filaments. An over-filling type synthetic boundary cell was used to form the enzyme layer in preference to the more commonly used Vinograd cell. The synthetic boundary cell enables the absorbance to be measured with a 'dual-beam' system and as a result the traces are much smoother than those obtained with a single beam system, which is compulsory with the Vinograd cell.

Synthetic filaments prepared from myosin A, were diluted to a concentration of 80µg/ml and made up to contain 10mM-$MgCl_2$ and 10mM-ATP. Into one sector of a 20mm pathlength synthetic boundary cell was placed 0.4ml of reaction mixture and into the other 0.45ml of synthetic filament solution. The centrifugation was carried out in the MSE Analytical Ultracentrifuge under the following conditions: speed, 12200rev./min; temperature, 22 - 25°C; scan time interval, 2min; wavelength, 340nm.

(c) Purified A-filaments

Active enzyme centrifugation of purified A-filaments was carried out in the same way as for synthetic myosin filaments with several minor modifications:

(i) since the density of purified A-filaments prepared on H_2O-D_2O gradients is greater than water (ρ = 1.07 - 1.08), the reaction mixture was made up in 100% D_2O. In practice, the 100% D_2O-relaxing medium was used and the additional components added to it, and the pD readjusted to 7.4.

(ii) the concentration of pyruvate kinase was increased to 40µg/ml (see V.3.8(a)).

(iii) the purified A-filament fractions were used within five hours after the time of collection from the H_2O-D_2O gradients. No further additions were made.

(iv) the centrifugation was carried out at various rotor speeds (12000 to 19700rev./min).

(v) purified A-filament fractions 6 and 7 were used because they were least contaminated by I-filaments.

V.2.10. Calculation of $s^o_{20,w}$

Sedimentation coefficients determined by active enzyme centrifugation can be calculated in the normal way from ln r versus time plots (Cohen and Mire, 1965). Radial position, r, was obtained from measurements made on the chart paper with the aid of a linear comparator (see II.2.5). To correct the observed sedimentation coefficient for A-filaments to $s^o_{20,w}$ the values for viscosity and density of D_2O were obtained from tables (from Kirschenbaum, 1951, pp.1 - 42). However, the effect of D_2O on proteins is well known (infact it provides a method of determining M and $\bar{v}$). Edelstein and Schachman (1967) used a correction factor, k, estimated for bovine serum albumin, but it was assumed to hold good for all proteins. The sedimentation coefficient was therefore corrected using the equation of Lee and Berns (1968):

$$s_{20,w} = s_{obs}\left[\frac{\eta_{t,D_2O}}{\eta_{20°,H_2O}} \cdot \frac{(1 - \bar{v}/\rho_{20°,H_2O})}{(1 - \frac{\bar{v}}{k}/\rho_{t,D_2O})}\right] \qquad (17)$$

where k = 1.0155 (from Edelstein and Schachman, 1967).

V.2.11. Estimation of ADP Concentration

The concentration of ADP in the A-filament fractions can be estimated by measuring the concentration of ATP in the H_2O-D_2O gradient in the absence of A-filaments and that in the purified A-filament fraction: the difference is the amount of ATP hydrolysed to ADP. The concentration of ATP was measured by the luciferin-luciferase assay procedure (also known as the firefly lantern assay) and this offers several advantages over measuring ADP concentration directly:

(i) ADP concentration is more difficult to measure; the ADP is first converted to pyruvate by using pyruvate kinase and excess PEP, the amount of pyruvate is then estimated from the absorbance at 460nm after the addition of 2,4 dinitrophenylhydrazine in HCl (Reynard et al., 1961).

(ii) The determination of ADP concentration by the above procedure may be affected by the high concentrations of ATP present.

(iii) The luciferen-luciferase assay procedure is sensitive to nmol amounts of ATP, thus only 10µl of sample is required to determine ATP concentration.

(iv) The luciferin-luciferase system is insensitive to ADP and can be accomplished within minutes.

Before measurement of the ATP concentration in A-filament fractions, a standard curve was first constructed using fresh solutions of ATP. Into a 1cm pathlength glass cuvette was placed 2.5ml distilled water followed by 0.5ml of a freshly made up solution containing 5mg/ml luciferin-luciferase

(from firefly lantern extract in a 0.05M-potassium arsenate, 0.02M-$MgSO_4$ buffer). The cuvette was reproducibly located in a holder in front of a photomultiplier in a curtained drawer in a dark room. The photomultiplier was connected to a high voltage supply from a Photomultiplier Photometer (Radiometer) provided by the Oriel Corporation, Stamford, Connecticut. The voltage was set at 550V and the meter adjusted to read 0% transmission. A 10µl sample of ATP solution was added to the cuvette and, after mixing, the transmission recorded at 15s intervals. The % transmission decreased rapidly at first then levelled out after 75 seconds. Transmission readings taken 90 seconds after mixing were used to construct a standard curve. Transmission readings for purified A-filament fractions or H_2O-D_2O gradients were determined in the same way using 10µl samples; readings taken 90 seconds after mixing were used to read off the ATP concentration from the standard curve.

V.3. Results

V.3.1. Myofibril Preparation

The procedure outlined in V.2.2 to prepare myofibrils from rabbit psoas muscle was always successful. A phase contrast microscope picture of a myofibril suspension is shown in Plate 10. Removal of M-line material by soaking myofibrils overnight in 5mM-Tris-HCl, 1mM-DTT, pH 7.8 at 4°C, did not produce any discernible change in the appearance of the myofibrils.

V.3.2. Crude A-filament Preparation

The blending conditions required to give an optimum yield of 'crude A-filaments' were critical: too little resulted in poor yield, too much produced highly degraded A-filaments. The removal of M-line protein had no obvious effect on increasing the yield of A-filaments (probably because

Plate 10. Phase contrast microscope picture of myofibrils.

The light areas are the I-bands in the middle of which is the Z-line. The dark bands are the A-bands and the less dense region in the middle is the H-zone.

Magnification: x1670.

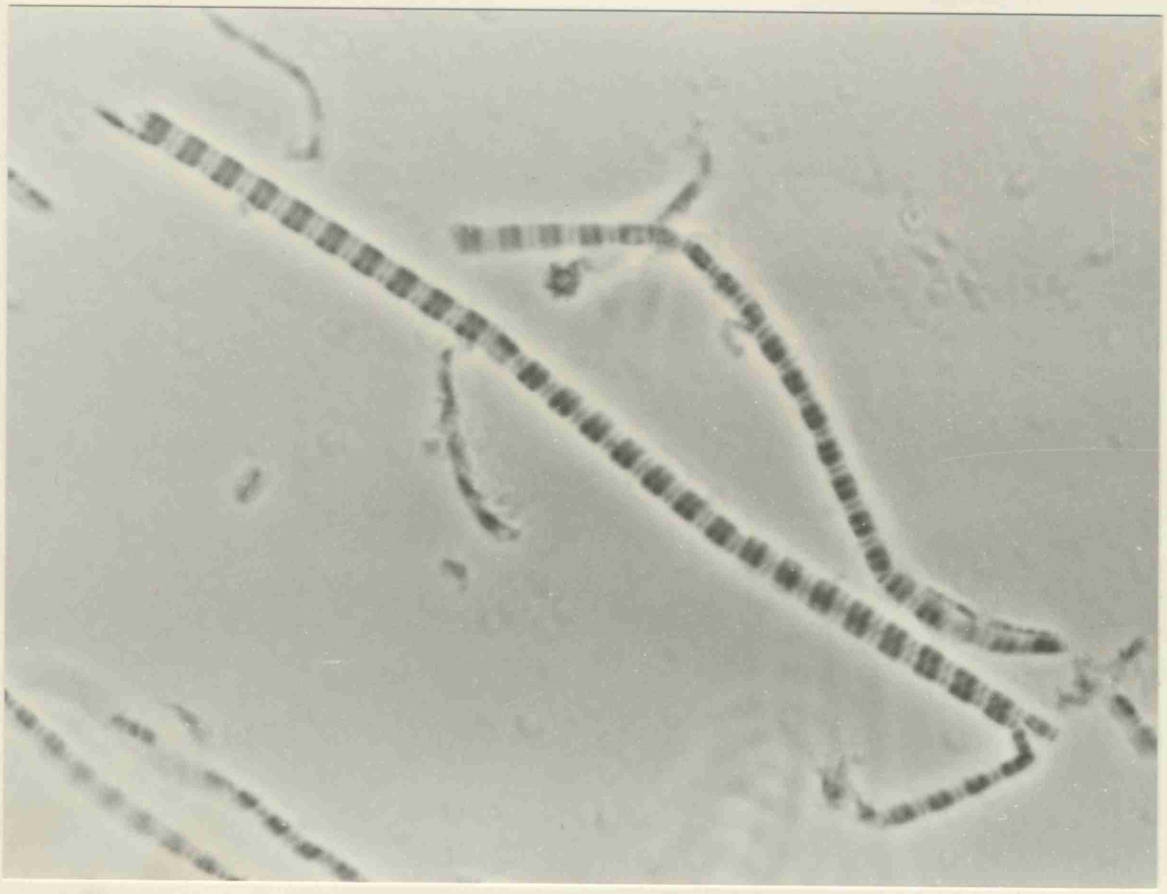

overnight soaking is insufficient to remove substantial amounts of M-line protein; Morimoto and Harrington (1973) used a period of 7 days to remove M-line protein). Due to the lack of an increase in yield, M-line removal was omitted from later crude A-filament preparations. Electron microscopy confirmed that the myofilament preparation contained both A- and I-filaments, Plate 11, and the analysis of the polypeptides by SDS gel electrophoresis is shown in Plate 12.

V.3.3. Isopycnic Banding

(a) D_2O-Fructose

Isopycnic banding of crude A-filaments was unsuccessful in separating A- and I-filaments. A single broad band was produced after overnight centrifugation, but electron microscopy revealed that the band contained 'super-filaments'. The filaments are shown in Plate 13 and it can be seen that they are both wider and very much longer than A-filaments. These 'super-filaments' are probably caused by interaction of actin and myosin filaments when the ATP is exhausted during the 16h centrifugation period. The high concentration of fructose required to generate the desired density gradient may cause the removal of some of the hydration layer of myosin or actin and promote filament interaction.

(b) D_2O-Metrizamide

It has been reported that the buoyant densities of proteins in metrizamide corresponds to the fully hydrated molecule (Birnie et al., 1973). Thus the use of metrizamide may reduce filament interaction by preserving the hydration layer. A 20 - 35% (w/w) D_2O-metrizamide gradient showed three bands after 16h centrifugation and all bands showed the presence of super-filaments. A further attempt was made to obtain concentrated purified A-filaments by decreasing the centrifugation time

Plate 11. Electron micrograph of a suspension of crude A-filaments.

The A- and I-filaments are indicated. 'B' signifies the bare-zone region.

Magnification: x64000.


A
A
B
I

Plate 12. SDS gels of crude A-filaments.

The bands were identified as (from the top): heavy chain (HC), C-protein (C), actin (A), troponin-T (TN-T), light chain 1 (LC1), troponin-I (TN-I), light chains 2 and 3 (LC2, LC3). Although LC3 was clearly observable in the original gel, it can only just be seen in the photograph.

100µg of crude A-filaments was applied.

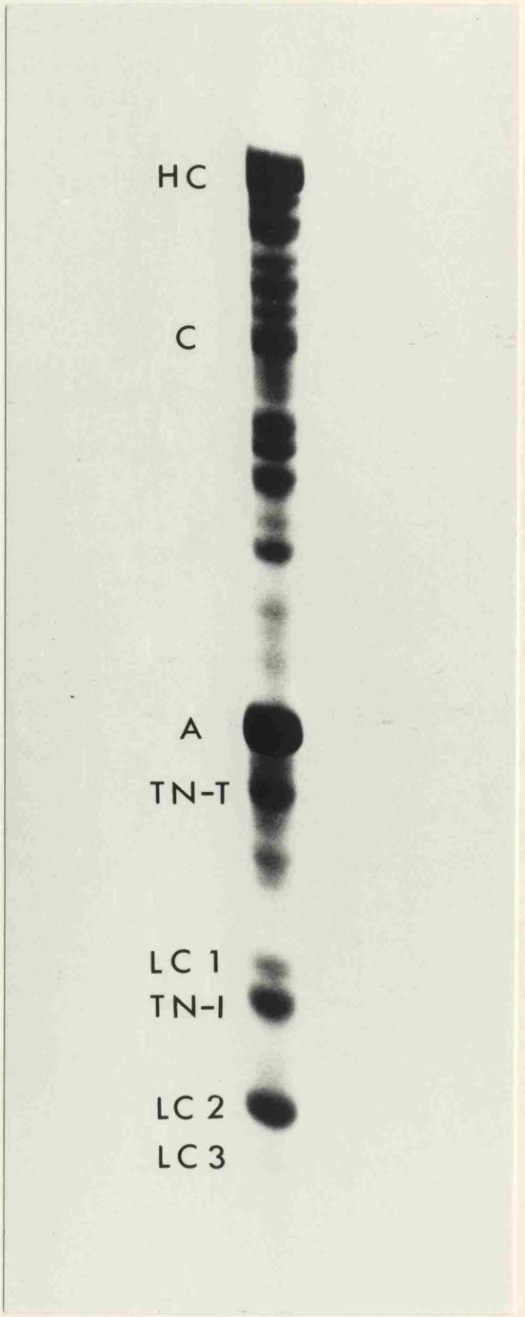
HC
C
A
TN-T
LC 1
TN-I
LC 2
LC 3

Plate 13. Electron micrograph of a crude A-filament suspension layered onto a D_2O-fructose density gradient.

Crude A-filaments were loaded onto a D_2O-fructose gradient (46%, w/w) and after 16h centrifugation one band was formed containing 'super-filaments' some of which showed this distinct 'hairy' feature.

Magnification: x64000.

(because of the low viscosity of metrizamide in solution, less time is required to reach equilibrium). With a shallower density gradient, 20 - 30% (w/w), and a very much shorter centrifugation time, 2 - 4h, only two bands were formed but both contained super-filaments. SDS gels of both bands show that each band is a mixture of actin and myosin, Plate 14. The radial positions of the two bands were greater for the longer centrifugation time indicating that at least 4h is needed to reach the isopycnic condition. Because of the interactions that occur in concentrated sugar solutions, further attempts to obtain concentrated purified A-filaments by isopycnic banding were abandoned. It should be emphasised that these experiments were performed in order to purify and concentrate A-filaments in a single operation. Although these attempts have failed, it may be possible to use isopycnic banding to concentrate A-filaments after removal of I-filaments. A zonal rotor would be ideal for this purpose as large volumes of purified A-filaments could be loaded onto a D_2O-metrizamide gradient.

V.3.4. Purification of A-filaments on H_2O-D_2O Gradients

The modified Trinick (1973) procedure used here has been extremely successful in providing purified A-filaments. This reliability does not involve any significant sacrifice in purity: the preparations used here are still contaminated by small amounts of I-filaments (about 2% by mass; c.f. Trinick,1973, who reported "under 2%"), as evidenced by electron microscopy and SDS gels. Fortunately, the active enzyme centrifugation technique described here is not affected by I-filaments, although purification is still an essential step to remove A-segments.

Plate 14. SDS gels of bands formed on D_2O-metrizamide gradients.

Two bands were formed on D_2O-metrizamide gradients loaded with crude A-filaments. Both bands contained actin and myosin ploypeptide chains (labelling as in Plate 12).

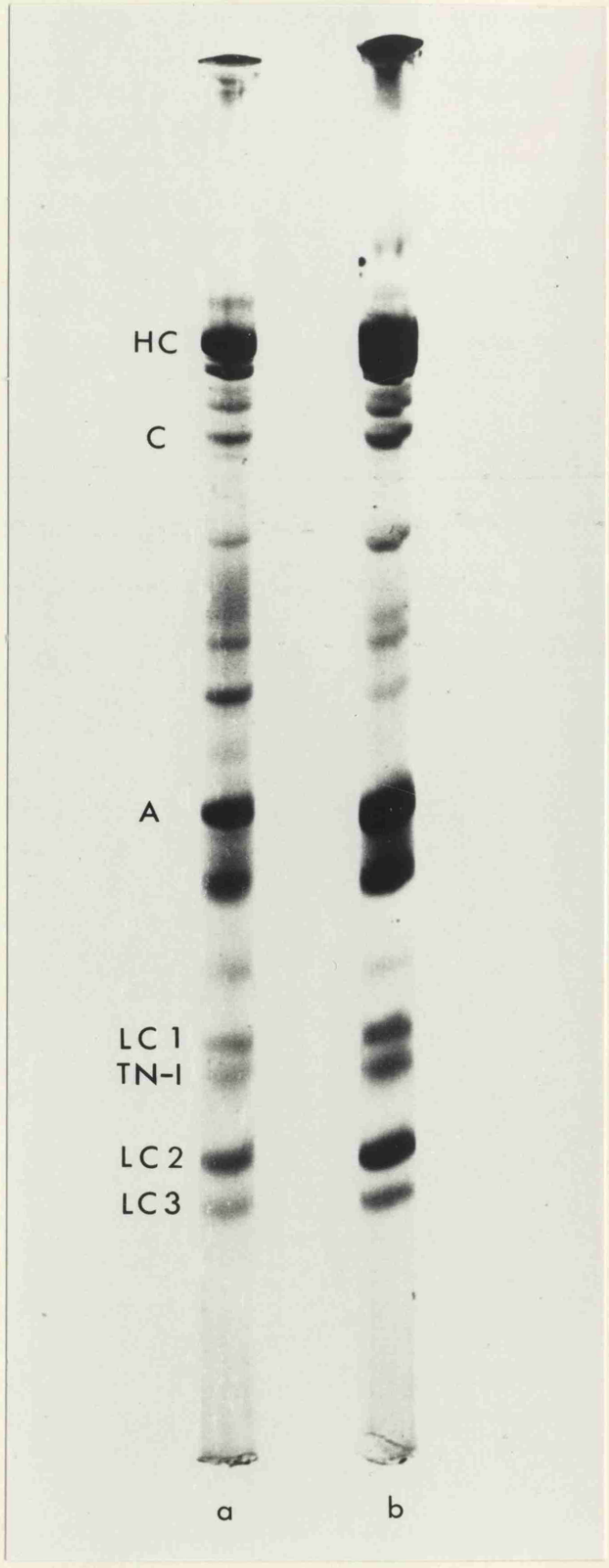
HC
C
A
LC 1
TN-I
LC 2
LC 3
a
b

V.3.5. Electron Microscopy

The electron microscope revealed that the middle fractions taken from H_2O-D_2O gradients contained A-filaments. These displayed the usual features of A-filaments (Huxley, 1963) namely tapered ends, surface projections and a bare central zone, see Plate 15. Fractions 6 and 7 showed the least contamination by I-filaments and the length distributions of three typical purified A-filament preparations are shown in Figure 24. Some breakage of the A-filaments had inevitably taken place during their preparation, however, the length-average length for the three preparations shown had a mean of 1.27μm. It should be noted that no filaments appeared with lengths greater than 1.7μm..

V.3.6. SDS gel Electrophoresis

The SDS gels of eight fractions collected from a single H_2O-D_2O gradient are shown in Plate 16. The actin band and the component polypeptide bands of myosin (heavy chains: HC; light chains: LC1, LC2, LC3) were identified by coelectrophoresis with a sample of myosin A. The other components of the I-filaments (troponin: TN-C, TN-T, TN-I; tropomyosin: α- and β-TM) were identified by their molecular weights. The bands corresponding to actin (41700, Elzinga et al., 1973) TN-T (38000, Wilkinson et al., 1972) and tropomyosin, α and β, (34000, Woods, 1969) can be seen to progressively decrease in intensity from the first fraction (light end) to the eighth fraction (heavy end). The actin : myosin ratio in each fraction was estimated from the peak areas of the microdensitometer traces in the following manner. Since the amount of LC2 (the so-called DTNB-light chains) in myosin is known (2 moles per mole of myosin) then the amount of myosin is proportional to the peak area of LC2. The actin and LC2 peaks were drawn onto tracing paper, cut out and weighed on an analytical balance; the ratio

Plate 15. Electron micrograph of negatively stained purified A-filaments.

The grids were first 'glow-discharged' before negative staining. The A-filaments can be seen to have tapered ends and surface projections along most of their length. The bare-zone is indicated (B).

Magnification: x140000.

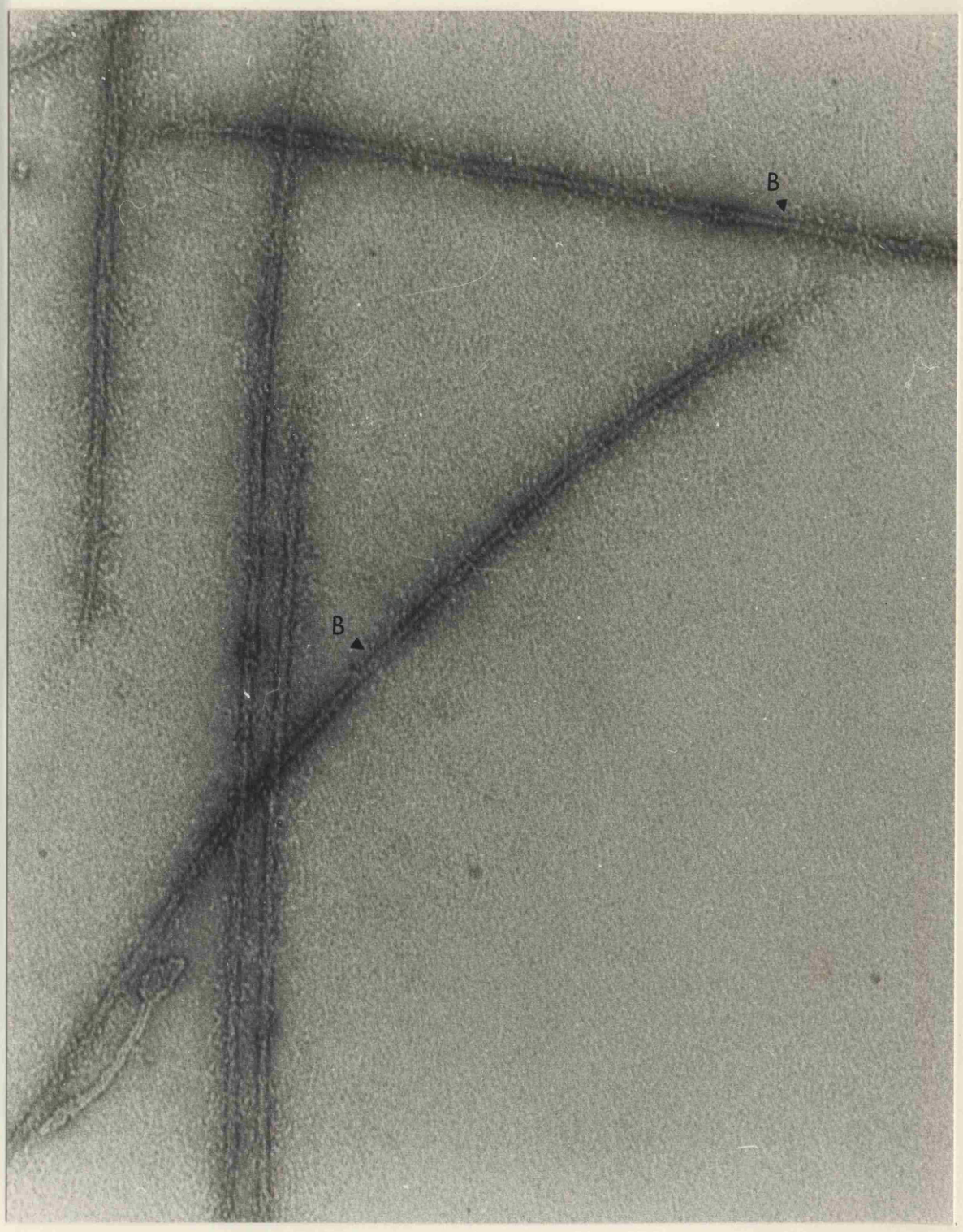
B
B

Plate 16. SDS gels of fractions collected from an H_2O-D_2O gradient loaded with crude A-filaments.

Fraction 1 is the light end (20% D_2O), fraction 8 is the heavy end (100% D_2O). The proteins associated with the I-filament (actin, troponin, tropomyosin) progressively decrease in concentration from fractions 1 to 8. Microdensitometer traces of the gels revealed that fractions 6 and 7 contained the least % by weight of actin. The bands are labelled (from the top): heavy chain (HC), B-protein (B), C-protein (C), F-protein (F), actin (A), troponin-T (TN-T), tropomyosin (TM), light chain 1 (LC1), troponin-I (TN-I), light chain 2 and 3 (LC2, LC3).

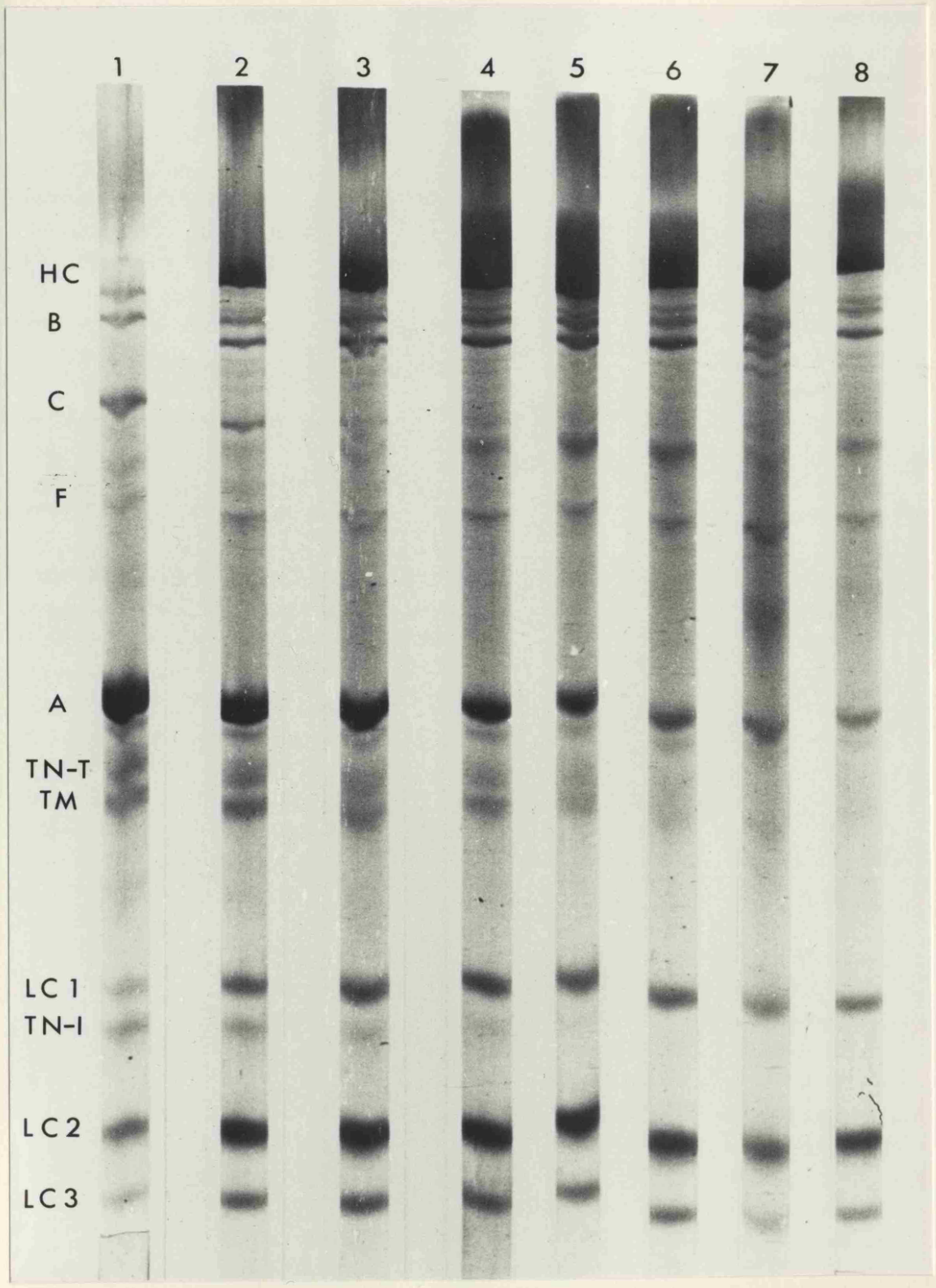
1
2
3
4
5
6
7
8
HC
B
C
F
A
TN-T
TM
LC 1
TN-I
LC 2
LC 3

Figure 24 Length distributions of three purified A-filament preparations

The number of filaments counted and the length-average length (l_{ave}) are shown.

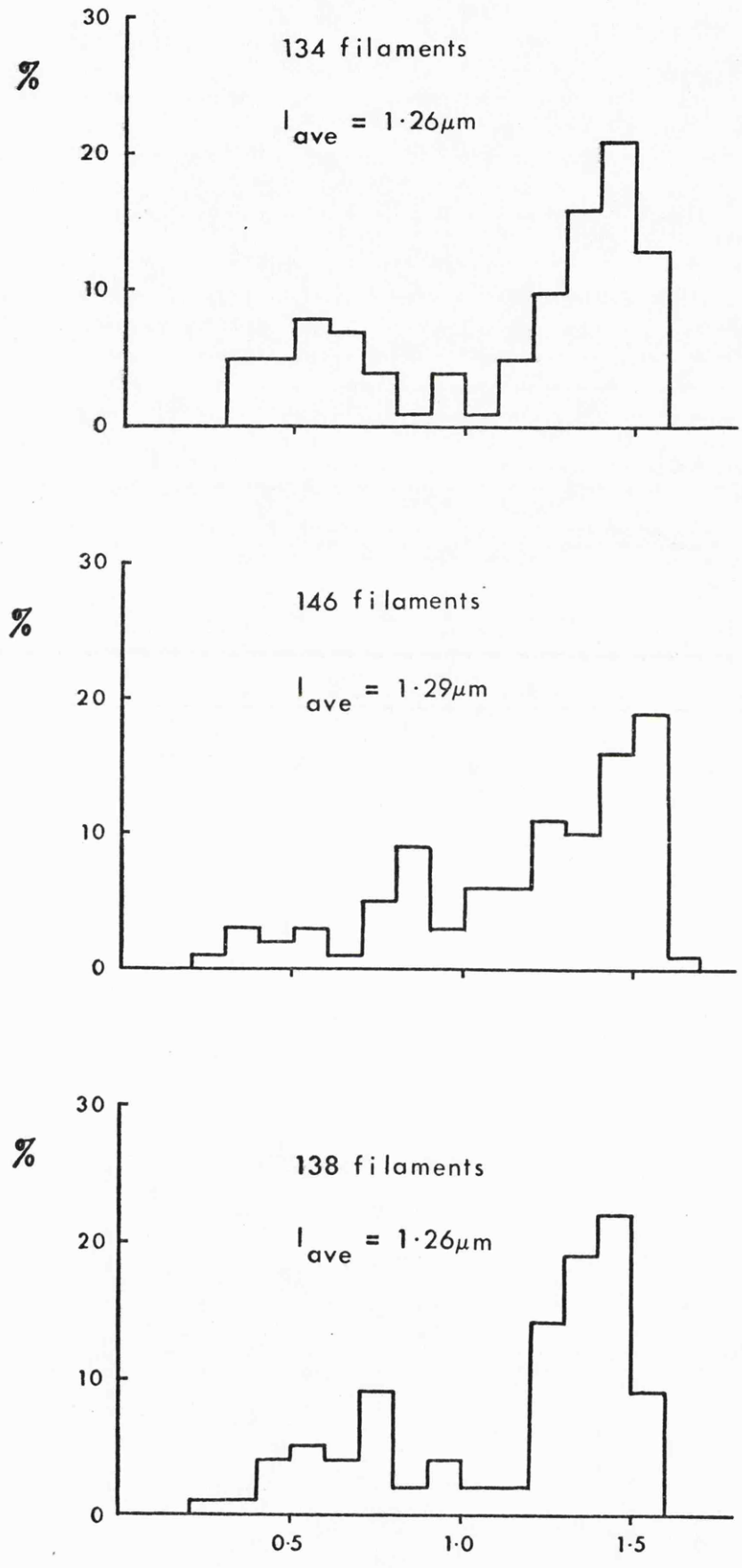
30
%
20
10
0
134 filaments
l_{ave} = 1·26μm
30
%
20
10
0
146 filaments
l_{ave} = 1·29μm
30
%
20
10
0
138 filaments
l_{ave} = 1·26μm
0·5
1·0
1·5
Length (μm)

of the weights gives the actin : LC2 ratio. But to obtain the % by weight of actin in each fraction this actin : LC2 ratio must be corrected for (a) the different staining intensities of actin and LC2 and (b) for the weight fraction of LC2 in the myosin molecule. For the former, I have used the estimate of Potter (1974) who reported that the staining intensity of actin was 20% greater than that of LC2. The results have also been corrected for the amount of light chain 2 in myosin (Sarkar, 1972; Weeds and Frank, 1972). Neglecting the presence of other protein components, the % by weight of actin in each fraction is shown in Table 5, column 3. As can be seen, the lowest amounts of actin are in fractions 5 to 7. The larger amount of actin in fractions 1 to 4 is due to I-filaments, that in fraction 8 is due to the presence of I-segments. These results confirm that the Trinick (1973) procedure for obtaining purified A-filaments can provide samples that are contaminated with only about 2% by weight of actin.

V.3.7. Problems Associated with Active Enzyme Centrifugation

(a) Control Runs

(i) NADH

The control active enzyme run of the reaction mixture in the absence of myosin filaments showed that the concentration of NADH did not alter during several hours of centrifugation. Furthermore, there was no appreciable sedimentation of NADH (the sedimentation coefficient, $s^{o}_{20,w}$, for NADH is 0.2S, Kemper and Everse, 1973).

(ii) ADP

The diffusion of ADP into the reaction mixture is shown as the 'apparent s value' as a function of rotor speed (Table 6). At high ADP concentrations and low rotor speed the 'apparent s value' increases, the effect being particularly marked at high concentrations, yielding s values

Table 5. The % by weight of actin found in purified A-filament fractions

Fraction	actin:LC2 ratio [a]	% by wt. of actin [b]
1	5.16	24.8
2	1.37	8.1
3	0.99	6.0
4	0.79	4.8
5	0.51	3.2
6	0.30	1.9
7	0.50	3.1
8	0.97	5.8

[a] estimated from the peak areas of actin and LC2 bands on SDS gels

[b] assuming actin stains 20% more intensely than LC2 (Potter, 1974) and that LC2 accounts for 8.14% of the myosin molecule by weight (Sarkar, 1972; Weeds and Frank, 1972).

Table 6. The 'apparent s values' created by the diffusion of ADP during active enzyme centrifugation as a function of ADP concentration and rotor speed.

1mM-ADP		10mM-ADP	
speed rev./min	apparent $s_{20,w}$ (S)	speed rev./min	apparent $s_{20,w}$ (S)
12310	82.4 ± 3.9	12150	236.9 ± 12.7
15240	51.7 ± 4.2	12500	235.4 ± 26.1
16730	39.3 ± 1.6	15270	163.1 ± 6.8
18830	31.2 ± 1.9	16670	135.9 ± 9.6

very much greater than that of the A-filament (about 136S, Trinick, 1973). This experiment shows quite clearly that by layering a purified A-filament solution, containing a high concentration of ADP (approaching 10mM), onto a reaction mixture and following the loss of absorbance at 340nm, the s value obtained would be a measure of the diffusion of ADP and not of the movement of the A-filament band. It is therefore imperative to estimate the concentration of ADP in the purified A-filament fractions.

(b) Estimation of ADP Concentration

The % transmission versus time curves obtained from luciferin-luciferase assays on five ATP concentrations are shown in Figure 25. The 90 second transmission readings were used to construct the standard curve, Figure 26. Transmission readings taken 90 seconds after mixing are shown for two fractions (fractions 6 and 7, i.e. those used for active enzyme centrifugation) for each of two A-filament preparations, Table 7. Also shown are transmission readings from the same fractions of two H_2O-D_2O gradients which were not loaded with A-filaments. The ratio of the two transmission readings gives the fraction of ATP hydrolysed by the A-filaments. The results show that 96.8 $\pm$ 0.8% (S.E.) of the original ATP concentration (10mM) was present in the purified A-filament fractions, this corresponds to about 0.3mM-ADP. In the previous section (V.3.7(a)) it was shown that the apparent s values caused by the diffusion of ADP were only greater than the s value of A-filaments (136 $\pm$ 25S, Trinick,1973) when the ADP concentration is high. For ADP concentrations less than 1mM, the apparent s values are only large at low rotor speed (below 12000rev./min). A lower limit to rotor speed is therefore set, below which the sedimentation coefficient of A-filaments cannot be measured by active enzyme centrifugation. Above this speed (12000rev./min) the effect of ADP can be ignored.

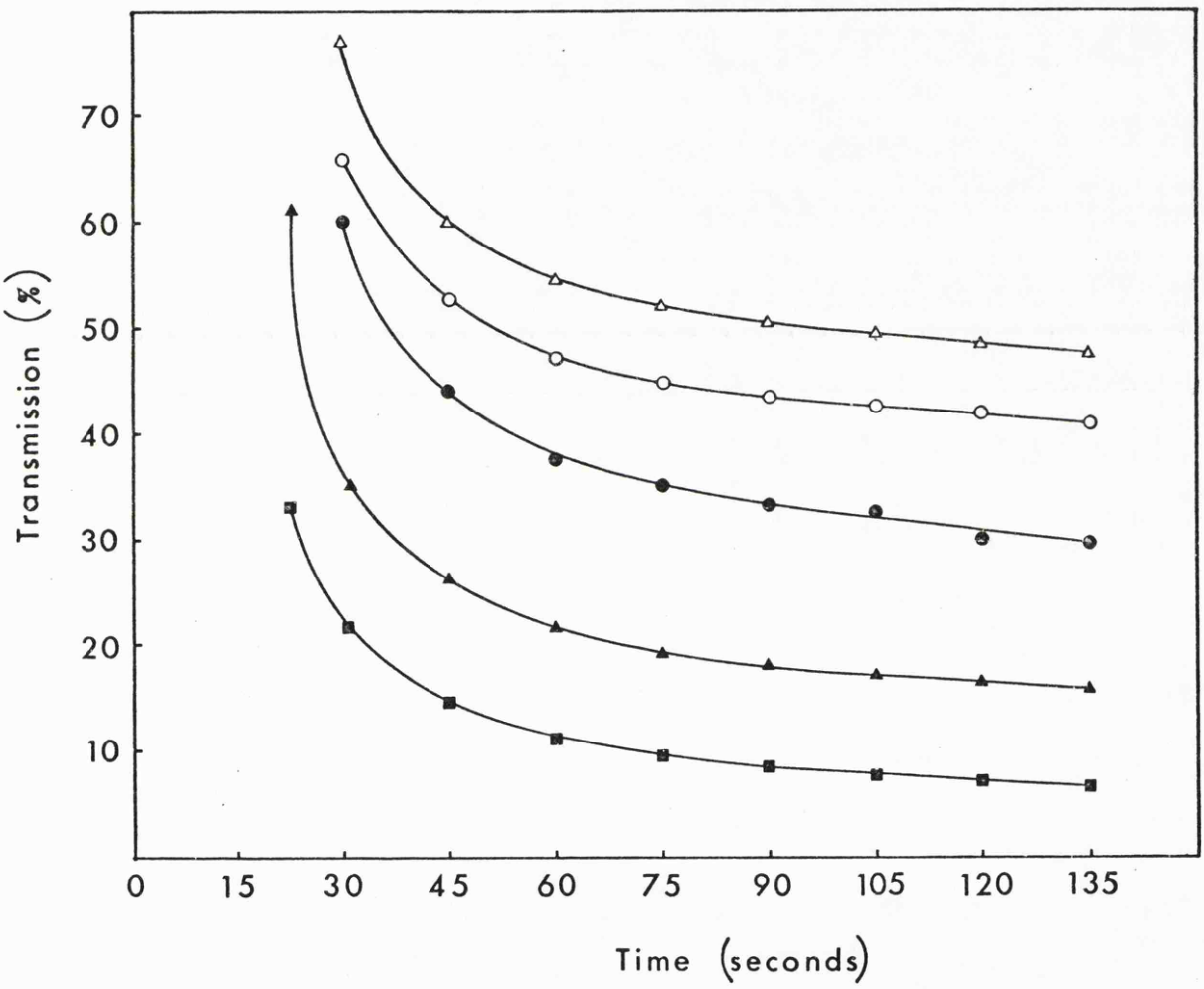

Figure 25 Response of luciferin-luciferase assay at various ATP concentrations

Percent transmission was recorded at 15 second intervals after mixing. The amounts of ATP (nmol) are: 100 (△), 75 (○), 50 (●), 25 (▲), 10 (■). Details of the assay are given in the text.

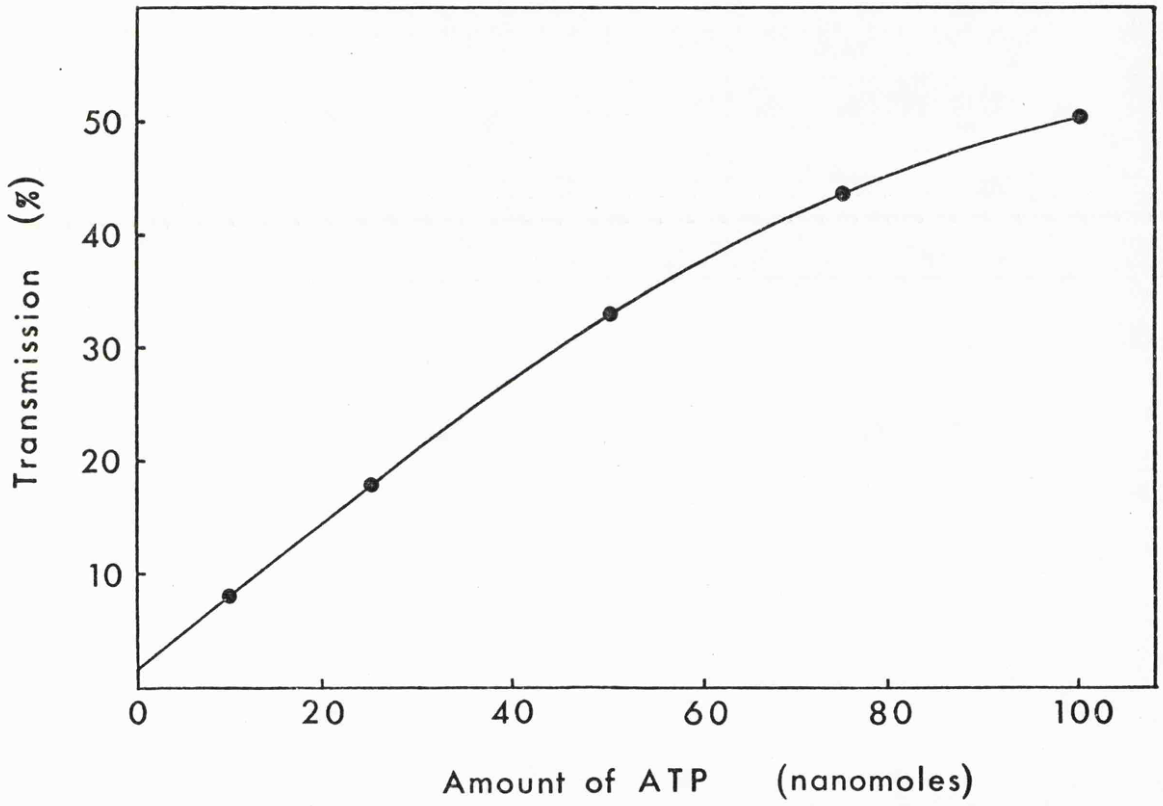

Figure 26 Standard curve for the luciferin-luciferase assay

The % transmission readings taken 90 seconds after mixing were plotted as a function of the amount of ATP.

Table 7. Estimation of the amount of ATP hydrolysed in purified A-filament fractions

Transmission readings quoted are those taken 90 seconds after addition of 10µl of the purified A-filaments.

A-fil. prepn.	Fractn.	Transmission reading		% of [a] ATP left
		A-fil. fractn.	control	
X	6	48.0	49.8	96.4
X	7	47.0	49.0	95.9
Y	6	47.3	49.4	95.7
Y	7	48.5	49.0	99.0

MEAN = 96.8 ± 0.8

[a] from the ratio of transmission readings taken 90 seconds after mixing.

V.3.8. Active Enzyme Centrifugation

(a) Synthetic Myosin Filaments

Active enzyme centrifugation of synthetic myosin filaments was carried out as described in V.2.9(b). The movement of the enzyme layer was successfully followed by the decrease in absorbance at 340nm caused by the oxidation of NADH to NAD^+. The sedimentation coefficient produced, corrected to 20°C and water, was 146.6 ± 2.6S (rotor speed = 12200rev./min). However, $s^o_{20,w}$ obtained for the same synthetic filament preparation by sedimentation velocity experiments at higher concentrations (and extrapolating to zero concentration) was 172 ± 5S. Mire (1967) explained that lower $s^o_{20,w}$ values could be obtained by active enzyme centrifugation when the speed of the linked enzyme reaction is too slow to follow the movement of the enzyme layer. The observed sedimentation coefficient is therefore a measure of the speed at which the linked enzyme system converts the product and is less than the true $s^o_{20,w}$. The centrifugation was repeated but the concentration of PK in the reaction mixture was increased to 40µg/ml to prevent the aforementioned effect. Under these conditions, active enzyme centrifugation gave an $s^o_{20,w}$ of 169.0 ± 3.7S at 12170rev./min which is not significantly different from the $s^o_{20,w}$ predicted from sedimentation velocity (that is to say the difference is no greater than two standard errors). This is the first successful report of the application of active enzyme centrifugation for the measurement of $s^o_{20,w}$ of synthetic myosin filaments.

(b) Purified A-filaments

The purified A-filaments were first checked for ATPase activity in a spectrophotometer by using the linked enzyme system to monitor the hydrolysis of ATP. Active enzyme centrifugation of purified A-filaments was performed as described in V.2.9(c). Movement of the A-filament layer was

detected by the loss of absorbance at 340nm caused by the oxidation of NADH to NAD^+. The NADH boundary remained sharp throughout most of the run (Plate 17) although some broadening did occur in the later stages of the run due to polydispersity. The ln r *versus* time plots were linear over the entire period, in contrast to the curvature seen in control runs with ADP, see Figure 27. Sedimentation coefficients were corrected to 20°C and water as described in V.2.10; no correction was made to zero concentration. Figure 28 shows values obtained for five different purified A-filament preparations as a function of rotor speed (three to four $s_{20,w}$ values were determined for each preparation). Sedimentation coefficients are independent of rotor speed over the range 12000 to 15500rev./min, but above 15500rev./min the $s_{20,w}$ values decrease with increasing rotor speed. The reason for these lower sedimentation coefficients has been given earlier for synthetic myosin filaments: the movement of the enzyme layer is faster than the rate at which the product (ADP) can be converted by the linked enzyme system (Mire, 1967). If the amounts of PK and LDH in the reaction mixture are increased the reaction rate should, in theory, be greater and true $s_{20,w}$ values should be obtained.

Attempts to obtain $s_{20,w}$ values in the range of 130S above a speed of 15500rev./min failed. Measurement of the enzyme rate in a spectrophotometer showed that the enzyme rate had been increased by only 12% with the addition of 50% more PK and LDH. The explanation is that the linked enzyme system used here is complex and under the influence of various activators and inhibitors (see V.1. (a)); increasing the amounts of PK and LDH does not automatically lead to an equivalent increase in reaction rate. To produce faster conversion of ADP it would be necessary to re-establish the concentrations of all the constituents of the reaction mixture. Since genuine $s_{20,w}$ values would be obtained upto, at most, 18000rev./min before

Plate 17. A trace recorded by the u-v scanner showing the NADH boundary formed during active enzyme centrifugation.

The trace records absorbance at 340nm (vertical direction) against radial position (horizontal direction). The sample was purified A-filaments layered onto a reaction mixture. Speed: 12330rev./min; temperature: 22.0°C. The direction of sedimentation is from right to left.

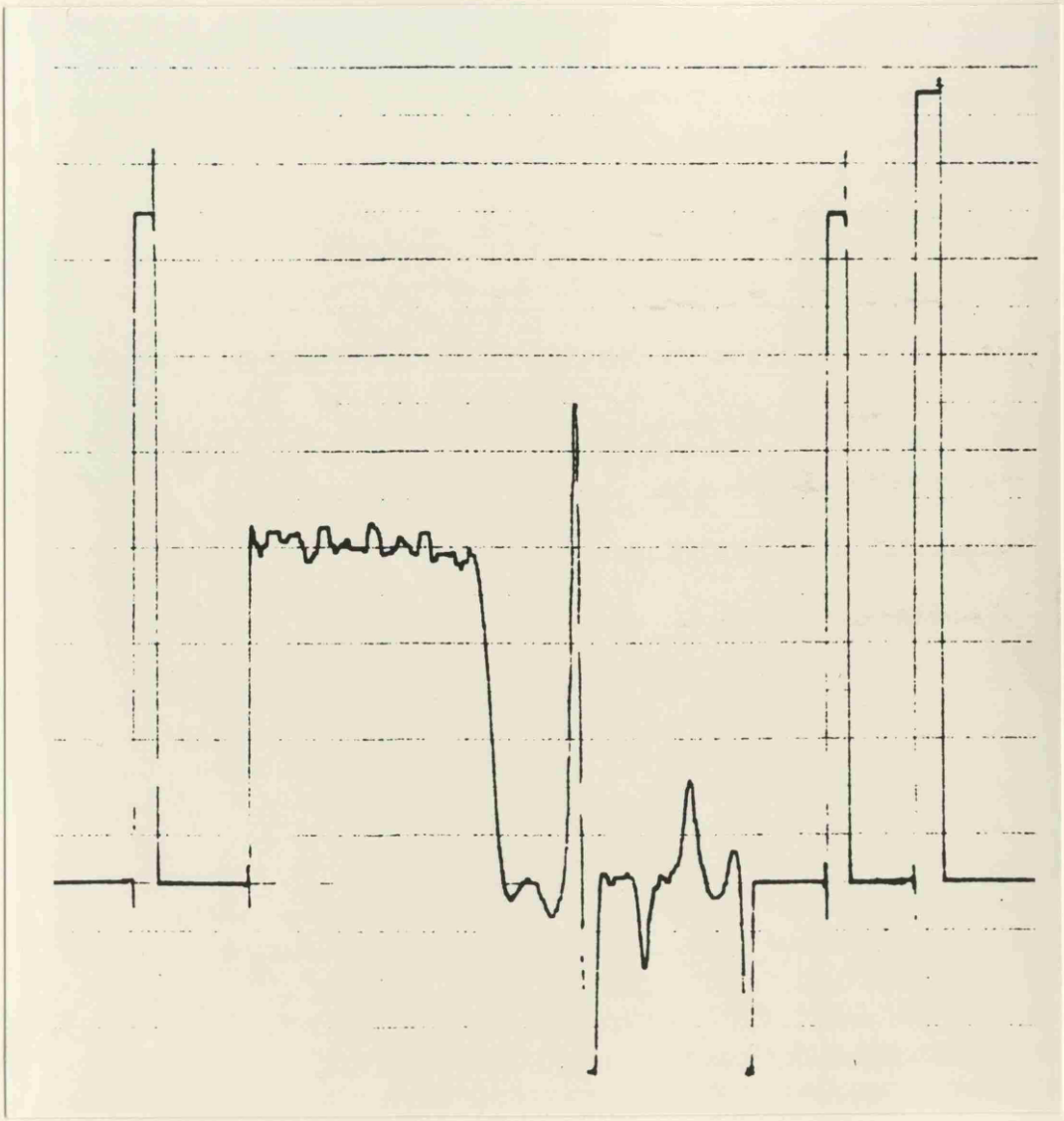

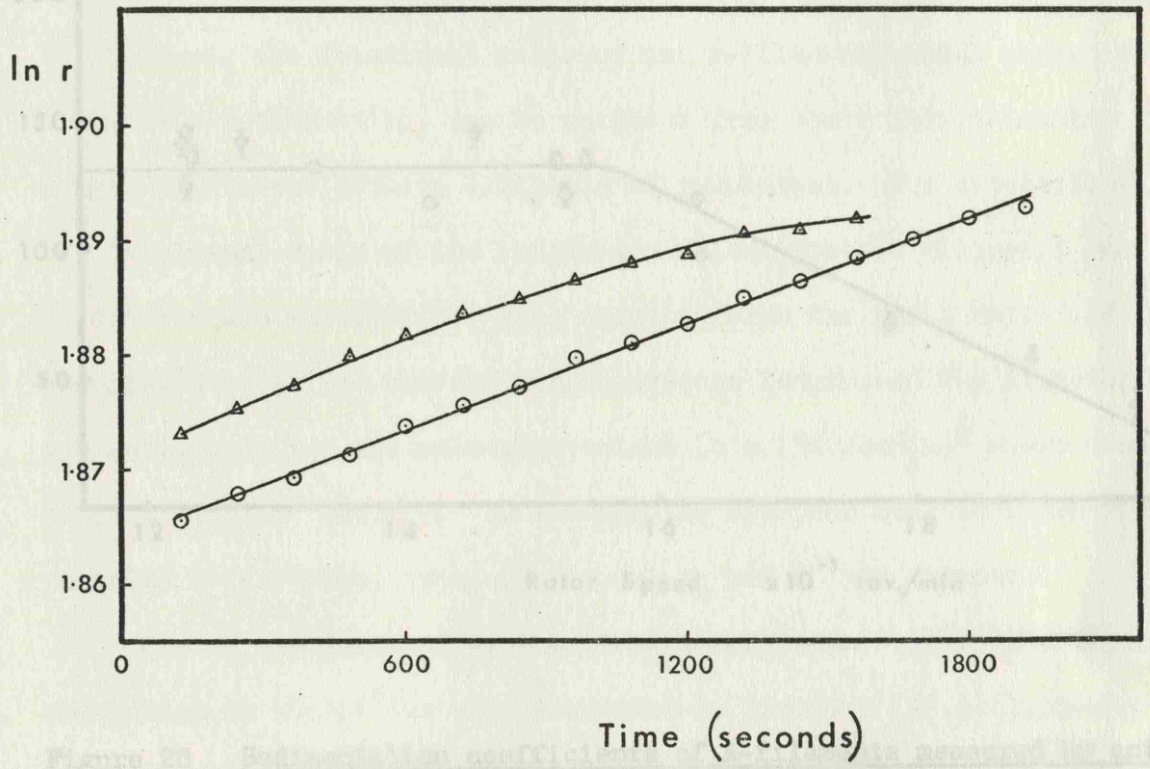

Figure 27 Ln r versus time plots from active enzyme centrifugation

The position of the NADH boundary (r) was measured from the scan traces. The results from active enzyme centrifugation of purified A-filaments (○) and 1mM-ADP (△) are shown. Rotor speed: about 12400rev./min in both cases; temperature: 22 °C.

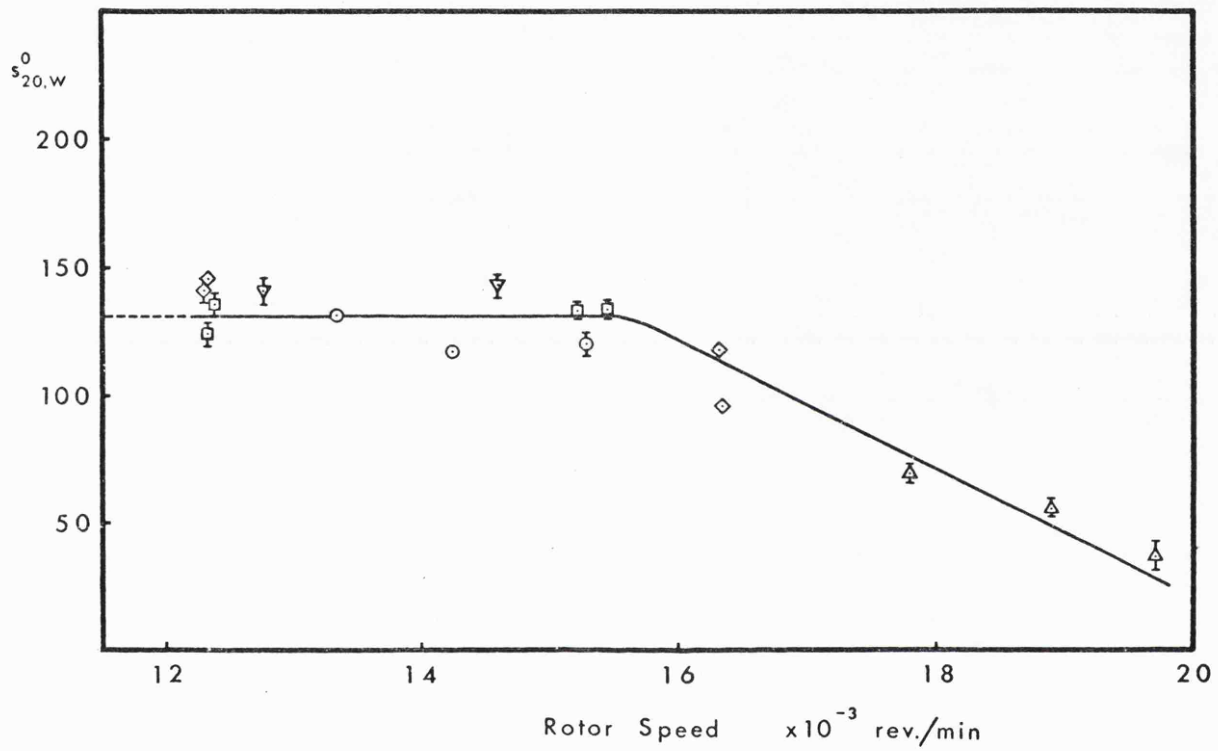

Figure 28 Sedimentation coefficients of A-filaments measured by active enzyme centrifugation as a function of rotor speed

The symbols signify different purified A-filament samples. Error bars have been drawn where the standard error is greater than 4%. Rotor speed as indicated; temperature: 22 - 25°C.

the same phenomenon occurred again, such experiments were not undertaken.

Sedimentation coefficients were not determined below 12000rev./min as the effect of diffusion of ADP becomes dominant in this range (see section V.3.7(b)). The mean $s^{o}_{20,w}$ of A-filaments of all the sedimentation coefficients measured in the range 12000 to 15500rev./min is 132 ± 3S.

V.3.9. Determination of Molecular Weight

In the introduction to this Chapter it was explained that the molecular weight of the A-filament could be determined from s^{o} and f/f_{o}. Furthermore, the frictional ratio of the A-filament, which cannot be measured experimentally, can be computed from the frictional ratio of the length-equivalent prolate ellipsoid of revolution. For synthetic filaments, the frictional ratio of the length-equivalent prolate ellipsoid was calculated via the Perrin (1936) equation from the axial ratio (IV.4.7): the length used (2a) was the length-average length and the diameter (2b) was estimated from the molecular weight ($b = (3M\bar{v}/4\pi N_{A}a)^{\frac{1}{2}}$ where M was obtained from s^{o} and k_{s}). An alternative approach must be found for purified A-filaments since, of course, k_{s} and M^{o} are unknown.

One of the features of the 'length-equivalent' prolate ellipsoid of revolution is that M^{o} is very sensitive to diameter (IV.4.6), being proportional to its square. Thus M^{o} of the length-equivalent prolate ellipsoid may be computed for a range of radii (see equation 18 below). But the axial ratio of the length-equivalent prolate ellipsoid can also provide the f/f_{o} of the same and, when corrected for the anomalous frictional increment, can be substituted into the Svedberg equation relating M^{o} and s^{o} of purified A-filaments. The unique solution to the molecular weight of the A-filament is obtained when these two equations (eqn. 18 and 24) are satisfied for a particular axial ratio. The equations

are, for a length-equivalent prolate ellipsoid of revolution:

$$M^{\circ} = \frac{4\pi N_A b^2 a}{3\bar{v}} \tag{18}$$

and for purified A-filaments:

$$M^{\circ} = \frac{N_A f s^{\circ}}{(1 - v\rho)} \tag{19}$$

where

$$f = \left(\frac{f}{f_o}\right)_{fil} \times f_o \tag{20}$$

and f_o is given by

$$f_o = 6\pi\eta a_e \tag{21}$$

f_o and a_e are the frictional coefficient and radius of the equivalent sphere, respectively.

$$a_e = \left(\frac{3 M \bar{v}}{4\pi N_A}\right)^{1/3} \tag{22}$$

The frictional ratio of the A-filament, $(f/f_o)_{fil}$ is related to that of the length-equivalent prolate ellipsoid by

$$\left(\frac{f}{f_o}\right)_{fil} = f_i \times \left(\frac{f}{f_o}\right)_{prol} \tag{23}$$

where f_i is the frictional, increment and is equal to 1.76 ± 0.11 (IV.4.7). Substituting equations 20, 21, 22 and 23 into 19 and rearranging, we have

$$M^{\circ} = \left[\frac{N_A s^{\circ} 6\pi\eta}{(1 - \bar{v}\rho)} \left(\frac{3\bar{v}}{4\pi N_A}\right)^{1/3} \cdot f_i \left(\frac{f}{f_o}\right)_{prol}\right]^{3/2} \tag{24}$$

Since $(f/f_o)_{prol}$ may be calculated from the axial ratio via the Perrin (1936) equation, M^o may be computed as a function of 'b', for a length-equivalent prolate ellipsoid (eqn. 18) and as a function of 'b', at constant s^o, for purified A-filaments (eqn. 24). In both cases, the length (2a) was taken as the 'length-average length' (1.27μm). The two curves obtained are shown in Figure 29. There is one point where the two functions are simultaneously satisfied, corresponding to a radius of 7.4nm (for the length-equivalent prolate ellipsoid) and a molecular weight of 1.2×10^8.

V.4. Discussion

The isopycnic banding experiments described here have shown that it is not possible to separate A- and I-filaments by this method. This is unfortunate because the isopycnic banding technique has the obvious advantage over zone velocity in that it concentrates the filaments within a band. There are several possibilities as to why these experiments failed. Firstly, there may be no difference between the buoyant densities of actin and myosin filaments, although this is unlikely because in all experiments more than one protein band was observed. Secondly, during long centrifugation times (16h) the ATP in the relaxing medium may become exhausted and so permit myosin and actin filaments to interact. Thirdly, myosin - actin interaction may be promoted (even in the presence of ATP) either by the removal of the hydration layer, thus 'unshielding' the charges on the proteins, or mediated by protein - metrizamide complexes. Concerning these last two points, if a difference between the buoyant densities does exist then one may explain the appearance of more than one protein band as to be due to a difference in myosin : actin ratios within the complexes.

The purification procedure for A-filaments that was adopted was that

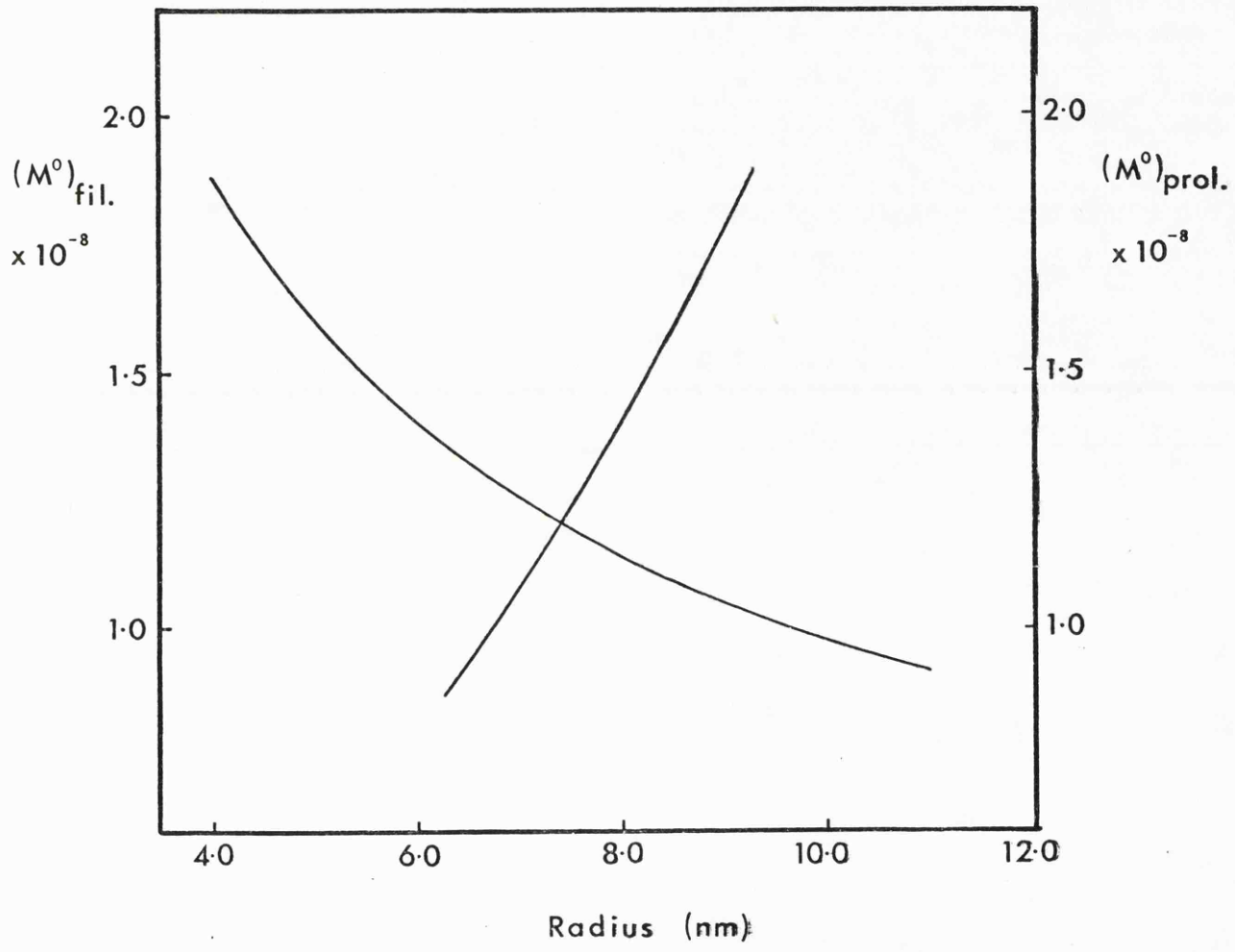

Figure 29 M^o of A-filaments and the length-equivalent prolate ellipsoid computed over the radius range shown

$(M^o)_{prol}$ was calculated via equation 18 and $(M^o)_{fil}$ via equation 24, see text. The length was taken as 1.27μm and s^o as 132S.

of Trinick (1973) using H_2O-D_2O gradients. This method offers distinct advantages over the purification technique reported by Morimoto and Harrington (1973) using 10 to 30% glycerol gradients. (i) H_2O-D_2O gradients have a low viscosity (100% D_2O has a viscosity of 2cp at 5°C) so zone velocity purification of A-filaments takes less time to complete, thus there is less likelihood that the ATP will be exhausted and hence permit interaction between actin and myosin filaments. (ii) The Morimoto and Harrington (1973) method involves removing the M-line material over a period of seven days. During this period depolymerization or proteolysis may occur and could result in degradation of the A-filaments (see iii below). The method used here enables all experiments on purified A-filaments to be completed within 40h after the death of the rabbit. (iii) The A-filaments purified by the Trinick (1973) procedure have a length-average length of 1.27μm, whereas those prepared by Morimoto and Harrington (1974b) have been judged to be far more seriously degraded by their sedimentation characteristics. No $s^{o}_{20,w}$ was reported by Morimoto and Harrington (1974b), although ds/dc ($=k_s.s^{o}$) was measured by the differential sedimentation technique (Kirschner and Schachman, 1971) and was quoted as -14.7S.ml/mg (in the presence or absence of Ca^{2+}). If an $s^{o}_{20,w}$ of 132S is assumed (and as we shall see below, s^{o} is approximately independent of length), then k_s = 111ml/g. The molecular weight of the A-filament, estimated from these values of s^{o} and k_s, is 6 x 10^7 showing that the A-filaments are about half their normal size *in vivo* and are far more degraded than predicted from the length distribution obtained from electron micrographs (Morimoto and Harrington, 1973, 1974b).

(iv) D_2O has been reported to stabilise polymer structures (Inoué *et al.*, 1965; Lee and Berns, 1968; Paglini and Lauffer, 1968; Henderson and Henderson, 1969). Several suggestions have been made to explain this

increased stability of the polymer caused by D_2O. Lee and Berns (1968) suggested it was due to intensification of hydrophobic bonds between aggregates. Henderson and Henderson (1969) proposed two possibilities (although a distinction between them has only been reported for DNA): the stability of the polymer may be increased due to replacement of bound water by D_2O, or by stabilising hydrogen bonds within helical structures (e.g. DNA or α-helix within protein) by replacement of hydrogen by deuterium atoms.

Zone velocity sedimentation using H_2O-D_2O gradients is a reliable method for obtaining A-filaments from which the contaminants (I-filaments and A- and I-segments) have, for the most part, been removed. The fractions containing purified A-filaments can be used immediately, without further treatment, to determine s^o by active enzyme centrifugation. As far as the author is aware, this is the first report of measurement of $s^o_{20,w}$ by active enzyme centrifugation in which a linked enzyme system involving <u>two</u> enzymes has been used. The $s^o_{20,w}$ for A-filaments also represents the highest s^o value determined in this way, being twice that of the largest s^o previously reported (Kolb, 1974). That the movement of the 'NADH boundary' can be attributed to the sedimentation of the A-filament layer is supported by five pieces of evidence: (i) synthetic filament solutions are devoid of ADP and A-segments and have been successfully detected by active enzyme centrifugation, (ii) the 'NADH boundary' in control runs with ADP is sharp initially, but rapidly becomes broader and ln r <u>versus</u> time plots show pronounced curvature; with A-filaments, although the 'NADH boundary' does spread during a run due to polydispersity, the broadening occurs less quickly and is less marked than with ADP, furthermore, ln r <u>versus</u> time plots are linear over the entire period, Figure 27, (iii) the ADP concentration in A-filament preparations is low, and in any case only has an

influence at low rotor speed, (iv) active enzyme centrifugation is capable of following only active enzyme species (the presence of I-filaments is unimportant) and (v) the other active enzyme species (namely A-segments) is removed during purification. On the basis of this evidence and the earlier report by Trinick (1973) that the s^o of A-filaments was 136 ± 25S (estimated from zone velocity experiments by the method of Strohmaier and Mussgay, 1959), it can be concluded that the $s^o_{20,w}$ value of 132 ± 3S is indeed the sedimentation coefficient of A-filaments.

An algorithm has been used to solve the equations relating M^o to axial ratio (a/b) of the length-equivalent prolate ellipsoid, and to s^o and f/f_o of purified A-filaments so that the unique value for M^o for the A-filament can be obtained. The number of myosins/14.3nm repeat, N, may be calculated from the molecular weight, after correcting for the weight fraction of C-protein, and the length-average length, but first the parameters used in the calculation will be considered, together with the possible sources of error in each.

V.4.1. Possible Sources of Error in M^o and N

(a) $s^o_{20,w}$

In the discussion above the weight of evidence indicated that the $s^o_{20,w}$ found did correspond to that of A-filaments. In the light of this conclusion, we may consider those factors which may influence the sedimentation coefficient.

(i) filament interaction

An erroneously high $s^o_{20,w}$ could be obtained if filament interaction (either between A-filaments or between A- and I-filaments) occurred. But the presence of Mg-ATP both prior to and during active enzyme centrifugation, ensures that interaction between A- and I-filaments is minimal.

Self-interaction of A-filaments may also be neglected because they are in dilute solution and, in spite of the 'absence of charge effects' condition for sedimentation, there will inevitably be a net charge on the A-filaments.

(ii) enzyme activity of A-filaments

Although D_2O has been reported to reduce enzyme rates (Bender and Hamilton, 1962; Thomson, 1963) it does not effect the ATPase activity of myosin B (i.e. actomyosin) at pH 7, Hotta and Morales (1960). Furthermore, a decrease in ATPase activity of A-filaments is reflected in the sensitivity of the linked enzyme system and in no way alters s^o: a prediction confirmed by the reproducibility of s^o values between different A-filament preparations.

(iii) enzyme activity of the linked enzyme system

The overall reaction rate of the linked enzyme system is under the influence of various effectors (see V.1.(a)). A possible decrease in enzyme rate caused by D_2O has already been mentioned. Although the reaction rate does have an effect at rotor speeds in excess of 15500rev./min, over the speed range of 12000 to 15500rev./min the sedimentation coefficient is, within experimental error, constant.

(iv) the effect of D_2O on $\bar{v}$

Heavy water tends to decrease $\bar{v}$ because some hydrogen atoms on the protein are exchanged for deuterium (Hvidt and Nielsen, 1966). This lower $\bar{v}$ was used in the correction factor to convert sedimentation coefficients to 20°C and water (V.2.10); the value of k used ($\bar{v}_{D_2O} = \bar{v}_{H_2O}/k$) was 1.0155 which was determined for bovine serum albumin (Edelstein and Schachman, 1967). The k factor is generally assumed to be the same for all proteins.

(v) correction to infinite dilution

Because of the low concentrations of enzyme used in active enzyme centrifugation, the $s_{20,w}$ obtained is usually assumed to be the same as

that at infinite dilution (Cohen and Mire, 1971b). The concentration dependence of the sedimentation coefficient of A-filaments is high (k_s was calculated to be 432ml/g, using $k_s = 2\bar{v}(V_s/\bar{v} + (f/f_o)^3)$ where $V_s/\bar{v} = 2.3$ and so the correction to infinite dilution should, strictly, be included. But the high k_s also tends to rapidly dilute the A-filament band during active enzyme centrifugation and so the actual concentration at which $s_{20,w}$ is measured is unknown, although it will certainly be small. The correction of $s_{20,w}$ to infinite dilution therefore has been neglected, but it is unlikely that this would introduce an error greater than 1%.

(b) Diameter

In the previous Chapter (IV.4.5) it was submitted that s^o was sensitive to changes in diameter. Although the exact diameter of the A-filament has been an elusive quantity (estimates are 12 - 14nm, Huxley, 1963; 11 - 13nm, Trinick, 1973; 18 - 20nm, Morimoto and Harrington, 1973) the uncertainty is probably a result of specimen preparation for the electron microscope rather than a genuine difference in diameter. This supposition is consistent with the observation that s^o values for the same or different A-filament preparations are reproducible.

(c) Anomalous Frictional Increment

The 'anomalous frictional increment' determined in the previous Chapter was used here to calculate f/f_o of A-filaments from the f/f_o of the equivalent close-packed prolate ellipsoid of revolution. It was found that this frictional increment estimated for synthetic filaments was independent of axial ratio over the range studied (see Table 4, section IV.4.5). It has also been suggested that the higher frictional ratio may be the result of a torque exerted on the myosin filament caused by the helical

arrangement of myosin heads (IV.4.8). If this hypothesis is correct, one would expect the frictional increment to be largely independent of axial ratio and it would therefore be valid to apply it to A-filaments with higher axial ratio.

(d) Algorithm for M^o

The molecular weight of the A-filament has been computed using an algorithm which solves the equations relating M^o to the axial ratio of the length-equivalent prolate ellipsoid on the one hand, to the s^o and f/f_o of purified A-filaments on the other. The f/f_o of the A-filament was predicted from the axial ratio of the length-equivalent prolate ellipsoid and corrected for the frictional increment, f_i. The two functions intersect at just one point (Figure 29) and therefore provide an accurate estimate of the weight-average molecular weight, M^o, 1.2×10^8. The radius at this point is, by definition, that of the prolate ellipsoid of revolution that has the same mass and length as purified A-filaments.

(e) Length-average Length

The justification for using 'weight-average length' to calculate f/f_o in preference to number-average length is because f/f_o is used in conjunction with the weight-average sedimentation coefficient in order to calculate M^o. The great advantage in using f/f_o and the sedimentation coefficient to calculate the mass/unit length of the A-filament is that N is largely independent of length by the following argument. At high axial ratio and constant mass/unit length, the molecular weight increases linearly with length. The number of myosins/14.3nm, N, is proportional to molecular weight and inversely proportional to length (eqn. 25), so that as length increases, N remains constant (a prediction that has been confirmed

by computation). On decreasing the length (and hence axial ratio) the molecular weight is no longer proportional to length and N will tend to increase, but even so N is tolerant of even large changes in length.

The method used previously (IV.3.4) to estimate the number of myosin molecules per 14.3nm (N) made use of the following equation:

$$N = \frac{\text{mol. wt. of filament} \times 0{\cdot}965}{\text{mol. wt. of myosin}} \times \frac{14{\cdot}3}{l_{ave}} \qquad (25)$$

where the molecular weight of the A-filament is corrected for 3.5% by weight of C-protein (Morimoto and Harrington, 1974a) and l_{ave} is the length-average length (1270nm). Substituting the molecular weight of the A-filament as 1.2×10^8 and the molecular weight of myosin as 470000, gives N = 2.8, which is consistent with three fold helical symmetry for the A-filament. But this equation is based upon two assumptions: (a) that myosin heads project at 14.3nm intervals down the entire length of the A-filament and (b) that there is constant mass per unit length. Strictly speaking, neither of these assumptions are true for native A-filaments. Firstly, there is a region in the middle of the A-filament which is devoid of cross-bridges, the so-called 'bare-zone'. The length of this region has been measured from electron micrographs of A-filaments and has been quoted as 160nm (Hanson et al., 1971; Knappeis and Carlsen, 1968; Morimoto and Harrington, 1973). However, by labelling glycerinated rabbit psoas muscle with antibodies to S-1 of myosin, Craig and Offer (1976a) have shown that the bare-zone is 154nm long, in good agreement with the value of 149 $\pm$ 2nm measured from A-segments stained with ammonium molybdate (Craig, 1975, 1977). To correct for the presence of a bare-zone of length 150nm, the length-average length used to calculate N via the equation above must be decreased by 150nm, assuming that A-filament fragments that contain no

bare-zone have a negligible effect upon the weight-average molecular weight.

There is a further correction to make because the mass/unit length is not constant for two reasons: (i) because of the location of other protein components of the thick filament and (ii) because of taper at the ends.

(i) Other protein components of the A-filament

Purification of A-filaments inevitably results in some breakage of the filaments and one would expect that the ends of the filament, which are tapered, are particularly susceptible. But the distribution of other protein components of the thick filament (M-line and C-protein) is not even: C-protein for example, is located at 43nm intervals over a distance of 0.16 to 0.51μm, measured from the centre of the A-band (Craig and Offer, 1976b). The correction for the weight fraction of non-myosin components in these purified A-filament samples would therefore be difficult, but in any case if it is ignored, the error introduced into N is only small (at most 3.5%).

(ii) The effect of taper

The ends of the full length A-filament are tapered and there is thus a decrease in mass/unit length. Estimation of the length of the A-filament from electron microscopy includes the tapered regions, and so if this length (1.57μm, Craig and Offer, 1976a) is used together with the molecular weight to calculate the number of myosins/14.3nm repeat, N, the answer will be too low. To determine the true value of N it is necessary to presume certain details of the packing arrangement in the tapered region: the argument is a worthwhile one for we shall see that the 'taper' has a considerable effect upon N. If we assume that the packing of myosins into the A-filament obeys 3-fold helical symmetry and that at the ends, 3 myosin molecules are consecutively omitted at each 14.3nm interval, then an A-filament,

containing 18 myosin tails in cross-section, will terminate after 6 x 14.3nm repeats. This progressive decrease in mass/unit length over 6 x 14.3nm at each end, is equivalent to a total of 6 'full crowns' missing per A-filament ignoring the 'empty crown' proposed by Craig and Offer (1976a). Thus a full length A-filament which contains 98 crowns (Craig and Offer, 1976a) has only 92 'full crowns' because of taper. An alternative method has therefore been used to estimate N from the number of myosins/A-filament and the number of 'full crowns'.

But there is a problem with purified A-filament preparations in that, for a typical preparation, only 32% of the A-filaments are close to 'full length', the remainder show various extents of degradation. It would be pushing the precision of these experiments too far to expect to correct for the percentage of the degraded A-filaments that display a taper. At best, the limits to the uncertainty in N can be established. If all the filaments have tapered ends, then correcting for taper, gives the minimum number of 'full crowns' and an upper limit to N. As the percentage of filaments with tapered ends decreases, then the number of 'full crowns' is progressively underestimated: the maximum number of full crowns is reached when all the filaments have broken (i.e. non-tapered) ends and this corresponds to the minimum N. The number of crowns for A-filaments of length-average length 1.27μm is 98 x 1.27 / 1.57 = 80 crowns. If the correction for taper is included, the number of full crowns is 74. The limits to N so obtained are 3.40 (for 100% tapered filaments, 74 full crowns) and 3.15 (0% tapered filaments, 80 full crowns) and the true value of N for a purified A-filament preparation lies between these two limits. It is clear that the consideration of whether degraded A-filaments have tapered ends is an important one affecting the estimation of N from molecular weight but was not considered in an earlier report (Morimoto and Harrington, 1974a).

In summary, the factors considered above do not create large errors in N with the notable exception of 'taper'. If an average value for N is chosen, 3.3, assuming that 50% of all the ends of the A-filaments are tapered, the maximum possible error, including the uncertainty in the sedimentation coefficient (132 $\pm$ 3S), is 3.3 $\pm$ 0.2. It can therefore be confidently concluded from this investigation that the A-filament shows 3-stranded helical symmetry with 1 myosin molecule per cross-bridge. An accurate estimate of the molecular weight of the full length A-filament can be obtained by assuming that there are 3 myosins/crown and that there are 92 'full crowns'. This gives a molecular weight of 1.27×10^8 from myosin alone and, with an additional 3.5% by weight of C-protein, as 1.31×10^8. This value for the molecular weight of the A-filament agrees very well with that estimated by Offer et al., 1973, (1.39×10^8) from the ratio of thick : thin filament protein (55 : 36, Huxley and Hanson, 1957) and the molecular weight of the thin filament (22.8×10^6) without making any assumptions as to the symmetry of the thick filament.

CHAPTER VI

Concluding Remarks

The research described in this thesis has made extensive use of new hydrodynamic procedures to examine some of the properties of myosin both as a molecule and in its aggregated form of the myofilament. Since these techniques have provided some hitherto unobtainable parameters they deserve some further comment.

A method has been described (Appendix I) by which it is possible to determine the molecular weight of a particle from s^o, k_s and $\bar{v}$, provided that there is no interaction taking place. If $\bar{v}$ is known, all that is required to determine M^o is an s *versus* concentration plot and since this type of analysis is often performed on solutions of uncharacterised proteins as a test for homogeneity, a reliable estimate of M^o can be obtained without the need for a separate determination of D. No assumptions are made as to shape and hydration, and f/f_o (derived from k_s) is the phenomenological frictional ratio of the particle. The molecular weight of myosin, calculated from s^o and k_s was found to be 470000 $\pm$ 27000 in good agreement with other estimates (III.4) and for the first time the molecular weights of synthetic myosin filaments have been obtained without the need to assume any hydrodynamic model.

A second feature of the s^o, k_s and M^o relationship is that if M^o and s^o of a monomer species are known, k_s is fixed. By this means it is possible to investigate self-interaction of sedimenting particles and predict, for the simple case of a monomer-dimer equilibrium, the approximate equilibrium constant, K. This analysis has been successfully used not only for myosin solutions (Chapter III) but also for α-chymotrypsinogen (J. R. Parkin and A. J. Rowe, unpublished), 16S RNA (Pearce *et al.*, 1975) and pyruvate dehydrogenase complex from *E. coli* (M. J. Danson, R. A. Perham and A. J. Rowe, unpublished). For the myosin solutions studied here it has

been shown that if a monomer-dimer equilibrium does exist, then K is less than 10ml/g.

Another approach has been to combine sedimentation and viscosity studies to determine the ratio $V_s/\bar{v}$ from k_η and k_s. The estimate of $V_s/\bar{v}$ is, in itself, an interesting quantity for muscle proteins and myofilaments since it can provide insight into the hydrodynamic forces exerted upon 'sliding filaments' during muscular contraction. In addition, the $V_s/\bar{v}$ method enables the 'goodness of fit' of a hydrodynamic model to be tested quantitatively, as $V_s/\bar{v}$ obtained from k_η and k_s makes no assumptions as to the shape of the particle. Application of this technique to myosin molecules and filaments has shown, perhaps not surprisingly, that neither may be adequately represented by an equivalent prolate ellipsoid of revolution.

Also presented here are details of a method to determine s^o of purified A-filaments by active enzyme centrifugation (Cohen, 1963). A dual linked enzyme system was successfully adapted to monitor the movement of A-filaments in the synthetic boundary cell of the ultracentrifuge. Active enzyme centrifugation is particularly suitable for determination of s^o of A-filaments as only low concentrations are required and non-myosin contaminants are ineffectual.

It has been possible to relate f/f_o of synthetic myosin filaments to f/f_o of the length-equivalent prolate ellipsoid and show that a 'frictional increment' is involved which is apparently independent of axial ratio. The frictional increment, f_i, has been used to predict f/f_o of purified A-filaments from the axial ratio of the length-equivalent prolate ellipsoid, a calculation based upon two assumptions: (i) $V_s/\bar{v}$ of synthetic filaments is the same as that of purified A-filaments (i.e. that f_i is the same for native A-filaments as it is for those formed <u>in vitro</u>) and (ii) that f_i is

independent of length upto high axial ratio. Certainly some kind of anomalous frictional increment is displayed by myosin filaments since, if f/f_o of the length-equivalent prolate ellipsoid is not corrected by this factor, the maximum value of N (assuming 100% of the filaments show taper) is 1.5. This number is inconsistent with the X-ray diffraction data on native thick filaments in resting muscle (Huxley and Brown, 1967) and also with the biochemical evidence of the amount of myosin in muscle (Hanson and Huxley, 1957; Huxley and Hanson, 1957). Thus the frictional ratio of A-filaments cannot be accounted for by a simple, close-packed prolate ellipsoid of revolution (as also suggested by Trinick, 1973). When the correction is made for the frictional increment and the effects of taper are considered, it is found that N lies in the range 3.1 - 3.5, which is consistent with three-fold helical symmetry for the A-filament. If a concentrated sample of purified A-filaments becomes available in the future then it will be possible to obtain M^o from s^o and k_s without the need to make this assumption. Of the types of packing arrangement of myosin molecules previously mentioned (I.1.3), two models are based upon 3-stranded symmetry and it is possible that one of these (the Rowe model) may represent the true packing arrangement since it is consistent with most of the observations made on vertebrate A-filaments.

N should of course be an integer if perfect helical symmetry is obeyed but the range of N determined here does not span an integer. The explanation may be that the A-filament does not show exact helical symmetry over part or all of its length (Huxley and Brown, 1967) and in this respect it should be remembered that X-ray diffraction of whole muscle gives an average pattern of the myosin head arrangement along the A-filament. Thus the helical repeat of 43nm and the subunit repeat of 14.3nm may only be approximate and this would create a non-integer value of N. A further

possibility is that the structure of the A-filament may not be as stable as supposed, indeed, Haselgrove (1975) has found that the subunit spacing is altered from 14.34nm in relaxed muscle to 14.48nm in 'activated muscle' and he interpreted this as a structural change occurring in the backbone of the filament when muscle contracts. Purified A-filaments may be used to test this hypothesis in that periodicities may be investigated (i) in the absence of I-filaments, (ii) without interference from adjacent sarcomeres and (iii) after specific removal of other protein components of the A-filament. However, this type of analysis must await further improvements in specimen preservation and in image analysis procedures.

There are still a number of unanswered questions concerning the structure of the A-filament but the determination of the symmetry goes part of the way in solving them. For example: (i) does the 43nm periodicity of C-protein reflect a true myosin repeat or is it a result of the binding of C-protein itself, (ii) what is the location and function of the other protein components of the thick filament, (iii) what is the significance of two isoenzymes of myosin and how are they arranged within A-filaments, (iv) how is the radial growth of the A-filament prevented *in vivo* and why is it non-functional *in vitro*, and (v) how is the length of the A-filament precisely determined?

As to this last point, there have been many speculations.
(a) A vernier mechanism has been proposed (Huxley, 1963; Huxley and Brown, 1967) involving a protein with a different periodicity to that of myosin. The two proteins copolymerize and a stable structure is formed when the two periods coincide. Evidence from several sources (from anti-C-protein studies, Craig, 1975; Craig and Offer, 1976b, from examination of negatively contrasted A-segments, Craig, 1977, from estimation of C-protein length by hydrodynamic studies, Offer *et al.*, 1973, and from the finding that

C-protein is unable to control self-assembly of myosin molecules, Katsura and Noda, 1973a; Moos et al., 1975; Pinset-Härström and Morel, 1975) suggests that C-protein is not the likely candidate for this second periodic structure. Rather, this second periodic structure may be some other protein component of the thick filament or even the thin filament.

(b) A 'steric hindrance' model was postulated by Katsura and Noda (1971) in an attempt to explain the absence of a length determining mechanism in LMM paracrystals. The HMM fragment is suggested to play an important role in the assembly of myosin molecules, perhaps by preventing further aggregation by the steric hindrance of myosin heads.

(c) A 'nucleation-growth' model has been used to interpret the mechanism of fibril formation in collagen (Wood, 1960) and aggregation of insulin (Waugh, 1957). But it is unlikely that such a mechanism is involved in myosin filament formation as there have been several reports (Katsura and Noda, 1971; Josephs and Harrington, 1966) that the filament length in vitro is independent of myosin monomer concentration, contrary to the behaviour predicted by the nucleation-growth model.

(d) Caspar (1966) submitted that the length of any biological structure formed by specific association of identical subunits may be an integral function of the subunit itself. Thus a linear aggregate in which the units assembled in a quasi-equivalent manner would have a self-determined length since the progressive disruption of the bonding pattern would increase until aggregation of further units became thermodynamically unstable. Where large numbers of subunits are involved, the conditions for the formation of the self-assembled structure are more critical. So the range of lengths found for synthetic filaments can simply be explained by the inability to exactly reproduce the ionic conditions necessary for the precise determination of length. Furthermore such structures are able to

undergo reversible changes in state in response to environmental changes: a property well-documented for synthetic filaments (Josephs and Harrington, 1966; Kaminer and Bell, 1966; Sunouchi et al., 1966; Sanger, 1971). The observation that synthetic filaments formed from vertebrate smooth muscle myosin and non-muscle myosin are shorter than those from vertebrate skeletal muscle myosin (Pollard and Weihing, 1974; Kaminer et al., 1976) may be accounted for by there being fewer specific assembly sites in the smooth and non-muscle myosins.

Purified A-filaments may be of use in testing these theories by investigating the ability of A-filaments to reform after depolymerization at high ionic strength.

Finally it is of interest to know how the A-filaments are assembled into the sarcomere so that their ends are in register and that they are arranged in a superlattice with a rotation of 2/3 of a repeat between neighbouring filaments. The sarcomere is, after-all, the basic contractile unit in vertebrate skeletal muscle and it is the events that take place within it, after stimulation by the nerve impulse, that lead to contraction.

APPENDICES

The following two appendices contain a summary of the relevant points from the paper by Rowe (1977). I am grateful to Dr A. J. Rowe for allowing me to quote extensively from his manuscript prior to publication.

Appendix I. The Concentration Dependence of the Sedimentation Coefficient

Determination of M^o from s^o and k_s and Estimation of Self-Interaction

The procedure used to determine M^o from s^o and k_s is based upon an equation relating k_s and the frictional ratio of the sedimenting particle. This equation can be derived from first principles by the following argument.

Definitions

We begin by supposing that there is a volume flux (J) associated with a sedimenting component in a closed system. Now in the closed system of a centrifuge cell the laws of conservation of mass operate, in other words, as the volume associated with the sedimenting particles moves towards the bottom of the cell, there is a movement of an equal volume of solvent 'backwards' (contrary to the behaviour in an open system in which there is no return flow). We may further define two theoretical frames of reference: a cell-fixed and a solvent-fixed frame of reference, denoted by the planes P_c and P_s, respectively, Figure 1. If V is the forward volume flux in a cell-fixed frame of reference (which is also equal to the backward volume flux) then the forward volume flux in a solvent-fixed frame of reference is 2V.

Basic Assumptions

(i) All sedimentation occurs at a fixed velocity of migration, u

(ii) The sedimentation coefficient of a particle in a solvent-fixed frame of reference is s^o (i.e. at infinite dilution).

The volume flux (J) associated with the sedimenting component may be specified in two ways:

(a) In terms of the frictional properties of the system (J_f)

One may write the generalised Stokes equation as:

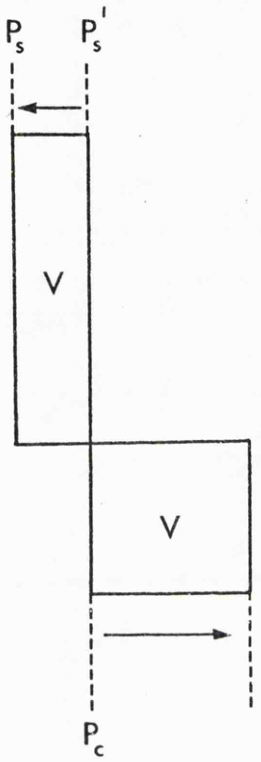

Figure 1 Relationship between the forward volume flux in a cell-fixed and solvent-fixed frame of reference

In a closed system, as the volume, V, associated with the sedimenting component moves across a plane in a cell-fixed frame of reference (P_c), then an equal volume of solvent moves backwards (as predicted by the laws of conservation of mass). If we consider a solvent-fixed frame of reference denoted by the plane P_s', then as the volume V moves forwards, the plane P_s' effectively moves backwards to position P_s. Thus the forward volume flux that has migrated across the plane P_s is 2V.

$$F = 6\pi\eta\left(\frac{3M}{4\pi N_A}\right)^{1/3}\left(\left(\frac{f}{f_o}\right)^3\bar{v}\right)^{1/3} u \qquad (1)$$

where F is the frictional resistance experienced by a particle moving at velocity u through a fluid of viscosity η. The second bracketed term in equation 1 is a mathematically defined parameter that may be considered as the effective specific volume: it has no real significance to the actual volume of the particle (just as the 'Stokes radius' has no real meaning).

The apparent frictional flux (J_f') associated with the solute at concentration c in a cell-fixed frame of reference may be defined as the product of specific volume and velocity:

$$J_f' = c\left(\frac{f}{f_o}\right)^3\bar{v}\,u \qquad (2)$$

For a solvent-fixed frame of reference, the volume flux is twice that in a cell-fixed frame of reference; hence

$$J_f' = 2c\left(\frac{f}{f_o}\right)^3\bar{v}\,u \qquad (3)$$

This relationship predicts that as $(f/f_o)\rightarrow 0$, $J_f'\rightarrow 0$ (the boundary condition at which f/f_o is zero is hypothetical only since it represents the condition underwhich there is zero slip at the particle surface), But since in any system, the volume flux of the component must at least be equal to the product of solute mass (cV_s) and the velocity of migration (u), it follows that J_f' is that part of the total flux associated with the frictional properties of the particle..

$$J_f = 2c\bar{v}\left(\frac{V_s}{\bar{v}} + \left(\frac{f}{f_o}\right)^3\right)u \qquad (4)$$

V_s is used here since both the bound and entrained solvent will sediment with the particle.

(b) In terms of the sedimenting properties of the system (J_s)

It can be shown that in a cell-fixed frame of reference, the volume flux (J_s) is given by

$$J_s = k_s c \omega^2 r s \tag{5}$$

on the following argument. If k_s is <u>defined</u> as the specific volume of the sedimenting component (c.f. Enokssen, 1948) then the sedimentation coefficient of solute at concentration c in a cell-fixed frame of reference is lower than that in a solvent-fixed frame of reference (s^o) by an amount given by

$$s = s^o (1 - k_s c) \tag{6}$$

This equation is the one conventionally used to determine k_s, which is now defined as the concentration dependence of s. If we now consider the volume flux in a solvent-fixed frame of reference, then equation 5 now becomes

$$J_s = k_s c s^o \omega^2 r (1 - k_s c) \tag{7}$$

where the bracketed term is the correction that must be made to maintain the isovelocity condition when going from a cell-fixed to a solvent-fixed frame of reference.

Since

$$J_f \equiv J_s \tag{8}$$

and, by definition,

$$s = \frac{u}{\omega^2 r} \tag{9}$$

Substituting eqn. 4, 7 and 9 into 8 and rearranging, we have

$$\frac{k_s}{\bar{v}} = 2\left(\frac{V_s}{\bar{v}} + \left(\frac{f}{f_o}\right)^3\right) \tag{10}$$

This generalised equation is valid for any sedimenting particle, as borne out by the experimental results on polystyrene latex spheres (Cheng and Schachman, 1955) and a wide range of other particles (including bovine serum albumin, fibrinogen, bushy stunt virus and paramyosin, Rowe, 1977). Equation 10 should be applied only when the following conditions are fulfilled:

(i) the solute concentrations must be absolute, i.e. related ultimately to a dry mass basis

(ii) the solute concentrations must be true sedimenting concentrations or alternatively the s values extrapolated for each run to zero time of sedimentation

(iii) the sedimentation coefficients must be fully corrected to a standard basis with no temperature or other ambiguities and must be corrected for solution (not solvent) density, Fujita (1962)

(iv) the ionic strength of the solvent must be sufficient to avoid charge effects.

The k_s' measured in practice is corrected to solvent density but can be related to that for solution density by the equation:

$$k_s = k_s' \left(1 - \frac{\bar{v}}{k_s'}\right) \qquad (11)$$

Infact no such correction has been made in the application of eqn. 10 in the determination of M^o for myosin molecules and filaments since, at high k_s' (greater than 90ml/g), the correction to solution density is negligible (less than 0.8%).

Determination of Molecular Weight, M^o

The sedimentation coefficient at infinite dilution is related to M^o and frictional coefficient by the Svedberg equation:

$$s^{\circ} = \frac{M^{\circ}(1-\bar{v}\rho)}{N_A f} \qquad (12)$$

where

$$f = \left(\frac{f}{f_o}\right) \times f_o \qquad (13)$$

$$f_o = 6\pi\eta\left(\frac{3M\bar{v}}{4\pi N_A}\right)^{1/3} \qquad (14)$$

By rearranging equation 10 and substituting into equation 12, we have

$$M^{\circ} = N_A\left[\frac{6\pi\eta s^{\circ}}{(1-\bar{v}\rho)}\right]^{3/2}\left[\left(\frac{3\bar{v}}{4\pi}\right)\left(\frac{k_s}{2\bar{v}} - \frac{V_s}{\bar{v}}\right)\right]^{1/2} \qquad (15)$$

an equation which enables us to determine M°, the ideal molecular weight of the solute from s°, k_s and $\bar{v}$. Since M° varies little over credible ranges of $V_s/\bar{v}$ (1.3 to 1.4 for proteins and nucleic acids) $V_s/\bar{v}$ may be assumed or determined experimentally, as described in Appendix II. Molecular weight may be estimated for a polydisperse sample provided a single sedimenting boundary exists. As with all M values obtained by substitution into the Svedberg equation, the value yielded is not an exactly defined average: however, numerical analysis shows that the method yields a reasonable approximation to the weight-average molecular weight at infinite dilution (M_w°), Rowe (1977).

The Study of Interacting Systems

Sedimentation velocity analysis has considerable application in the study of solutes showing appreciable interaction. Until now it has been necessary to assume k_s of the individual species and thus the precision of interaction constants which have been estimated has been limited. But the

theory described above enables the k_s to be predicted for a given solute species provided M^o, s^o and $\bar{v}$ are known. Hence even a small amount of self-interaction can be detected from any difference between experimental and predicted k_s. The details of the procedure for predicting k_s are as follows. The sedimentation coefficient at infinite dilution of the equivalent sphere (s^o_{sp}) of the same mass and $\bar{v}$ as the particle, is estimated from the Svedberg equation (eqn. 12) substituting $f/f_o = 1$, thus

$$s^o_{sp} = \frac{M^o(1 - \bar{v}\rho)}{N_A 6\pi\eta\left(\frac{3M\bar{v}}{4\pi N_A}\right)^{1/3}} \qquad (16)$$

The frictional ratio of the particle is given by

$$\frac{f}{f_o} = \frac{s^o_{sp}}{s^o} \qquad (17)$$

and the predicted k_s can be estimated via equation 10 assuming a value of $v_s/\bar{v}$.

Appendix II. The Concentration Dependence of Reduced Viscosity

The addition of a macromolecular solute at concentration c to a solvent results in an increase in viscosity, characterised by η_{sp}/c, the reduced specific viscosity of the final solution. At infinite dilution η_{sp}/c is denoted by $[\eta]$, the intrinsic viscosity of the solute. The concentration dependence of reduced viscosity may be written as

$$\frac{\eta_{sp}}{c} = [\eta] + K[\eta]^2 c \qquad (18)$$

where K is the Huggins constant. But an alternative equation may be written which is analogous to that of sedimentation

$$\frac{\eta_{sp}}{c} = [\eta](1 + k_\eta c) \qquad (19)$$

where $k_\eta = K[\eta]$. Although a general qualitative resemblance between the concentration dependence of sedimentation and reduced viscosity has often been noted, no exact quantitative theory is currently available relating k_η to k_s. The relationship can be shown to be a simple one under certain conditions and is derived in the following way.

Figure 2 shows the flow pattern adjacent to one side of a particle in solution undergoing viscous flow. Once again if we choose a solvent-fixed frame of reference, in this case a point sufficiently distant from the particle at which the solvent is unperturbed, then the particle can be considered to migrate in a direction opposite to the solvent flow. Analogously, a similar construction for the opposite side of the particle shows that it migrates in the direction of the solvent flow. Thus the particle convects solvent with it but since there is no net solvent flux across the solvent-fixed frame of reference (since the defined migrations are opposite on either side of the particle) then the system can be

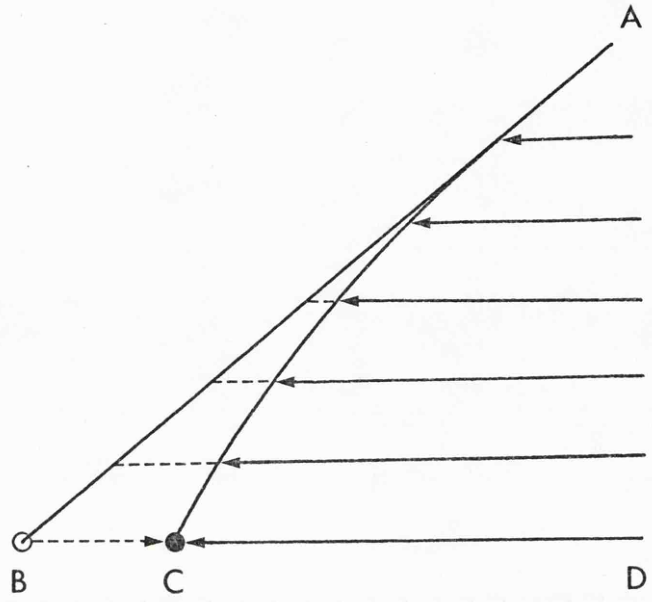

Figure 2 Velocity profile of a particle undergoing viscous flow

As the particle moves from D to C it convects solvent with it (as shown by the arrows) but a point is reached, sufficiently distant from the particle, where the solvent is unperturbed. In a solvent-fixed frame of reference, defined by the axes BD, BA, the particle effectively moves from B to C, i.e. opposite to the direction of flow. A similar construction for the opposite side of the particle reveals that the effective migration of the particle is in the direction of flow. Thus there is no net solvent flux across the plane of the particle and the system may be considered as closed and therefore analogous to sedimentation in a centrifuge cell.

regarded as 'closed' and the induced flow of convected solvent will cause a 'backflow' of unperturbed solvent. This construction has the immediate consequence that the concentration dependence of reduced viscosity exhibited upon addition of a macromolecular solute is identical to the concentration dependence associated with the solute when induced to migrate in another way (e.g. by centrifugal force).

However this treatment considers the concentration in volume terms for which the analogous equation for the concentration dependence of the sedimentation coefficient (eqn. 6) may be rewritten as:

$$s = s^0 \left(1 - \frac{k_s}{\bar{v}} \phi\right) \simeq s^0 \left(1 + \frac{k_s}{\bar{v}} \phi\right)^{-1} \qquad (20)$$

where ϕ $(=cV_s)$ is defined as the volume concentration (v/v) and $k_s/\bar{v}$ represents the concentration dependence expressed in <u>thermodynamic</u> volume terms (c.f. eqn. 10). If reduced viscosity shows the same concentration dependence upon ϕ then

$$\frac{\eta_{sp}}{\phi} = \left[\frac{\eta_{sp}}{\phi}\right]_{\phi \to 0} \left(1 + \frac{k_s}{\bar{v}} \phi\right) \qquad (21)$$

or

$$\frac{\eta_{sp}}{c} = [\eta] \left(1 + \frac{V_s}{\bar{v}} k_s c\right) \qquad (22)$$

Comparing equation 22 with equation 19 we see that

$$k_\eta = \frac{V_s}{\bar{v}} k_s \qquad (23)$$

Thus from the ratio k_η/k_s the swelling of the solute $(V_s/\bar{v})$ may be estimated independently of any assumed shape model.

<u>A Quantitative Test for Hydrodynamic Models</u>

The phenomenological frictional ratio is generally considered to be the product of two factors due to swelling and asymmetry (Tanford, 1963).

$$\left(\frac{f}{f_o}\right)^3 = \frac{V_s}{\bar{v}}\left(\frac{f}{f_o}\right)^3_{a/b} \qquad (24),$$

where $(f/f_o)_{a/b}$ is the shape factor signifying the frictional ratio of a particle of axial ratio a/b. For ellipsoids of revolution $(f/f_o)_{a/b}$ is defined by the well-known Perrin function (Perrin, 1936). The intrinsic viscosity may be likewise accounted for in terms of swelling and asymmetry

$$[\eta] = \frac{V_s}{\bar{v}}\,\bar{v}\,\nu \qquad (25)$$

where ν is the viscosity increment and can be computed for ellipsoids of revolution using the equations of Simha (1940).

Combining equations 10, 24 and 25 we have

$$\frac{k_s}{[\eta]} = \frac{2\left(1 + \left(\frac{f}{f_o}\right)^3_{a/b}\right)}{\nu} \equiv R \qquad (26)$$

The function R depends solely on the particle asymmetry and is independent of swelling. It may be computed for ellipsoids of revolution or indeed for any model for which frictional and viscosity functions are available. Computations of R for ellipsoids of revolution of axial ratio from 1 : 100 and 100 : 1 has shown that R is a sensitive function even for low a/b, Figure 3. Also shown is the dependence of the β-factor upon a/b which is a similar function computed from M^o, s^o, $[\eta]$ and $\bar{v}$ (Scheraga and Mandelkern, 1953). The R-function, however, has considerable advantages over the β-function.

(i) R is far more sensitive to a/b than β, the latter varies only slowly with a/b ($a/b < 4$) for prolate ellipsoids and hardly at all with a/b for oblate ellipsoids.

(ii) The R-function does not require knowledge of the absolute concentration since it cancels in the ratio $k_s/[\eta]$.

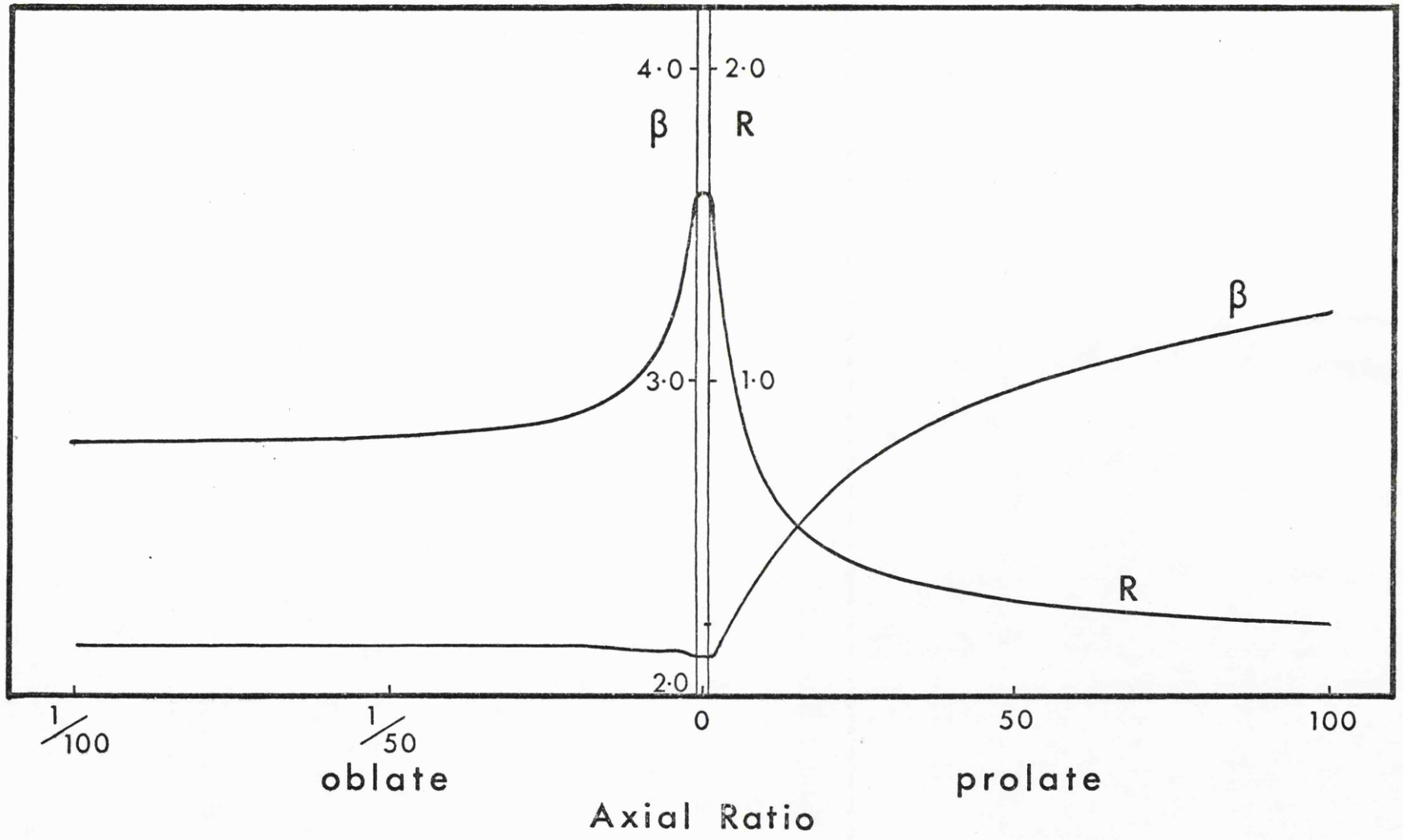

Figure 3 R and β computed as a function of axial ratio for ellipsoids of revolution.

(iii) R is much more tolerant of errors involved in its calculation than is the β-function.

For these reasons the R-function may largely replace the β-function in the estimation of a/b for particles whose shapes can be legitimately represented by ellipsoids of revolution. But the very lack of variation of β with a/b for oblate ellipsoids may make it possible to distinguish between an oblate or prolate ellipsoid of revolution where the R-function is unable to do so. The a/b of the ellipsoid of revolution which is consistent with the calculated value of R can be used to estimate the viscosity increment, ν, and hence $V_s/\bar{v}$ via equation 25. This model-dependent $V_s/\bar{v}$ can be compared to the model-independent value given by k_η/k_s. If the two values agree one may conclude that under the solvent conditions used the particle may be represented by an equivalent ellipsoid of revolution of defined a/b; where the two values disagree one may surmise that the hydrodynamic model is a poor one.

BIBLIOGRAPHY

Bibliography

Belton, P. S. and Packer, K. J. (1974)
Biochim. Biophys. Acta 354, 305 - 314

Belton, P. S., Jackson, R. R. and Packer, K. J. (1972)
Biochim. Biophys. Acta 286, 16 - 25

Bender, M. L. and Hamilton, G. A. (1962)
J. Amer. Chem. Soc. 84, 2570 - 2576

Birnie, G. D., Rickwood, D. and Hell, A. (1973)
Biochim. Biophys. Acta 331, 283 - 294

Bloomfield, V. A., Dalton, W. O. and Van Holde, K. E. (1967)
Biopolymers 5, 135 - 148

Boyer, P. D., Lardy, H. A. and Phillips, P. H. (1942)
J. Biol. Chem. 146, 673 - 682

Boyer, P. D., Lardy, H. A. and Phillips, P. H. (1943)
J. Biol. Chem. 149, 529 - 541

Brahms, J. and Kay, C. M. (1962)
J. Mol. Biol. 5, 132 - 137

Busch, H. and Nair, P. V. (1957)
J. Biol. Chem. 229, 377 - 387

Caillé, J. P. and Hinke, J. A. M. (1974)
Can. J. Physiol. Pharmacol. 52, 814 - 828

Carlson, F. D. and Herbert, T. J. (1972)
J. de Physique 33 (suppl. C1), 157 - 161

Carney, J. A. and Brown, A. L. (1966)
J. Cell Biol. 28, 375 - 389

Caspar, D. L. D. (1966)
in 'Molecular Architecture in Cell Physiology' (Hayashi, T. and Szent-Györgyi, A. G., eds.), pp.191 - 207, Prentice-Hall, New Jersey

Cheng, P. Y. and Schachman, H. K. (1955)
J. Polymer Soi. 16, 19 - 30

Chowrashi, P. K. and Pepe, F. A. (1971)
First European Biophysics Congress, Baden, 429 - 436

Chung, C. S., Richards, E. G. and Olcott, H. S. (1967)
Biochemistry 6, 3154 - 3161

Cohen, R. (1963)
C. R. Acad. Soi. 256, 3513 - 3515

Cohen, R and Hahn, C. W. (1965)
C. R. Acad. Sci. 260, 2077 - 2080

Cohen, R. and Mire, M. (1971a)
Eur. J. Biochem. 23, 267 - 275

Cohen, R. and Mire, M. (1971b)
Eur. J. Biochem. 23, 276 - 281

Connell, J. J. (1958)
Biochem. J. 70, 81 - 91

Connell, J. J. and Mackie, I. M. (1964)
Nature (London), 201, 78 - 79

Craig, R. (1975)
Ph. D. thesis, University of London

Craig, R. (1977)
J. Mol. Biol. 109, 69 - 81

Craig, R. and Offer, G. (1976a)
J. Mol. Biol. 102, 325 - 332

Craig, R. and Offer, G. (1976b)
Proc. Roy. Soc. B, 192, 451 - 461

Dreizen, P. and Gershman, L. C. (1970)
Biochemistry, 9, 1688 - 1693

Dreizen, P., Gershman, L. C., Trotta, P. P. and Stracher, A. (1967)
J. Gen. Physiol. Suppl. 50, 85 - 113

Eaton, B. L. and Pepe, F. A. (1974)
J. Mol. Biol. 82, 421 - 423

Edelstein, S. J. and Schachman, H. K. (1967)
J. Biol. Chem. 242, 306 - 311

Edsall, J. T. (1953)
in 'The Proteins' (Neurath, H. and Bailey, K., eds.), vol. 1B, pp. 549 - 726,
Academic Press, London and New York

Ellenbogen, E., Iyengar, R., Stern, H. and Olson, R. E. (1960)
J. Biol. Chem. 235, 2642 - 2648

Elliott, A., Offer, G. and Burridge, K. (1976)
Proc. Roy. Soc. B, 193, 45 - 53

Endo, M., Nonomura, Y., Masaki, T., Ohtsuki, I. and Ebashi, S. (1966)
J. Biochem. 60, 605 - 608

Elzinga, M., Collins, J. H., Kuehl, W. M. and Adelstein, R. S. (1973)
Proc. Nat. Acad. Sci., U. S. A. 70, 2687 - 2691

Enokssen, B. (1948)
Nature (London), 161, 934 - 935

Fairbanks, G., Steck, T. L. and Wallach, D. F. H. (1971)
Biochemistry, 10, 2606 - 2617

Fujita, H. (1962)
in 'Mathematical Theory of Sedimentation Analysis', Academic Press, London and New York

Fung, B. M. and McGaughy, T. W. (1974)
Biochim. Biophys. Acta 343, 663 - 673

Fung, B. M., Wassil, D. A., Durham, D. L., Chestnut, R. W., Durham, N. N. and Berlin, K. D. (1975)
Biochim. Biophys. Acta 385, 180 - 187

Gellert, M. F. and Englander, S. W. (1963)
Biochemistry 2, 39 - 42

Gergely, J. (1966)
Ann. Rev. Biochem. 35, 691 - 722

Gershman, L. C., Stracher, A. and Dreizen, P. (1969)
J. Biol. Chem. 244, 2726 - 2736

Gibbs, A. J. and Rowe, A. J. (1974)
I. C. R. S. (Biochemistry), 2, 1092

Gilbert, G. A. (1959)
Proc. Roy. Soc. A, 250, 377 - 388

Gilbert, L. M. and Gilbert, G. A. (1973)
in 'Methods in Enzymology' (Hirs, C. W. and Timasheff, S. N., eds.)
vol. 27D, pp. 273 - 296, Academic Press, London and New York

Glascoe, P. K. and Long, F. A. (1960)
J. Phys. Chem. 64, 188 - 190

Godfrey, J. E. and Harrington, W. F. (1970a)
Biochemistry 9, 886 - 893

Godfrey, J. E. and Harrington, W. F. (1970b)
Biochemistry 9, 894 - 908

Gordon, A. M., Huxley, A. F. and Julian, F. J. (1966)
J. Physiol. 184, 143 - 169

Guba, F. and Straub, F. B. (1943)
Studies Inst. Med. Chem. 3, 46 - 48

Hamoir, G., McKenzie, H. A. and Smith, M. B. (1960)
Biochim. Biophys. Acta 40, 141 - 149

Hanson, J. and Huxley, H. E. (1957)
Biochim. Biophys. Acta 23, 250 - 260

Hanson, J., O'Brien, E. J. and Bennett, P. M. (1971)
J. Mol. Biol. 58, 865 - 871

Harrington, W. F. and Burke, M. (1972)
Biochemistry 11, 1448 - 1455

Harrison, R. G., Lowey, S. and Cohen, C. (1971)
J. Mol. Biol. 59, 531 - 535

Haselgrove, J. C. (1975)
J. Mol. Biol. 92, 113 - 143

Hazlewood, C. F., Chang, D. C., Nichols, B. L. and Woessner, D. E. (1974)
Biophys. J. 14, 583 - 606

Henderson, R. F. and Henderson, T. R. (1969)
Arch. Biochem. Biophys. 129, 86 - 93

Herbert, T. J. and Carlson, F. D. (1971)
Bioploymers 10, 2231 - 2252

Holtzer, A. and Lowey, S. (1959)
J. Amer. Chem. Soc. 81, 1370 - 1377

Holtzer, A., Lowey, S. and Schuster, T. M. (1961)
in 'Symposium on the Molecular Basis of Neoplasia', pp. 259 - 280,
University of Texas Press, Austin, Texas

Hotta, K. and Morales, M. F. (1960)
J. Biol. Chem. 235, PC 61

Hu, A. S. L., Bock, R. M. and Halvorson, H. O. (1962)
Anal. Biochem. 4, 489 - 504

Hüttermann, A. and Wendlberger, G. (1975)
Methods Cell Biol. 13, 153 - 170

Huxley, H. E. (1957)
J. Biophys. Biochem. Cytol. 3, 631 - 648

Huxley, H. E. (1963)
J. Mol. Biol. 7, 281 - 308

Huxley, H. E. (1968)
J. Mol. Biol. 37, 507 - 520

Huxley, H. E. (1972)
in 'The Structure and Function of Muscle', (Bourne, G. H., ed.), 2nd edn., vol. 1, pp. 301 - 387

Huxley, H. E. and Brown, W. (1967)
J. Mol. Biol. 30, 383 - 434

Huxley, H. E. and Hanson, J. (1957)
Biochim. Biophys. Acta 23, 229 - 249

Hvidt, A. and Nielsen, S. O. (1966)
Adv. Protein Chem. 21, 287 - 386

Inoué, S., Sato, H., Kane, R. E. and Stephens, R. E. (1965)
J. Cell Biol. 27, 115 - 116A

Jakus, M. A. and Hall, C. E. (1947)
J. Biol. Chem. 167, 705 - 714

Johnson, P. and Rowe, A. J. (1960)
Biochem. J. 74, 432 - 440

Johnson, P. and Rowe, A. J. (1961)
Biochem. J. 79, 524 - 530

Jolly, D. J. and Josephs, R. (1975)
Abstract, Second International Congress of Biorheology, Rehovot, Israel

Josephs, R. and Harrington, W. F. (1966)
Biochemistry 5, 3474 - 3487

Kachmar, J. F. and Boyer, P. D. (1956)
J. Biol. Chem. 200, 669 - 682

Kaminer, B. (1969)
J. Mol. Biol. 39, 257 - 264

Kaminer, B. and Bell, A. L. (1966)
J. Mol. Biol. 20, 391 - 401

Kaminer, B., Szonyi, E. and Belcher, C. D. (1976)
J. Mol. Biol. 100, 379 - 386

Katsura, I. and Noda, H. (1971)
J. Biochem. 69, 219 - 229

Katsura, I. and Noda, H. (1973a)
J. Biochem. 73, 245 - 256

Katsura, I. and Noda, H. (1973b)
J. Biochem. 73, 257 - 268

Kay, C. M. (1960)
Biochim. Biophys. Acta 38, 420 - 427

Kemper, D. L. and Everse, J. (1973)
in 'Methods in Enzymology' (Hirs, C. W. and Timasheff,S. N., eds.)
vol. 27D, pp. 67 - 82, Academic Press, London and New York

King, M. V. and Young, M. (1972)
J. Mol. Biol. 65, 519 - 523

Kirschenbaum, I. (1951)
in 'Physical Properties and Analysis of Heavy Water', pp. 1 - 42,
McGraw-Hill Book CO., New York

Kirschner, M. W. and Schachman, H. K. (1971)
Biochemistry 10, 1919 - 1925

Knappeis, G. G. and Carlsen, F. (1968)
J. Cell Biol. 38, 202 - 211

Koizumi, T. (1974)
J. Biochem. 76, 431 - 439

Kolb, H. J. (1974)
Hoppe-Seylers Z. Physiol. Chem. 355, 401 - 409

Kuno, H. and Kihara, H. K. (1967)
Nature (London) 215, 974 - 975

Laki, K. and Carroll, W. (1955)
Nature (London) 175, 389 - 390

Lardy, H. A. and Zeigler, J. A. (1945)
J. Biol. Chem. 159, 343 - 351

Lauffer, M. A. (1951)
J. Amer. Chem. Soc. 73, 2370 - 2371

Lee, J. J. and Berns, D. S. (1968)
Biochem. J. 110, 465 - 470

Linderstrøm-Lang, K. (1949)
Cold Spring Harb. Symp. Quant. Biol. 14, 117 - 125

Lowey, S. (1971)
in 'Subunits in Biological Systems', (Timasheff, S. N. and Fasman, G. D., eds.), Part A, pp. 201 - 259, Marcel Dekker Inc., New York

Lowey, S. (1972)
in 'Protein-Protein Interactions', (Jaenicke, R. and Helmreich, E., eds.), pp. 317 - 342, Springer-Verlag, Berlin

Lowey, S. and Cohen, C. (1962)
J. Mol. Biol. 4, 293 - 308

Lowey, S. and Risby, D. (1971)
Nature (London), 234, 81 - 85

Lowey, S., Goldstein, L., Cohen, C. and Luck, S. M. (1967)
J. Mol. Biol. 23, 287 - 304

Lowey, S., Slayter, H. S., Weeds, A. G. and Baker, H. (1969)
J. Mol. Biol. 42, 1 - 29

Lowry, O. H., Rosebrough, N. J., Farr, A. L. and Randall, R. J. (1951)
J. Biol. Chem. 193, 265 - 275

Luchi, R. J., Kritcher, E. M. and Conn, H. L. (1965)
Circ. Res. 16, 74 - 82

McQuate, J. T. and Utter, M. F. (1959)
J. Biol. Chem. 234, 2151 - 2157

Mihalyi, E. and Rowe, A. J. (1966)
Biochem. Z. 345, 267 - 285

Mire, M. (1967)
C. R. Acad. Sci. 264, 1896 - 1899

Moos, C., Offer, G., Starr, R. and Bennett, P. (1975)
J. Mol. Biol. 97, 1 - 9

Morimoto, K. and Harrington, W. F. (1973)
J. Mol. Biol. 77, 165 - 175

Morimoto, K. and Harrington, W. F. (1974a)
J. Mol. Biol. 83, 83 - 97

Morimoto, K. and Harrington, W. F. (1974b)
J. Mol. Biol. 88, 693 - 709

Mueller, H. (1964)
J. Biol. Chem. 239, 797 - 804

Nishihara, T. and Doty, P. (1958)
Proc. Nat. Acad. Sci., U. S. A. 44, 411 - 417

Noda, H. and Ebashi, S. (1960)
Biochim. Biophys. Acta 41, 386 - 392

Offer, G., Moos, C. and Starr, R. (1973)
J. Mol. Biol. 74, 653 - 676

Ohtsuki, I. and Wakabayashi, T. (1972)
J. Biochem, 72, 369 - 377

Oosawa, F. and Kasai, M. (1971)
in 'Subunits in Biological Systems', (Timasheff, S. N. and Fasman, G. D., eds.), Part A, pp. 261 - 322, Marcel Dekker Inc., New York

Paglini, S. and Lauffer, M. A. (1968)
Biochemistry 7, 1827 - 1835

Peacocke, A. R. and Schachman, H. K. (1954)
Biochim. Biophys. Acta 15, 198 - 210

Pearce, T. C., Rowe, A. J. and Turnock, G. (1975)
J. Mol. Biol. 97, 193 - 201

Pepe, F. A. (1966)
J. Cell Biol. 28, 505 - 525

Pepe, F. A. (1967)
J. Mol. Biol. 27, 203 - 225

Pepe, F. A. (1971)
Prog. Biophys. Molec. Biol. 22, 75 - 96

Pepe, F. A. (1972)
Cold Spring Harb. Symp. Quant. Biol. 37, 97 - 108

Pepe, F. A. (1975)
J. Histochem. Cytochem. 23, 543 - 562

Pepe, F. A. and Drucker, B.(1972)
J. Cell Biol. 52, 255 - 260

Pepe, F. A. and Drucker, B.(1975)
J. Mol. Biol. 99, 609 - 617

Perrin, F. (1936)
J. Phys. Radium. 7, 1 - 10

Perry, S. V. (1967)
Prog. Biophys. Molec. Biol. 17, 325 - 381

Pinset-Härström, I. and Morel, J. E. (1975)
in 'Proteins of Contractile Systems' (Biró, E. N. A., ed.), pp. 193 - 203,
North Holland, Amsterdam

Pollard, T. D. (1974)
J. Cell Biol. 63, 273a

Pollard, T. D. and Weihing, R. R. (1974)
CRC Crit. Rev. Biochem. 2, 1 - 65

Potter, J. D. (1974)
Arch. Biochem. Biophys. 162, 436 - 441

Reisner, A. H. and Rowe, J. (1971)
Anal. Biochem. 41, 1 - 15

Reynard, A. M., Hass, L. F., Jacobsen, D. D. and Boyer, P. D. (1961)
J. Biol. Chem. 236, 2277 - 2283

Richards, E. G., Chung, C. S., Menzel, D. B. and Olcott, H. S. (1967)
Biochemistry 6, 528 - 540

Rickwood, D., Hell, A., Birnie, G. D. and Gilhuus-Moe, C. C. (1974)
Biochim. Biophys. Acta 342, 367 - 371

Rowe, A. J. (1960)
Ph. D. thesis, University of Cambridge

Rowe, A. J. (1964)
Proc. Roy. Soc. B, 160, 437 - 441

Rowe, A. J. (1977)
Biopolymers, in press

Sanger, J. W. (1971)
Cytobiol. 4, 450 - 466

Sarkar, S. (1972)
Cold Spring Harb. Symp. Quant. Biol. 37, 14 - 17

Sarkar, S., Streter, F. A. and Gergely, J. (1971)
Proc. Nat. Acad. Sci., U. S. A. 68, 946 - 950

Scheraga, H. A. and Mandelkern, L. (1953)
J. Amer. Chem. Soc. 75, 179 - 184

Schmitt, B. (1975)
Biochimie, 57, 1001 - 1004

Siemankowski, R. F. and Dreizen, P. (1974)
Fed. Proc. 33, 1579

Siemankowski, R. F. and Dreizen, P. (1975)
Biophys. J. 15, 236a

Simha, R. (1940)
J. Phys. Chem. 44, 25 - 34

Slayter, H. S. and Lowey, S. (1967)
Proc. Nat. Acad. Sci., U. S. A. 58, 1611 - 1618

Small, J. V. and Squire, J. M. (1972)
J. Mol. Biol. 67, 117 - 149

Sobieszek, A. (1972)
J. Mol. Biol. 70, 741 - 744

Squire, J. M. (1971)
Nature (London), 233, 457 - 462

Squire, J. M. (1972)
J. Mol. Biol. 72, 125 - 138

Squire, J. M. (1973)
J. Mol. Biol. 77, 291 - 323

Squire, J. M. (1974)
J. Mol. Biol. 90, 153 - 160

Squire, J. M. (1975)
A. Rev. Biophys. Bioeng. 4, 137 - 163

Stambaugh, R. and Post, D. (1966)
J. Biol. Chem. 241, 1462 - 1467

Starr, R. and Offer, G. (1971)
F. E. B. S. Letters, 15 40 - 44

Starr, R. and Offer, G. (1973)
J. Mol. Biol. 81, 17 - 36

Stracher, A. (1969)
Biochem. Biophys. Res. Comm. 35, 519 - 525

Strohmaier, K. and Mussgay, M. (1959)
Science, 130, 217

Sunouchi, E., Maruyama, K. and Noda, H. (1966)
Biochim. Biophys. Acta 120, 229 - 238

Szent-Györgyi, A. (1945)
Acta Physiol. Scand. 9, suppl. 25

Szent-Györgyi, A. (1951)
in 'Chemistry of Muscular Contraction', 2nd rev. edn., Academic Press, London and New York

Tanford, C. (1963)
in 'Physical Chemistry of Macromolecules', Chapter 6, John Wiley & Sons, Inc., New York

Thomson, J. F. (1963)
in 'Biological Effects of Deuterium', McMillan, New York

Tomimatsu, Y. (1964)
Biopolymers 2, 275 - 277

Tonomura, Y., Appel, P. and Morales, M. (1966)
Biochemistry 5, 515 - 521

Trautman, R. (1956)
J. Phys. Chem. 60, 1211 - 1217

Trayer, I. P. and Perry, S. V. (1966)
Biochem. Z. 345, 87 - 100

Tregear, R. T. and Squire, J. M. (1973)
J. Mol. Biol. 77, 279 - 290

Trinick, J. A. (1973)
Ph. D. thesis, University of Leicester

Vallejo, C. G. and Lagunas, R. (1970)
Anal. Biochem. 36, 207 - 212

Waugh, D. F. (1954)
Adv. Protein Chem. 9, 325 - 437

Waugh, D. F. (1957)
J. Cell. Comp. Physiol. 49, Suppl. 1, 145 - 164

Weber, A. and Murray, J. M. (1973)
Physiol. Rev. 53, 612 - 673

Weeds, A. G. and Frank, G. (1972)
Cold Spring Harb. Symp. Quant. Biol. 37, 9 - 14

Weeds, A. G. and Lowey, S. (1971)
J. Mol. Biol. 61, 701 - 725

Wilkinson, J. M., Perry, S. V., Cole, H. A. and Trayer, I. P. (1972)
Biochem. J. 127, 215 - 228

Williams, R. C. and Backus, R. C. (1949)
J. Amer. Chem. Soc. 71, 4052 - 4057

Williams, R. C., Backus, R. C. and Steere, R. L. (1951)
J. Amer. Chem. Soc. 73, 2062 - 2066

Wood, G. C. (1960)
Biochem. J. 75, 598 - 605

Woods, E. F. (1969)
J. Biol. Chem. 242, 2859 - 2871

Woods, E. F., Himmelfarb, S. and Harrington, W. F. (1963)
J. Biol. Chem. 238, 2374 - 2385

Yang, J. T. (1961)
Adv. Protein Chem. 16, 323 - 400

Young, M. (1969)
Ann. Rev. Biochem. 38, 913 - 950

Young, M., King, M. V., O'hara, D. S. and Molberg, P. J. (1972)
Cold Spring Harb. Symp. Quant. Biol. 37, 65 - 76

Zewe, V. and Fromm, H. J. (1962)
J. Biol. Chem. 237, 1668 - 1675

Zimm, B. (1946)
J. Chem. Phys. 14, 164 - 179

Zimm, B. H. (1948)

J. Chem. Phys. 16, 1099 - 1116

Zobel, C. R. and Carlson, F. D. (1963)

J. Mol. Biol. 7, 78 - 89

Abstract

A procedure has recently been derived which makes it possible to determine the molecular weight of a particle from sedimentation velocity studies alone. Application of this new theory has enabled the molecular weight of both the myosin molecule and the myosin filament isolated from rabbit skeletal muscle to be determined. It has further been demonstrated by exhaustive curve-fitting that myosin A solutions contain no appreciable amounts of dimer at high ionic strength. This is in direct contradiction to the prediction by Godfrey and Harrington (1970a,b) and Harrington and Burke (1972) that a monomer-dimer equilibrium existed in myosin solutions. An analysis has been presented which shows that these latter results may be satisfactorily explained without recourse to a monomer-dimer hypothesis.

A detailed analysis of the hydrodynamic properties of synthetic A-filaments has shown that they display a feature not previously demonstrated heretofore; namely that they invariably possess a range of frictional ratios some 75% higher than can be accounted for in terms of the length-equivalent prolate ellipsoids of revolution. On the assumption that preparations of natural A-filaments exhibit similar frictional properties as those formed in vitro, it has been possible to determine the helical symmetry of purified natural A-filaments by measuring their sedimentation coefficient.

The sedimentation coefficient close to infinite dilution has been estimated for purified A-filaments by the technique of active enzyme centrifugation yielding a value of 132 ± 3S (in agreement with the earlier but less precise estimate of 136 ± 25S, Trinick, 1973). It was found that native A-filaments contain between 3.15 and 3.40 myosins/14.3nm axial repeat and this is regarded as good evidence in favour of a 3-stranded model for the A-filament.

References

Godfrey, J. E. and Harrington, W. F. (1970a)
Biochemistry 9, 886 - 893

Godfrey, J. E. and Harrington, W. F. (1970b)
Biochemistry 9, 894 - 908

Harrington, W. F. and Burke, M. (1972)
Biochemistry 11, 1448 - 1455

Trinick, J. A. (1973)
Ph.D. thesis, University of Leicester